

Synthetic Procedures for the Functionalisation of the $\text{Re}(\text{CO})_3^+$ unit

A thesis submitted to the Cardiff University

By

Afroza Banu

in candidature of the degree of

Doctor of Philosophy

February 2009

Department of Chemistry
Cardiff University

UMI Number: U585155

All rights reserved

INFORMATION TO ALL USERS

The quality of this reproduction is dependent upon the quality of the copy submitted.

In the unlikely event that the author did not send a complete manuscript and there are missing pages, these will be noted. Also, if material had to be removed, a note will indicate the deletion.



UMI U585155

Published by ProQuest LLC 2013. Copyright in the Dissertation held by the Author.
Microform Edition © ProQuest LLC.

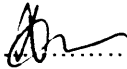
All rights reserved. This work is protected against
unauthorized copying under Title 17, United States Code.



ProQuest LLC
789 East Eisenhower Parkway
P.O. Box 1346
Ann Arbor, MI 48106-1346


DECLARATION

This work has not previously been accepted in substance for any degree and is not concurrently submitted in candidature for any degree.

Signed  (candidate) Date 16/02/09.....


STATEMENT 1

This thesis is being submitted in partial fulfillment of the requirements for the degree of PhD

Signed  (candidate) Date 16/02/09.....

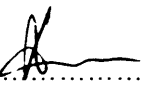
STATEMENT 2

This thesis is the result of my own independent work/investigation, except where otherwise stated.
Other sources are acknowledged by explicit references.

Signed  (candidate) Date 16/02/09.....

STATEMENT 3

I hereby give consent for my thesis, if accepted, to be available for photocopying and for inter-library loan, and for the title and summary to be made available to outside organisations.

Signed  (candidate) Date 16/02/09.....

My mum and Asif

DEDICATED TO

ACKNOWLEDGEMENTS

I want to express my sincerest gratitude to my supervisors Professor Peter G. Edwards and Dr. Angelo J. Amoroso for the idea of this research. Special thanks go to Dr. Angelo J. Amoroso for his careful guidance and unlimited patience throughout the last couple of years.

I would like to thank Dr. K. M. A. Malik and Dr. Liling Ooi for performing crystallography, described in this thesis.

I would also like to thank Dr. Ian A. Fallis, Dr. S. Aldridge, Dr. Nancy Dervisi and Dr. James Platts for their helpful discussion during viva.

Thanks go to all the technical staffs- Rob Jenkins, Alan, Robin, Ricky, Sham, John Bowly and Gary for helping me to work smoothly.

Thanks also go to everyone in the Labs 1.124 and 1.125 specially Mark, Lisa, Neha, Cerys, Tim, Amal, Debbie, Becky, Bres, Ruth, Anne, Graham, Tom for making the work enjoyable.

Finally, I would like thank my husband Golzar and my lovely son Asif for their support and inspiration throughout the research works.

ABSTRACT

This thesis mainly describes the synthesis of functionalised $\text{Re}(\text{CO})_3^+$ units with polypyridine ligands and their characterization by spectroscopic and X-ray crystallographic methods.

Chapter 1 includes general introduction of rhenium and its carbonyl compounds, their preparation, substitution of carbonyls in general organometallic compounds and in rhenium carbonyl compounds. This chapter also describes the photophysical and redox active properties of rhenium.

There have been numerous reports that have used the $\text{Re}(\text{bpy})(\text{CO})_3\text{Cl}$ moiety as building blocks for supramolecular species, sub-units of photodevices or even as potential biological labels. Chapter 2 and 3 describe the investigation of new potential complexes where the bipyridyl ligand has been replaced by a ligand which offers greater possibilities in functionalisation. These include $\text{Re}(\text{I})$ -complexes containing 2,2';6',2''-terpyridine and 2,2';6',2'';6'',2'''-quaterpyridine ligands. A number of novel rhenium compounds have been synthesized and their coordinative and spectroscopic properties have been elucidated. The complexes also characterized by X-ray crystallographic studies.

In chapter 4, a number of $\text{Re}(\text{bpy})(\text{CO})_3^+$ complexes containing thiourea, pyridyl terpyridine and 1-methyl-4-pyridyltetrahydropyridine ligands have been prepared and their anion binding, cation binding and redox active properties have been described. The rhenium compound of 1-methyl-4-pyridyltetrahydropyridine may prove to be useful molecular probe for the biochemical research into the origin of Parkinsons-like conditions. This chapter also dealt with the synthesis of water soluble $\text{Re}(\text{bpy})(\text{CO})_3^+$ analogues using disodium bathophenanthroline sulphonate ligand.

ABBREVIATIONS

bpy	2,2'-bipyridine
qpy	2,2':6',2'':6'',2'''-quaterpyridine
terpy	2,2':6',2''-terpyridine
IPQP	4',4''-bis(4-isopropylphenyl)- 2,2':6',2'':6'',2'''-quaterpyridine
Ph2qtpy	4',4''-diphenyl-2,2':6',2'':6'',2'''- quaterpyridine
pyterpy	4'-(4'''-pyridyl)-2,2':6',2''-terpyridine
4,4'-bpy	4,4'-bipyridine
MQ ⁺	N-methyl-4,4'-bipyridinium
MPyTP	1-methyl-4-pyridyltetrahydropyridine
BPSA	Bathophenanthroline disulphonic acid disodium salt
phen	1,10-phenanthroline
bpm	2,2'-bipyrimidine
dpq	4-(3,5-dimethyl-4-oxo-2,5- cyclohexadienylidene)-2,6-dimethyl-2,5- cyclohexadienone, diphenyl quinone
DMF	dimethylformamide
DMSO	dimethylsulfoxide
phen	1,10-phenanthroline
Å	Angström (1 Å = 10 ⁻¹⁰ cm)
λ	Wavelength
V	Cell volume
a, b, c	Cell axes
α, β, γ	Cell angles

(°)	degree centigrade (Celcius)
cm	centimeter
cm ⁻¹	Reciprocal centimeters
g	gram
ml	milliliter
mmol	millimole
ppm	Parts per million
IR	Infrared
UV	ultraviolet
ε	Absoption coefficient
MS	Mass spectroscopy
ES	Electrospray
FAB	Fast atom bombardment
NMR	Nuclear magnetic resonance
s	Singlet
d	Doublet
t	Triplet
dd	Doublet of doublets
td	Triplet of doublets
m	Multiplet
sh	Shoulder

TABLE OF CONTENTS

TITLE	I
DECLARATION	II
DEDICATED TO	III
ACKNOWLEDGEMENT	IV
ABSTRACT	V
ABBREVIATIONS	VI

Chapter 1 Introduction

1.1 Introduction to Rhenium	1
1.1.1 Chemistry of Rhenium	1
1.1.2 Rhenium use in therapeutic complexes	2
1.2 Metal carbonyls	5
1.2.1 Preparation of metal carbonyls	6
1.2.2 Substitution of carbonyl ligands in organometallic species	7
1.2.2.1 General carbonyl activation	8
1.2.2.2 Thermal activation	8
1.2.2.3 Photochemical activation	8
1.2.2.4 Chemical activation	9
1.2.3 Substitution reaction of rhenium carbonyls and their derivatives	10
1.2.3.1 Mono-substituted rhenium carbonyl complexes	11
1.2.3.2 Disubstituted rhenium carbonyl complexes	12
1.2.3.3 Trisubstituted rhenium carbonyl complexes	13
1.2.3.4 Substitution by Chelating ligands	13
1.3 Metals in biological applications	16
1.4 Luminescence	16
1.4.1 Organic luminescent complexes	17
1.4.2 Lanthanide luminescent complexes	18
1.4.3 Luminescent transition metal complexes & switches	18
1.5 Rhenium complexes	18

1.5.1 Photochemical properties of rhenium complexes	20
1.5.2 Redox active sensors	21
1.5.3 Supramolecular switches	23
1.6 Aims of the work	23
References	26

Chapter 2 Terpyridine complexes of $\text{Re}(\text{CO})_3^+$ moiety

2.1 Introduction	29
2.1.1 Synthesis of 2,2':6',2''-terpyridine (terpy)	30
2.1.2 4'-Substituted-2,2':6',2''-terpyridines	32
2.1.3 Coordination of 2,2':6',2''-terpyridine with metals	34
2.1.4 Rhenium compounds of terpyridine	35
2.1.5 Aim of the work	36
2.2 Results and Discussion	37
2.2.1 Synthesis of Rhenium complexes	37
2.2.2 Coordinative Properties of the pendent pyridine moiety	40
2.2.3 Spectroscopic Studies	40
2.2.3.1 ^1H NMR	40
2.2.3.2 IR Spectroscopy	43
2.2.4 X-ray Crystallographic Studies	45
2.2.4.1 Crystallographic data for $\text{Re}(\sigma^2\text{-terpy})(\text{CO})_3\text{Cl}$ (1)	45
2.2.4.2 Crystallographic data for $[\text{Re}(\sigma^2\text{-terpy})(\text{CO})_3\text{CH}_3\text{CN}]\text{PF}_6$ (2)	48
2.2.4.3 Crystallographic data for $[\text{Re}(\sigma^2\text{-terpyMe})(\text{CO})_3\text{I}]^+\text{PF}_6^-$ (3)	50
2.2.4.4 Crystallographic data for $[\text{Re}(\sigma^2\text{-terpyMe})(\text{CO})_3\text{Cl}]^+\text{BF}_4^-$ (4)	52
2.2.4.5 Crystallographic data for $[\text{Re}(\sigma^2\text{-terpyMe})(\text{CO})_3\text{CH}_3\text{CN}](\text{PF}_6)_2$ (5)	53
2.2.5 Luminescence	54
2.2.6 Cyclic Voltammetry	56
2.2.7 Concluding remarks	58
2.3 Experimental	58
References	65

Chapter 3 Quaterpyridine complexes of $\text{Re}(\text{CO})_3^+$ moiety

3.1 Introduction	69
3.1.1 Synthesis of 2,2':6',2'':6'',2'''-quaterpyridine (qpy)	69
3.1.2 Coordination of 2,2':6',2'':6'',2'''-quaterpyridine with metals	71
3.1.3 Organometallic compounds of quaterpyridine	73
3.1.4 Solubility of 2,2':6',2'':6'',2'''-quaterpyridine	74
3.1.5 Aim of the work	75
3.2 Results and Discussion	76
3.2.1 Synthesis of the ligand	76
3.2.2 Synthesis of $[\{\text{ReCl}(\text{CO})_3\}_2\text{L}](\mathbf{8})$ [L=4',4''-bis(4-iso-propylphenyl)-2,2':6',2'':6'',2'''-quaterpyridine (IPQP) and 4',4''-diphenyl-2,2':6',2'':6'',2'''-quaterpyridine(Ph ₂ qtpy)]	77
3.2.3 Synthesis of $[\text{Re}_2(\text{IPQP})(\text{CO})_6(\text{CH}_3\text{CN})\text{Cl}]\text{PF}_6(\mathbf{10})$	79
3.2.4 Synthesis of $[\text{Re}_2(\text{IPQP})(\text{CO})_6(\text{py}-3\text{-NH}_2)\text{Cl}]\text{PF}_6(\mathbf{11})$	80
3.2.5 Attempted synthesis of $[\text{Re}(\text{IPQP})(\text{CO})_6(\mu\text{-Cl})]\text{PF}_6(\mathbf{12})$	81
3.2.6 Spectroscopic Studies	81
3.2.6.1 IR and Mass Spectra	81
3.2.6.2 NMR Spectra	83
3.2.7 X-ray Crystallographic Studies	86
3.2.7.1 Crystallographic data for $\text{Re}_2(\text{IPQP})(\text{CO})_6\text{Cl}_2$ (8)	86
3.2.7.2 Crystallographic data for $\text{Re}_2(\text{Ph}_2\text{qpy})(\text{CO})_6(\mu\text{-OH})\text{ReO}_4$ (9)	87
3.2.7.3 Crystallographic data for $[\text{Re}_2(\text{IPQP})(\text{CO})_6(\text{CH}_3\text{CN})\text{Cl}]\text{PF}_6$ (10)	91
3.2.7.4 Crystallographic data for $[\text{Re}_2(\text{IPQP})(\text{CO})_6(\text{py}-3\text{-NH}_2)\text{Cl}]\text{PF}_6$ (11)	92
3.2.8 Absorption spectra and luminescence properties	94
3.2.9 Concluding remarks	95
3.3 Experimental	95
References	100

Chapter 4 Functionalisation of the $\text{Re}(\text{CO})_3(\text{bpy})^+$ unit

4.1 Introduction	103
4.1.1 Ruthenium based sensors	103
4.1.2 Rhenium based sensors	105

4.1.3 Aim of the work	107
4.2 Results and Discussions	107
4.2.1 Anion binding switches	107
4.2.1.1 N-(3-pyridyl)-N'-phenylthiourea (L^1)	107
4.2.1.2 $[\text{Re}(\text{CO})_3(\text{bpy})(L^1)]\text{PF}_6$ (13)	108
4.2.1.3 Test for anion binding	109
4.2.1.4 $[\text{ReCl}(\text{CO})_3(L^1)_2]$ (14)	110
4.2.2 Cation binding switches	113
4.2.2.1 $[\text{Re}(\text{CO})_3(\text{bpy})(L^2)]\text{PF}_6$ (15)	114
4.2.2.2 $[\text{Re}(\text{CO})_3(\text{bpy})(L^2)]_2\text{M}(\text{PF}_6)_2$ [M= Zn(16) and Fe(17)]	117
4.2.2.3 $[\text{Re}(\text{CO})_3(\text{bpy})]_n\text{L}^3(\text{PF}_6)_n$ [n=1(18) and 2(19), $L^3 = 4,4'$ -bpy]	122
4.2.3 Redox-active switches	128
4.2.3.1 N-methyl-4,4'-bipyridinium(MQ^+) PF_6^-	128
4.2.3.2 1-methyl-4-pyridyltetrahydropyridine (MPyTP)	129
4.2.3.3 $[\text{Re}(\text{CO})_3(\text{bpy})L^4][\text{PF}_6]$ [$L^4 = \text{MQ}^+\text{PF}_6^-$ (20) and MPyTP (21)]	130
4.2.3.4 Cyclic Voltammetry	131
4.2.3.5 Luminescence	135
4.2.4 Water-soluble rhenium(I) complexes	136
4.2.5 Rhenium(I)-based supramolecules	139
4.2.5.1 Synthesis of $\text{Re}(\text{CO})_3(\text{CH}_3\text{CN})_3\text{PF}_6$ (25)	139
4.2.5.2 Attempted preparation of $[\text{Re}(\text{CO})_3]_{12} [4,4'\text{-bpy}]_8 [\text{PF}_6]_{12}$	142
4.2.5.3 $[\text{Re}(\text{CO})_3(\text{MQ})_3][\text{PF}_6]_3$ (26)	143
4.3 Experimental	144
References	155

Chapter 1

Introduction

1.1 Introduction to Rhenium

The element rhenium was discovered in 1925 by the Noddachs and is one of the rarest elements, occurring in a mixture of two radioactive isotopes ^{185}Re (37.4%) and ^{187}Re (62.6%). It is not found free in nature and the only commercial source is as a by-product of the molybdenum industry. However, the extraction of the metal from molybdenite is expensive. It is among the ten most expensive metals on earth, so the common starting materials of rhenium chemistry are precious.

The chemistry of rhenium rather closely resembles that of technetium.¹ There are also remote similarities between rhenium and isoelectronic complexes of molybdenum², tungsten³ and osmium⁴ since Re belongs to group VIIA of the periodic table along with Mn and Tc. However, the chemistries of Tc and Re are much more similar to each other than that of Mn. This is because of the filling of the seven 4f orbitals (comprising the fourteen lanthanide elements) between the five 4d (comprising the ten transition metals of the second row) orbitals and the five 5d (comprising the ten transition metals of the third row) orbitals. These fourteen 4f electrons do not effectively shield their associated fourteen positively charged protons, and thus the 5d electrons experience a relatively large effective nuclear charge and are drawn closer to the nucleus than would be normally expected. Due to this effect of “lanthanide contraction”, the atomic radius of technetium is only slightly smaller than that of rhenium. The most stable form of these metals is the pertechnetate ion, $[\text{TcO}_4]^-$, and the perrhenate ion, $[\text{ReO}_4]^-$, which resemble the permanganate ion, $[\text{MnO}_4]^-$ but are much weaker oxidants.

1.1.1 Chemistry of Rhenium

The high rhenium-element bond strengths and variable oxidation states, ranging from +7 to -3 produces unusual and fascinating structural motifs. The chemistry of higher oxidation states of rhenium is dominated by the presence of multiply bonded ligands such as O^{2-} , N^{3-} or NR^{2-} . Salts of the perrhenate anion are the most important group of starting materials for the synthesis of other rhenium compounds and they are also of importance in catalysis and other commercial processes.

Rhenium(VI) complexes, which contain the metal in a d^1 configuration are comparatively rare. They are often formed as transient states during the reduction of Re(VII)

or the oxidation of Re(V) compounds and readily undergo further redox processes. The chemistry of Re(V) is vast due to the high stability of rhenium(V) oxo, nitride and imido cores with a great variety of ligand systems. Moreover, these complexes are frequently used as nonradioactive model compounds for the development of technetium radiopharmaceutical.

Complexes containing rhenium in the oxidation state +IV are comparatively rare. The stabilization of rhenium (IV) centres requires a well balanced donor-acceptor behavior of the ligands. So, none of the classical π -donor ligands such as oxide or nitride or π -acceptors such as carbonyls or nitrosyls are characteristic for this oxidation state. The d^4 configuration of rhenium(III) centre can readily be stabilized by ligands with pronounced donor and π -acceptor properties. Most of the rhenium (III) complexes are stable against hydrolysis rendering them suitable for nuclear medical applications. Rhenium has little cationic chemistry and forms only a few compounds in the oxidation state II whereas the most stable and characteristic oxidation state of its congener, manganese is II.

The d^6 configuration of rhenium(I) requires ligand systems which are able to accept electron density from the electron-rich metal centre. Thus, frequently phosphines, nitrogen heterocycles, carbonyls or isocyanides are encountered. Most of the octahedral products possess a high thermodynamic stability and kinetic inertness as is expected for an 18-electron d^6 system.

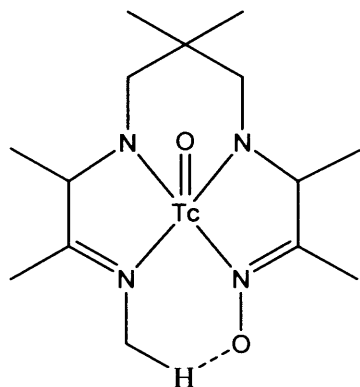
The element also has a tendency to form a Re-Re multiple metal bonds. For example, several complexes containing trinuclear rhenium clusters have been extensively studied. The $[\text{Re}_2\text{Cl}_8]^{2-}$ ion was the first stable chemical entity shown to possess a quadruple bond.⁵

1.1.2 Rhenium use in therapeutic complexes

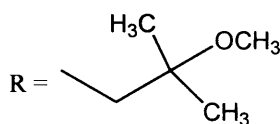
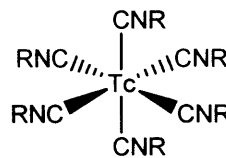
The research of rhenium in the field of organometallic chemistry has developed significantly since the mid 1980s. Before that period rhenium found only a limited use in catalysis.

In the 1980s a series of neutral amine-oxime complexes were developed by the University of Missouri and later further development by Amersham International and lead to the commercial CeretecTM ⁶ (Figure 1.1), a ⁹⁹Tc radiopharmaceutical, used in brain imaging. The other ⁹⁹Tc complexes, CardioliteTM ($[\text{}^{99\text{m}}\text{Tc}(\text{MIBI})_6]^+$, where MIBI is 2-methoxy-2-methylpropyl-isocyanide)⁷ and MyoviewTM ($[\text{}^{99\text{m}}\text{TcO}_2(\text{P53})_2]^+$, dioxobisdiphosphine-

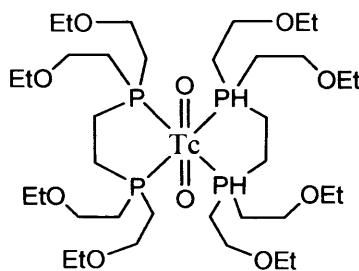
complex)⁸, are also used as cardiac imaging agent. ^{99m}Tc-HIDA (HIDA is 2,6-dimethylphenylcarbamoylmethyl)⁹ gave good performance as a liver imaging agent.



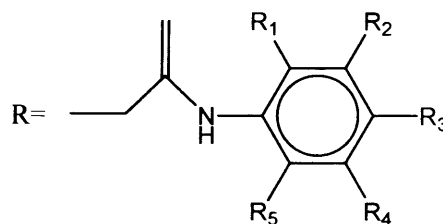
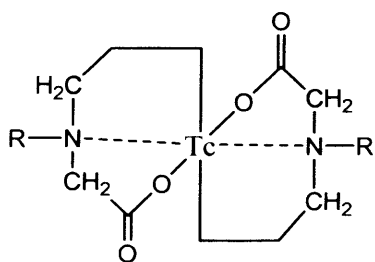
Ceretec™



Cardiolite™



Myoview™



Lidoferin $R_1 = \text{CH}_3$

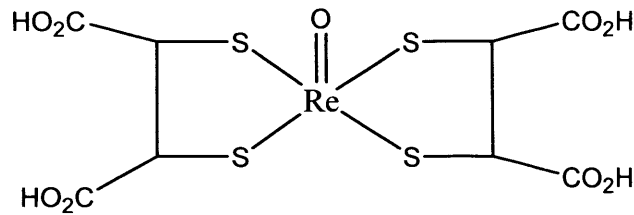
Disoferin $R_1 = \text{isopropyl}$

Mebrofenin $R_1=R_3=\text{CH}_3$, $R_2 = \text{Br}$

⁹⁹Tc-HIDA analogue

Figure 1.1 ^{99m}Tc imaging agents

Tc(V) complex of dimercaptosuccinic acid (DMSA) is widely used in thyroid carcinoma imaging. The Re(V) complex of DMSA (Figure 1.2) also shows selective uptake of tumour tissue analogous to Tc species and offers a possibility of therapeutic treatment of the disease.¹⁰



Re-DMSA complex

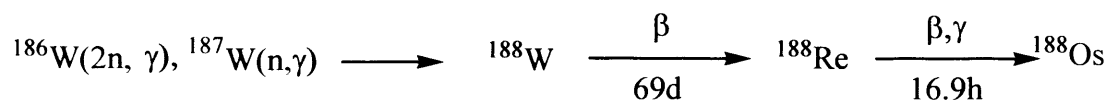
Figure 1.2 ^{99m}Re imaging agent

Rhenium has potential to be used as a therapeutic agent in the form of ¹⁸⁶Re and ¹⁸⁸Re radioisotopes. Their properties are indicated in table 1.

Table 1 Properties of ¹⁸⁶Re and ¹⁸⁸Re.

	Half-life (h)	Max β energy (MeV)	Range in Tissue (mm)	γ-energy (Kev)
¹⁸⁶ Re	90	1.07 (71%)	5	137 (10%)
¹⁸⁸ Re	17	2.1 (100%)	11	155 (15%)

¹⁸⁶Re is generated by neutron radiation of ¹⁸⁵Re whereas ¹⁸⁸Re is available by radioactive decay of ¹⁸⁸W (Scheme 1.1).



(n, γ) = single neutron capture followed by γ-decay

Scheme 1.1 Production root of ¹⁸⁸Re and further decay .

Technetium does not occur in any stable isotope form and the handling of this metal requires radiation safety procedures. ^{99}Tc emits low-energy (0.292 MeV and specific activity of $17 \mu\text{Ci/mg}$) β -particle and decays with a half-life of 2.12×10^5 years to the stable ^{99}Ru .

As rhenium and technetium show similar chemistry and rhenium isotopes can be handled more safely than that of technetium, rhenium chemistry may be explored in a greater extent than technetium in research and development for clinical and therapeutic investigations.

1.2 Metal carbonyls

We are interested in chemistry of low-valent rhenium complexes, specifically d^6 Re(I) carbonyl complexes. A characteristic of the *d*-group transition metal atoms is their ability to form complexes with a variety of neutral molecules such as carbon monoxide and ligands such as 2,2'-bipyridine and 1,10-phenanthroline. In many of these complexes, the metal atoms are in a low-positive, zero or negative formal oxidation states. It is a characteristic of these ligands that they can stabilize low oxidation states. This property is associated with the fact that these ligands have vacant π -orbitals in addition to lone pairs. The vacant orbitals accept electron density from filled metal orbitals to form a type of π bonding that supplements the σ bonding arising from lone pair donation. It is the ability of these ligands to accept electron density into their low lying empty π orbitals that makes them Lewis-acids.¹¹

Carbon monoxide is a common ligand in transition metal chemistry, in part due to the synergistic nature of its bonding to transition metals. The bonding of CO to a metal can be described as consisting of two components. The first component is a two electron donation of the lone pair on the carbon into a vacant metal $d\sigma$ -orbital. This electron donation makes the metal more electron rich, and in order to compensate for this increased electron density, a filled metal $d\pi$ -orbital may interact with the empty π^* orbital on the carbonyl ligand to relieve itself of the added electron density. This second component is called π -backbonding or π -back-donation, illustrated in Figure 1.3.

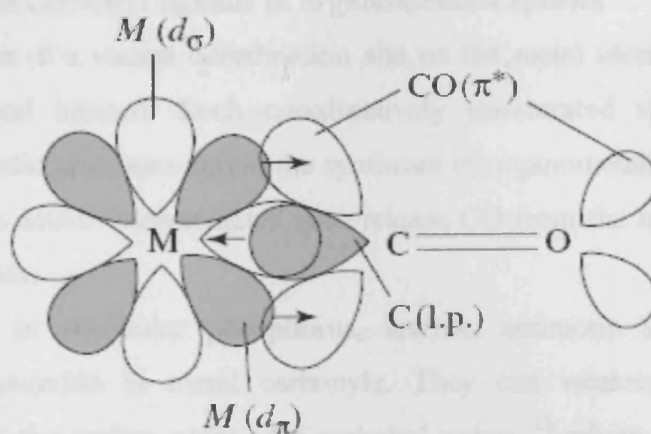
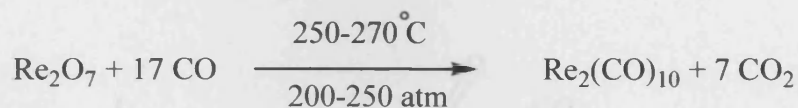


Figure 1.3 shows how the CO HOMO, the carbon lone pair, donates electron to the metal LUMO, the empty $M(d_{\sigma})$ orbital, and metal HOMO, the filled $M(d_{\pi})$ orbital, back donates to the CO LUMO

The two components of this bonding are synergistic. The more sigma donation of electrons by the carbonyl occurs (or other sigma-donors on the metal center), the stronger the π -back bonding interaction.

1.2.1 Preparation of metal carbonyls

Metal carbonyls like $\text{Ni}(\text{CO})_4$ and $\text{Fe}(\text{CO})_5$ are normally formed by the treatment of the metals with CO. However, most metal carbonyls are prepared less directly. The other homoleptic carbonyls are usually made by reductive carbonylation of metal salts or metal oxides under a high pressure of CO in autoclave (Scheme 1.2).



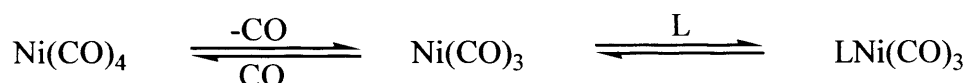
Scheme 1.2 Synthesis of metal carbonyls

Once prepared, these homoleptic carbonyls undergo extensive substitution and redox reactions.

1.2.2 Substitution of carbonyl ligands in organometallic species

The generation of a vacant coordination site on the metal atom in a metal carbonyl complex is of general interest. Such coordinatively unsaturated species are important intermediates in catalytic processes and in the syntheses of organometallic compounds.¹² One way to generate these active intermediates is to release CO from the metal atom in a stable metal carbonyl complex.

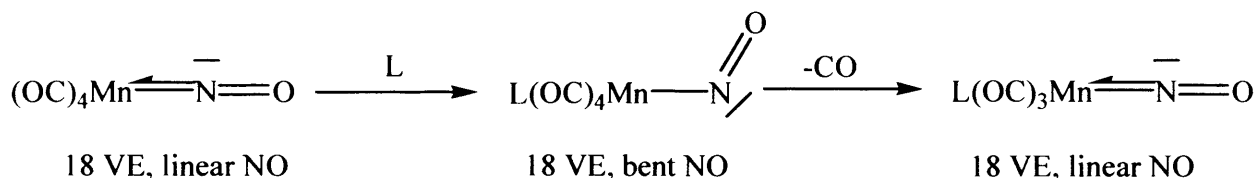
Lewis bases, in particular phosphorus, arsenic, antimony and nitrogen donors, substitute carbon monoxide in metal carbonyls. They can weaken the M-C bond by nucleophilic attack at the carbon atom of a carbonyl group,¹³ which decreases the π -back bonding from metal to CO. The reactions mainly follow S_N1 or D mechanism, in which the initial rate determining dissociation of CO gives a coordinatively unsaturated intermediate that is followed by uptake of the ligand L (Scheme 1.3).



Scheme 1.3 Substitution of CO by L in Ni(CO)₄

Ni(CO)_4 reacts rapidly at room temperature to give a series of substituted derivatives $\text{Ni(CO)}_3\text{L}$, $\text{Ni(CO)}_2\text{L}_2$, Ni(CO)L_3 and NiL_4 . The extent of the reaction of excess L depends largely on the steric bulk of L.

In the case of allyl or nitrosyl type ligands, which can change from a 3- to 1-electron donor mode, associative substitution can take place with coordinatively unsaturated 4 or 5-coordinate complexes avoiding an electron counting of more than 18 (Scheme 1.4).



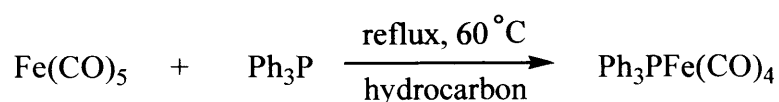
Scheme 1.4 Associative substitution by electron transfer catalysis.

1.2.2.1 General carbonyl activation

As CO is a small and strongly coordinated ligand, the substitution of CO is generally achieved either by thermal or photochemical activation or by the chemical reaction with trimethylamine oxide, iodosobenzene etc.

1.2.2.2 Thermal activation

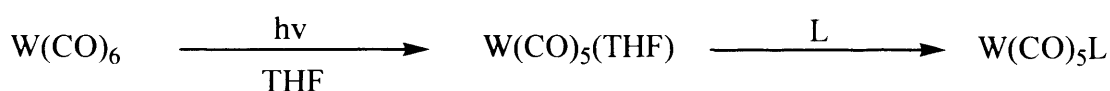
This method involves providing enough energy by thermal excitation of the molecules from ground states to transition states, which then is followed by cleavage of the M-C bond to generate coordinatively unsaturated intermediates. For example, the substitution of CO from metal carbonyls by a ligand occurs in refluxing hydrocarbons is shown below (Scheme 1.5).



Scheme 1.5 Thermal substitution of CO in Fe(CO)₅

1.2.2.3 Photochemical activation

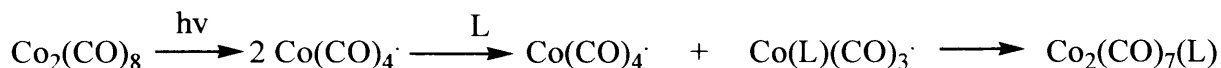
Photochemical substitution usually involves milder reaction conditions and allows the synthesis of less highly substituted or more labile products. Complexes of labile THF, nitrile or alkene ligands are convenient synthons in organometallic chemistry. For example, irradiation of W(CO)₆ by UV light in THF produce W(CO)₅(THF) (Scheme 1.6).



Scheme 1.6 Photochemical substitution of CO in W(CO)₆

W(CO)₅(THF) is a useful synthetic reaction intermediate because it reacts with a variety of ligands (L) to give W(CO)₅L rather than more highly substituted species *fac*-W(CO)₃L₃, which was obtained from W(CO)₅(THF) and L on heating. The mechanism for such reactions is the photoinduced promotion of dπ electron into a dσ level, which is M–L σ-antibonding in character, and so dissociative substitution is more rapid in the excited state.

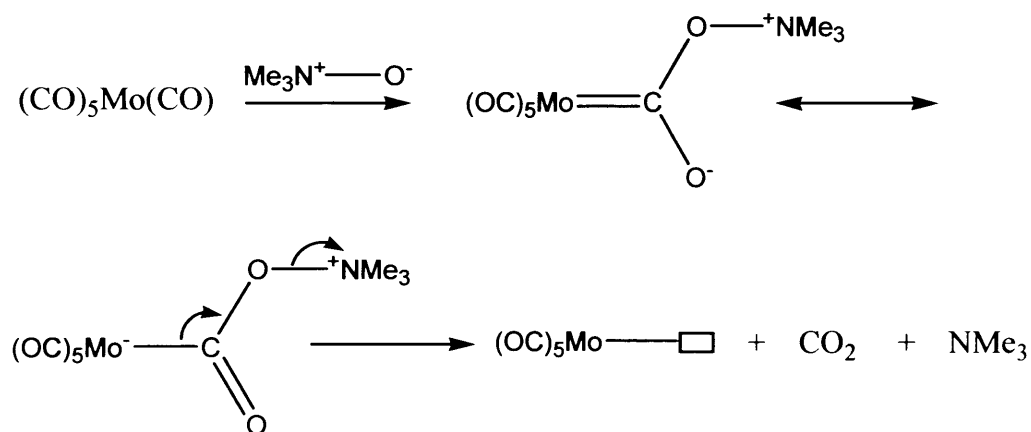
Substitution reactions of binuclear complexes with metal-metal bonds involve electronically unsaturated radical species through M-M bond homolysis (Scheme 1.7).



Scheme 1.7 Photochemical substitution of CO in bimetallic $\text{Co}_2(\text{CO})_8$

1.2.2.4 Chemical activation

Amine N-oxides can act as O-atom transfer reagents and facilitate the reaction for the substitution of a CO group from many metal carbonyls.¹⁴ The reaction is believed to involve nucleophilic attack of an oxygen atom at the carbon atom of a carbonyl group, which annihilates CO as a ligand due to transforming it into the good leaving group CO_2 (Scheme 1.8). This results in the formation of an active coordination site on the metal, rendering it useful in syntheses of organometallic compounds and in applications as a homogeneous catalyst.

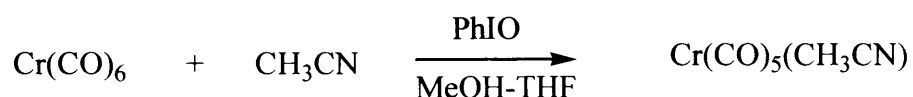


Scheme 1.8 Substitution of CO by Me_3NO

This reaction is particularly important because it is one of the rare ways in which tightly bound CO can be removed to generate an open site at the metal. In this way a ligand L, which would normally not be sufficiently strongly binding to replace the CO, can now do so.

Its application has been especially successful in the syntheses of substituted metal carbonyl clusters.¹⁵

Another important O-atom transfer reagent is iodosobenzene (PhIO). Substitution of CO from Cr(CO)₆ with acetonitrile proceeds in presence of PhIO (Scheme 1.9).¹⁶ The mechanism of the reaction is believed to be similar to that for Me₃NO.

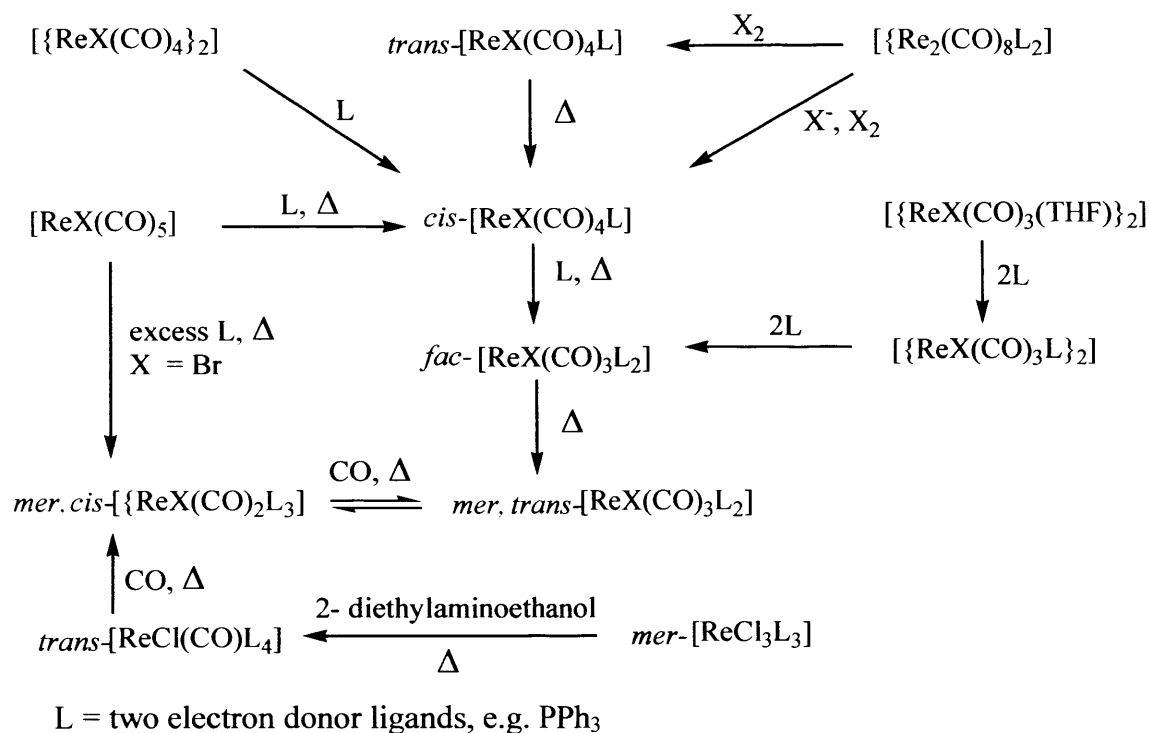


Scheme 1.9 Substitution of CO by PhIO

1.2.3 Substitution reaction of rhenium carbonyls and their derivatives

The rhenium species [Re₂(CO)₁₀] is the most important starting material for its low-valent chemistry. In general, the dimeric complex is oxidized to [MX(CO)₅], which is then used as a synthon for subsequent substitution reactions. Rhenium pentacarbonyl halides [Re(CO)₅X] (X= Cl, Br and I) were first prepared by Schulten¹⁷ by the action of carbon monoxide on the corresponding hexahalogenorhenates. Compounds of the [Re(CO)₃]⁺ moiety have been traditionally prepared from Re(CO)₅Cl or Re₂(CO)₁₀.

The majority of complexes arises by displacement of carbon monoxides or weakly bound solvent molecules (e.g. THF). Like other metal carbonyls, substitution is achieved either thermally or photochemically or reaction with trimethylamine oxides. Schematic representation of substitution of CO in mononuclear and dinuclear rhenium carbonyl complexes is as follows (Scheme 1.10):



Scheme 1.10 Substitution of CO in rhenium carbonyl complexes

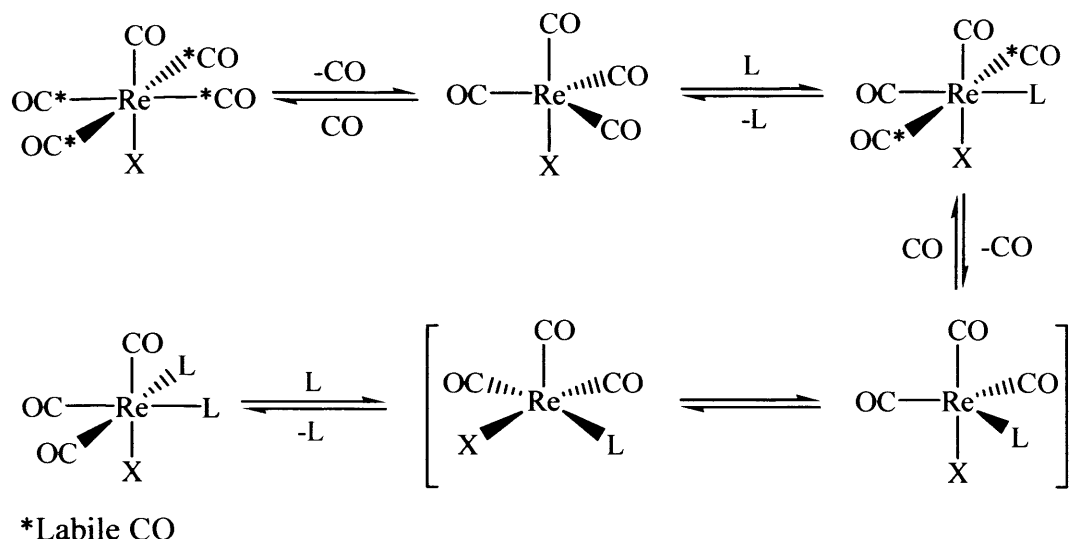
1.2.3.1 Mono-substituted rhenium carbonyl complexes:

Monosubstitution of $\text{ReX}(\text{CO})_5$ is achieved by treatment of one equivalent of donor ligand in a refluxing solvent. Cleavage of the bridged dihalides $\{[\text{ReX}(\text{CO})_4]_2\}$ with donor ligands also produce $\text{cis-}[\text{ReX}(\text{CO})_4\text{L}]$ species. An order of cis labilizing ability $\text{L} = \text{py} > \text{PPh}_3 > \text{P}(\text{OPh}_3) = \text{CO}$ has been determined for $[\text{ReX}(\text{CO})_4\text{L}]$ ¹⁸. However, under certain circumstances the trans isomer may be isolated. On heating this isomerizes to the more stable cis form.¹⁹

Actually, most substitution products have been derived from monosubstituted complex $[\text{M}(\text{CO})_5\text{L}]^+$ in which L is an easily displaced ligand, such as acetonitrile. These easily substituted complexes can be obtained by the oxidation of $[\text{M}_2(\text{CO})_{10}]$ in acetonitrile either chemically²⁰ (e.g. NOPF_6) or electrochemically or by halide extraction from $[\text{ReX}(\text{CO})_5]$ with silver salts in the appropriate solvent. $[\text{Re}(\text{CO})_5(\text{NCMe})]\text{PF}_6$ ²¹ and $[\text{Re}(\text{CO})_5(\text{SO}_2)]\text{AsF}_6$ ²² have been synthesized in this manner.

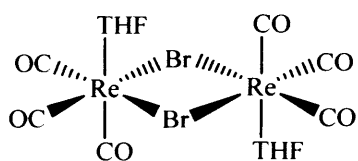
1.2.3.2 Disubstituted rhenium carbonyl complexes:

The disubstituted complexes $[\text{Re}_2(\text{CO})_8\text{L}_2]$ are only obtained as the diaxial ($\text{L} = \text{PPh}_3, \text{P}(\text{OPh})_3$)²³ or diequatorial ($\text{L} = \text{PMe}_2\text{Ph}, \text{AsMe}_2\text{Ph}, \text{PMePh}_2, \text{py}$)^{19, 24} isomers. The complexes *fac*- $[\text{ReX}(\text{CO})_3\text{L}_2]$ are generally synthesized by refluxing $[\text{ReX}(\text{CO})_5]$ with two equivalents of L by following scheme 1.11.



Scheme 1.11 Synthesis of disubstituted rhenium carbonyl complexes

Treatment of rhenium halocarbonyls with THF generates a dinuclear complex with bridging halides (Figure 1.4).²⁵



Donor ligands such as N-heterocycles, amines and phosphines readily substitute THF to form mononuclear *fac*- $[\text{ReX}(\text{CO})_3\text{L}_2]$ complexes. The disubstituted complexes *fac*- $[\text{ReX}(\text{CO})_3\text{L}_2]$

Figure 1.4

undergo isomerization to the *mer*, *trans*- $[\text{ReX}(\text{CO})_3\text{L}_2]$ complexes on heating. This process is hindered by the presence of excess ligand, but aided by sodium borohydride or by oxidation with NOPF_6 followed by reduction. The isomerization appears to be related to a release of steric strain.²⁶ A proposed mechanism involving facial rotation is shown below (Figure 1.5).²⁶

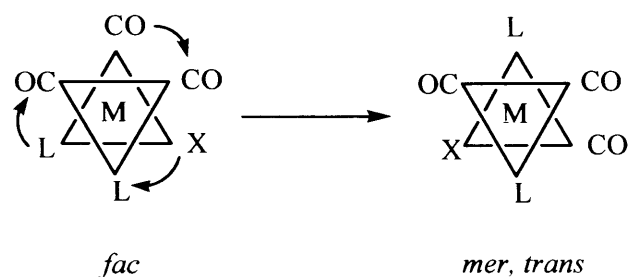


Figure 1.5 Isomerization of $[\text{ReX}(\text{CO})_3\text{L}_2]$ complexes

1.2.3.3 Trisubstituted rhenium carbonyl complexes:

Trisubstitution can occur in dimeric complexes and several isomers have been described (Figure 1.6).¹⁹ Further substitution leads to the formation of mononuclear species, possibly for steric factors.

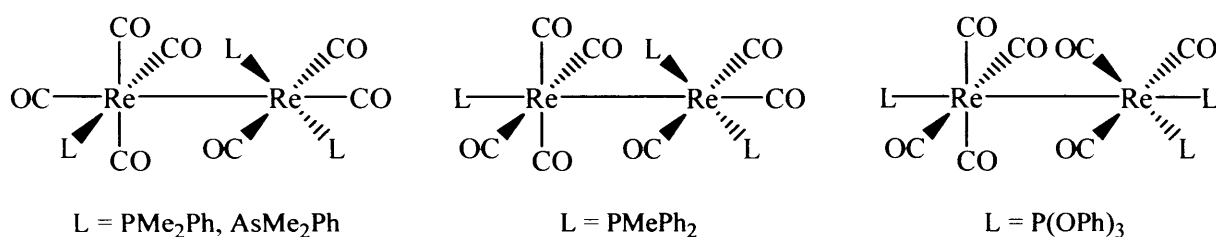
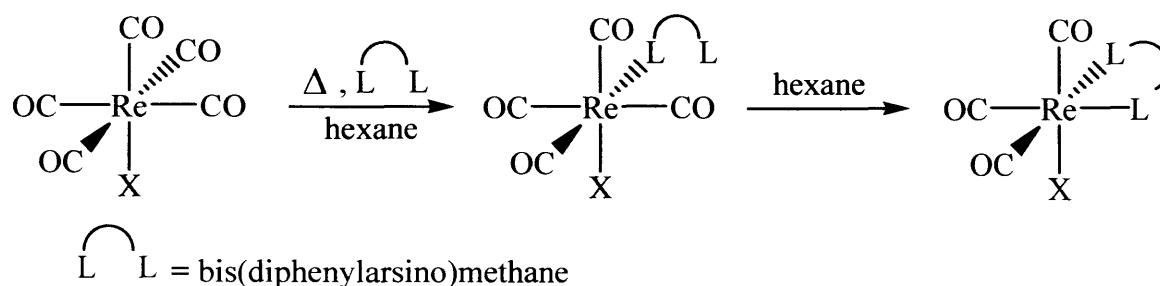


Figure 1.6 Trisubstituted rhenium dinuclear complexes

Refluxing $[\text{ReBr}(\text{CO})_5]$ with excess donor ligand produces *mer, cis*- $[\text{ReBr}(\text{CO})_2\text{L}_3]$ complexes, but further substitution of the parent halocarbonyl has not been observed. Trisubstituted cations $[\text{Re}(\text{CO})_3\text{L}_3]^+$ ($\text{L} = \text{MeCN}, \text{Me}_2\text{CO}, \text{PrNH}_2$)²⁷ have been prepared through arene substitution of $[\text{Re}(\text{CO})_3(\text{arene})]^+$. The substitution proceeds through an associative mechanism rather than dissociative mechanism. $[\text{ReX}_3(\text{CO})_3]^+$ is the starting points of choice for many syntheses of rhenium(I) carbonyl compounds today.

1.2.3.4 Substitution by Chelating ligands:

Chelating donor ligands also form dinuclear and mononuclear complexes.²⁸ The reaction scheme of bis(diphenylarsino)methane with $[\text{ReX}(\text{CO})_5]$ is as follows:



Scheme 1.12 Substitution of CO by chelating ligands

Ligands containing sp^2 -hybridized nitrogen atoms, especially when the N atom is part of an aromatic system, have an extensive coordination chemistry, in particular when they are multidentate ligands. One of the first substitution reactions of $[\text{ReCl}(\text{CO})_5]$ investigated in 1941 was the one with the diimine ligand 1,10-phenanthroline.²⁹ Substitution of two carbonyl ligands occurred and the complex *fac*- $[\text{ReCl}(\text{phen})(\text{CO})_3]$ was isolated. The compound possesses remarkable photochemical properties, especially a long-living, emissive excited state, which can be studied by spectroscopy even at room temperature.³⁰ This is very peculiar for a metal carbonyl complex, which in most cases are known to undergo rapid excited state decay *via* carbonyl loss. Many *fac*- $[\text{Re}(\text{CO})_3\text{L}_2\text{X}]^+$ [L_2 is a chelating ligand] complexes were studied afterwards to investigate their excited state properties. The chelating ligands normally used were as follows (Figure 1.7).

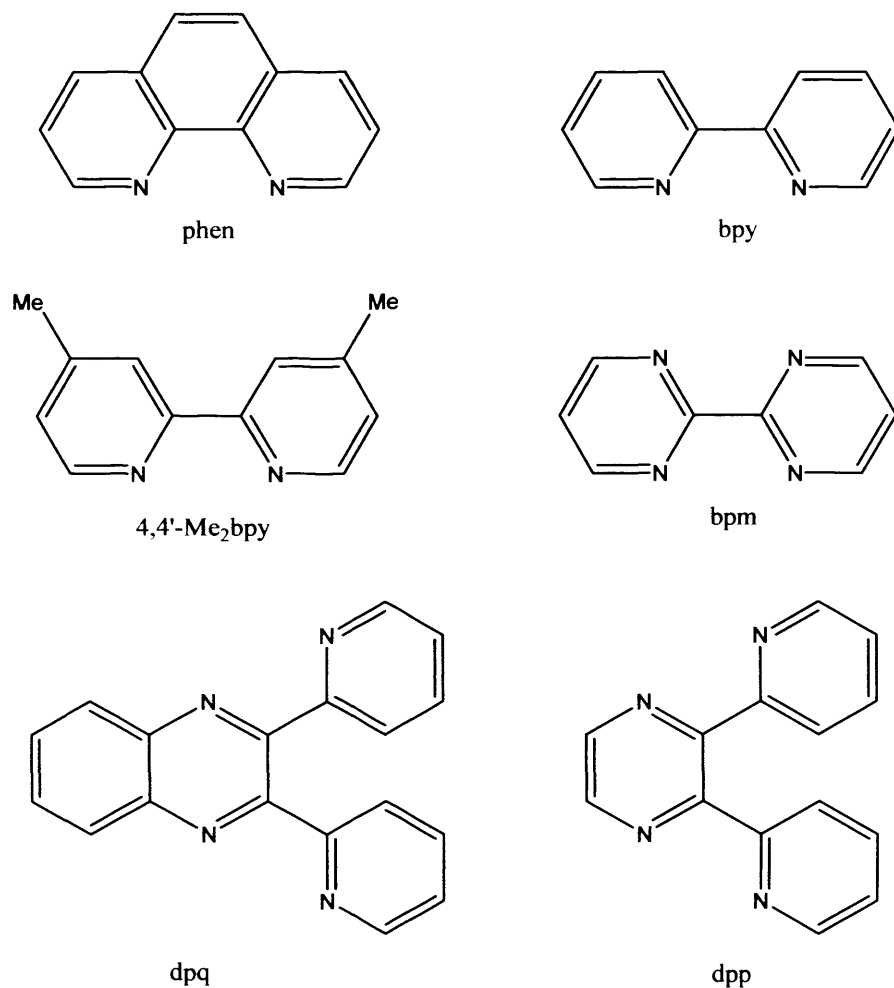
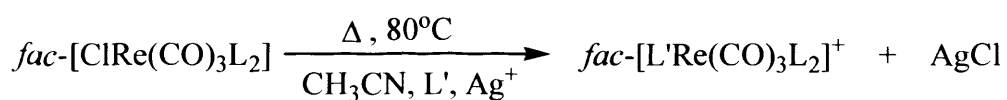


Figure 1.7 Structural representation of selected α -diimine ligands.

The halide, X, in fac -[Re(CO)₃L₂X], can be replaced by L' [L' is a neutral donor such as MeCN, PhCN, py, piperidine, THF etc.) by reaction with a silver salt. For example, fac -[(CH₃CN)Re(CO)₃L₂]⁺ is formed by the reaction of an equimolar amount of fac -[Re(CO)₃L₂X] and silver perchlorate in refluxing acetonitrile.³¹



Scheme 1.12 Substitution of X by L' in fac -[Re(CO)₃L₂X]⁺ complexes

They are extremely air/moisture-stable, which lends a great deal of flexibility to the study of both their ground and excited-state chemistry. They luminesce at room temperature both in solid state and solution. Their luminescent properties arise from the metal-to-ligand charge transfer (MLCT) between the $d\pi$ (Re) orbitals and the π^* orbitals on the corresponding diimine. A number of useful luminescent Re(I) complexes have been synthesized in a straightforward manner from $[\text{Re}(\text{CO})_3(\text{bpy})(\text{CH}_3\text{CN})]^+$, where the acetonitrile group can readily be replaced by a variety of pyridines and their photophysical, photochemical and redox properties have been studied. Alternatively rhenium compounds containing weakly coordination species, $[\text{Re}(\text{CO})_3(\text{bpy})(\text{L})]^+$ (L= perchlorate or hexafluorophosphate) undergo rapid substitution with chloride, bromide ions and acetone to give the respective rhenium compound.³² Thus they occupy an important position in the field of rhenium chemistry.

1.3 Metals in biological applications

Many metallic elements play a crucial role in living systems. A characteristic of metals is that they easily lose electrons from their metallic or familiar elemental state to form positively charged ions which tend to be soluble in biological fluids. This cationic form plays a role in biology. While metal ions are electron deficient, most biological molecules are electron rich, paving the way for interaction between these metals and biological systems. Metals also tend to bind to the smaller molecules essential for life. For example, haemoglobin, an iron containing protein carries oxygen throughout the body through its binding to iron.

Molecular probes for biomolecular recognition are of great importance in the field of chemistry, biology, and medical sciences as well as biotechnology. These probes have been used in studies of biological functions and in ultrasensitive detection of biological species responsible for many diseases. Many methods such as atomic absorption, ion selective electrodes etc. are available but fluorescent sensors offer the distinct advantage of high sensitivity.

1.4 Luminescence

The fluorescence technique provides an important alternative to radioimmunoassay, which is the most widely used technique in the detection and quantification of important

biological molecules, even though it presents drawback related to radioactivity. Fluorescent materials can be used as a molecular tag to follow reactions. The use of this property in bioanalytical assays requires development of specific chelate technologies for labelling i.e., binding of the ion to bioaffinity reagents, carrying it through the assay procedure, creating the optimal environment for emission and so forth. Moreover, these materials can also be used as a reporter group for molecular sensors for biological target groups as well as tracing environmental pollutants. Fluorescent complexes indicate metal ion concentration or the polarity of the solvent or environment in which they are present or they will be indicative of the local potential for reduction or oxidation.

Both organic and inorganic fluorescence contrast agents are now available for chemical conjugation to targeting molecules.

1.4.1 Organic luminescent complexes

The labelling of biological substrates with fluorescent organic compounds (Figure 1.8) is a routine procedure now a days. But conventional organic fluorophores suffer from significant limitations.

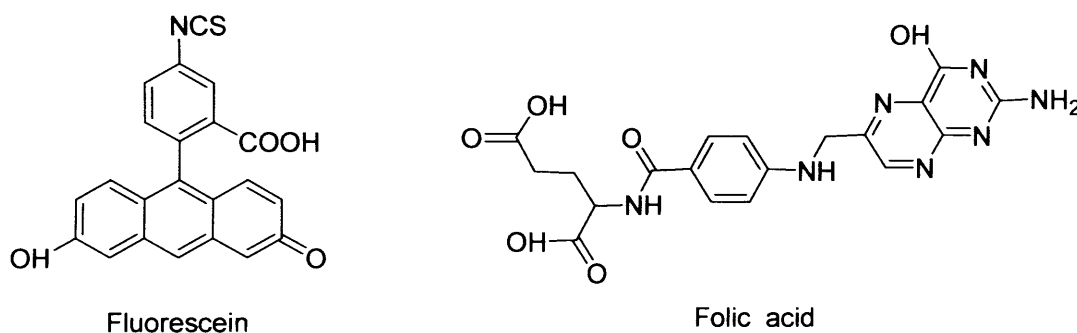


Figure 1.8 Fluorescent organic dyes

Firstly, it is difficult to control excitation and emission wavelengths that are dependent on chemical structure, and tuning a conventional fluorophore to precise wavelengths requires sophisticated chemistry. Again, the short fluorescence lifetimes, self-quenching effects, photobleaching and pH-dependence of these compounds are still significant disadvantages.

1.4.2 Lanthanide luminescent complexes

The uses of lanthanide complexes as diagnostic luminescence imaging agents such as europium and terbium in the development of time-resolved luminescent assays have been documented. These complexes generally have long-lived and good emissive characteristics. Their emission spectra show narrow bands. But they are often difficult to synthesize and their emission frequency are insensitive to surroundings, that is, the wavelengths do not shift on changing the conditions such as temperature or the coordination site due to the shielding of f-electrons. Lanthanide ions have very weak absorption bands with molar absorption coefficients usually $< 1 \text{ dm}^{-3} \text{ mol}^{-1} \text{ cm}^{-1}$. This is due to the fact that the transitions occurring involve the same f^n configuration which are parity forbidden. The second problem relates to deactivation of metal emissive states by vibrational energy transfer. Unfortunately, the lanthanides are strong coordinators of bases such as water molecules.

1.4.3 Luminescent transition metal complexes & switches

Transition metal complexes by virtue of their variable oxidation state i.e., the d-electrons, unique photophysical and photochemical properties, and variable coordination geometries, have been covalently linked to different biomolecules in electron transfer studies and other analytical applications. Numerous luminescent transition-metal complexes, Re (I)-, Ru(II)- and Os(II)-based polypyridyl chromophores have been studied. They usually exhibit fairly strong luminescence in the visible region and the photophysical properties are relatively easily tuned by simply modifying the coordinated ligands. These compounds also have the advantage of being relatively stable with respect to photodecomposition. The emission from the complexes usually originates from triplet metal-to-ligand charge transfer ($^3\text{MLCT}$) excited states and has the added feature of being typically sensitive to its nature and environment, being influenced by solvent, temperature, and pH.³³ For example, the widely studied complex, $[(\text{bpy})_2\text{Ru}^{2+}(\text{dppz})]^{2+}$ which is not photoluminescent in aqueous solvent, shows typical emission from the $^3\text{MLCT}$ state after binding with DNA.³⁴

1.5 Rhenium complexes

Rhenium (I) d^6 low spin complexes have attracted our attention. The $[\text{Re}(\text{CO})_3(\text{diimine})\text{X}]$ complexes absorb visible light up to wavelengths of 500nm. When

excited with light of about 400nm wavelength, a rather strong luminescence is observed with an emission maximum between 500 and 600nm. They show a great potential to be developed in bioanalytical applications in view of their photophysical and photochemical properties.

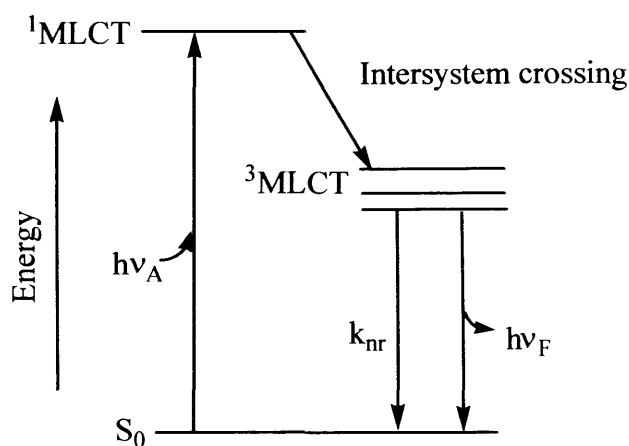


Figure 1.9 Jablonski diagram for a metal to ligand complex.

The intense and long-lived photoluminescence properties of rhenium polypyridine complexes can be exploited in the development of luminescent labelling reagents for biomolecules as they possess the following fundamental properties.

- The use of various diimine ligands for the rhenium complexes can alter the MLCT (Figure 1.9) emission energy and give rise to a series of multicolour labelling reagents.
- The large Stokes' shift could minimise self-quenching effects which are commonly observed in multiple labelling of biomolecules with fluorescent organic dyes.
- The long emission lifetimes of rhenium polypyridine complexes could be applied in time-resolved detection techniques that can offer high sensitivity.

In this regard, polypyridyl Re(I) tricarbonyl complexes have been widely used in a variety of techniques, including fundamental excited-state properties such as photo induced electron and energy transfer and potential applications such as luminescent sensors,³⁵ probes for polymerisation,³⁶ photocleavage of DNA,³⁷ non-linear optical materials³⁸ and optical switches.³⁹ Recently, studies on the utilization of luminescent rhenium polypyridine complexes as a DNA probe using extensively planar diimine ligands have been reported.

However, to date, a systematic design of luminescent polypyridine complexes as a label for biological substrates, such as DNA and proteins, has not been realised.

1.5.1 Photochemical properties of rhenium complexes

The photochemical and photophysical properties of Re(I) carbonyl–bpy complexes, $fac-[ReE(diimine)(CO)_3]^{0/+}$, have attracted much research interest ever since their intriguing excited state properties were first recognised in the mid-1970s.³⁰ The excited state was assigned to be a metal to ligand charge transfer (MLCT) excited state, with the photoelectron ejected from a metal centred π -d orbital into a vacant ligand centred π^* orbital. The energy scheme for $[ReE(diimine)(CO)_3]^{0/+}$ complexes is presented in Figure 1.10. The photoexcitation process here is a metal-centred oxidation and a ligand-centred reduction. The lifetimes of the excited states are strongly dependent on both diimine and the ligand E.

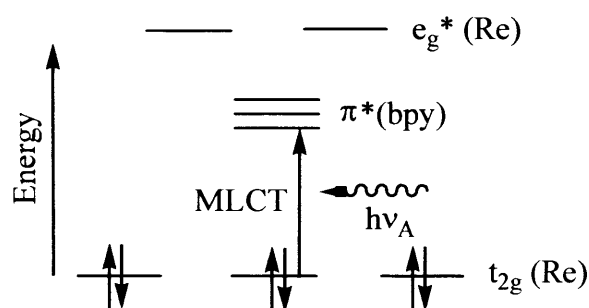


Figure 1.10 Metal to ligand charge transfer (MLCT) in $[ReE(bpy)(CO)_3]$.

A great variety of these compounds may be synthesized since the nature of the axial ligand E can be varied broadly, ranging from anionic ligands, halides or CN^- , to neutral phosphines, pyridine derivatives, isonitriles, etc. Alkyls or metal containing fragments like Ph_3Sn or $M(CO)_5$ ($M=Re, Mn$) were also employed as axial ligands.

It was shown that the increasing π -donor strength of an axial ligand, such as a halide changes the character of the lowest excited state from MLCT to LLCT. On the other hand, the presence of a covalently bound axial ligand in the coordination sphere introduces a $\sigma\pi^*$ lowest excited state that involves an excitation of an electron from the rhenium–ligand σ -bonding orbital to the π^* orbital of the diimine. The excited state properties of the Re-carbonyl–bpy

complexes can be controlled by a sensible choice of the axial and bipy ligands and by the medium. These relations can be employed to design new functional molecular photonic materials, e.g. sensitizers, luminophores, photocatalysts, radical photoinitiators, luminescent probes or sensors.

Their photobehavior reflects the structural dependence of the nature of their low-lying excited states. The presence of an electron-accepting α -diimine ligand in the coordination sphere allows for charge transfer (CT) electronic transitions directed to the diimine ligand, while the origin of the excited electron depends strongly on the nature of the axial ligand. So, the photobehavior of Re(I) carbonyl diimine complexes depends on four limiting types of excited states.

- M→diimine metal-to-ligand charge transfer states, MLCT.
- E→diimine ligand-to-ligand charge transfer states, LLCT.
- Transition from the M-E σ -bonding orbital to the diimine ligand, $\sigma\pi^*$.
- Intraligand (diimine) $\pi\pi^*$ states, IL.

1.5.2 Redox active sensors

Early work has demonstrated that the excited state of $[\text{Re}(\text{E})(\text{CO})_3(\text{diimine})]^{0/+}$ complexes are both strong reductants and oxidants.^{30,40-41} Excited states of $[\text{Re}(\text{E})(\text{CO})_3(\text{diimine})]^{0/+}$ complexes are often sufficiently long-lived (ns- μ s) to become engaged in fast bimolecular reactions similar to $[\text{Ru}(\text{bpy})_3]^{2+}$ and related polypyridyl complexes. However, in spite of their higher stability towards photochemical ligand loss, the $[\text{Re}(\text{E})(\text{CO})_3(\text{diimine})]^{0/+}$ complexes found less application in light energy conversion because of a limited stability of their reduced or oxidized form. Again, the high reactivity of the reduced species can be utilized in photocatalysis. For example, photoexcitation of $[\text{Re}(\text{Cl})(\text{CO})_3(\text{bpy})]$ in the presence of a reductive quencher like triethanolamine, produces $[\text{Re}(\text{Cl})(\text{CO})_3(\text{bpy})]^-$, which loses the Cl⁻ ligand. A further reaction with CO₂, present in the solution, results in the photocatalytic CO₂ reduction to CO via a rather complicated mechanism. The $[\text{Re}(\text{E})(\text{CO})_3(\text{diimine})]^{0/+}$ complexes also undergo intramolecular electron transfer reactions on excitation, provided that the axial ligand E or the diimine bears a redox active substituent.

An electron-accepting axial ligand introduces a (Re→E) MLCT state which may be populated either by a $\text{bpy}^- \rightarrow \text{E}$ intramolecular electron transfer from the (Re→bpy) MLCT state: $[\text{Re}^{\text{II}}(\text{E})(\text{CO})_3(\text{bpy}^-)] \rightarrow [\text{Re}^{\text{II}}(\text{E}^-)(\text{CO})_3(\text{bpy})]$, or by a direct, usually weak, (Re→E) MLCT transition (Figure 1.11).⁴² The intramolecular electron transfer actually amounts to a non-radiative transition between two different MLCT excited states. For E=*N*-methyl-4,4'-bipyridinium, MQ^+ , it is fully completed in 7 ns.⁴²

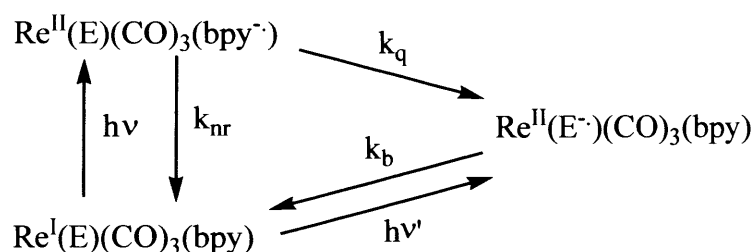


Figure 1.11 Mechanism of the population of the (Re→E) MLCT states in complex with reducible axial ligand MQ^+ .

An intramolecular $\text{E} \rightarrow \text{Re}^{\text{II}}$ electron transfer occurs from (Re→bpy) MLCT states of those complexes containing an axial ligand E that bears a reducing group, e.g., py-PTZ (Figure 1.12).⁴³⁻⁴⁶ Optical excitation of $[\text{Re}^{\text{I}}(\text{py-PTZ})(\text{CO})_3(\text{bpy})]^+$ first populates the $[\text{Re}^{\text{II}}(\text{py-PTZ})(\text{CO})_3(\text{bpy}^-)]^+$ MLCT excited state. Then, an electron is transferred from py-PTZ to Re^{II} with a rate constant of $4.8 \times 10^9 \text{ s}^{-1}$ or faster.⁴³ The species produced, $[\text{Re}^{\text{I}}(\text{py-PTZ}^+(\text{CO})_3(\text{bpy}^-))]^+$ may be viewed as a py-PTZ→diimine ligand to ligand charge transfer, LLCT, excited state. It was identified by time-resolved resonance Raman and UV-vis absorption spectroscopies that showed features characteristic of the reduced bpy^- and oxidised PTZ^+ moieties.^{43, 45-46} This LLCT state decays to the ground state by another intramolecular electron transfer, $\text{bpy}^- \rightarrow \text{py-PTZ}^+$.

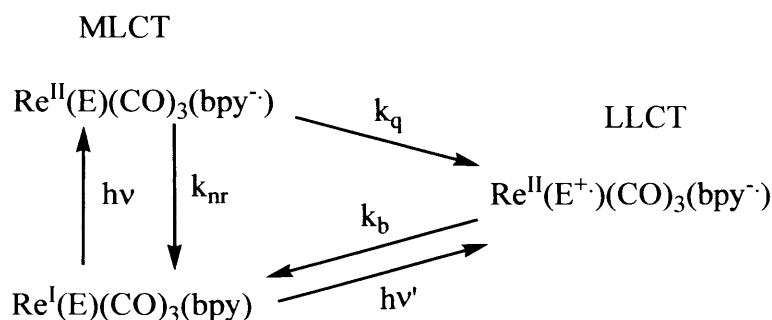


Figure 1.12 Mechanism of the population of the (E → bpy) LLCT states in complex with reducing axial ligand py-PTZ.

1.5.3 Supramolecular switches

In recent years attention has been paid to transition-metal-directed self-assembly to construct many different shaped supramolecules such as squares, boxes, helices and many interesting three-dimensional structures. Among these complexes, Re(I)-, Ru(II)- and Os(II)-based polypyridyl chromophores are commonly studied because they exhibit fairly strong luminescence in the visible region and the photophysical properties are easily tuned by modifying the coordinated ligands. They are relatively stable with respect to photodecomposition. These luminescent compounds with large cavity play an important role in host-guest chemistry.

There are only a few examples of Re(I)-containing rectangles and squares.⁴⁷⁻⁴⁸ The incorporation of potentially luminescent *fac*-tricarbonyl Re(I) chromophores into the macrocyclic structures offers rich photophysical properties and potential application as sensors and ultrafine sieves.⁴⁹⁻⁵⁰

1.6 Aims of the work

The research discussed herein describes the synthesis of novel rhenium complexes of $\text{Re}(\text{CO})_3^+$ core and the study of the influence of various ligand substituents on their luminescence properties. The intense and long-lived photoluminescence properties of low spin d^6 Re(I) polypyridine complexes can be exploited in the development of luminescent sensors. To achieve this goal, two possible sites of modification of the widely studied $[\text{Re}(\text{CO})_3(\text{bpy})\text{Cl}]$ complex were planned (Figure 1.13).

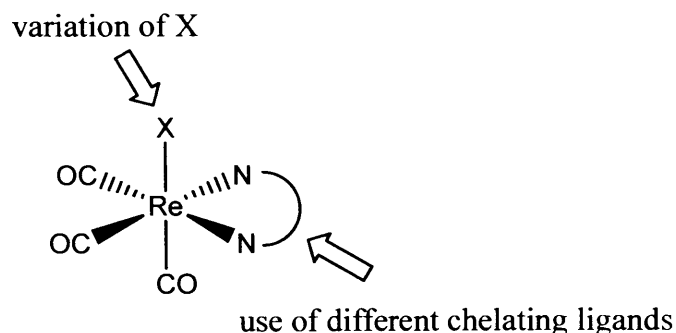


Figure 1.13 Ideas for the modified polypyridyl Re(I) complexes different from the normally used compound $[Re(CO)_3(bpy)Cl]$

- Instead of 2,2'-bpy, different chelating ligands such as 2,2';6',2''-terpyridine and 2,2';6',2'';6'',2'''-quaterpyridine can be introduced to the $Re(CO)_3^+$ core since they offer greater possibilities in functionalisation.
- Introduction of different axial ligands, such as py-3-NH₂, to the related $Re(CO)_3^+$ core.

The pendant pyridine ring of the rhenium terpyridine complexes could be utilized in binding cations and the methylation of the pendant unit could facilitate the synthesis of molecules capable of performing as reversible redox active luminescent switches.

The ligand, quaterpyridine, forms dimeric rhenium complexes that may have enhanced luminescent properties when compared with their mononuclear bipyridine analogues. Again, it was hoped to form mononuclear quaterpyridine rhenium complexes containing a pendant bipyridyl unit. The bipyridyl unit can then be coordinated to different metals or metal complexes to form dinuclear asymmetric complexes.

In addition, the axial ligand of $[Re(CO)_3(bpy)Cl]$ complex could be replaced with the potential ligands, such as, 4,4'-bpy, py-terpy, thiourea, MQ⁺ and MPyTP. It was expected that these complexes can be utilized (1) to detect and quantify biologically or environmentally important anionic (thiourea) and cationic (4,4'-bpy, py-terpy) species and (2) to develop redox active molecular switches (MQ⁺ and MPyTP). We were also interested in synthesising water-soluble analogues of the bpy complexes using disodium bathophenanthroline sulphonate and in assessing their photophysical properties.

Finally, attempts will be made to synthesis supramolecular rhenium complexes using the precursor complex, $[\text{Re}(\text{CO})_3(\text{CH}_3\text{CN})_3]^+$.

References

- 1 K. V. Kotegov, O. N. Pavlov and V. P. Shvedov, *Advan. Inorg. Chem. Radiochem.*, 1968, **11**, 1.
- 2 P. C. H. Mitchell, *Coord. Chem. Rev.*, 1966, **1**, 315.
- 3 R. V. Parish, *Advan. Inorg. Chem. Radiochem.*, 1966, **9**, 315.
- 4 W. P. Griffith, *Quart. Rev.; Chem. Soc.*, 1965, **19**, 254.
- 5 F. A. Cotton, B. A. Frenz, J. R. Ebner and R. A. Walton, *Inorg. Chem.*, 1976, **15**, 1630.
- 6 J. P. Leonard, D. P. Novotnik and R. D. Neirinckx, *J. Nucl. Med.*, 1986, **27**, 1819.
- 7 B. L. Holman, A. G. Jones, J. Lister-James, A. Davison, M. J. Abrams, J. M. Kirschenbaum, S. S. Tubeh and R. J. English, *J. Nucl. Med.*, 1984, **25**, 1350.
- 8 E. Barbarics, J. F. Kronauge, A. Davison and A. G. Jones, *Nucl. Med. Biol.*, 1998, **25**, 667.
- 9 A. R. Fritzberg, S. Kasina, D. Eshima and D. L. Johnson, *J. Nucl. Med.*, 1986, **27**, 111.
- 10 P. J. Blower, J. Singh, S. E. M. Clarke, M. M. Bisundan and M. J. Went, *J. Nucl. Med.*, 1990, **31**, 768.
- 11 F. A. Cotton, G. Wilkinson, P. L. Gaus, *Basic Inorganic Chemistry*, Second Edition, 1987.
- 12 G. W. Parshall and S. D. Ittell, *Homogeneous Catalysis*, Wiley, New York, 2nd edn., 1992.
- 13 J.D. Atwood and T.L. Brown, *J. Am. Chem. Soc.*, 1976, **98**, 3160; D. J. Darensbourg, N. Walker and M. Y. Darensbourg, *J. Am. Chem. Soc.*, 1980, **102**, 1212.
- 14 D. S. C. Black, G. B. Deacon and N. C. Thomas, *Inorg. Chim. Acta*, 1982, **65**, L75.
- 15 T. Y. Luh, *Coord. Chem. Rev.*, 1984, **60**, 255.; B. G. F. Johnson, J. Lewis and D. Pippard, *J. Organomet. Chem.*, 1978, **160**, 263.; G. F. Stunz and J. R. Shapley, *J. Organomet. Chem.*, 1981, **213**, 389.
- 16 J. K. Shen, Y. C. Gao, Q. Z. Shi and F. Basolo, *Organometallics*, 1988, **7**, 531.
- 17 Z. Schulten, *Anorg. Chem.*, 1939, **243**, 164.
- 18 J. D. Atwood and T. L. Brown, *J. Am. Chem. Soc.*, 1976, **98**, 3160.

- 19 J. T. Moelwyn-Hughes, A. W. B. Garner and N. Gordon, *J. Organomet. Chem.*, 1971, **26**, 373; E. Singleton, J. T. Moelwyn-Hughes and A. W. B. Garner, *J. Organomet. Chem.*, 1970, **21**, 449.
- 20 D. Drew, D. J. Darensbourg and M. Y. Darensbourg, *Inorg. Chem.*, 1975, **14**, 1579.
- 21 R. H. Reimann and E. Singleton, *J. Organomet. Chem.*, 1973, **59**, C24.
- 22 R. Mews, *AngewChem., Int. Ed. Engl.*, 1975, **14**, 640.
- 23 D. G. Dewitt, J. P. Fawcett and A. Poe, *J. Chem Soc., Dalton Trans.*, 1976, 528.
- 24 U. Kolle, *J. Organomet. Chem.*, 1971, **155**, 53.
- 25 F. Calderazzo, I. P. Mavani, D. Vitali, I. Bernal, J. D. Korp and J. L. Atwood, *J. Organomet. Chem.*, 1978, **160**, 207.
- 26 A. M. Bond, R. Colton and M. E. McDonald, *Inorg. Chem.*, 1978, **17**, 2842.
- 27 L. A. P. Kane-Maguire and D. A. Sweigart, *Inorg. Chem.*, 1979, **18**, 100.
- 28 M. Freni, D. Giusto and P. Romiti, *J. Inorg. Nucl. Chem.*, 1971, **33**, 4093; N. Flitcroft, J. M. Leach and F. J. Hopton, *J. Inorg. Nucl. Chem.*, 1970, **32**, 137.
- 29 W. Hieber and H. Fuchs, *Z. Anorg. Allg. Chem.*, 1941, **248**, 269.
- 30 J. C. Luong, L. Nadjo and M. S. Wrighton, *J. Am. Chem. Soc.*, 1978, **100**, 5790.
- 31 T. D. Westmoreland, H. Le Bozec, R. W. Murray, and T. J. Meyer, *J. Am. Chem. Soc.*, 1983, **105**, 5952.
- 32 E. Horn and M. R. Snow, *Aust. J. Chem.*, 1980, **33**, 2369.
- 33 A. J. Lees, *Chem. Rev.*, 1987, **87**, 711.
- 34 R. Nair, B. Cullam and C. Murphy, *Inorg. Chem.*, 1997, **36**, 962.
- 35 V. W. –W. Yam, K. M. –C. Wong, V. W. –M. Lee, K. K. –W. Lo and K. –K. Cheung, *Organometallics*, 1995, **14**, 4034; L. Sacksteder, M. Lee, J. N. Demas and B. A. DeGraff, *J. Am. Chem. Soc.*, 1993, **115**, 8230.
- 36 T. J. Kotch, A. J. Lees, S. J. Fuerniss, K. Papathomas and I. R. W. Snyder, *Inorg. Chem.*, 1993, **32**, 2570.
- 37 V. W. –W. Yam, K. K. –W. Lo, K. –K. Cheung and R. Y. –C. Kong, *J. Chem Soc., Dalton Trans.*, 1997, 2067.
- 38 T. T. Ehler, N. Malmberg, K. Carron, B. P. Sullivan and L. J. Noe, *J. Phys. Chem. B.*, 1997, **101**, 3174.

- 39 V. W. –W. Yam, V. C. –Y. Lau and K. –K. Cheung, *J. Chem Soc., Chem. Commun.*, 1995, 259.
- 40 K. Kalyanasundaram, *J. Chem. Soc. Faraday Trans.*, 1986, **2**, 2401.
- 41 W.B. Connick, A.J. Di Bilio, M.G. Hill, J.R. Winkler and H.B. Gray, *Inorg. Chim. Acta*, 1995, **240**, 169.
- 42 J.R. Schoonover, P. Chen, W.D. Bates, R.B. Dyer and T.J. Meyer, *Inorg. Chem.*, 1994, **33**, 793.
- 43 P. Chen, T.D. Westmoreland, E. Danielson, K.S. Schanze, D. Anthon, P.E. Neveux Jr and T.J.Meyer, *Inorg. Chem.*, 1987, **26**, 1116.
- 44 P. Chen, R. Duesing, D.K. Graff and T.J. Meyer, *J. Phys. Chem.*, 1991, **95**, 5850.
- 45 J.R. Schoonover, G.F. Strouse, P. Chen, W.D. Bates and T.J. Meyer, *Inorg. Chem.*, 1993, **32**, 2618.
- 46 R.J. Shaver, M.W. Perkovic, D.P. Rillema and C. Woods, *Inorg. Chem.*, 1995, **34**, 5446.
- 47 R. V. Slone, D. I. Yoon, R. M. Calhoun and J. T. Hupp, *J. Am. Chem. Soc.*, 1995, **117**, 11813.
- 48 K.D. Benkstein, J.T. Hupp and C.L. Stern, *J. Am. Chem. Soc.*, 1998, **120**, 12982.
- 49 D. Curiel and P. D. Beer, *Chem. Commun.*, 2005, 1909.
- 50 S. S. Sun and A. J. Lees, *Chem. Commun.*, 2000, 1687.

Chapter 2

**Terpyridine complexes of $\text{Re}(\text{CO})_3^+$
moiety**

2.1 Introduction

The 2,2':6',2''-terpyridine molecule is widely used in the development of modern inorganic chemistry.¹ The ligand possesses vacant low-lying π^* orbitals

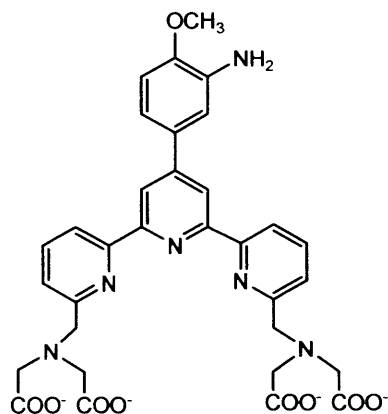


Figure 2.1: TMT

capable of accepting electron density from a metal, and these orbitals played a vital role in the ligand coordinative capabilities. The ability of this ligand to chelate to a wide range of metal ions has led to its incorporation in macrocyclic ligands.²⁻⁴ Again, lanthanide complexes of 2,2':6',2''-terpyridine ligand with multiple carboxylate groups are attracting interest as luminescent agents for protein labelling.⁵⁻⁷

A. K. Saha⁷ and his group designed Eu^{3+} -TMT [terpyridine-bis(methylenamine) tetracetic acid] [Figure 2.1] as a DNA binding probe where the aromatic terpyridyl system provided the chelated Eu^{3+} ion with a relatively hydrophobic environment for maximal emission and lifetime.

Chiral 2,2':6',2''-terpyridine ligands are being designed as reagents for enantioselective synthesis.⁸ Cu(I)-complexes of the following ligands have been used for catalytic asymmetric cyclopropanation of styrene by ethyl diazoacetate and the chiral substituent used on the terpyridine ring is 6,6-dimethyl-norbornan-2-yl [Figure 2.2].

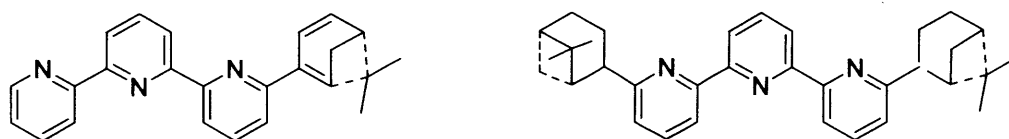


Figure 2.2: Chiral 2,2':6',2'' terpyridines.

In addition, appropriately functionalized 2,2':6',2''-terpyridines have been anchored to oxide surfaces, permitting the build up of a monolayer or a thin film of coordination complexes.⁹ Electron-withdrawing and -releasing substituents may be used to alter the redox and photophysical properties of the complexes.^{10, 11} Moreover,

4'-Aryl-substituted-2,2':6',2'' terpyridines have been found to be highly sensitive reagents for the colorimetric determination of iron(II)¹, with some finding potential applications in clinical chemistry.¹² [2,6-bis(4-phenyl-2-pyridyl)-4-phenyl-pyridine] (terosite) and tripyridyl triazene (TPTZ) [Figure 2.3] was used to determine the iron in serum along with the possibility of the interference of copper and zinc.

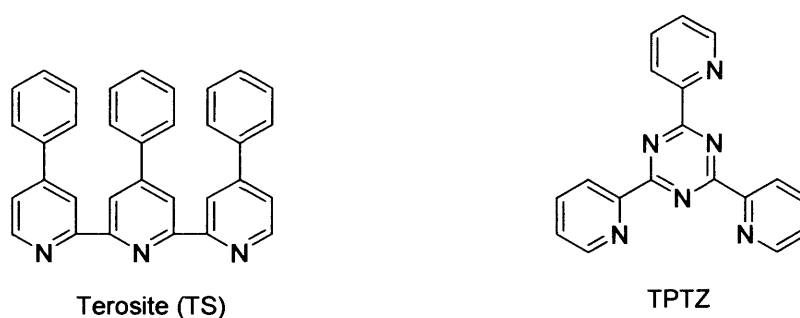


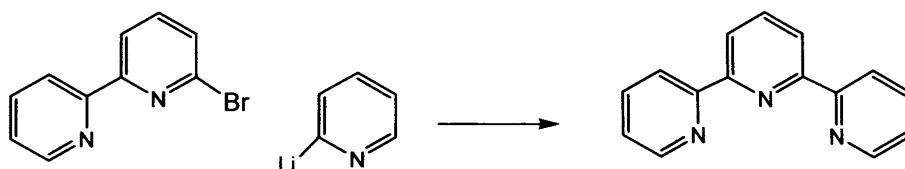
Figure 2.3: 4'-Aryl-substituted-2,2':6',2'' terpyridines used in colorimetric determination of iron(II)

Again, the phenyl, furyl and thienyl analogues exhibit significant cytotoxicity against human tumour cells.¹³

In this chapter we are interested in exploring this constructive ligand in the development of potential inorganic luminescent materials.

2.1.1 Synthesis of 2,2':6',2''-terpyridine (terpy)

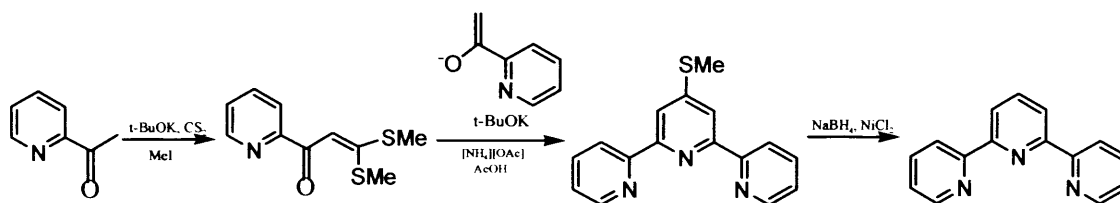
The two common synthetic approaches to terpyridine involve either the coupling of three pyridine units, or the synthesis of either the central or the two terminal pyridine rings. The ligand 2,2':6',2'' terpyridine was first isolated by Morgan and Burstall in the 1930s as one of the numerous products obtained in a low yield from the oxidative coupling of pyridine by iron(III) chloride at elevated temperature and pressure in a steel autoclave.^{14,15} The organometallic coupling of 2,2'-bipyridine with 2-pyridyllithium in ether at -40°C afforded 2,2':6',2'' terpyridine in 39% yield (Scheme 2.1).



Scheme 2.1: Synthesis of 2,2':6',2'' terpyridine by coupling reaction.

Constable's group prepared 2,2':6',2''-terpyridine in 64% yield from the condensation of N -{1-(2-pyridyl)1-oxo-2'-ethyl}pyridinium iodide with 2-(2'-pyrrolidino-propionyl)-pyridine in the presence of ammonium acetate. The ligand is isolated as its iron(II) salt which was then demetallated by oxidative cleavage of the complex with hydrogen peroxide.¹⁶

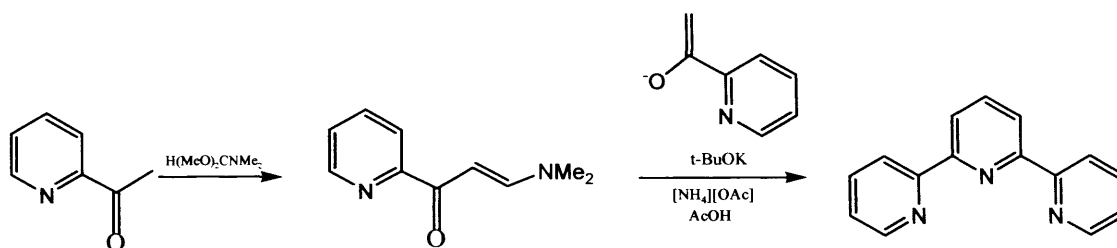
Potts *et al* have reported a three step synthesis of terpy in high yield which involves first the synthesis of the bisthiomethylpropenone intermediate from 2-acetyl pyridine (Scheme 2.2).



Scheme 2.2: Potts' synthesis of 2,2':6',2'' terpyridine.

This enone is then cyclized to the 4'-thiomethyl terpy, which is finally reduced to 2,2':6',2'' terpyridine using Raney nickel¹⁷ or nickel boride (generated from sodium borohydride and nickel(II) chloride hexahydrate)¹⁸. The use of Raney nickel results in the contamination of the product with about 15% of 4'-ethoxy-2,2':6',2'' terpyridine, while the use of sodium borohydride is expensive.

The most efficient synthesis of 2,2':6',2'' terpyridine is Jameson's two step method which proceeds through the formation of enaminone and produces the desired terpy in 47% overall yield (Scheme 2.3).¹⁹



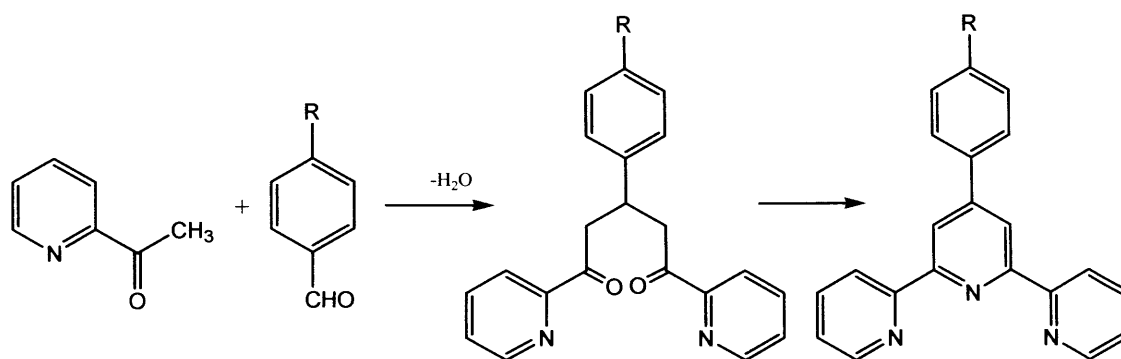
Scheme 2.3: Synthesis of 2,2':6',2'' terpyridine by Jameson's method.

Stille coupling has been used to prepare terpy using two complementary routes. Either 2-trimethylstannylpyridine may be coupled with 2,6-dibromopyridine, or 2,6-di-(trimethylstannyl)pyridine may be coupled with 2-bromopyridine, to afford terpy in yields of 74% and 72%, respectively.²⁰

2.1.2 4'-Substituted-2,2':6',2''-terpyridines

Substituted derivatives of 2,2':6',2''-terpyridine (terpy) are interesting ligands whose rich coordination chemistry affords compounds of use in supramolecular chemistry,²¹ molecular biology,²² photochemistry,²³ and potential pharmaceutical applications.²⁴ Among a series of terpy ligand derivatives, the substituents at the 4'-position provide a ligand which still retains the C_2 symmetry of the parent molecule.

Several reactions, such as the Hantzsch, the Kröhnke and the Chichibabin lead to the formation of 4'-substituted terpyridine derivatives in which the central pyridine ring is built up in a condensation process.²⁵ The reaction of benzaldehyde, or the relevant substituted benzaldehyde, with 2-acetylpyridine gives a 1,5-diketone intermediate. Ring closure with ammonium acetate in air provides the final terpy in a yield of 47% (Scheme 2.4). The basic ingredient is acetylpyridine which provides the two distal rings of terpy, as well as C2', C3', C5' and C6' of the central ring.



Scheme 2.4: Synthesis of 4'-substituted terpyridine derivatives where $R = \text{H}^{26}$, $\text{CH}_3^{11,27}$, OCH_3^{27} , $\text{OH}^{27,28}$, Cl^{27} , Br^{27} etc.

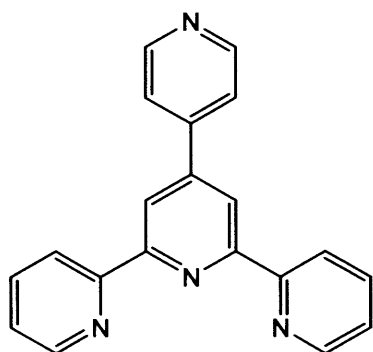
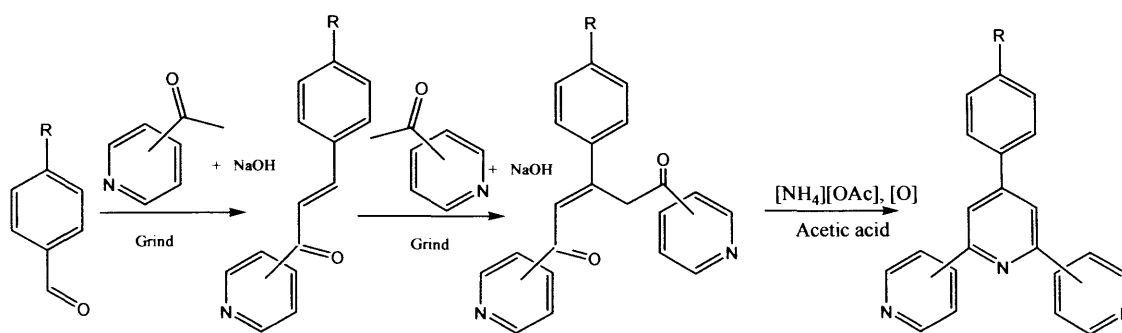


Figure 2.4: 4'-(4'''-Pyridyl)-2,2':6',2''-terpyridine

Constable and co-workers²⁹ have prepared 4'-(4'''-pyridyl)-2,2':6',2''-terpyridine (Figure 2.4) from the reaction of 2-acetylpyridine and 4-pyridinecarboxaldehyde and by isolating the 1,5-diketone intermediate followed by ring closure with ammonium acetate. This ligand is an important synthon in supramolecular chemistry. Many other groups^{28,30} have prepared a variety of 4'-substituted

2,2':6',2''-terpyridines using this general methodology. But this methodology displays moderate to low yields, utilizes large volumes of toxic and volatile organic solvents, has low atom efficiency and requires extensive purification.

In view of the limitations of this conventional method a new and more versatile solventless method has been developed by applying the principles of 'green chemistry'.³¹ The aldol condensation of an enolisable ketone and a benzaldehyde followed by Michael addition to the enone, with a second enolisable ketone, leads to the quantitative formation of 1,5-diketone, either symmetrical or unsymmetrical with respect to the aromatic rings. Both steps involve grinding with solid NaOH. The corresponding terpyridine is then easily formed in high yield via a double condensation in the presence of ammonium acetate in acetic acid (Scheme 2.5).

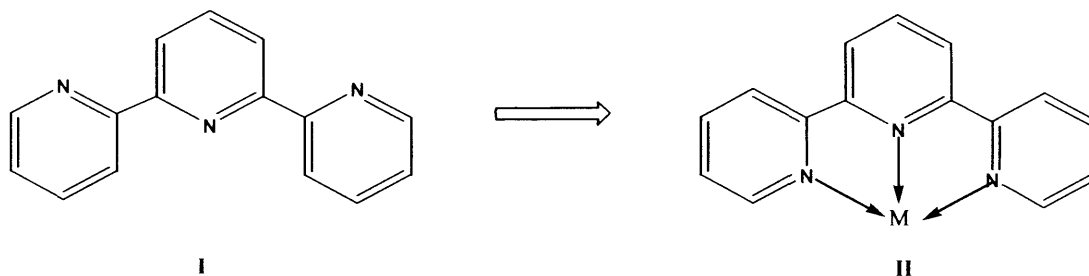


Scheme 2.5: Reaction scheme for the Roston style synthesis of terpyridine.

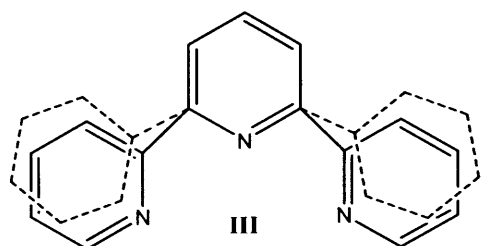
This new method is simple, occurs under mild conditions and has lower costs. This method is accessible to unsymmetrical bpy or terpy simply by adding a different aryl ketone to the enone in the Michael addition step of the reaction prior to the ring closure.^{32, 33} However, this solventless methodology is restricted to highly exothermic reaction. Still this type of situation can be overcome by using water soluble, non-toxic poly(ethyleneglycol) reaction medium.³⁴

2.1.3 Coordination of 2,2':6',2''-terpyridine with metals

The ligand terpy, **I**, and its derivatives adopt a planar conformation with the nitrogen atoms in adjacent rings *trans* to each other to minimize the repulsion between the nitrogen atom lone pairs. The adoption of the *trans* conformation in the solid state has been confirmed crystallographically for 2,2':6',2''-terpyridine³⁵, 4'-phenyl-2,2':6',2''-terpyridine²⁶, 4'-(4-pyridyl)-2,2':6',2''-terpyridine³⁶ and 6',6''-dibromo-4'-phenyl-2,2':6',2''-terpyridine³⁷. But on coordination to a metal ion the majority of complex contain a terdentate planar *cis,cis* ligand **II**.¹



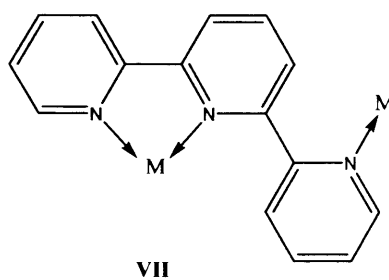
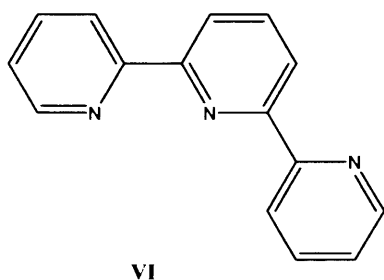
The ligand 2,2':6',2''-terpyridine exhibits very extensive coordination chemistry. It can demonstrate a variety of bonding modes to metals such as monodentate, bidentate, terdentate and bridging. However, it almost invariably functions as a terdentate chelating ligand, with the majority of complexes exhibiting 1:1 or 1:2 metal to ligand ratios.^{1, 25}



The 1:2 complexes are based upon an octahedral geometry and exhibit D_{2d} local symmetry. It is also apparent that for terpy to act as an efficient terdentate, it is necessary to

distort the ligand and reduce the interannular angle between the central and terminal pyridine rings, **III**.

There are a number of compounds have been reported which contain bidentate terpy ligands,³⁸ the first structurally characterized examples were $[\text{Ru}(\text{terpy})(\text{CO})_2\text{Br}_2]^{39}$ and $[\text{Ru}(\text{Hterpy})(\text{phen})(\text{CO})_2]^{3+}$.⁴⁰ The two rings of terpy that are coordinated to the ruthenium are in a near planar cis conformation. However, the non-coordinated ring is now no longer coplanar with the other two leading to a non-planar arrangement about the C-C bond between coordinated and non-coordinated rings **VI**. This principle is important for the formation of polynuclear systems where terpyridine act as bridging ligand between two metal centres. In this case, there will be a non-planar arrangement between rings coordinated to different metal centres **VII** in such a system.



The extensive coordination chemistry of 2,2':6',2''-terpyridine and its derivatives with different metals has already been reviewed by E.C. Constable.¹

2.1.4 Rhenium compounds of terpyridine

The work on Re(I) complexes was initiated by Wrighton's pioneering studies. In the meantime many other groups contributed to this subject. The main interest has been directed to the behaviour of $\text{Re}^1(1,2\text{-diimine})(\text{CO})_3\text{X}$ compounds in their MLCT excited states. There have been numerous reports that have used the $\text{Re}(\text{bipy})(\text{CO})_3\text{Cl}$ moiety as building blocks for supramolecular species,⁴¹ sub-units of photodevices⁴² or even as potential biological labels.⁴³ While similar chemistry has been carried out using pyridine and terpyridine, neither has been reported as being luminescent. The $\text{Re}(\text{py})_2(\text{CO})_3\text{Cl}$ species was reported by Wrighton⁴⁴ in the same publication as the bipyridine species and its lack of luminescence was an indicator of the CT based origin of the emission. The reaction of $\text{Re}(\text{CO})_5\text{Cl}$ with various nitrogen containing heterocycles, including 2,2':6',2'' terpyridine, was carried out by Juris *et al.*⁴⁵ While the compound was initially thought to be $\text{Re}(\sigma^3\text{-terpy})(\text{CO})_2\text{Cl}$, with the terpyridine meridionally co-ordinated, the compound was later characterised⁴⁶ as *fac*- $\text{Re}(\sigma^2\text{-terpy})(\text{CO})_3\text{Cl}$. While this compound is not luminescent in solution at room temperature, it is nonetheless, an interesting compound that has two obvious sites of reactivity: substitution of the chloride ligand and addition to pendant pyridine group.

2.1.5 Aim of the work

The main goal of this work was to prepare molecular switches. We tried to utilize *fac*- $\text{Re}(\sigma^2\text{-terpy})(\text{CO})_3\text{Cl}$ for metal binding domains through the coordination of the pendant pyridine unit with different metal centres to observe any switchable luminescence properties. Subsequently, we were also interested in methylation of the pendant pyridine unit. It was hoped that the inclusion of the pyridinium group with the molecule might allow reversible redox behaviour that will facilitate on-off switching of the luminescence. Again, the successive substitution of the chloride ion with efficient ligands can lead to the synthesis of molecules with high emission quantum yield, oxidizing/reducing ability of the MLCT excited states⁴⁷ responding to changes in the electronic distribution at the Re centre.^{48,49} Since the isothiocyanate moiety of various rhenium(I) polypyridine complexes⁵⁰ were used as biological labeling reagents, we were also interested to see the potential of the corresponding terpyridine complex as a biological substrate.

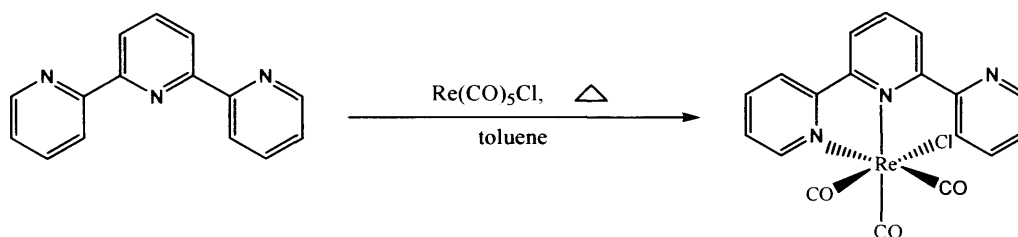
In brief, this work describes subsequent modifications to *fac*- $\text{Re}(\sigma^2\text{-terpy})(\text{CO})_3\text{Cl}$ and the effects that the changes have on the photophysical and electrochemical properties of the resulting compounds.

2.2 Results and Discussion

This section includes the result and discussion on the synthesis of rhenium complexes (2.2.1), their coordinative properties (2.2.2), followed by their spectroscopic studies (2.2.3): IR and Mass spectra (2.2.3.1) and ^1H NMR spectra (2.2.3.2), X-ray crystallographic studies (2.2.4), luminescence properties (2.2.5) and electrochemical properties (2.2.6).

2.2.1 Synthesis of Rhenium Complexes

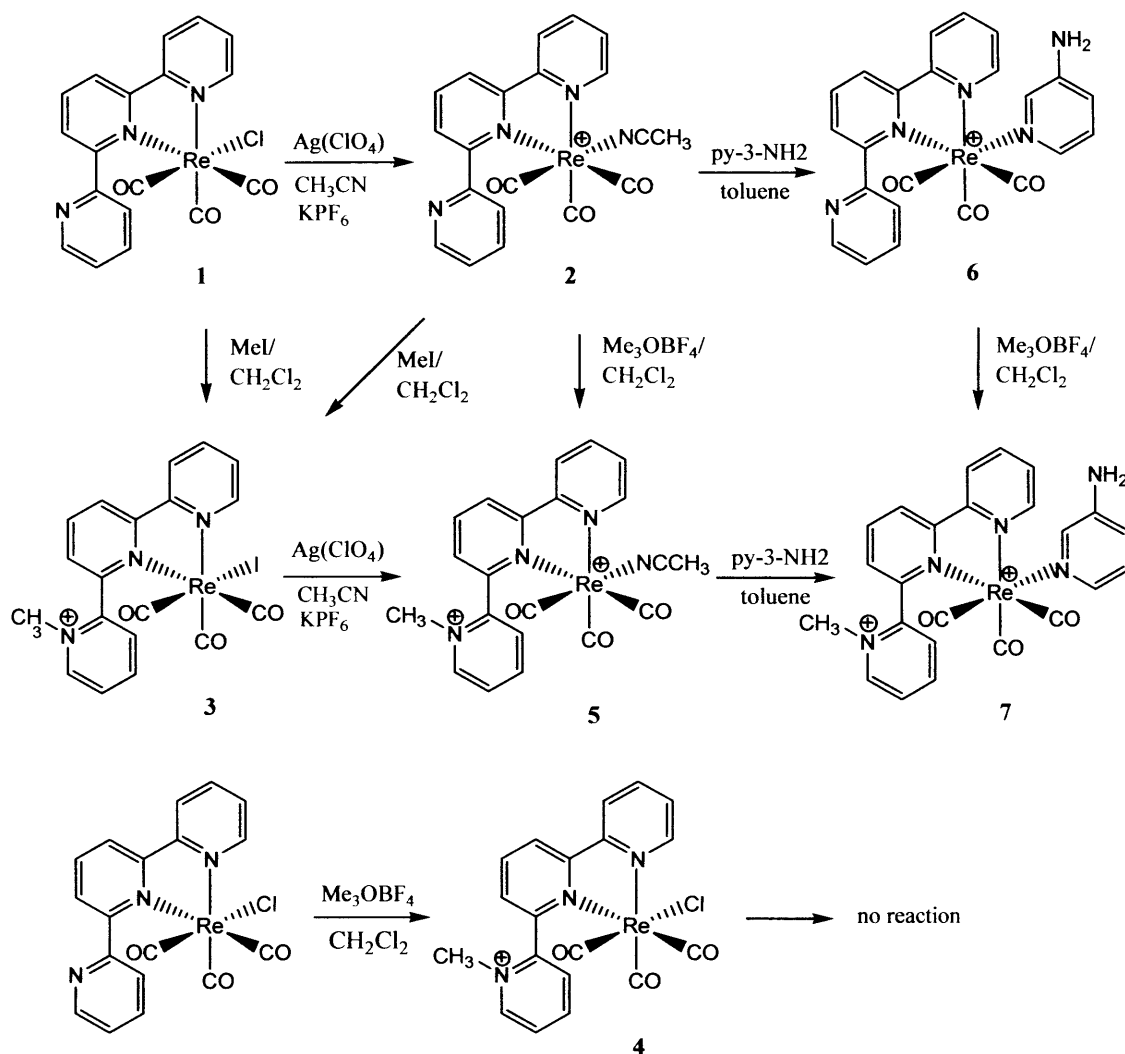
The reaction of $\text{Re}(\text{CO})_5\text{Cl}$ with one equivalent of terpyridine in refluxing toluene results in the formation of $\text{Re}(\sigma^2\text{-terpy})(\text{CO})_3\text{Cl}$, **1**, as previously described (Scheme 2.6).⁵¹



Scheme 2.6: Synthesis of $\text{Re}(\sigma^2\text{-terpy})(\text{CO})_3\text{Cl}$ (1**)**

This air stable compound may be reacted with $\text{Ag}(\text{ClO}_4)$ in acetonitrile to yield $\text{Re}(\sigma^2\text{-terpy})(\text{CO})_3(\text{CH}_3\text{CN})^+$, **2**, in a reaction analogous to that utilised by Meyer⁵¹ for the synthesis of $\text{Re}(\text{bipy})(\text{CO})_3(\text{CH}_3\text{CN})^+$ [Scheme 2.7]. The complex is typically isolated by its precipitation as the hexafluorophosphate salt from aqueous solutions. Unsurprisingly, attempts to rearrange the compound to give the *mer*- $\text{Re}(\sigma^3\text{-terpy})(\text{CO})_3^+$ species, by adding two equivalents of silver perchlorate and heating 48-72 hours, have been unsuccessful and typically result in decomposition or the isolation of the starting material. The compound is stable at room temperature in solution and crystals suitable for x-ray crystallographic studies were obtained by the

slow vapour diffusion of diethyl ether into an acetonitrile solution of the compound. Details of the solid state structure are discussed in the crystallographic section.



Scheme 2.7: Synthesis of complexes 2-7.

Alternatively, rather than substituting the chloride in $\text{Re}(\sigma^2\text{-terpy})(\text{CO})_3\text{Cl}$, we may further derivatise the compound by the alkylation of the pendant pyridine group. It was hoped that the inclusion of the pyridinium group with the molecule may allow reversible redox behaviour which will facilitate on-off switching of the luminescence. Initial attempts to alkylate the pyridine group were carried out by the reaction of the complex with a large excess of methyl iodide in refluxing acetonitrile. A compound

was isolated by the addition of an aqueous KPF_6 solution. While the product does contain the pyridinium moiety, the use of methyl iodide also results in the substitution of the chloride for iodide and the species isolated was determined to be $[\text{Re}(\sigma^2\text{-terpyMe})(\text{CO})_3\text{I}]^+\text{PF}_6^-$, **3**. Previously, most crystallographically characterised $\text{Re}(\text{CO})_3\text{I}(\text{N-N})$ species were synthesised from $\text{Re}(\text{CO})_5\text{I}$ ⁵² starting material, although recently Gladysz has reported similar halide substitution reactions using NaI .⁵³ To avoid this halide exchange, the chloride species was synthesised by the reaction of $\text{Re}(\sigma^2\text{-terpy})(\text{CO})_3\text{Cl}$ with trimethyloxonium tetrafluoroborate, in a 1: 1 molar ratio, in acetonitrile at room temperature. The reaction proceeded smoothly and after ion exchange gave the desired product, $[\text{Re}(\sigma^2\text{-terpyMe})(\text{CO})_3\text{Cl}]^+\text{PF}_6^-$, **4**, in high yield. The compound was isolated by simply removing the solvent and the product was typically pure enough to use in subsequent steps.

The methylated species, **4**, was reacted with $\text{Ag}(\text{ClO}_4)$ in acetonitrile to try to form the dicationic species $[\text{Re}(\sigma^2\text{-terpyMe})(\text{CO})_3(\text{CH}_3\text{CN})]^{2+}$, **5**, however no reaction was observed. However, the reaction of the iodide complex, **3**, was successful, and reaction with AgClO_4 gave the target molecule. Alternatively, the compound may also be synthesised by the reaction of $[\text{Re}(\sigma^2\text{-terpy})(\text{CO})_3(\text{CH}_3\text{CN})]^+\text{PF}_6^-$ with $\text{Me}_3\text{O}^+\text{BF}_4^-$ to give $[\text{Re}(\sigma^2\text{-terpyMe})(\text{CO})_3(\text{CH}_3\text{CN})]^{2+}\text{PF}_6^-\text{BF}_4^-$. It was observed that the length of time in this reaction was important. The reaction was monitored by solution IR spectroscopy, and it was observed that the reaction was complete within one hour at which point the product may be precipitated from solution by the addition of hexane. If the reaction mixture is left for a longer period of time, further reaction was observed to occur, giving a mixture of uncharacterised products. If the methylation of $[\text{Re}(\sigma^2\text{-terpy})(\text{CO})_3(\text{CH}_3\text{CN})]^+\text{PF}_6^-$ is carried out using MeI rather than $\text{Me}_3\text{O}^+\text{BF}_4^-$, then $[\text{Re}(\sigma^2\text{-terpyMe})(\text{CO})_3\text{I}]^+\text{PF}_6^-$ is isolated.

Finally, the acetonitrile adducts, **2** and **5**, were found to be substitutionally reactive with the acetonitrile group being readily replaced by a variety of pyridines. The reactions were typically carried out in refluxing THF with a large excess of the pyridine present. Typically the reaction had reached completion after 2-4 hours and the product was isolated by the addition of n-hexanes, which caused the precipitation of crystalline product. Accordingly, the reaction of **2** with 3-aminopyridine results in $[\text{Re}(\sigma^2\text{-terpy})(\text{CO})_3(\text{py-3-NH}_2)]^+\text{PF}_6^-$, **6** while **5** doesn't give the expected complex

due to the lower solubility of the dicationic species in THF. However, the expected complex $[\text{Re}(\sigma^2\text{-terpyMe})(\text{CO})_3(\text{py-3-NH}_2)]^{2+}\text{PF}_6^-$, **7** was synthesised by the methylation of the pendant pyridine in complex **6**. The reaction was carried out successfully by using trimethyloxonium in acetonitrile at room temperature.

2.2.2 *Coordinative Properties of the pendent pyridine moiety*

Compounds **1**, **2** and **6** all contain a pendant pyridyl group. We were interested in determining the coordinative abilities of these somewhat sterically hindered donors. Due to the mono-cationic charge on **2** and **6**, we decided to initially investigate the ability of the neutral complex **1** to co-ordinate to first row transition metals. Reactions were carried out using an acetonitrile solution of $\text{M}(\text{H}_2\text{O})_6^{2+}$ with 2-4 equivalents of **1**. Reactions were initially carried out using Zn^{2+} , due to its diamagnetism and its lack of stereochemical preferences which could allow less sterically demanding, tetrahedral species to form. It was surprising to observe that the reaction in fact resulted in the formation of $\text{Re}(\sigma^2\text{-terpy})(\text{CO})_3(\text{CH}_3\text{CN})^+$, **2**, with the transition metal abstracting the chloride atom. It was even more surprising that the reaction still proceeded when the zinc chloride salt was used in place of the more typically used perchlorate salt. While halide abstraction by Ag^+ and Tl^+ is common, and on a few occasions has been achieved electrochemically, the abstraction by Zn^{2+} has not previously been reported and is most unexpected.

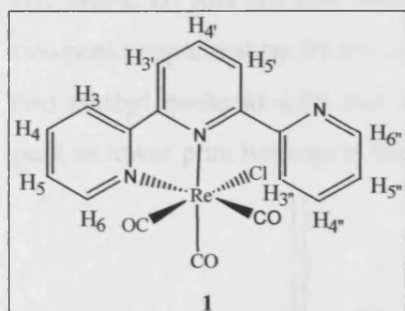
Similar reactions were carried out using compounds **2** and **6**. The attempted co-ordination of **2** and **6** with Zn^{2+} was on all occasions unsuccessful, with the isolation of starting materials being observed. All species crystallised from solution gave spectroscopic data identical to the starting materials and it was concluded that the coulombic repulsion that would result from aggregating the mono-cationic Re complexes about a dicationic metal centre was too unfavourable.

2.2.3 Spectroscopic Studies

2.2.3.1 $^1\text{H NMR}$

The $^1\text{H NMR}$ of complex **1** has been reported by Westmoreland⁴⁶ and is a useful guide in the assignment of derivatives of this complex. The $^1\text{H NMR}$ spectra for complexes 1-6 are given in Table 1. The spectra of complexes 2-6 were assigned

by comparison to the shift observed for **1** and $\text{Re}(\text{CO})_3(\text{bipy})\text{Cl}$, as well through analysis of COSY H-H NMR spectra.



though small shift in other protons are observed.

The biggest complication to the spectra occurs when the enantiomeric species, e.g. **1** and **2**, becomes a diastereomer when the pendant pyridine has restricted rotation (e.g. **4** and **5**). For complexes **3**, **4** and **5**, due to a mixture of diastereomers, we clearly observe two sets of signals for some given protons. These protons are those which have been assigned to be in close proximity to the axial centre. In these compounds double signals are observed for H_{5'}, H_{3'} and the CH₃ group of the methylated pyridine. A slight splitting is also observed for H_{4'}.

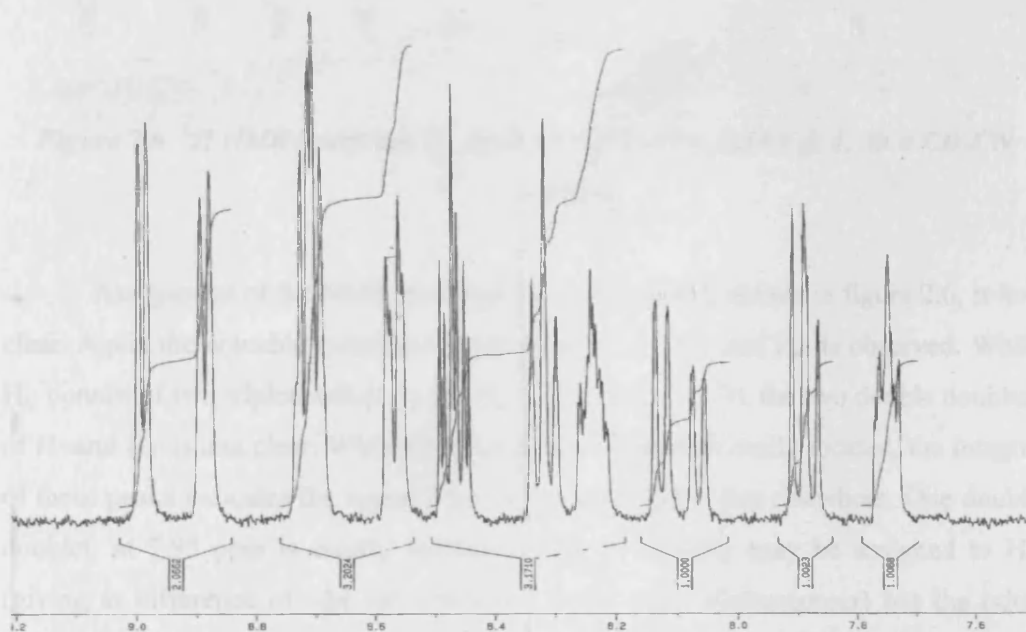


Figure 2.5 ¹H NMR Spectrum of $[\text{Re}(\text{CO})_3(\text{terpyMe})(\text{CH}_3\text{CN})]^+[\text{PF}_6]_2^-$, **5**, in a CD_3CN solution.

For example, compound **5** is shown in figure 2.5, and the signal for H_3 consists of two signals offset by ~ 2 Hz, while H_4 consists of two signals offset by ~ 3 Hz. While H_5 and H_5' also show signs of consisting of two peaks, H_3'' clearly gives two peaks separated by 24 Hz in a 3:2 ratio. This ratio is confirmed by the presence of two methyl peaks at 4.04 and 4.09 ppm in the same proportions although now the peak at lower ppm belongs to the major diastereomer.

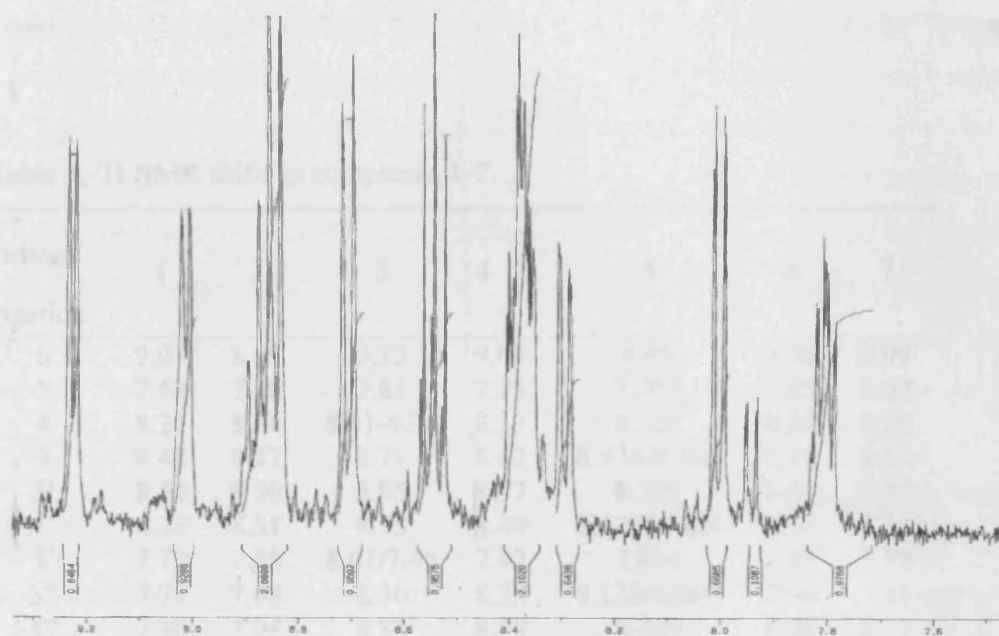


Figure 2.6 ^1H NMR Spectrum of $[\text{Re}(\text{CO})_3(\text{terpyMe})(\text{I})][\text{PF}_6]$, **3**, in a CD_3CN solution.

Assignment of the NMR spectrum for compound **3**, shown in figure 2.6, is less clear. Again the notable splitting of peaks due to H_5 , H_3'' and H_4 is observed. While H_4 consist of two triplets offset by 2.4 Hz (in a ratio of $\sim 1:3$), the two double doublets of H_5 and H_3'' is less clear. While the major diastereomer is easily located, the integral of these peaks indicates the signal from the minor species lies elsewhere. One double doublet, at 7.95 ppm is clearly identified and presumably may be assigned to H_5 (giving at difference of ~ 24 Hz compared to the other diastereomer) but the other peak due to the minor diastereomer is not clearly obvious, but the integrals suggest it lies within the multiplets at 8.36-8.41 also assigned to H_4 and H_5'' . Again, the methyl peak is split into two signals at 4.30 and 4.07 ppm in a 3:1 ratio.

Finally, **7** has an unexpected spectrum, with the proposed methylated pyridine ring showing very little shift in ppm. Clearly a new species has been formed which contains both the terpyridine and the 3-amino-pyridine moieties. Two possibilities exist, either the aniline has been methylated or the complex of interested has been formed but the steric congestion of complex causes very different ring effects compared with other complexes.

Table 1. ^1H NMR shifts in complexes 1-7

Proton Position	1	2	3	4	5	6	7
6	9.05	8.99	9.23	9.09	8.99	9.26	8.99
5	7.62	7.66	7.81	7.75	7.751	7.85	7.67
4	8.21	8.24	8.41-8.36	8.33	8.321	8.34	8.25
3	8.48	8.47	8.71	8.62	8.574/8.568	8.41	8.50
3'	8.50	8.50	8.85	8.77	8.705	8.43	8.55
4'	8.28	8.31	8.55	8.49	8.475/8.468	8.34	8.34
5'	7.79	7.80	8.01/7.95	7.92	7.894	7.85	7.79
3''	7.78	7.68	8.30	8.24	8.128/8.069	7.96	7.83
4''	7.96	7.94	8.88	8.79	8.709	8.08	8.12
5''	7.55	7.53	8.41-8.36	8.29	8.24	7.67	7.67
6''	8.76	8.72	9.02	8.94	8.89	8.86	8.75
a						7.35	7.87
b						7.21	7.79
c						6.92	7.55
d						7.01	7.61

2.2.3.2 IR Spectroscopy

The complex $\text{Re}(\text{CO})_3(\text{bpy})\text{Cl}$ possess C_s geometry with three IR active vibrational modes [$A'(1)+A'(2)+A''$], corresponding to three carbonyl ligands in a facial arrangement.⁵⁴⁻⁵⁶ When the axial Cl ligand is substituted by an N-donor ligand the local coordination around the Re metal center possesses pseudo- C_{3v} symmetry, resulting in the observance of only two IR active bands; the higher energy band assigned to an A_1 vibrational mode while the broad lower energy (E) band is a convolution of the previously mentioned $A'(2) + A''$ bands. For the complex *fac*- $[\text{Re}(\text{CO})_3(\text{bpy})\text{Cl}]$, the νCO bands are observed at 2024, 1917 and 1900cm^{-1} in CH_3CN solution. The position of these carbonyl bands is greatly affected by the $d\pi$

electron density of the rhenium centre as a result of π -back donation and the π -acceptor capabilities of the coordinated polypyridyl ligand.

The solution IR data of the carbonyl region for these compounds is very diagnostic and informative when following the course of a reaction. The IR data of these complexes can be found in Table 2. Typical trends are observed in the CO stretching frequency, with the cationic species showing absorbances at higher wavenumbers due to decreased back-bonding into the π^* orbital of the carbonyl ligands. It was curious to note, despite numerous measurements of several samples, we observed the absorbance of the pyridine substituted complex **6** to be at lower frequency than that of the acetonitrile complex **2**. A possible explanation for this may be that, although one might expect pyridine to be a better π acceptor, and perhaps reduce the electron density on the metal, it is also a better σ donor than acetonitrile and the net effect of replacing an acetonitrile ligand with a pyridine donor is an increase in electron density on the metal centre, leading to a reduction in the stretching frequency of the carbonyl groups.

The methylation of the pendant pyridine of the terpyridine ligand does have a significant effect on the stretching frequencies of the carbonyl groups, with, in all cases, a shift to higher frequencies in relation to five wavenumbers being observed. Finally, the methylation of $[\text{Re}(\text{terpy})(\text{CO})_3(\text{py-3-NH}_2)]\text{PF}_6$ lead to a species with an IR spectrum which was inconsistent with the methylation of the terpyridines and while the new compound may be due to the methylation of the aminopyridine moiety, it is unclear why this would not also lead to an increase in the stretching frequency. With both the NMR and IR data for **7** being unexpected, its characterisation as $[\text{Re}(\text{terpyMe})(\text{CO})_3(\text{py-3-NH}_2)]^+$ is tentative.

Table 2. Infra-red and mass spectroscopic data for complexes 1-7.

Compound	IR/ ν_{max} ($\text{CH}_3\text{CN}/\text{cm}^{-1}$)	MS m/z (es)
$\text{Re}(\sigma^2\text{-terpy})(\text{CO})_3\text{Cl}$, (1)	2024, 1920, 1898	540/504/511 /483/455
$\text{Re}(\sigma^2\text{-terpy})(\text{CO})_3(\text{CH}_3\text{CN})^+ \text{PF}_6^-$, (2)	2040, 1941, 1930	545
$[\text{Re}(\sigma^2\text{-terpyMe})(\text{CO})_3\text{I}]^+ \text{PF}_6^-$, (3)	2031s, 1939s, 1908vs	664
$[\text{Re}(\sigma^2\text{-terpyMe})(\text{CO})_3\text{Cl}]^+ \text{BF}_4^-$, (4)	2036, 1941, 1907	552/4
$[\text{Re}(\sigma^2\text{-terpyMe})(\text{CO})_3(\text{CH}_3\text{CN})]^{2+} \text{PF}_6^- \text{BF}_4^-$, (5)	2044, 1944, 1931, 1916	560
$[\text{Re}(\sigma^2\text{-terpy})(\text{CO})_3(\text{NH}_2\text{C}_5\text{H}_5\text{N})]^+ \text{PF}_6^-$, (6)	2027s, 1937ssh, 1926vs	598/504
$[\text{Re}(\sigma^2\text{-terpyMe})(\text{CO})_3(\text{NH}_2\text{C}_5\text{H}_5\text{N})]^{2+} \text{BF}_4^- \text{PF}_6^-$, (7)	2024, 1919, 1895	613

The mass spectra of the complexes yield the parent ions of the complexes and suitable fragmentation patterns. The electron impact mass spectrum of compound **1** showed the main peak centred at m/z 540 corresponding to $[\text{Re}(\sigma^2\text{-terpy})(\text{CO})_3\text{Cl} + \text{H}]$. A relatively smaller peak corresponding to the loss of chloride [m/z 504, $\text{Re}(\sigma^2\text{-terpy})(\text{CO})_3^+$] was also observed, as are much smaller fragmentation peaks corresponding to $\text{Re}(\sigma^2\text{-terpy})(\text{CO})_2\text{Cl}$ (m/z 511), $\text{Re}(\sigma^2\text{-terpy})(\text{CO})\text{Cl}$ (m/z 483) and $\text{Re}(\sigma^2\text{-terpy})\text{Cl}$ (m/z 455). The FAB mass spectra of compounds **2**, **3** and **5** demonstrated parent peaks centred at m/z 545 [$\text{Re}(\sigma^2\text{-terpy})(\text{CO})_3(\text{CH}_3\text{CN})^+$], m/z 664 $\{[\text{Re}(\sigma^2\text{-terpyMe})(\text{CO})_3]^{2+} + \text{PF}_6\}$ and m/z 560 $[[\text{Re}(\sigma^2\text{-terpyMe})(\text{CO})_3(\text{CH}_3\text{CN})]^{2+}]$, respectively. The electro spray mass spectrum of complex **4** gave the main peak at m/z 552/4 [$\text{Re}(\sigma^2\text{-terpyMe})(\text{CO})_3\text{Cl}]^+$. The FAB mass spectra of compound **6** showed the main peak centred at m/z 598 corresponding to $[\text{Re}(\sigma^2\text{-terpy})(\text{CO})_3(\text{py-3-NH}_2)^+]$ with a smaller peak corresponding to the loss of 3-aminopyridine group [m/z 504, $\text{Re}(\sigma^2\text{-terpy})(\text{CO})_3^+$]. Despite several attempts for obtaining the mass spectra results for compound **7** neither the parent peak nor any fragments were observed.

2.2.4 X-ray Crystallographic Studies

2.2.4.1 Crystallographic data for $\text{Re}(\sigma^2\text{-terpy})(\text{CO})_3\text{Cl}$ (**1**)

$\text{Re}(\sigma^2\text{-terpy})(\text{CO})_3\text{Cl}$ was obtained by the reaction of $\text{Re}_2(\text{CO})_{10}$ with terpyridine and three equivalents of trimethylamine oxide in CH_2Cl_2 which was then recrystallized as yellow crystals by slow vapour diffusion of diethyl ether into chloroform solution of the compound. The solid-state structure of $\text{Re}(\sigma^2\text{-terpy})(\text{CO})_3\text{Cl}$ was determined (Figure 2.7). This is a polymorph of the previously reported structure⁴⁶ with same space group but different unit cell dimensions. The asymmetric unit of the structure contains two crystallographically independent complex units and two CDCl_3 molecules. The two complex units are similar, with relatively minor differences in bond lengths, angles and ring torsion angles between them. Crystallographic data and relevant bond lengths and angles are shown in Table 4 and 3.

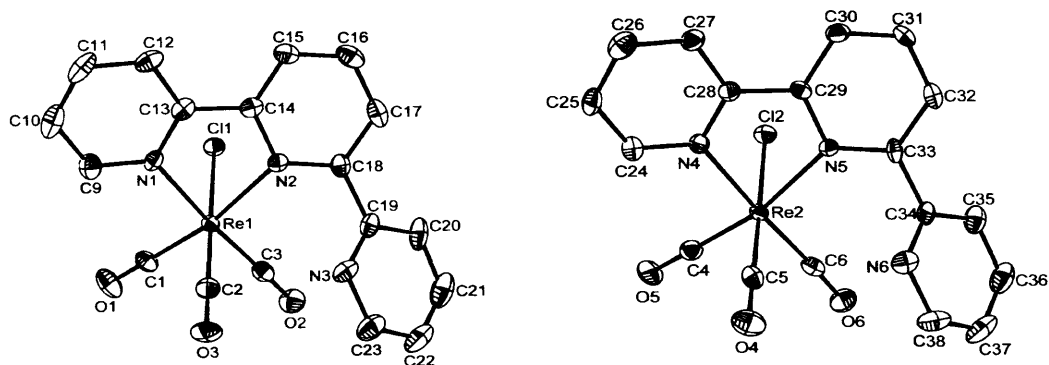


Figure 2.7 Two molecules in the asymmetric unit of the structure of $\text{Re}(\sigma^2\text{-terpy})(\text{CO})_3\text{Cl}$ (1). Thermal ellipsoids are drawn at 50% probability.

The coordination geometry at each rhenium atom is distorted octahedral with the three carbonyl ligands arranged in a *fac* fashion. The terpy ligand acts as a bidentate chelating ligand with a *cis* conformation of the coordinated rings. Surprisingly, the uncoordinated pyridine ring is also in a *cis* orientation to the coordinated pyridine rings, opposite to the previously reported structure⁴⁶. In solving the structure of this compound, we tried exchanging the positions of N3 and C20 atoms (and N6 and C35 atoms) but this gave an unsatisfactory solution with the R factor being very high. The bond lengths and bond angles are similar to those found in $\text{Re}(\sigma^2\text{-terpy})(\text{CO})_3\text{Cl}$ ⁴⁶, $\text{Re}(\sigma^2\text{-terpy})(\text{CO})_3\text{Br}$ ⁵⁷ and $\text{Re}(\sigma^2\text{-terpy})(\text{CO})_3\text{Cl}\cdot\text{H}_2\text{O}$ ⁵⁸ complexes and are summarized in Table 4. The Re-N bond distance of the central pyridine is 0.074 Å longer than the outer pyridine. This is a common feature for $\sigma^2\text{-terpy}$ complexes, e.g. $[\text{Ru}(\sigma^2\text{-terpy})(\text{CO})_2\text{Br}_2]$ ³⁹ where the M-N bond length of the central pyridine is 0.054 Å longer than the outer pyridine. But this observation is in contrast to the situation observed for $\sigma^3\text{-terpy}$ complexes, eg, $[\text{Ru}(\sigma^3\text{-terpy})(\text{CO})\text{Cl}_2]$ ³⁹, where the M-N distance of the central ring is approximately 0.06 Å shorter than that of the outer rings. Actually, in $\text{Re}(\sigma^2\text{-terpy})(\text{CO})_3\text{Cl}$ the steric bulk of the uncoordinated pyridyl, which is effectively a substituent on the central pyridyl, prevents close approach to the rhenium centre and the Re-N(2) distance is longer than the Re-N(1) distance. The distortions from regular octahedral geometry mainly arise due to the angles N-Re-N [74.59(14)° and 74.30(13)°], N(2)-Re(1)-C(3) [100.67(17)°] and N(5)-Re(2)-C(6) [102.19(17)°]. The former values are typical for $\text{Re}(\text{bpy})(\text{CO})_3^+$

^{59, 60} units and the latter values probably arise from the steric interaction between the pendant rings and the corresponding carbonyl groups.

The torsion angles between the central pyridine ring and the pendant pyridine rings of the two structures are $-40.16(6)^\circ$ [N(2)-C(18)-C(19)-N(3)] and $-43.48(6)^\circ$ [N(5)-C(33)-C(34)-N(6)] and smaller than that of the reported $\text{Re}(\text{terpy})(\text{CO})_3\text{Cl}$ [$-130.0(3)^\circ$] where the pendant ring is *trans* to the adjacent coordinated ring. The corresponding torsion angle of the hydrate complex is -114.9° . The difference can be attributed to interaction of the uncoordinated nitrogen atom with water in the hydrated crystal.

2.2.4.2 Crystallographic data for $[\text{Re}(\sigma^2\text{-terpy})(\text{CO})_3\text{CH}_3\text{CN}]\text{PF}_6$ (2)

A suitable single crystal of $[\text{Re}(\sigma^2\text{-terpy})(\text{CO})_3\text{CH}_3\text{CN}]\text{PF}_6$ was obtained by slow vapour diffusion of diethyl ether into dichloromethane solution of the compound. The crystallographic structure of $[\text{Re}(\sigma^2\text{-terpy})(\text{CO})_3\text{CH}_3\text{CN}]\text{PF}_6$ is shown in Figure 2.8. Corresponding bond lengths and angles and other relevant crystallographic properties are given in Table 4 and 3.

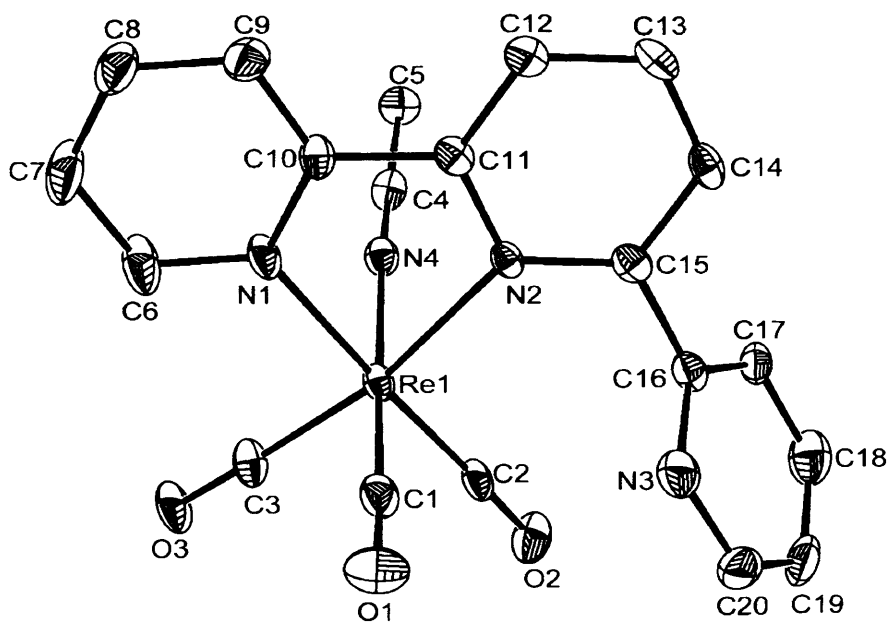


Figure 2.8 Ortep diagram of the cation present in $[\text{Re}(\sigma^2\text{-terpy})(\text{CO})_3\text{CH}_3\text{CN}]\text{PF}_6$ (2).

Thermal ellipsoids are drawn at 50% probability.

The coordination geometry at rhenium centre is almost identical with that of complex 1. The rhenium atom in the complex is six coordinated and possesses a distorted octahedral geometry with facially arranged carbonyl groups, a bidentate terpy and an acetonitrile donor. The ligand lies in a *cis,cis* orientation of the pyridine rings similar to that observed for 1. The $\text{Re}(1)\text{-N}(2)$ bond distance is 0.051 \AA longer than that of $\text{Re}(1)\text{-N}(1)$ due to the steric bulk of the uncoordinated pyridine ring, as found in complex 1. This steric bulk also affects the angle $\text{N}(2)\text{-Re}(1)\text{-C}(2)$ [$103.0(2)^\circ$], which is the largest angle between any two *cis* angles in the complex and leads to the distortion of its regular octahedral geometry. The Re-N bond distances arising from the acetonitrile moiety is

2.150(7) Å and may be compared to the corresponding bond lengths in complexes $\{\text{Re}(\text{CO})_3(\text{CH}_3\text{CN})[\text{CH}_2(\text{S-tim})_2]\}\text{PF}_6$ [2.1404(16)Å]⁶¹ (tim=1-methyl-thioimidazolyl), $[\text{NEt}_4][\text{Re}(\text{NO})\text{Br}_4(\text{CH}_3\text{CN})]$ [2.153(11)Å]⁶², $[(\text{CO})_3\text{Re}(\text{NCCH}_3)_3]\text{BF}_4$ (2.132-2.125 Å)⁶³ and $[\text{Re}(\text{bpy})(\text{CO})_3(\text{CH}_3\text{CN})]\text{ClO}_4$ [2.140(3) Å]⁶⁴.

The torsion angle between two co-ordinated pyridines is -4.6° and the torsion angle between the central pyridine and the non-coordinated pyridine is -61.7° [N(2)-C(15)-C(16)-N(3)] which is larger than the corresponding angle in compound 1.

Table 3. Crystal and structure refinement data for compounds 1-5.

Compound	1	2	3	4	5
Empirical formula	$\text{C}_{19}\text{H}_{12}\text{Cl}_4$ $\text{N}_3\text{O}_3\text{Re}$	$\text{C}_{20}\text{H}_{14}\text{F}_6\text{N}_4\text{O}_3$ PRe	$\text{C}_{19}\text{H}_{14}\text{F}_6\text{IN}_3\text{O}_3$ PRe	$\text{C}_{19}\text{H}_{14}\text{ClF}_6\text{N}_3$ O_3PRe	$\text{C}_{21}\text{H}_{17}\text{F}_{12}\text{N}_4\text{O}_3$ P_2Re
Formula weight	658.32	689.52	790.40	698.95	849.53
Temperature K	150(2)	150(2)	150(2)	150(2)	150(2)
Crystal system	Triclinic	Triclinic	Triclinic	Triclinic	Monoclinic,
Space group	P-1	P-1	P-1	P-1	P2(1)/n
a Å	9.8147(2)	8.3282(2)	6.9323(2)	6.8448(2)	11.3456(3)
b Å	14.8166(2)	10.9366(3)	13.0225(4)	12.7464(4)	12.0228(3)
c Å	16.3480(3)	13.5483(4)	13.5441(5)	13.4209(5)	20.3267(6)
α°	69.3790(7)	70.6089(12)	70.4699(11)	71.4100(10)	
β°	80.9599(7)	78.2809(11)	86.0787(12)	83.9550(10)	91.8990(10)
γ°	79.9672(8)	86.0682(13)	81.1926(18)	78.6090(10)	
Volume Å ³	2179.13(7)	1139.74(5)	1138.58(6)	1086.84(6)	2771.16(13)
Z	4	2	2	2	4
Density (Mg/m ³)	2.007	2.009	2.306	2.136	2.036
Absorption coefficient, mm ⁻¹	6.093	5.481	6.839	5.867	4.614
F(000)	1256	660	740	668	1632
Crystal size, mm	0.25 × 0.15 × 0.12	0.15 × 0.12 × 0.04	0.25 × 0.15 × 0.15	0.25 × 0.20 × 0.06	0.25 × 0.20 × 0.18
θ -range for data collection	2.92 - 27.46	2.94 - 27.53	2.97 - 27.40	3.04 - 27.54	3.14 - 27.58
Limiting indices	-12 ≤ h ≤ 12 -18 ≤ k ≤ 19 -21 ≤ l ≤ 21	-10 ≤ h ≤ 10, - 13 ≤ k ≤ 14 -17 ≤ l ≤ 17	-8 ≤ h ≤ 8 -16 ≤ k ≤ 16 -17 ≤ l ≤ 17	-8 ≤ h ≤ 8 -16 ≤ k ≤ 16 -17 ≤ l ≤ 17	-14 ≤ h ≤ 14 -14 ≤ k ≤ 15 -26 ≤ l ≤ 26
Reflections Collected/unique	35230 / 9846	17820 / 5172	21851 / 5122	19562 / 4959	18125 / 6233
R(int)	0.0760	0.1193	0.0948	0.0710	0.0745
Completeness to $\theta = 27.47^\circ$ %	98.7 %	98.4	99.0	98.7	97.0
Max. and min. transmission	0.5284 and 0.3111	0.8106 and 0.4936	0.4269 and 0.2797	0.7198 and 0.3217	0.4905 and 0.3917
Data / restraints / parameters	9846 / 0 / 541	5172 / 0 / 317	5122 / 0 / 308	4959 / 0 / 308	6233 / 30 / 426
Goodness-of-fit on F ²	1.038	1.053	1.046	1.038	1.016
Final R indices [I > 2 σ (I)]	R ₁ = 0.0346, wR ₂ = 0.0736	R ₁ = 0.0507, wR ₂ = 0.1208	R ₁ = 0.0413, wR ₂ = 0.0918	R ₁ = 0.0388, wR ₂ = 0.0793	R ₁ = 0.0448, wR ₂ = 0.0978
R indices (all data)	R ₁ = 0.0456, wR ₂ = 0.0787	R ₁ = 0.0614, wR ₂ = 0.1271	R ₁ = 0.0570, wR ₂ = 0.0986	R ₁ = 0.0507, wR ₂ = 0.0843	R ₁ = 0.0448, wR ₂ = 0.0978
Largest diff. peak and hole, e.Å ⁻³	3.813 and - 1.657	2.046 and - 2.397	1.787 and - 1.898	1.665 and - 1.937	2.870 and - 2.394

Table 4: Bond lengths (Å) and bond angles (°) for complexes

Compound	1	2	3	4	5
Re(1)-C(1)	1.905(5)	1.922(8)	1.919(8)	1.909(6)	1.907(7)
Re(1)-C(2)	1.915(5)	1.928(8)	1.913(8)	1.915(6)	1.924(6)
Re(1)-C(3)	1.923(5)	1.919(7)	1.900(7)	1.920(6)	1.918(6)
Re(1)-N(1)	2.159(4)	2.159(6)	2.149(6)	2.155(5)	2.164(4)
Re(1)-N(2)	2.234(4)	2.210(5)	2.206(5)	2.198(4)	2.191(4)
Re(1)-Cl(1)/N(4)/I(1)	2.5005(12)	2.150(7)	2.8138(5)	2.4997(15)	2.126(5)
C(1)-Re(1)-C(2)	88.4(2)	89.6(3)	86.1(3)	88.8(3)	83.8(2)
C(1)-Re(1)-C(3)	87.7(2)	89.0(3)	91.4(3)	85.5(2)	91.1(3)
C(2)-Re(1)-C(3)	86.5(2)	87.4(3)	91.2(3)	89.3(2)	89.3(3)
C(1)-Re(1)-N(1)	96.84(19)	94.2(3)	93.1(3)	95.0(2)	97.1(2)
C(2)-Re(1)-N(1)	96.06(17)	94.3(3)	94.6(3)	94.0(2)	94.3(2)
C(3)-Re(1)-N(1)	174.87(17)	175.9(3)	175.4(2)	177.2(2)	176.2(2)
C(1)-Re(1)-N(2)	169.60(19)	169.1(3)	166.9(3)	167.8(2)	170.6(2)
C(2)-Re(1)-N(2)	98.18(17)	94.3(3)	97.5(2)	97.4(2)	94.7(2)
C(3)-Re(1)-N(2)	100.67(17)	103.0(2)	103.3(2)	104.7(2)	103.6(2)
N(1)-Re(1)-N(2)	74.59(14)	75.0(2)	75.2(2)	74.47(17)	75.07(17)
C(1)-Re(1)-Cl(1)/N(4)/I(1)	92.01(15)	93.8(3)	89.0(2)	91.41(18)	89.3(2)
C(2)-Re(1)-Cl(1)/N(4)/I(1)	179.43(15)	174.6(2)	179.6(2)	177.36(18)	178.2(2)
C(3)-Re(1)-Cl(1)/N(4)/I(1)	93.17(15)	95.2(3)	89.0(2)	93.33(18)	92.5(2)
N(1)-Re(1)-Cl(1)/N(4)/I(1)	84.23(11)	82.3(2)	86.50(13)	85.78(13)	83.91(16)
N(2)-Re(1)-Cl(1)/N(4)/I(1)	81.42(10)	81.0(2)	82.34(12)	80.04(12)	84.69(16)

2.2.4.3 Crystallographic data for $[\text{Re}(\sigma^2\text{-terpyMe})(\text{CO})_3\text{I}]^+\text{PF}_6^-$ (3)

Recrystallization of $[\text{Re}(\sigma^2\text{-terpyMe})(\text{CO})_3\text{I}]^+\text{PF}_6^-$ from acetonitrile solution of the complex gave orange crystals suitable for X-ray crystallography studies. The solid-state structure of $[\text{Re}(\sigma^2\text{-terpyMe})(\text{CO})_3\text{I}]\text{PF}_6$ was determined (Figure 2.9). Relevant bond lengths and angles as well as unit cell parameters are shown in Table 4 and 3.

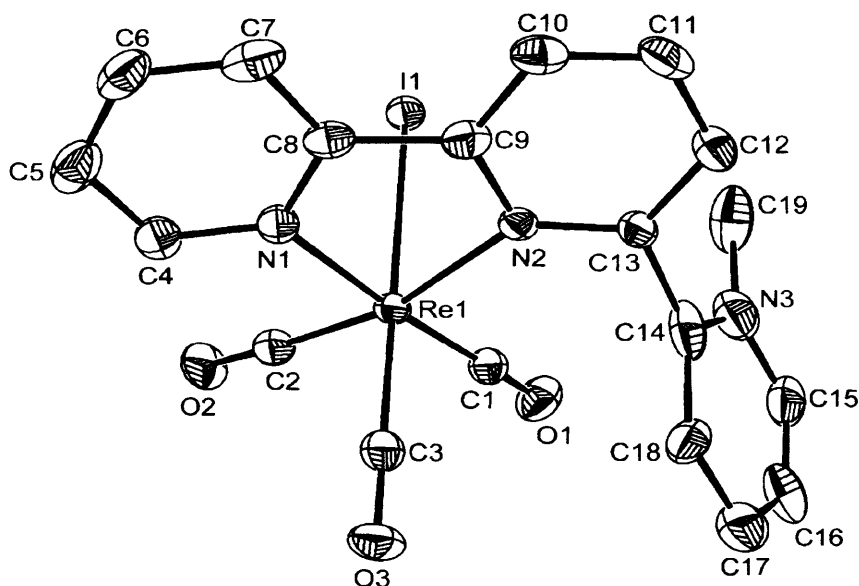


Figure 2.9 Ortep diagram of the cation present in $[\text{Re}(\sigma^2\text{-terpyMe})(\text{CO})_3\text{I}]\text{PF}_6$ (**3**).

Thermal ellipsoids are drawn at 50% probability.

The structure of the compound can be compared to that of the previously reported $\text{Re}(\sigma^2\text{-terpy})(\text{CO})_3\text{Cl}\cdot\text{H}_2\text{O}$ ⁵⁵. As expected, the methylated terpy ligand is coordinated in a bidentate η^2 mode, with the rhenium centre taking up a distorted octahedral coordination geometry containing facially arranged carbonyl groups. An iodide donor occupies the sixth coordination site. The terpy ligand is in *cis,trans* orientation, unlike compound **1** and **2**, to facilitate the introduction of the methyl group. Again, the $\text{Re}(1)\text{-N}(2)$ bond distance is 0.057 Å longer than that of $\text{Re}(1)\text{-N}(1)$, the same as shown in complex **1** and **2**. The distortion from regular octahedral geometry arises from the deviation of *cis* angles [75.2(2)°-103.3(2)°] and *trans* angles [166.9(3)°-179.6(2)°]. The two coordinated pyridyl rings are distorted away from planarity by a twist angle of -0.9°, while the central pyridyl ring and the methylated pyridine ring are distorted by an angle 112.9°. This latter torsion angle is comparable to that of the reported $\text{Re}(\sigma^2\text{-terpy})(\text{CO})_3\text{Cl}\cdot\text{H}_2\text{O}$ ⁵⁵. The Re-I bond length is 2.8138(5) Å which is comparable to the corresponding bond lengths 2.721(9) Å in $(\eta^5\text{-C}_5\text{H}_5)\text{Re}(\text{NO})(\text{PPh}_3)(\text{I})$ ⁶⁵.

Table 5. Comparison of torsion angles between the central pyridine ring and the non-coordinated or methylated pyridine rings of complexes **1-5**.

Compound	Torsion angle ($^\circ$)
$\text{Re}(\sigma^2\text{-terpy})(\text{CO})_3\text{Cl}$, 1	40.16(6)
$\text{Re}(\sigma^2\text{-terpy})(\text{CO})_3(\text{CH}_3\text{CN})^+\text{PF}_6^-$, 2	61.7(9)
$[\text{Re}(\sigma^2\text{-terpyMe})(\text{CO})_3\text{I}]^+\text{PF}_6^-$, 3	112.9(8)
$[\text{Re}(\sigma^2\text{-terpyMe})(\text{CO})_3\text{Cl}]^+\text{PF}_6^-$, 4	109.9(6)
$[\text{Re}(\sigma^2\text{-terpyMe})(\text{CO})_3(\text{CH}_3\text{CN})]^{2+}\text{PF}_6^-\text{BF}_4^-$, 5	96.3(7)

2.2.4.4 Crystallographic data for $[\text{Re}(\sigma^2\text{-terpyMe})(\text{CO})_3\text{Cl}]^+\text{BF}_4^-$ (**4**)

Crystallographic quality crystals of $[\text{Re}(\sigma^2\text{-terpyMe})(\text{CO})_3\text{Cl}]^+\text{BF}_4^-$ were obtained by slow vapour diffusion of diethyl ether in to an acetonitrile solution of the compound and the structure is shown in Figure 2.10. The bond lengths and bond angles are given in Table 4.

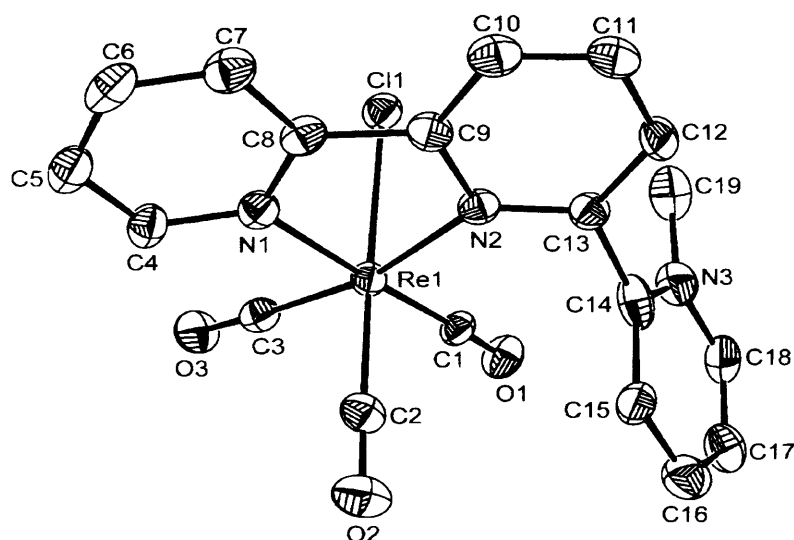


Figure 2.10 Ortep diagram of the cation present in $[\text{Re}(\sigma^2\text{-terpyMe})(\text{CO})_3\text{Cl}]^+\text{PF}_6^-$ (**4**).

Thermal ellipsoids are drawn at 50% probability.

The coordination geometry at the Re atom is again distorted octahedral with *trans* angles at the Re site ranging from $167.8(2)^\circ$ - $177.36(18)^\circ$. Like compound **3**, the terpy ligand is coordinated in a bidentate η^2 mode with the rhenium centre and affords *cis,trans* conformation in this structure. A chloride donor occupies the sixth coordination site of rhenium. The Re-C and Re-N bond distances lie in the range 1.909(6)-1.920(6) Å and 2.155(5)-2.198(4) Å respectively, similar to those found in complex **1**, **2** and **3** and other

$\text{Re}(\text{I})$ -polypyridine complexes⁶⁶. The torsion angle between the two coordinated pyridine rings is -3.7° , while the torsion angle between the central pyridine ring and the methylated pyridine is 109.9° .

2.2.4.5 Crystallographic data for $[\text{Re}(\sigma^2\text{-terpyMe})(\text{CO})_3\text{CH}_3\text{CN}](\text{PF}_6)_2$ (5)

$[\text{Re}(\sigma^2\text{-terpyMe})(\text{CO})_3\text{CH}_3\text{CN}](\text{PF}_6)_2$ was obtained from the acetonitrile reaction of complex 3 and recrystallized as greenish yellow crystals by slow vapour diffusion of diethyl ether into chloroform solution of the compound. The solid-state structure of $[\text{Re}(\sigma^2\text{-terpyMe})(\text{CO})_3(\text{CH}_3\text{CN})](\text{PF}_6)_2$ was determined (Figure 2.11). Relevant bond lengths and angles are shown in Table 4.

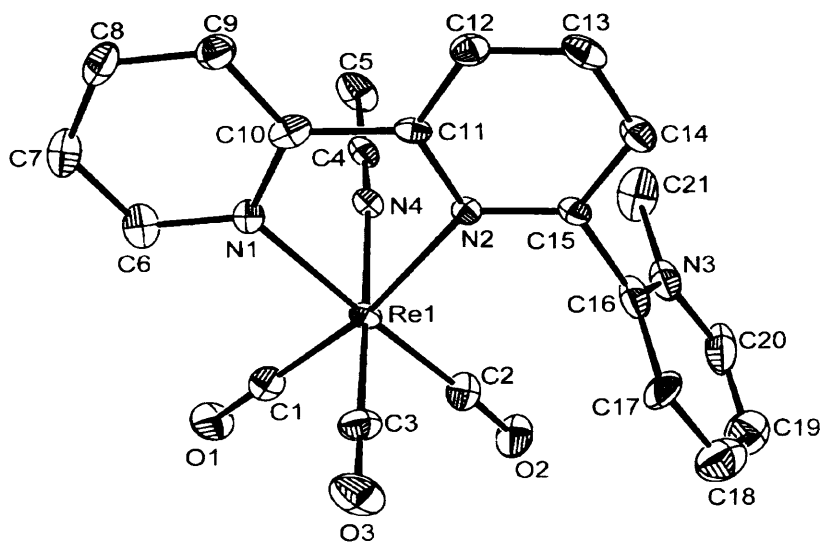


Figure 2.11 Ortep diagram of the cation present in $[\text{Re}(\sigma^2\text{-terpyMe})(\text{CO})_3\text{Cl}]\text{PF}_6$ (5). Thermal ellipsoids are drawn at 50% probability.

The rhenium atom in the complex is six coordinated and possesses distorted octahedral geometry with facially arranged carbonyl groups, a methylated terpy ligand having bidentate η^2 mode and an acetonitrile donor. The Re-C and Re-N bond distances are similar to those found in complexes 1, 2, 3 and 4. The *cis* angles at the Re centre vary from $75.07(17)^\circ$ - $103.6(2)^\circ$ and the *trans* angles vary from $170.6(2)^\circ$ - $178.2(2)^\circ$ which are also similar to those in the previous structures. The Re-N bond distance arising from the acetonitrile moiety is $2.216(5)^\circ$ which is comparable to complex 2 and other related complexes in the literature⁶¹⁻⁶⁴. The two coordinated pyridyl rings are distorted away from planarity by a twist angle of 4.3° , while the central pyridyl ring and the methylated

pyridine ring are distorted by an angle 96.3° . The latter angle is smaller than the corresponding angle in complexes **3** and **4** (Table-5).

2.2.5 Luminescence

The luminescence of $\text{Re}(\text{CO})_3(\text{bpy})\text{Cl}$ is well documented and has been the subject of numerous studies, as has been many of its derivatives, with the pyridine and acetonitrile adducts showing greatly improved quantum yields. On the other hand, $\text{Re}(\text{CO})_3(\text{terpy})\text{Cl}$ has been prepared previously and been reported as non-luminescent and no other derivatives of this compound have been reported. A possible explanation for the difference between the terpyridine and bipyridine complexes is that, in the former, there is substantial competition between emission from the MLCT state and that from MC state to which it is thermally coupled. In the bpy compound, this competition is diminished by the larger energy separation between the two states.⁶⁷ The absorption spectra of rhenium terpyridine complexes in the UV-Vis region occurs between 320-400 nm due to MLCT transitions [$\text{Re } d\pi \rightarrow \pi^*$ (LL)] and between 250-300 nm due to ligand centred $\pi \rightarrow \pi^*$ transitions. This is a common feature for rhenium(I) polypyridine complexes.^{47, 68}

Table 6. Excitation and emission wavelengths of 10^{-4} M solution of compound 1-5.

Compound	Excitation (λ_{max} , nm)	Emission (λ_{max} , nm)
$\text{Re}(\sigma^2\text{-terpy})(\text{CO})_3\text{Cl}$, 1	360	506
$\text{Re}(\sigma^2\text{-terpy})(\text{CO})_3(\text{CH}_3\text{CN})^+\text{PF}_6^-$, 2	360	510
$[\text{Re}(\sigma^2\text{-terpyMe})(\text{CO})_3\text{I}]^+\text{PF}_6^-$, 3	332	557
$[\text{Re}(\sigma^2\text{-terpyMe})(\text{CO})_3\text{Cl}]^+\text{PF}_6^-$, 4	335	556
$[\text{Re}(\sigma^2\text{-terpyMe})(\text{CO})_3(\text{CH}_3\text{CN})]^{2+}\text{PF}_6^-\text{BF}_4^-$, 5	330	560

Thus we have carried out initial studies to determine if any of the synthesised complexes are luminescent. Since dissolved oxygen does quench the MLCT excited state and rhenium complexes are extremely sensitive to the presence of oxygen, the measurements were carried out in degassed acetonitrile at room temperature to avoid quenching by oxygen. The luminescence measurements were performed in various concentrations of the compound in order to use the least concentrated sample and to avoid the inner filter effect. Except **6** and **7**, the MLCT excited state of these complexes is weakly to moderately emissive, both in solid state and in solution at room temperature.

Complexes **1** and **2** appear weakly luminescent. The principal emission peaks of 10^{-4} M solutions of **1** and **2** in acetonitrile are centred at 506 and 510 nm, respectively, for the MLCT excitation wavelength of 360 nm (Table 6), whereas the analogous bipyridine compounds showed strong emission under identical condition.^{47, 51} Compound **6** gives only ligand centred emission.

Only the methylated species **3**, **4** and **5** were found to be moderately luminescent in solid state as well as in solution at room temperature. This observation is in contrast with that of the published compounds like, $[\text{Re}(\text{bpm})(\text{CO})_3(\text{MQ}^+)]^{2+}$,⁶⁹ $[\text{Re}(\text{bpy})(\text{CO})_3(\text{MQ}^+)]^{2+}$,⁷⁰ $[\text{Os}(\text{bpy})_2(\text{CO})(\text{MQ}^+)]^{3+}$,⁷⁰ $[\text{MQ}^+=\text{N-methyl-4,4-bipyridinium ion}]$ and $[\text{Pt}(\text{C}^{\wedge}\text{N}^{\wedge}\text{C})\text{MQ}]\text{PF}_6$ ⁷¹ $[\text{HC}^{\wedge}\text{N}^{\wedge}\text{CH}=\text{2,6-diphenylpyridine}]$ where protonation or methylation generally lowered the energy of the π^* orbital of the ligand, shifted the MLCT transition to the lower energy and caused the quantum yield to drop.

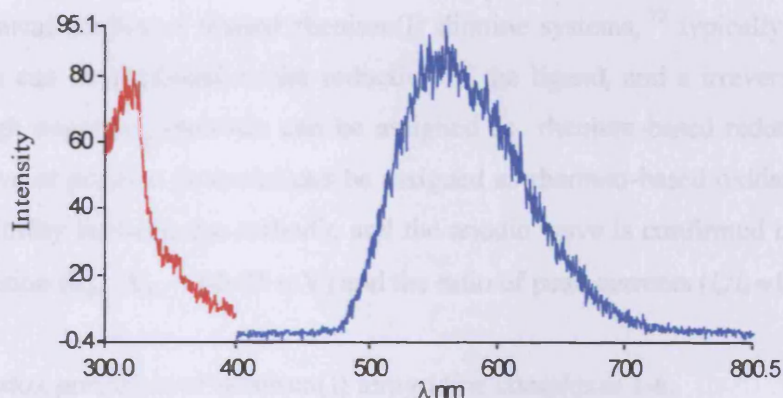


Figure 2.12 Excitation and emission spectra of compound **5** (10^{-4} M) in deoxygenated CH_3CN solution at 298K.

The emission peaks for the methylated complexes are red-shifted compared to that of the pendant pyridine ring containing complexes. The principal emission peaks of 10^{-4} M solutions of **3**, **4** and **5** in acetonitrile were centred at 550-560 nm for the excitation wavelength range 330-340 nm. Crude comparisons suggest complex **5** shows moderate emissive properties (Figure 2.12) compared to complexes **3** and **4**. However, as the emissions were not studied using isoabsorbing solutions, the emission spectrum of complex **5** may indicate a higher extinction coefficient rather than a higher quantum yield.

Complex **7** does not show any luminescence either in solid state or in solution. These preliminary observations are very surprising and as such warrant further investigation, as it was certainly expected that the presence of the methyl group would quench the luminescence with perhaps the luminescence being restored on the reduction of the metal centre.

2.2.6 Cyclic Voltammetry

The redox behavior of these complexes was studied by cyclic voltammetry. The electrochemical data are presented in Table 7. The measurements were performed using acetonitrile distilled over calcium hydride, with 0.1 M $[\text{NBu}_4][\text{PF}_6]$, as supporting electrolyte and 1-2 mM concentration of the sample at room temperature. Ferrocene was added at the end of each experiment as an internal reference, and all redox potentials are quoted vs. the ferrocene-ferrocenium couple. The measurements were carried out in the region from +2.00 to -2.00 V with a scan rate of 200 mVs^{-1} . With reference to previous electrochemical studies of related rhenium(I) diimine systems,⁷² typically the reversible redox wave can be attributed to the reduction of the ligand, and a irreversible reduction wave at high negative potentials can be assigned as rhenium-based reduction ($\text{Re}^0/\text{Re}^{\text{I}}$) and the wave at positive potential can be assigned as rhenium-based oxidation ($\text{Re}^{\text{I}}/\text{Re}^{\text{II}}$). The reversibility between the cathodic and the anodic wave is confirmed by the peak-to-peak separation ($E_{\text{pa}} - E_{\text{pc}} = 60\text{-}75 \text{ mV}$) and the ratio of peak currents ($i_{\text{a}}/i_{\text{c}} \approx 1$).

Table 7. Redox potentials of rhenium(I) terpyridine complexes **1-6**.

Compound	Reduction (V)	Oxidation(V)
$\text{Re}(\sigma^2\text{-terpy})(\text{CO})_3\text{Cl}$, 1	-1.741	0.786 ^{irr}
$\text{Re}(\sigma^2\text{-terpy})(\text{CO})_3(\text{CH}_3\text{CN})^+\text{PF}_6^-$, 2	-1.595, -1.797 ^{irr}	-
$[\text{Re}(\sigma^2\text{-terpyMe})(\text{CO})_3\text{I}]^+\text{PF}_6^-$, 3	-1.409 ^{irr} , -1.837 ^{irr}	1.047 ^{irr}
$[\text{Re}(\sigma^2\text{-terpyMe})(\text{CO})_3\text{Cl}]^+\text{PF}_6^-$, 4	-1.627 ^{irr} , -1.828 ^{irr}	0.841 ^{irr}
$[\text{Re}(\sigma^2\text{-terpyMe})(\text{CO})_3(\text{CH}_3\text{CN})]^{2+}\text{PF}_6^-\text{BF}_4^-$, 5	-1.353 ^{irr} , -1.609, -1.826 ^{irr}	-
$[\text{Re}(\sigma^2\text{-terpy})(\text{CO})_3(\text{NH}_2\text{C}_5\text{H}_5\text{N})]^+\text{PF}_6^-$, 6	-1.540	1.128 ^{irr}

The electrochemically irreversible oxidation observed in the region 0.786-1.128 V for compound **1**, **3**, **4** and **6** can be assigned to the oxidation of rhenium(I) centre. In contrast, no oxidation waves were seen for any of the acetonitrile complexes, **2** and **5**, suggesting that the rhenium oxidation peak is shifted past the anodic solvent limit for such

cationic species. This observation is also supported by the previous cyclic voltammetric studies of $\text{Re}(\text{bppz})(\text{CO})_3(\text{CH}_3\text{CN})^+$, $\text{Re}(\text{ppz})(\text{CO})_3(\text{CH}_3\text{CN})^+$ and $\text{Re}(\text{ddpq})(\text{CO})_3(\text{CH}_3\text{CN})^+$.⁷³

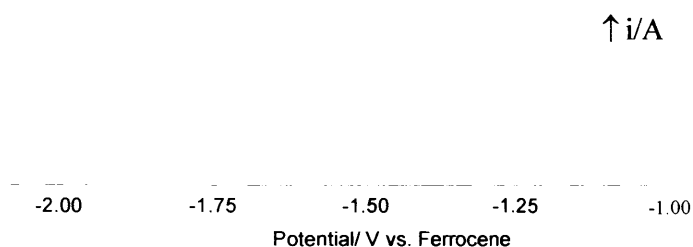


Figure 2.13 Cyclic voltammograms in the negative potential region of **5** measured in acetonitrile solution containing $n\text{-Bu}_4\text{NBF}_4$ (0.1 M) as an electrolyte.

The reductive waves are displayed in the region from -1.353 to -1.828 V (Figure 2.13). Most of the complexes showed a one electron reduction which can be attributed to the ligand centred process, except compound **3**. This reduction occurs at moderate potentials (~ -1.6 V) and is reversible for all the complexes, except compound **4**. Compound **1** displayed reduction at a higher negative potential compared to the rest of the complexes. This result is similar to the previously reported⁷⁴ electrochemical study of compound **1**. The irreversible reductions at higher negative potentials (~ -1.8 V) of compounds **2-5** can be assigned to the rhenium based reduction. Compounds **1** and **6** do not show Re^0/Re^1 reduction within the solvent range. However, the corresponding

reduction may be observed at potentials >-2.0 V. The reduction potential of the lower negative region (~ -1.4 V) demonstrated by compounds **3** and **5** can be confidently assigned to the pyridinium based reduction. These reductions are irreversible and are in good agreement with the reduction potentials of rhenium(I) polypyridine complexes containing pyridinium moiety^{69, 75}. In contrast, no such reduction was observed for the methylated species **4**. It is of note that the reduction potential of compound **4** at -1.627 V, which was assigned earlier of this study as terpyridine based reduction, was not reversible. So, one might expect this irreversible reduction for compound **4** as pyridinium based reduction.

2.2.7 Concluding remarks

The novel complexes $[\text{Re}(\sigma^2\text{-terpy})(\text{CO})_3(\text{CH}_3\text{CN})]\text{PF}_6$ (**2**), $[\text{Re}(\sigma^2\text{-terpyMe})(\text{CO})_3\text{I}]\text{PF}_6$ (**3**), $[\text{Re}(\sigma^2\text{-terpyMe})(\text{CO})_3\text{Cl}]\text{PF}_6$ (**4**), $[\text{Re}(\sigma^2\text{-terpyMe})(\text{CO})_3(\text{CH}_3\text{CN})](\text{PF}_6)_2$ (**5**), $[\text{Re}(\sigma^2\text{-terpy})(\text{CO})_3(\text{py-3-NH}_2)]\text{PF}_6$ (**6**) and $[\text{Re}(\sigma^2\text{-terpyMe})(\text{CO})_3(\text{py-3-NH}_2)][\text{PF}_6]_2$ (**7**) were successfully prepared in a reasonable yield. These complexes have been characterized by ^1H NMR, IR, mass spectroscopy and 2-D COSY spectrum. Complexes **1-5** have also been characterized by X-ray crystallography. Attempts to coordinate different metals to the pendant pyridine by the reactions of **1** in an acetonitrile solution of $\text{M}(\text{H}_2\text{O})_6^{2+}$ resulted in halide abstraction from the rhenium centre. Most of these complexes are weakly luminescent. However, **5** is interesting as it shows moderate luminescence. This is unusual considering other pyridinium containing complexes, such as $[\text{Re}(\text{bpy})(\text{CO})_3(\text{MQ})]^{2+}$ ($\text{MQ}^+ = \text{N-methyl-4,4'-bipyridinium}$), are typically quenched. Moreover, the compound undergoes reversible reduction which could be analyzed using cyclic voltammetry. Further work may focus on the substitution of **7**, so that it may be readily attached to biological molecules of interest.

2.3 Experimental

All preparations were carried out under an oxygen free inert atmosphere. Solvents were dried by standard procedures, distilled and used directly from the still. $\text{Re}(\text{CO})_5\text{Cl}$ and $\text{Re}(\text{CO})_{10}$ were purchased and were used without further purification. IR spectra were recorded in NaCl solution cells or in compressed KBr discs on a Perkin-Elmer 1600 or a Jasco 660 spectrophotometers. ^1H NMR was recorded on Bruker DP-400 spectrometer. Electronic spectra were run in HPLC grade acetonitrile on a Perkin-Elmer

20 or a Jasco V-570 UV-Vis spectrophotometer. Cyclic voltammograms were recorded with Autolab PGSTAT 12 Potentiometer with a Ag/AgNO_3 (0.1 M) reference electrode (BAS Non-aqueous Reference Electrode Kit). Electrochemical measurements were carried out in acetonitrile with 0.1 M $[\text{NBu}_4][\text{PF}_6]$ as supporting electrolyte. The supporting electrolyte was dried prior to use. Fluorescence spectra were recorded with Perkin-Elmer LS 50B luminescence spectrometer. Spectra measured in quartz SUPRASIL precision fluorescence cell. When necessary, samples were degassed by bubbling nitrogen through the solution. Perchlorate salts are potentially explosive. All compounds containing perchlorate should be handled with great care and in small amounts.

2.3.1 Preparation of 2,2':6',2'' terpyridine

A flame dried 1L 2-neck flask was purged with argon. Anhydrous THF (400 ml) and potassium t-butoxide (20g, 0.179mol) was added followed by 2-acetylpyridine(10.34g, 85.4 mmol). The solution was stirred at room temperature for two hours until a white solid formed. The β -(dimethyl-amino)vinyl 2-pyridyl ketone (15.03g, 85.4 mmol) was added in a single portion and the solution, which gradually turns a very deep red, was stirred at room temperature for 40-60 hours. The reaction mixture was cooled in ice and a solution of ammonium acetate (64.1g, 0.833mol) in acetic acid (200ml) was added with stirring. Methanol (40ml) was added, the flask fitted with a distillation head, the mixture heated to reflux and the THF gradually removed by distillation over a five-hour period. The distillation continued until the head temperature reached 115°C . The mixture was poured into water (400ml) and the acetic acid neutralized with sodium carbonate (~300g). Toluene (120ml) and celite (20g) was added and the mixture stirred and heated at 80°C . The mixture was cooled to room temperature and filtered through a pad of celite. The solid was broken up into a powder and washed with toluene (3x75ml). The organic layer of the filtrate was separated and the aqueous layer extracted with toluene (2x100ml). The combined organic layers were stirred with 25g of alumina(II) and filtered. The powder was evaporated down to give a brown oil which was dissolved in 80ml of chloroform and 40g of alumina(II) was added. The powder was added to the top of alumina(II) column and eluted with 20:1 cyclohexane/ethyl acetate. A light yellow fraction was collected and evaporated down to yield the pure product. Yield: 57%.

δ_{H} (400MHz, CDCl_3): 8.65(2H, ddd, J 4.7, 2.0, 0.9, $\text{H}_{6+6''}$), 8.58(2H, d, J 7.9, $\text{H}_{3+3''}$), 8.41(2H, d, J 7.7, $\text{H}_{3'+5'}$), 7.93(1H, t, J 7.4, H_4), 7.82(2H, m, $\text{H}_{4+4''}$), 7.30(2H, ddd, J 7.3, 4.8, 1.3, $\text{H}_{5+5''}$).

2.3.2 Preparation of $\text{Re}(\sigma^2\text{-terpy})(\text{CO})_3\text{Cl}$ (1):

Rhenium pentacarbonyl chloride (100 mg, 0.276 mmol) and 2,2':6',2''-terpyridine (64 mg, 0.014 mmol) were allowed to reflux in toluene (30 cm^3) under a nitrogen atmosphere for 1 hour. After the CO evolution had ceased, the precipitated complex, formed upon cooling to room temperature, was filtered out, washed with diethyl ether and dried under vacuum (60%).

Anal. Found: C 40.23, H 2.07, N 7.57%. Calc. for $\text{Re}(\sigma^2\text{-terpy})(\text{CO})_3\text{Cl}$: C 40.11, H 2.06, N 7.8%. IR (KBr): 2023s, 1922s, 1866s cm^{-1} . Mass spectrum (ES): m/z 540 (100) [M+H], 504 (95) [M-Cl], 511 (73) [M-CO], 483 (40) [M-2CO], 455 (39) [M-3CO].

δ_{H} (400MHz, CDCl_3): 9.05(1H, d, J 5.0, H_6), 8.76(1H, d, J 4.8, $\text{H}_{6''}$), 8.50(1H, d, J 8.6, $\text{H}_{3'}$), 8.48(1H, d, J 8.3, H_3), 8.28(1H, t, J 7.9, H_4), 8.21(1H, t, J 7.3, H_4), 7.96(1H, t, J 7.9, H_4), 7.79(1H, d, J 8.1, H_5), 7.78(1H, d, J 7.9, $\text{H}_{3''}$), 7.49(1H, t, J 5.2, H_5), 7.55(1H, t, J 4.7, $\text{H}_{5''}$)

2.3.3 Preparation of $[\text{Re}(\sigma^2\text{-terpy})(\text{CO})_3(\text{CH}_3\text{CN})]\text{PF}_6$ (2):

$\text{Re}(\text{terpy})(\text{CO})_3\text{Cl}$ (100 mg, 0.185 mmol) and silver perchlorate (41 mg, 0.197 mmol) were allowed to reflux in acetonitrile (100 cm^3) under nitrogen atmosphere in the dark for overnight. After cooling, the solution was filtered to remove insoluble AgCl and concentrated aqueous solution of potassium hexafluorophosphate was added to the reaction mixture. Partial removal of the solvent under vacuum and addition of water gave light green precipitates which were collected and recrystallized by slow diffusion of diethyl ether into an acetonitrile solution of the compound to yield the hexafluorophosphate complex in about 63% yield.

Anal. Found: C 34.86, H 2.07, N 7.99%. Calc. for $[\text{Re}(\sigma^2\text{-terpy})(\text{CO})_3\text{CH}_3\text{CN}]\text{PF}_6$: C 34.84, H 2.05, N 8.13%. IR(KBr): 2040s, 1941s cm^{-1} ; Mass spectrum (FAB): m/z 545 (100) [M- PF_6]; δ_{H} (400MHz, CD_3CN): 8.99(1H, d, J 5.3, H_6), 8.72(1H, d, J 4.6, $\text{H}_{6''}$), 8.50(1H, d, J 8.3, $\text{H}_{3'}$), 8.47(1H, d, J 8.5, H_3), 8.31(1H, t, J 8.0, H_4), 8.24(1H, t, J 8.0, H_4), 7.94(1H, td, J 7.9, 0.9, $\text{H}_{4''}$), 7.80(1H, d, J 7.7, H_5), 7.68(1H, d, J 7.6, $\text{H}_{3''}$), 7.66(1H, t, J 7.8, H_5), 7.53(1H, t, J 7.8, $\text{H}_{5''}$);

2.3.4 Preparation of $[\text{Re}(\sigma^2\text{-terpyMe})(\text{CO})_3\text{I}]\text{PF}_6$ (3):

$\text{Re}(\text{terpy})(\text{CO})_3\text{Cl}$ (160 mg, 0.2 mmol) and methyl iodide (1 g, 7.04 mmol) were allowed to reflux in acetonitrile (80 cm^3) under nitrogen atmosphere for overnight. After cooling the solution, concentrated aqueous solution of potassium hexafluorophosphate was added to the reaction mixture and acetonitrile was removed by slow evaporation under vacuum. The product was obtained as bright yellow powder (60%).

Anal. Found: C 28.57, H 1.84, N 5.64%. Calc. for $[\text{Re}(\sigma^2\text{-terpyMe})(\text{CO})_3\text{I}]\text{PF}_6$: C 28.87, H 1.79, N 5.32%; IR(CH_3CN), $\nu(\text{cm}^{-1})$ 2031s, 1939s, 1908vs; Mass spectrum (positive FAB): m/z 664 (100) $[\text{M-I}]$; δ_{H} (400MHz, CD_3CN): 9.23(1H, d, J 5.5, H_6), 9.02(1H, d, J 6.1, H_6^{r}), 8.88(1H, t, J 7.3, H_4^{r}), 8.85(1H, d, J 8.2, H_3^{r}), 8.71(1H, d, J 8.3, H_3), 8.55(1H, t, J 8.0, H_4^{r}), 8.41-8.36(2H, m, $\text{H}_4+\text{H}_5^{\text{r}}$), 8.30(1H, d, J 7.8, H_3^{r}), 8.01 + 7.95(1H (4:1), dd, J 1.1, 7.8, H_5^{r}), 7.81(1H, td, J 7.1, 1.3, H_5), 4.30 + 4.07(3H (3:1), s, $-\text{CH}_3$).

2.3.5 Preparation of $[\text{Re}(\sigma^2\text{-terpyMe})(\text{CO})_3\text{Cl}]\text{PF}_6$ (4):

$\text{Re}(\text{terpy})(\text{CO})_3\text{Cl}$ (168 mg, 0.31 mmol) and $(\text{CH}_3)_3\text{OBF}_4$ (46 mg, 0.31 mmol) were allowed to reflux in acetonitrile (80 cm^3) under nitrogen atmosphere for 1h. The product was obtained by complete evaporation of the solvent in a yield of 70%.

Anal. Found: C 32.42, H 1.84, N 5.64%. Calc. for $[\text{Re}(\sigma^2\text{-terpyMe})(\text{CO})_3\text{Cl}]\text{PF}_6$: C 32.65, H 2.02, N 6.01%; IR(CH_3CN), $\nu(\text{cm}^{-1})$ 2036s, 1941vs, 1907vs; Mass spectrum (ES): m/z 552/4 (50/100) $[\text{M-PF}_6]$; δ_{H} (400MHz, CD_3CN): 9.09(1H, dd, J 1.0, 5.5, H_6), 8.94(1H, d, J 6.6, H_6^{r}), 8.79(1H, td, J 8.0, 0.9, H_4^{r}), 8.77(1H, dd, J 1.0, 8.2, H_3^{r}), 8.62(1H, d, J 8.2, H_3), 8.49(1H, t, J 8.1, H_4^{r}), 8.33(1H, td, J 8.1, 1.6, H_4), 8.29(1H, td, J 7.9, 1.5, H_5^{r}), 8.24(1H, d, J 7.9, H_3^{r}), 7.92(1H, dd, J 1.2, 7.8, H_5^{r}), 7.75(1H, td, J 6.4, 1.3, H_5),

2.3.6 Preparation of $[\text{Re}(\sigma^2\text{-terpyMe})(\text{CO})_3(\text{CH}_3\text{CN})](\text{PF}_6)_2$ (5):

This complex was prepared in an analogous way to 2. $[\text{Re}(\text{terpy})(\text{CO})_3\text{I}]\text{PF}_6$ (32 mg, 0.057 mmol) and silver perchlorate (0.012 g, 0.057 mmol) were allowed to reflux in acetonitrile (30 cm^3) under nitrogen atmosphere in the dark for overnight. After cooling, the solution was filtered, concentrated aqueous solution of KPF_6 was added and the reaction mixture was reduced to 5 cm^3 by slow evaporation under vacuum and left in the

refrigerator for cooling. After two days light green crystals were obtained in a yield of 50%.

Anal. Found: C 29.54, H 1.78, N 6.34%. Calc. for $[\text{Re}(\sigma^2\text{-terpyMe})(\text{CO})_3(\text{CH}_3\text{CN})](\text{PF}_6)_2$: C 29.69, H 2.02, N 6.60%; IR(CH_3CN), $\nu(\text{cm}^{-1})$ 2043s, 1943s, 1931vs, 1915m; Mass spectrum (positive FAB): m/z 560 (8) $[\text{M}-2\text{PF}_6]$; δ_{H} (400MHz, CD_3CN): 8.99(1H, d, J 5.2, H_6), 8.89(1H, d, J 6.1, H_6^{a}), 8.709(1H, t, J 6.4, H_4^{a}), 8.705(1H, d, J 1.0, 8.2, H_3^{a}), 8.574 + 8.568(1H(3:2), d, J 8.3/8.1, H_3), 8.475 + 8.468(1H (3:2), t, J 8.0/8.0, H_4^{a}), 8.32(1H, t, J 7.9, H_4), 8.26-8.22(1H, m, H_5^{a}), 8.128+8.069(1H (3:2), d, J 7.8/7.0, H_3^{a}), 7.89(1H, t, J 7.7, H_5^{a}), 7.75(1H, t, J 8.0, H_5), 4.09 + 4.04(3H (3:2), s, $-\text{CH}_3$)

2.3.7 Preparation of $[\text{Re}(\sigma^2\text{-terpy})(\text{CO})_3(\text{py-3-NH}_2)]\text{PF}_6$ (6):

$[\text{Re}(\text{terpy})(\text{CO})_3(\text{CH}_3\text{CN})]\text{PF}_6$ (70 mg, 0.101 mmol) and 3-aminopyridine (191 mg, 2.03 mmol) were allowed to reflux in THF (50 cm^3) under nitrogen atmosphere for two hours. After the solution had cooled, cold hexane was added, resulting in the precipitation of the product, which was then filtered and dried (yield 80%).

Anal. Found: C 37.01, H 2.47, N 9.13%. Calc. for $[\text{Re}(\sigma^2\text{-terpy})(\text{CO})_3(\text{py-3-NH}_2)]\text{PF}_6$: C 37.2, H 2.31, N 9.43%; IR(CH_3CN), $\nu(\text{cm}^{-1})=2035, 1935, 1923$; Mass spectrum (positive FAB): m/z 598 (48) $[\text{M}-\text{PF}_6]$, 504 (25) $[\text{M}-\text{PF}_6-\text{NH}_2\text{C}_5\text{H}_5\text{N}]$; δ_{H} (400MHz, CD_3CN): 9.26(1H, d, J 5.2, H_6), 8.86(1H, d, J 4.0, H_6^{a}), 8.43(1H, d, J 7.8, H_3^{a}), 8.41 (1H, d, J 7.9, H_3), 8.34(2H, t, J 8.0, $\text{H}_{4+4^{\text{a}}}$), 8.08(1H, t, J 7.4, H_4^{a}), 7.96(1H, d, J 7.2, H_3^{a}), 7.85(2H, d, J 7.4, $\text{H}_5+\text{H}_5^{\text{a}}$), 7.67(1H, t, J 5.9, H_5^{a}), 7.35 (1H, d, J 2.4, a, py-NH_2), 7.21 (1H, d, J 5.2, b, py-NH_2), 7.01 (1H, m, d, py-NH_2), 6.92(1H, m, c, py-NH_2), 3.52 (2H, s, $-\text{NH}_2$).

2.3.8 Preparation of $[\text{Re}(\sigma^2\text{-terpyMe})(\text{CO})_3(\text{py-3-NH}_2)][\text{PF}_6]_2$ (7):

$[\text{Re}(\text{terpy})(\text{CO})_3(\text{py-3-NH}_2)]\text{PF}_6$ (27 mg, 0.036 mmol) and Me_3OBF_4 (6 mg, 0.036 mmol) were allowed to reflux in acetonitrile (20 cm^3) under nitrogen atmosphere for overnight. Acetonitrile was then removed by evaporation under vacuum. (yield 40 %).

Anal. Found: C 31.78, H 2.11, N 7.65%. Calc. for $[\text{Re}(\sigma^2\text{-terpyMe})(\text{CO})_3(\text{py-3-NH}_2)][\text{PF}_6]_2$: C 31.94, H 2.23, N 7.76%; IR (KBr), $\nu(\text{cm}^{-1}) = 2023.6, 1918.5, 1895.3$; Mass spectrum (positive FAB): m/z 613 (35) $[\text{M}-\text{PF}_6]_2$; δ_{H} (400MHz, CD_3CN): 8.99(1H, d, J 5.6, H_6), 8.75(1H, d, J 4.8, H_6^{a}), 8.55(1H, dd, J 7.2, 0.8, H_3^{a}), 8.50(1H, d, J 8.4, H_3),

8.34(1H, t, J 8.0, H_4), 8.25 (1H, td, J 7.9, 0.6, H_4), 8.12(1H, td, J 7.6, 0.6, H_4), 7.87 (1H, d, J 2.4, a, py-NH₂), 7.83(1H, dd, J 8, 0.8, H_3), 7.79 (2H, m, H_5 + b, py-NH₂), 7.67(2H, d, J 6.8, $\text{H}_{5+5'}$), 7.61(1H, m, d, py-NH₂), 7.55 (1H, m, c, py-NH₂).

2.3.9 Attempted preparation of $[\text{Re}(\sigma^2\text{-terpy})(\text{CO})_3(\phi\text{-thiourea})]\text{PF}_6$

$[\text{Re}(\text{terpy})(\text{CO})_3(\text{py-3-NH}_2)]\text{PF}_6$ (15 mg, 0.013 mmol) and phenyl isothiocyanate (2.7 mg, 0.013 mmol) were added to a mixture of acetonitrile (5 cm³) and triethylamine (0.5 cm³). The mixture was then incubated in dark for overnight. The resulting mixture was sticky and despite numerous attempts the product could not be purified.

2.3.10 Attempted to coordinate the pendant N-atom of $\text{Re}(\text{CO})_3(\sigma^2\text{-terpy})\text{Cl}$:

1. $\text{Re}(\text{CO})_3(\text{terpy})\text{Cl}$ (50 mg, 0.092 mmol), $\text{Fe}(\text{CO})_5$ (40 mg, 0.0178 mmol) and Me_3NO (14 mg, 0.125 mmol) were dissolved in dichloromethane (30 cm³) in ice bath under nitrogen. The reaction mixture was then warmed to room temperature and stirred to react for several hours. The solvent was then evaporated under vacuum and the product was collected. IR (KBr): ν (cm⁻¹) = 2018.2, 1925.5, 1912.9, 1891.4. The IR spectrum is identical to that of the starting materials providing no evidence of complex formation, with no peaks due to a $\text{Fe}(\text{CO})_5$ species.

2. $\text{Re}(\text{CO})_3(\text{terpy})\text{Cl}$ (50 mg, 0.092 mmol) and $\text{W}(\text{CO})_6$ (40 mg, 0.092 mmol) were allowed to reflux in acetonitrile (30 cm³) under nitrogen for overnight. The solvent was then evaporated to obtain the product. IR (KBr): ν (cm⁻¹) = 2018.7, 1924.3, 1913.5, 1891.1. The IR spectrum is identical to that of the starting materials providing no evidence of complex formation, with no peaks due to a $\text{W}(\text{CO})_5$ species.

3. $\text{Re}(\text{CO})_3(\text{terpy})\text{Cl}$ (50 mg, 0.092 mmol) and $\text{Zn}(\text{ClO}_4)_2$ (17.2 mg, 0.046 mmol) were allowed to stir in acetonitrile (30 cm³) under nitrogen for overnight. Concentrated aqueous KPF_6 was then added and acetonitrile was removed by slow evaporation under vacuum. IR (CH_3CN): ν (cm⁻¹) = 2039.5, 1940.4, 1932.8. The IR spectrum is identical to that of compound **2**. The formation of **2** is also confirmed by ¹H NMR spectrum.

4. $\text{Re}(\text{CO})_3(\text{terpy})\text{Cl}$ (50 mg, 0.092 mmol) and $\text{Fe}(\text{ClO}_4)_2$ (7 mg, 0.027 mmol) were allowed to stir in acetonitrile under nitrogen for 4 hr. Concentrated aqueous KPF_6 was then added and acetonitrile was removed by slow evaporation under vacuum. IR

(CH_3CN): ν (cm^{-1}) = 2039.6, 1941.1, 1930. The IR spectrum is identical to that of compound **2**.

5. $\text{Re}(\text{CO})_3(\text{terpy})\text{Cl}$ (40 mg, 0.074 mmol) and ZnCl_2 (10 mg, 0.073 mmol) were allowed to stir in acetonitrile under nitrogen for overnight. Acetonitrile was then evaporated to obtain the product. IR (CH_3CN): ν (cm^{-1}) = 2039.5, 1939.2. The IR spectrum also suggests the formation of compound **2**.

References

1. E. C. Constable, *Adv. Inorg. Chem. Radiochem.*, 1986, **30**, 69.
2. E. C. Constable and J. Lewis, *Polyhedron*, 1982, **1**, 303.
3. E. C. Constable, F. K. Khan, J. Lewis, M. C. Liptort and P. R. Raithby, *J. Chem. Soc., Dalton Trans.*, 1985, 333.
4. A. Livoreil, C. O. Dietrich-Buchecker and J. -P. Sauvage, *J. Am. Chem. Soc.*, 1994, **116**, 9399.
5. V. -M. Mikkala, M. Helenius, I. Hemmila, J. Kanare and H. Takalo, *Helv. Chim. Acta*, 1993, **76**, 1361.
6. V. Hemmila, V. -M. Mikkala, M. Latva and P. Kiilholma, *J. Biochem. Biophys. Methods*, 1993, **26**, 283.
7. A. K. Saha, K. Kross, E. D. Kloszewski, D. A. Upson, J. L. Toner, R. A. Snow, C. D. V. Black and V. C. Desai, *J. Am. Chem. Soc.*, 1993, **115**, 1032.
8. G. Chelucci, M. A. Cabras and A. Saba, *J. Mol. Catal. A*, 1995, **95**, L7.
9. Y. Liang and R. H. Schmehl, *J. Chem. Soc. Chem. Commun.*, 1995, 1007.
10. J. -P. Collin, S. Guillerez and J. -P. Sauvage, *J. Chem. Soc. Chem. Commun.*, 1989, 776.
11. J. -P. Collin, S. Guillerez, J. -P. Sauvage, F. Barigelletti, L. De Cola, L. Flamigni and V. Balzani, *Inorg. Chem.*, 1991, **30**, 4230.
12. B. Zak, E. S. Baginski, E. Epstein and L. M. Weiner, *Clin. Chim. Acta.*, 1970, **29**, 77.
13. L. -X. Zhao, T. S. Kim, S.-H. Ahn, T.-H. Kim, E.-K. Kim, W.-J. Cho, H. Choi, C.-S. Lee, J.-A. Kim, T.C. Jeong, C.-J. Chang and E.-S. Lee, *Bioorganic & Medicinal Chemistry Letters*, 2001, **11**, 2659.
14. G.T. Morgan and F.H. Burstall, *J. Chem. Soc.*, 1932, 20.
15. G.T. Morgan and F.H. Burstall, *J. Chem. Soc.*, 1937, 1649.
16. E. C. Constable, M. D. Ward, *Inorg. Chim. Acta*, 1988, **141**, 201-203.
17. K. T. Potts, P. Ralli, G. Theodoridis and P. Winslow, *Org. Synth.*, 1986, **64**, 189.
18. K. T. Potts, D. A. Usifer, A. Guadalupe and H. D. Abruna, *J. Am. Chem. Soc.*, 1987, **109**, 3961.
19. D. L. Jameson and L. E. Guise, *Tetrahedron Lett.*, 1991, **32**, 1999-2002.
20. Y. Yamamoto, T. Tanaka, M. Yagi and M. Inamoto, *Heterocycles*, 1996, **42**, 189-194.

21. J. P. Sauvage, J. P. Collin, J. C. Chambron, S. Guillerez, C. Coudret, V. Balzani, F. Barigelletti, L. De Cola and L. Flamigni, *Chem. Rev.*, 1994, **94**, 993.
22. B. N. Trawick, A. T. Daniher and J. K. Bashkin, *Chem Rev.*, 1998, **98**, 939.
23. A. Harriman and R. Ziessel, *Coord. Chem. Rev.*, 1998, **171**, 331.
24. H. M. Brothers and N. M. Kostic, *Inorg. Chem.*, 1988, **27**, 1761.
25. A. M. W. C. Thompson, *Coord. Chem. Rev.*, 1997, **160**, 1-52.
26. E. C. Constable, J. Lewis, M. C. Liptort and P. R. Raithby, *Inorg. Chim. Acta*, 1990, **178**, 47.
27. W. Spahni and G. Calzaferri, *Helv. Chim. Acta*, 1984, **67**, 450.
28. M. Licini, J. A. G. Williams, *Chem. Commun.*, 1999, 1943.
29. E. C. Constable and A. M. W. C. Thompson, *J. Chem. Soc., Dalton Trans.*, 1992, 2947.
30. V. Hedge, Y. Jahng, R.P. Thummel, *Tetrahedron Lett.*, 1987, **28**, 4023.
31. G. W. V. Cave, C. L. Raston and J. L. Scott, *Chem. Commun.*, 2001, 2159.
32. G. W. V. Cave and C. L. Raston, *Chem. Commun.*, 2000, 2199.
33. G. W. V. Cave, M. J. Hardie, B. A. Roberts and C. L. Raston, *Eur.J. Org. Chem.*, 2001, 3227.
34. C. B. Smith, C. L. Raston and A. N. Sobolev, *Green Chem.*, 2005, **7**, 650.
35. C. A. Bessel, R. F. See, M. R. Churchill and Takeuchi, *J. Chem. Soc., Dalton Trans.*, 1992, 3223.
36. E. C. Constable, C. E. Housecroft, M. Neuburger, D. Phillips, P. R. Raithby, E. Schofield, E. Sparr, D. A. Tocher, M. Zehnder and Y. Zimmermann, *J. Chem. Soc., Dalton Trans.*, 2000, 2219.
37. E. C. Constable, F. K. Khan, V. E. Marquez and P. R. Raithby, *Acta Crystallogr. Sect. C*, 1992, **48**, 932.
38. R. D. Chapman, R. T. Loda, J. P. Riehl and R. W. Schwartz, *Inorg. Chem.*, 1984, **23**, 1652. E. W. Abel, N. J. Long, K. G. Orrell, A. G. Osborne, H. M. Pain and V. Sik, *J. Chem. Soc., Chem. Commun.*, 1992, 303. A. L. Crumbliss and A. T. Poulos, *Inorg. Chem.*, 1975, **14**, 1529.
39. G. B. Deacon, J. M. Patrick, B. W. Skelton, N. C. Thomas and A. H. White, *Aust. J. Chem.*, 1984, **37**, 929.
40. N. C. Thomas and J. Fisher, *J. Coord. Chem.*, 1990, **21**, 119.
41. C.A. Berg-Brennan, D.I. Yoon, R.V. Slone, A.P. Kazala and J.T. Hupp. *Inorg. Chem.*, 1996, **35**, 2032.

42. V.W.-W. Yam, V.C.Y.-Lau, K.-K. Cheung, *J. Chem. Soc. Chem. Commun.*, 1995, 259.
43. K.K.-W. Lo, D. C.-M Ng, W.-K. Hui and K.-K. Cheung, *J. Chem. Soc., Dalton Trans.*, 2001, 2634; K.K.-W. Lo, W.-K. Hui, D. C.-M Ng and K.-K. Cheung, *Inorg. Chem.*, 2002, **41**, 40.
44. M. Wrighton and D.L. Morse, *J. Am. Chem. Soc.*, 1974, **96**, 998.
45. A. Juris, S. Campagna, I. Bidd, J.-M. Lehn and R. Ziessel, *Inorg. Chem.*, 1988, **27**, 4007.
46. E.R. Civitello, P.S. Dragovich, T.B. Karpishin, S.G. Novick, G. Bierach, J.F. O'Connell and T.D. Westmoreland, *Inorg. Chem.*, 1993, **32**, 237.
47. L. A. Worl, R. Duesing, P. Y. Chen, C. L. Della, T. J. Meyer, *J. Chem. Soc., Dalton Trans.*, 1991, 849.
48. J. J. Turner, M. W. George, F. P. A. Johnson, J. R. Westwell, *Coord. Chem. Rev.*, 1993, **125**, 101.
49. J. R. Schoonover, C. A. Bignozzi, T. J. Meyer, *Coord. Chem. Rev.*, 1997, **165**, 239.
50. K. K.-W. Lo, W.-K. Hui, C.-K. Chung, K. H.-K. Tsang, D. C.-M. Ng, N. Zhu, K.-K. Cheung, *Coord. Chem. Rev.*, 2005, **249**, 1434.
51. J.V. Casper and T.J. Meyer, *J. Phys. Chem.*, 1983, **87**, 952.
52. W. J. Kirkham, A. G. Osborne, R. S. Nyholm and M.H.B. Stiddard, *J. Chem. Soc.*, 1965, 550.
53. G. D. Hess, F. Hampel, J. A. Gladysz, *Organometallics*, 2007, **26**, 5129.
54. J.C. Luong, L. Nadjo and M.S. Wrighton, *J. Am. Chem. Soc.*, 1978, **100**, 5790;
55. L.W. Houk and G.R. Dobson, *Inorg. Chem.*, 1966, **5**, 2119.
56. G.J. Stor, S.L. Morrison, D.J. Stufkens and A. Oskam, *Organometallics*, 1994, **213**, 2641.
57. E. W. Abel, V. S. Dimitrov, N. J. Long, K. G. Orrell, A. G. Osborne, H. M. Pain, V. Sik, M. B. Hursthouse and M. A. Mazid, *J. Chem. Soc., Dalton Trans.*, 1993, 597.
58. P. A. Anderson, F. R. Keene, E. Horn, and E. R. T. Tiekink, *Appl. Organomet. Chem.*, 1990, **4**, 523.
59. Y. Chen, L. Zhang and Z. Chen, *Acta Cryst.*, 2003, **E59**, m429.
60. S. H-F. Chong, S. C-F. Lam, V. W-W. Yam, N. Zhu, K-K. Cheung, S. Fathallah, K. Costuas and J-F. Halet, *Organometallics*, 2004, **23**, 4924.

61. R. M. Silva, B. J. Liddle, S. J. Lindeman, M. D. Smith and J. R. Gardinier, *Inorg. Chem.*, 2006, **45**, 6802.
62. G. Ciani, D. Giusto, M. Manassero and M. Sansoni, *J. Chem. Soc., Dalton Trans.*, 1975, 2156.
63. L. Y. Y. Chan, E. E. Isaacs and W. A. G. Graham, *Can. J. Chem.*, 1977, **55**, 111.
64. Y. -D. Chen, L. -Y. Zhang and Z. -N. Chen, *Acta Crystallogr. Sect. E*, 2005, **44**, 9601.
65. C. H. Winter, W. R. Veal, C. M. Garner, A. M. Arif and J. A. Gladysz, *J. Am. Chem. Soc.*, 1989, **111**, 998.
66. L. Wallace, C. Woods and D. P. Rillema, *Inorg. Chem.*, 1995, **34**, 2875.
67. K. Kalyanasundaram, Polypyridyl complexes of Ru, Os and Fe. In *Photochemistry of Polyridine and porphyrin Complexes*; Academic Press, San Diego, 1992; p 105.
68. J. D. Dattelbaum, O. O. Abugo and J. R. Lakowicz, *Bioconjugate Chem.*, 2000, **11**, 533.
69. R. J. Shaver, M. W. Perkovic, D. P. Rillema and C. Woods, *Inorg. Chem.*, 1995, **34**, 5446.
70. P. Chen, M. Curry and T. J. Meyer, *Inorg. Chem.*, 1989, **28**, 2271.
71. W. L. Michael, C. W. Chan, K. K. Cheung, and C. M. Che, *Organometallics*, 2001, **20**, 2477-2486.
72. F. Paolucci, M. Marcaccio, C. Paradisi, S. Roffia, C. A. Bignozzi and C. Amatore, *J. Phys. Chem. B*, 1998, **102**, 4759; S. Frantz, J. Fiedler, I. Hartenbach, T. Schleid and W. Kaim, *Organometallics*, 2004, **689**, 3031.
73. B. J. Yoblinski, M. Stathis and T. F. Guarr, *Inorg. Chem.*, 1992, **31**, 5.
74. A. Klein, C. Vogler and W. Kaim, *Organometallics*, 1996, **15**, 236.
75. S. Berger, A. Klein and W. Kaim, *Inorg. Chem.*, 1998, **37**, 5664.

Chapter 3

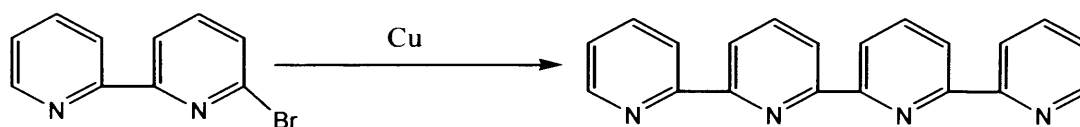
**Quaterpyridine complexes of $\text{Re}(\text{CO})_3^+$
moiety**

3.1. Introduction

The tetradentate chelating ligand 2,2':6',2'':6'',2'''-quaterpyridine fills an intermediate position between 2,2'-bipyridine and 2,2':6',2''-terpyridine, which are mononucleating, and the higher oligopyridines which may be polynucleating.¹ While 2,2'-bipyridine and 2,2':6',2''-terpyridine and their substituted derivatives have been subjected to extensive works, there are comparatively fewer studies on 2,2':6',2'':6'',2'''-quaterpyridine.²

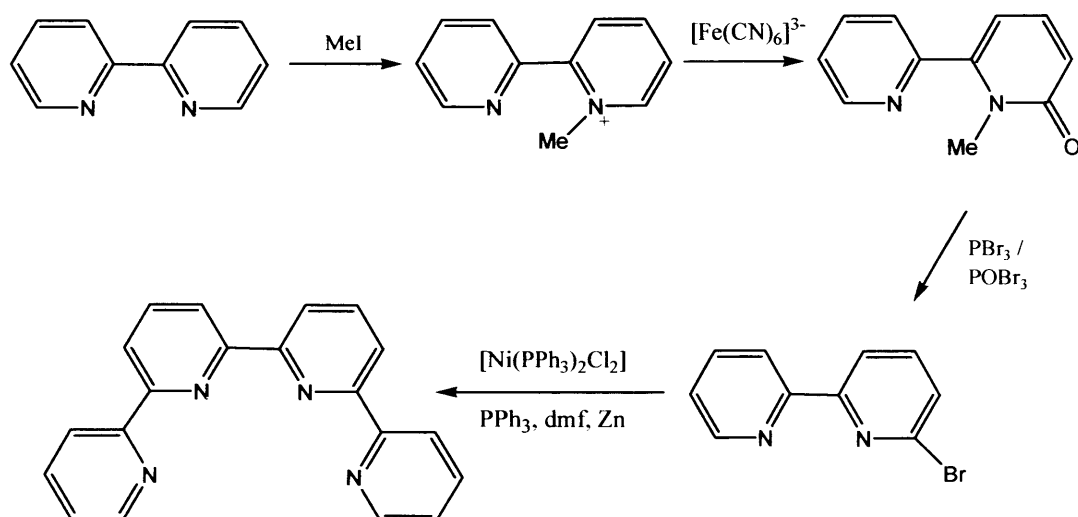
3.1.1 Synthesis of 2,2':6',2'':6'',2'''-quaterpyridine (qpy)

Oligopyridines containing even numbers of pyridine rings can be synthesized by either the symmetrical coupling of smaller units or by the formation of pyridine rings from acyclic precursors. Hence 2,2':6',2'':6'',2'''-quaterpyridine and its derivatives may be prepared using coupling methods.³ 2,2':6',2'':6'',2'''-quaterpyridine was first synthesized in 1938 by the high temperature coupling of 6-halo-2,2'-bipyridines in the presence of copper powder⁴ (scheme 3.1), which was reported to give a yield of 30%. The yield varies depending of the nature of copper used and the purity of the 6-halo-2,2'-bipyridine.



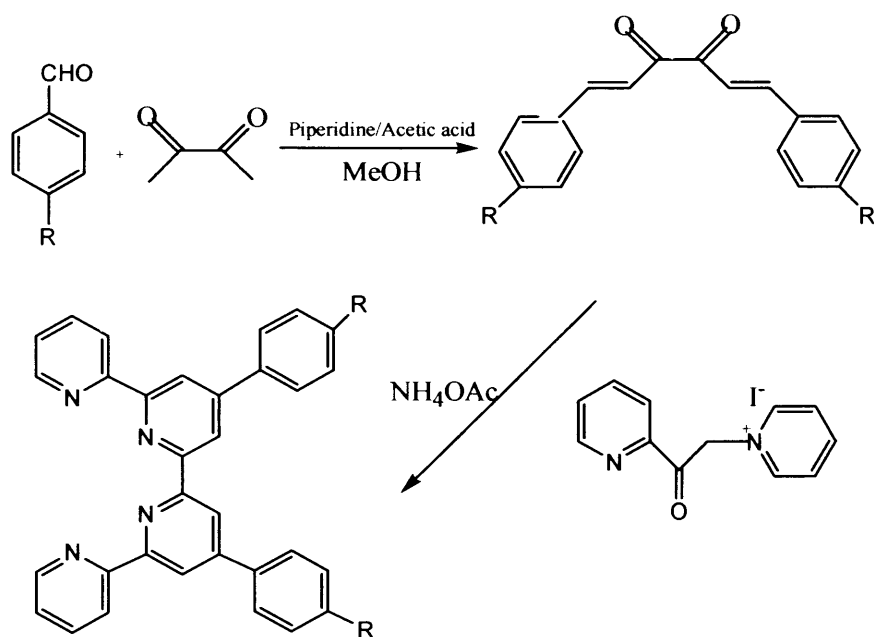
Scheme 3.1 Synthesis of 2,2':6',2'':6'',2'''-quaterpyridine by the high temperature coupling of 6-halo-2,2'-bipyridines

A metal directed synthetic route for the preparation of 2,2':6',2'':6'',2'''-quaterpyridine has also been reported.⁵ A stoichiometric amount of a nickel(0) species generated *in situ* by zinc reduction of $[\text{NiCl}_2(\text{PPh}_3)_2]$ in dimethylformamide in the presence of an excess of triphenylphosphine has been used (scheme 3.2). The reaction initially yields a nickel (II) complex of 2,2':6',2'':6'',2'''-quaterpyridine which may be demetallated by treatment with NaCN. Yields of the ligand were typically in the range of 40-45%.



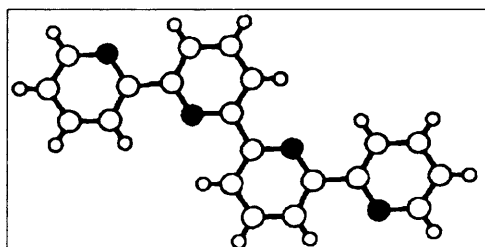
Scheme 3.2 Synthesis of 2,2':6',2'':6'':2'''-quaterpyridine by using Nickel.

The preparation of 4',4''-disubstituted ligands by the coupling reactions of halo-2,2'-bipyridines is not easy. Constable *et al*⁶ developed an easy route to synthesize 2,2':6',2'':6'':2'''-quaterpyridine and its derivatives by the generation of a central 2,2'-bipyridine unit from the acyclic moiety 1,6-diaryllhexa-1,5-diene-3,4-dione. Utilizing the methodology described by Sorenson and co-workers⁷, 1,6-diaryllhexa-1,5-diene-3,4-dione was prepared as orange crystals from the reaction of diacetyl with an excess of appropriately substituted benzaldehyde in methanol using piperidinium acetate as catalyst. The product undergoes cyclization by the reaction with the Kröhnke reagent *N*-[2-(2-pyridyl)-2-oxoethyl]pyridinium iodide⁸ in the presence of ammonium acetate (scheme 3.3) to give 4',4''-diaryl-2,2':6',2'':6'':2'''-quaterpyridines as a colourless solid in a yield of 50% after recrystallization.



Scheme 3.3 Synthesis of substituted quaterpyridines where $R = \text{H}, \text{CMe}_3, \text{Me}, \text{OMe}, \text{CF}_3, \text{Cl}$.

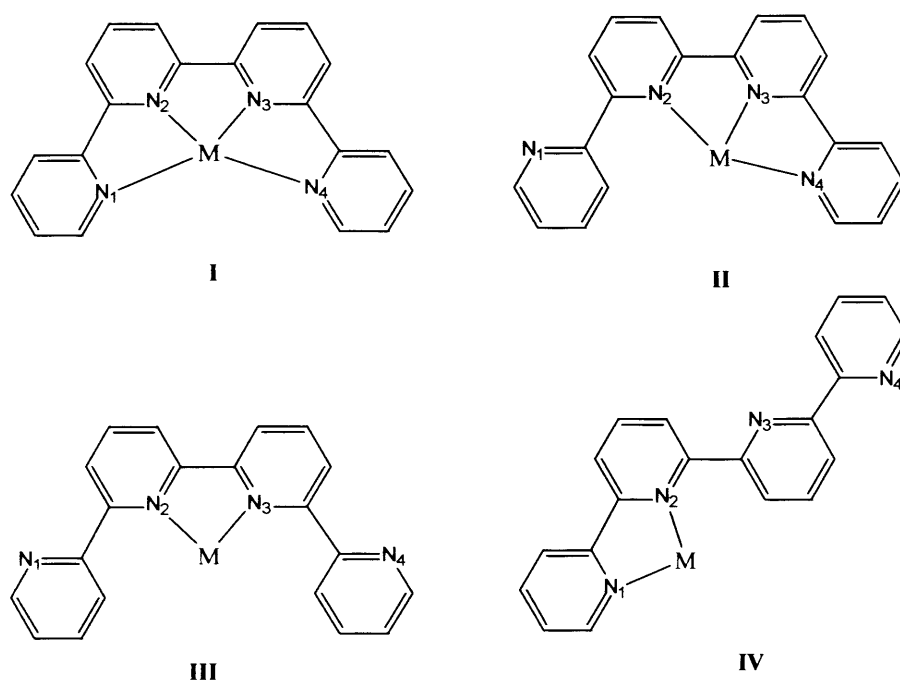
3.1.2 Coordination of 2,2':6',2'':6'',2'''-quaterpyridine with metals



Scheme 3.4 *Trans, trans, trans* conformation of qpy

The ligand qpy is planar with a trans, trans, trans conformation in the solid state⁶ (scheme 3.4). On coordination, the ligand may bind in several different modes (scheme 3.5), such as a planar quaterdentate ligand, I, a terdentate ligand with a non-coordinated pyridine, II, and as a bidentate ligand with either two non-coordinated terminal pyridines containing N1 and N4 nitrogen atoms, III, or a non-coordinated bipyridine involving N3 and N4 nitrogen atoms (or the equivalent N1 and N2 nitrogen atoms), IV.

The planar quaterdentate mode is primarily associated with metal ions with a ligand-field preference for square-planar or octahedral coordination geometry and has been structurally confirmed for a range of metal ions.^{5, 9-19} In the case of an octahedral centre, the ligand will occupy the four equatorial sites. Thus the majority of the complexes of qpy contain a near-planar ligand. This is found for the octahedral $[\text{Ni}(\text{qpy})(\text{MeCN})_2]^{2+}$ complex and the square planar $[\text{Pd}(\text{qpy})]^{2+}$ complex.^{5,9}

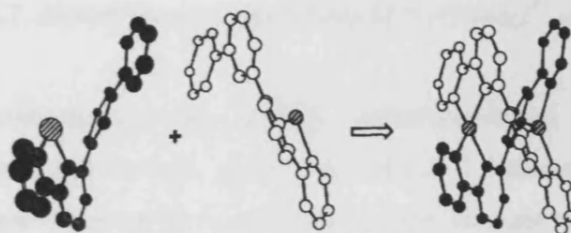


Scheme 3.5 Possible bind modes of 2,2':6',2'':6'',2'''-quaterpyridine

The complex in which qpy ligand coordinates to a six-coordinated metal centre in a hypodentate tridentate mode is $[\text{Ru}(\text{tpy}-\text{N},\text{N}',\text{N}'')(\text{qtpy}-\text{N},\text{N}'\text{N}'')](\text{PF}_6)_2$ ²⁰⁻²¹. If a metal ion is too small for the coordination cavity, resulting from the all cis conformation of the ligand, it is expected to coordinate to only some, but not all, of the donor atoms. Similarly, if a metal ion is too large for the coordination cavity in the all cis conformation, twisting should occur to minimize unfavourable steric interaction. Coordination of qpy to a larger metal ion with a preference for a high coordination number also results in the formation of a complex containing a planar quaterdentate qpy ligand, as seen in the complex cation $[\text{Y}(\text{qpy})(\text{NO}_3)_2(\text{H}_2\text{O})]^{+}$ ²² in

which the yttrium(III) centre ($r = 1.075 \text{ \AA}$) has no ligand field imposed geometries, but has a charge imposed preference for higher coordination number.

The situation is rather different for large metal ions of low charge. A d^{10} metal ion such as copper (I) and silver (I) has a steric preference for a tetrahedral arrangement. On coordination with qpy they form dinuclear double-helical complexes (scheme 3.6) where qpy behaves as a bridging ligand.^{18, 23} Helication derives from the twisting about the interannular C-C bond of the coordinated qpy.

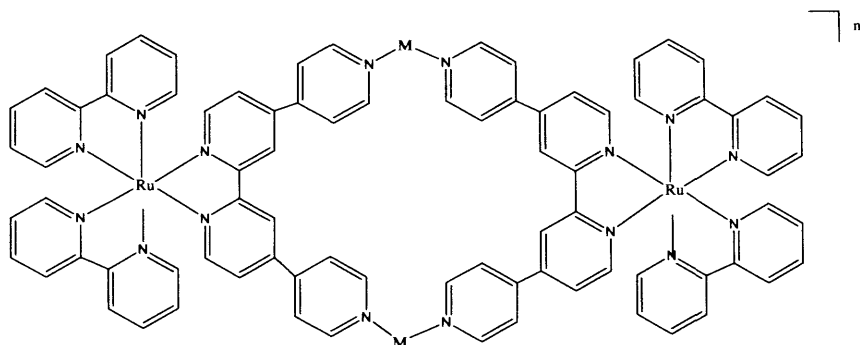


Scheme 3.6 Helical complex of quaterpyridine

We will not discuss helication to any further extent, as our works did not involve the synthesis of quaterpyridine helices but organometallic compounds of qpy, however for further reading the topic has recently been reviewed by Constable.^{18-19, 23-24}

3.1.3 Organometallic compounds of quaterpyridine

The complexes of Re^I and Pt^{IV} with 2,2':6',2'':6'',2'''-quaterpyridine [$\{\text{Re}(\text{CO})_3\text{Br}\}_2\text{L}$] {where $\text{L} = 2,2':6',2'':6'',2'''$ -quaterpyridine (QP), 4',4''-bis(4-*tert*-butylphenyl) -2,2':6',2'':6'',2'''-quaterpyridine (BPQP), 5,5',3'',5'''-tetramethyl-2,2':6',2'':6'',2'''-quaterpyridine (Me_4QP), $[\text{ReBr}(\text{CO})_3\text{QP}]$ and $[(\text{PtI}\text{Me}_3)_2(\text{QP})]$, have been studied previously.²⁵ Only [$\{\text{Re}(\text{CO})_3\text{Br}\}_2(\text{Me}_4\text{QP})$] was found to be luminescent in fluid solution at room temperature. The complexes of 2,2':4,4'':4',4'''-quaterpyridine (qtpy) with Re^I , Pt^{II} and Pd^{II} metal centres, $[\text{Re}(\text{qtpy})(\text{CO})_3\text{X}]$ ($\text{X} = \text{Cl}$, Br or CH_3CN), $[\text{M}(\text{qtpy})\text{L}]^{2+}$ ($\text{M} = \text{Pt}^{II}$ or Pd^{II} and $\text{L} = \text{en}$ or dppp), have recently been reported.²⁶ These complexes can be used as building blocks in the synthesis of metallomacrocycles. An example of metallomacrocycles²⁷ is shown in scheme 3.7.



Scheme 3.7 Metallomacrocycles where $M = [\text{Pd}(\text{en})]^{2+}$ or $\text{Re}(\text{CO})_3\text{Cl}$

These metallomacrocycles display ruthenium-based luminescence. The interaction of mono- and bicyclic molecules such as 1,4-dimethoxybenzene and 1-naphthanol with these macrocycles in aqueous solution changes the absorption spectra. As a result these complexes can be used to recognize aromatic molecules in water by luminescence titrations.²⁷

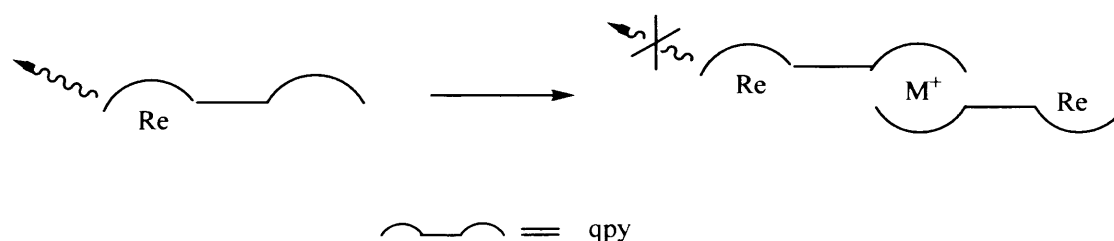
3.1.4 Solubility of 2,2':6',2'':6'',2''':6''',2''''-quaterpyridine

The quaterpyridine ligand tends to be extremely insoluble, although interaction with metal ions yields soluble ionic complexes. The insolubility of the free ligand is primarily due to the efficient graphitic stacking of the planar molecules in crystal lattice. In view of this limitation, Potts has introduced alkylthio substituents to aid the solubility of the ligands.^{28,29} The thioether substituents may be converted to other functional groups, but yields are not always high. The introduction of the phenyl substituents into the 4' and 4'' positions of the quaterpyridine was found to have little effect on the formation and the behaviour of complexes with metal ions compared to those formed with the unsubstituted quaterpyridine. Although this ligand had limited solubility in organic solvents, it was sufficiently soluble to allow its characterization by the usual spectroscopic techniques. Subsequently, Constable has introduced aryl substituents upon the periphery of oligopyridines utilizing Krohnke methodology.¹⁹ The introduction of 4-*tert*-butylphenyl substituents onto 2,2':6',2'':6'',2''':6''',2''''-quaterpyridine enhanced the solubility of the ligand and its complexes in common organic solvents.³⁰ While using the ligand 4',4''-diphenyl-2,2':6',2'':6'',2''':6''',2''''-quaterpyridine, we have also experienced difficulties in preparing and characterizing the rhenium complexes due to the insolubility of the ligand. To overcome this

situation we have prepared 4',4''-bis(4-*iso*-propylphenyl) -2,2':6',2'':6'',2'''-quaterpyridine, which is better in terms of solubility, and used this ligand for the synthesis of the rhenium complexes.

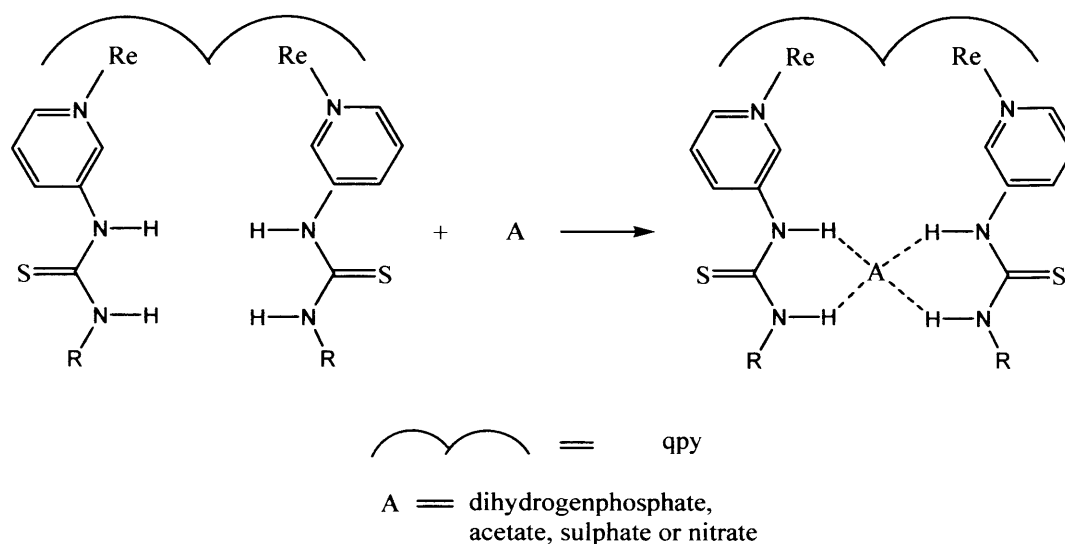
3.1.5 Aim of the work

Our aims are to synthesis multinuclear polyridine complexes containing more than one bipyridine unit and investigate their spectroscopic and photophysical properties. These complexes may then be explored for the construction of hosts with potentially luminescent centres. In this context, the reaction of d^6 $\text{Re}(\text{I})$ metal centre has been investigated. Rhenium complexes of quaterpyridine ligand were prepared to construct mononuclear and dinuclear luminescent rhenium centres. The mono-rhenium complexes of quaterpyridine can be used to bind cations to the pendant bipyridine units. The binding of the cation can then be observed by following changes in luminescence in the complexes (scheme 3.8).



Scheme 3.8 Cation bind mode of mono-rhenium quaterpyridine complex

Therefore, these complexes might be used in the detection of metal ions in biological systems. In case of the dirhenium complexes, the substitution of chloride ions with moieties such as thiourea, can lead to host molecules containing bidentate receptor sites (scheme 3.9). The host molecule may then bind anions, such as, dihydrogenphosphate, acetate, sulphate or nitrate through hydrogen bonding in solution that can be observed by change in luminescence. Thus useful bimetallic sensors can be built.



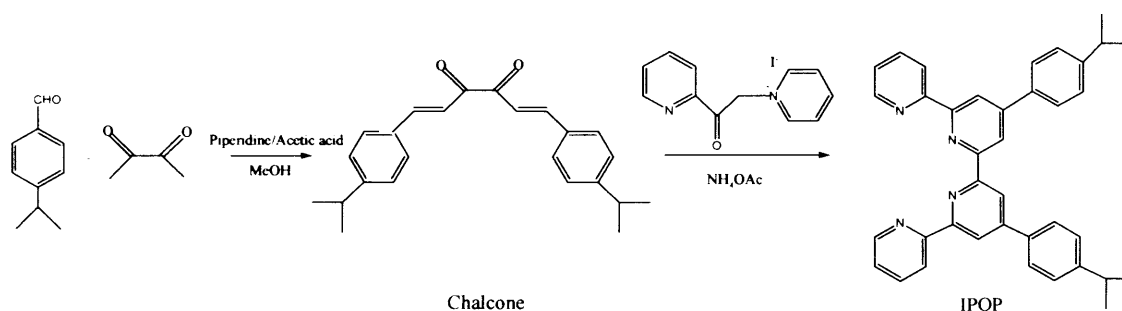
Scheme 3.9 Anion bind mode of dirhenium quaterpyridine complex

3.2 Results and Discussion

This section includes the synthesis of the ligand (3.2.1) and rhenium complexes (3.2.2-5), followed by their spectroscopic studies: IR and mass spectra (3.2.6.1) and ^1H NMR spectra (3.2.6.2), X-ray crystallographic studies (3.2.7) and electronic and luminescence properties (3.2.8).

3.2.1 Synthesis of the ligand

The ligand IPQP was prepared in 3 steps (scheme 3.10), analogous to a literature procedure,³⁰ where the 4-*tert*-butylphenyl quaterpyridine was prepared using Krohnke methodology.



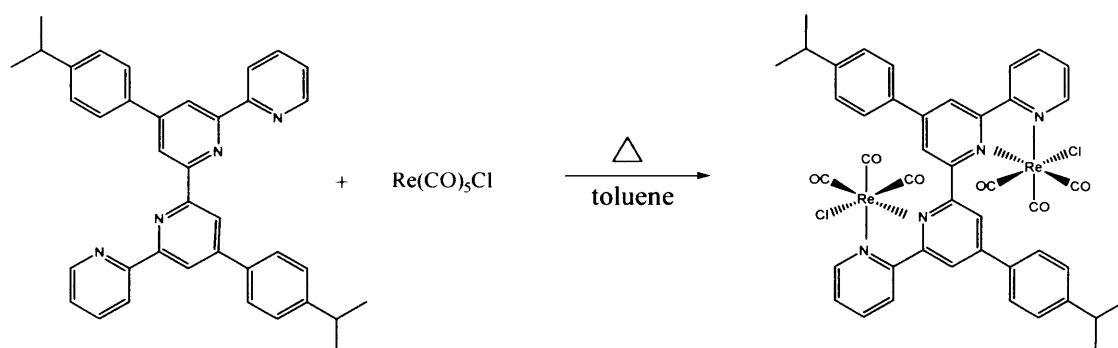
Scheme 3.10 Preparation of 4',4''-bis(4-iso-propylphenyl)-2,2':6',2''-quaterpyridine (IPQP)

The reaction of diacetyl with *iso*-propyl benzaldehyde in MeOH with piperidinium acetate as catalyst resulted in the formation of 1, 6-*bis*(4-*iso*-propylphenyl)-1,5-diene-3,4-dione as bright orange crystals in a yield of 9%. Although the yield was poor, unreacted material can be recovered. The convenience of this synthesis and the low cost of the starting material, isopropyl benzaldehyde compared to *tert*-butylbenzaldehyde, make this chalcone an attractive intermediate for the synthesis of IPQP. 4',4''-*bis*(4-*iso*-propylphenyl) -2,2':6',2'':6'',2'''-quaterpyridine was isolated as an off-white solid, in a yield of 34% from the reaction of chalcone with *N*-[1-oxo-2-(2-pyridyl)ethyl]pyridinium iodide in the presence of ammonium acetate. It is readily soluble in common organic solvents such as chloroform, dichloromethane and acetonitrile. This new ligand was characterized by the presence of a molecular ion at m/z 546 in its EI mass spectrum. In addition, the ^1H NMR spectra showed the expected number of peaks, as will be discussed later in this chapter.

4',4''-diphenyl -2,2':6',2'':6'',2'''-quaterpyridine was also prepared by following this 3 step route where benzaldehyde was used instead of isopropyl benzaldehyde.

3.2.2 Synthesis of $\{\{\text{ReCl}(\text{CO})_3\}_2\text{L}\}$ (8) [$\text{L}=4',4''\text{-bis}(4\text{-iso-propylphenyl})\text{-}2,2':6',2'':6'',2'''\text{-quaterpyridine}$ (IPQP) and 4',4''-diphenyl-2,2':6',2'':6'',2'''-quaterpyridine(Ph_2qtpy)]

The reaction of 4',4''-*bis*(4-*iso*-propylphenyl)-2,2':6',2'':6'',2'''-quaterpyridine with an equimolar amount of $\text{Re}(\text{CO})_5\text{Cl}$ was carried out in toluene under nitrogen using conditions similar to a literature procedure (scheme 3.11).³¹ The product was precipitated from the solution.



Scheme 3.11 Preparation of $\{\{\text{ReCl}(\text{CO})_3\}_2(\text{IPQP})\}$ (8)

The compound was initially expected to be mononuclear $[\text{ReCl}(\text{CO})_3(\text{IPQP})]$. However, the presence of eight resonances instead of sixteen resonances (for monorhenium species) in the aromatic region of NMR spectrum provides the evidence of the formation of dinuclear $[\{\text{ReCl}(\text{CO})_3\}_2(\text{IPQP})]$ complex, **8**. The FAB mass spectrum of the complex gave peaks that were consistent with the molecular ion $[\{\text{ReCl}(\text{CO})_3\}_2(\text{IPQP})]^+$ and the molecular ion minus halogen $[\{\text{Re}(\text{CO})_3\}_2(\text{IPQP})\text{Cl}]^+$. The yield of the reaction is only 42%. This low yield suggests that mono-rhenium compound was also formed and remained in the solution while comparatively heavier compound, **8**, precipitated out. The solvent was completely evaporated from the solution to obtain the solid product. However, the IR spectrum of the solid was not consistent with $[\text{Re}(\text{CO})_3]^+$ moiety which indicates that neither mono- nor di-rhenium complexes were present in the solution.

Higher yields (81%) of compound **8** were obtained by running the reaction stoichiometrically, that is, 4',4''-bis(4-iso-propylphenyl)-2,2':6',2'':6'',2'''-quaterpyridine with two equivalents of $\text{Re}(\text{CO})_5\text{Cl}$ under same reaction conditions. The compound **8** is stable at room temperature in solution and orange crystals were obtained by the slow vapour diffusion of diethyl ether into an acetonitrile solution of the compound. Attempts to prepare the 1:1 complex using an excess amount of ligand were also unsuccessful. The only product obtained during the reaction is 2:1 complex that was characterized by NMR and mass spectrometry. 4',4''-diphenyl-2,2':6',2'':6'',2'''-quaterpyridine also gave 2:1 complex, $[\{\text{ReCl}(\text{CO})_3\}_2(\text{Ph}_2\text{qtpy})]$, with $\text{Re}(\text{CO})_5\text{Cl}$ in refluxing toluene. This compound is less soluble in most of the solvents compared to compound **8** and difficult to use for further reaction.

The formation of 1:1 complexes $[\text{Re}(\text{CO})_3(\text{qpy})\text{Br}]$, $[\text{Re}(\text{CO})_3(\text{BPQNP})\text{Br}]$ (qpy = 2,2':6',2'':6'',2'''-quaterpyridine, BPQNP=4',4'''-bis(4-tert-butylphenyl)-2,2':6',2'':6'',2''':6''',2''''-quinquepyridine) have been reported by *Gelling et al*²⁴ though they have experienced difficulty in synthesizing these mononuclear complexes due to the strong electron donor properties of the two pairs of pyridyl N atoms. They have used the bromide species that might facilitate the reaction to occur for steric reason, while we failed to obtain mono-rhenium complexes by using chloride species. Otherwise, there might be two possibilities why we were unable to obtain monorhenium compound (1) The solubility of the ligand in toluene or (2) the formation of the monorhenium compound has been pre-organised which leads the

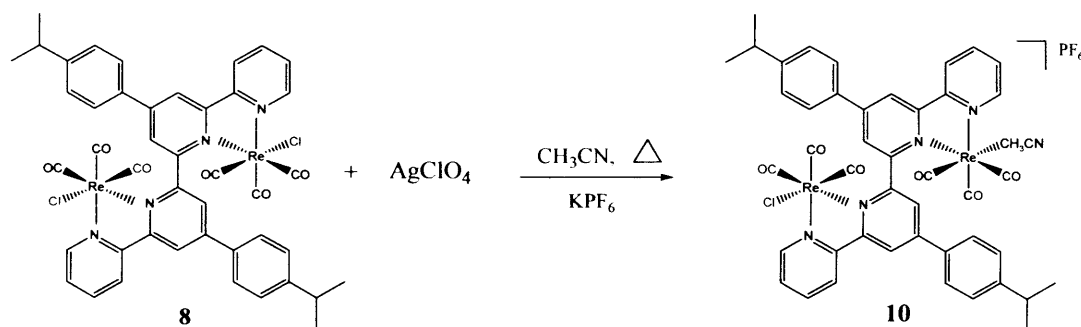
other rhenium to react with the 1:1 complex rather than the ligand itself. However, the reason is uncertain in this case.

An alternative synthesis was attempted. The reaction of $\text{Re}_2(\text{CO})_{10}$ with 4',4''-diphenyl-2,2':6',2'':6'',2'''-quaterpyridine and four equivalents of trimethylamine oxide was carried out in CH_2Cl_2 . The solution slowly turned yellow in colour. The solvent was removed under reduced pressure. The IR spectrum of the compound was encouraging. It was similar to the *fac*- $\text{ReX}(\text{CO})_3$ moiety. But ^1H NMR spectrum of the compound does not bear a resemblance to that of compound **8**. The product was recrystallised from acetonitrile solution by the slow diffusion of diethyl ether vapour. A few light orange crystals were obtained together with a yellow powder. The crystals were separated and the X-ray crystallography studies revealed the formation of $[\text{Re}_2(\text{Ph}_2\text{qtpy})(\text{CO})_6(\mu\text{-OH})][\text{ReO}_4]$, **9**. However, this was not stoichiometric and compound **9** can be considered as a by-product of the reaction.

Although compound **8** has weak luminescence both in solid state (visual) and in solution, it might be possible that the luminescence may be tuned by substituting the chloride ligand of compound **8** with a nitrogen donor ligand. However, the absence of a chloride atom and being a by-product of the reaction no further investigation was carried out with compound **9**.

3.2.3 Synthesis of $[\text{Re}_2(\text{IPQP})(\text{CO})_6(\text{CH}_3\text{CN})\text{Cl}]\text{PF}_6$ (**10**)

$\text{Re}_2(\text{IPQP})(\text{CO})_6\text{Cl}_2$ was reacted with two equivalents of $\text{Ag}(\text{ClO}_4)$ in acetonitrile in a reaction analogous to the synthesis of $[\text{Re}(\text{bipy})(\text{CO})_3(\text{CH}_3\text{CN})]\text{PF}_6$ (scheme 3.12)³².



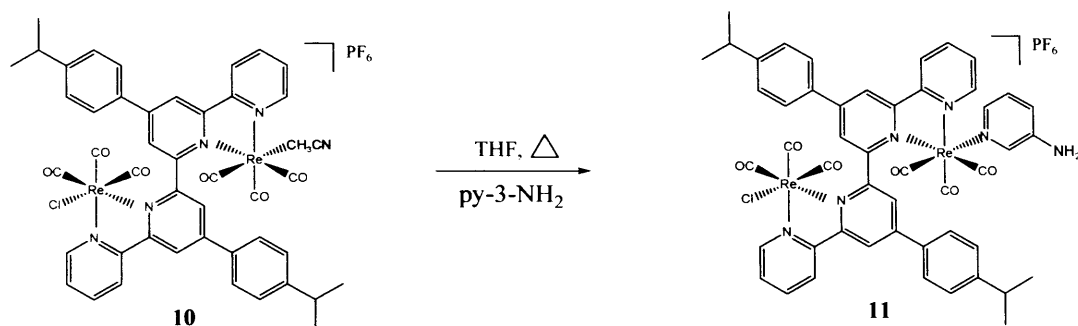
Scheme 3.12 Preparation of $[\text{Re}_2(\text{IPQP})(\text{CO})_6(\text{CH}_3\text{CN})\text{Cl}]\text{PF}_6$ (**10**)

The reaction was monitored by observing the change of the solution IR spectrum at 30 min intervals. A band at 2039 cm^{-1} gradually grew indicating the formation of the cationic species along with the band at 2020 cm^{-1} for chloride species slowly diminishing. After 4 hrs these two bands became equal in size. The reaction was left for overnight, anticipating a complete disappearance of the carbonyl stretch due to the neutral chloride containing moiety. However, no further change in IR spectrum was observed. Thus infrared spectrum of the product is consistent with the formation of the mono-acetonitrile complex $[\text{Re}_2(\text{IPQP})(\text{CO})_6(\text{CH}_3\text{CN})\text{Cl}]\text{PF}_6$, **10** rather than bis-acetonitrile compound, $[\text{Re}_2(\text{IPQP})(\text{CO})_6(\text{CH}_3\text{CN})_2](\text{PF}_6)_2$. The formation of compound **10** is also indicated by its NMR spectrum since all 16 ring hydrogens become NMR distinguishable. The crystals obtained from the vapour diffusion of diethyl ether were solvent dependent. Needle-shaped crystals of **10**, suitable for X-ray crystallographic studies were obtained by layer diffusion of water on to an acetonitrile solution of the compound.

Several attempts to prepare dicationic complexes using excess $\text{Ag}(\text{ClO}_4)$ or prolonging the time of the reaction were unsuccessful. As we have seen during the alkylation of $\text{Re}(\sigma^2\text{-terpy})(\text{CO})_3\text{Cl}$ with methyl iodide $[\text{Re}(\sigma^2\text{-terpyMe})(\text{CO})_3\text{I}]\text{PF}_6$ was formed, substituting chloride for iodide, and iodide is more readily replaced than chloride we aimed to prepare $\text{Re}_2(\text{IPQP})(\text{CO})_6\text{I}_2$ by the reaction of $\text{Re}_2(\text{IPQP})(\text{CO})_6\text{Cl}_2$ and $(\text{Bu})_4\text{NI}$ in refluxing toluene to facilitate the formation of dicationic species. However, in this case no substitution reaction was observed as the IR spectrum of the resulting compound is identical with that of the starting material.

3.2.4 Synthesis of $[\text{Re}_2(\text{IPQP})(\text{CO})_6(\text{py-3-NH}_2)\text{Cl}]\text{PF}_6$ (**11**)

The acetonitrile group can be replaced by a variety of pyridines. The reaction of **10** was typically carried out in refluxing THF with a large excess of 3-aminopyridine (scheme 3.13). Normally the reaction had reached completion after 2-4 hours, as indicated by solution IR spectrum. The product $[\text{Re}_2(\text{IPQP})(\text{CO})_6(\text{py-3-NH}_2)\text{Cl}]\text{PF}_6$, **11** was isolated by the addition of n-hexanes, which caused the precipitation of the bright yellow crystalline product in a yield of 60%.



Scheme 3.13 Preparation of $[\text{Re}_2(\text{IPQP})(\text{CO})_6(\text{py-3-NH}_2)\text{Cl}]\text{PF}_6$ (11)

This air stable product was recrystallised by slow vapour diffusion of diethyl ether into an acetonitrile solution of the compound and X-ray quality crystals were obtained.

3.2.5 Attempted synthesis of $[\text{Re}(\text{IPQP})(\text{CO})_6(\mu\text{-Cl})]\text{PF}_6$ (12)

Since quaterpyridine formed a bridging hydroxide compound with rhenium in compound **9**, the formation of a chloride-bridged species may be possible. $[\text{Re}(\text{IPQP})(\text{CO})_6(\text{CH}_3\text{CN})\text{Cl}]\text{PF}_6$ was heated in refluxing toluene in order to remove the acetonitrile ligand and cause the chloride to bridge the two metals. The orange coloured products were precipitated by the addition of hexane to the cooled solution. The resulting product may be the bridging halide compound, $[\text{Re}_2(\text{IPQP})(\text{CO})_6(\mu\text{-Cl})]\text{PF}_6$, **12**. The formation of compound **12** has been supported by IR and mass spectrum, as will be discussed in the section 3.2.6.1. But several attempts to obtain clear ^1H NMR spectrum were unsuccessful. So, it is not obvious that compound **12** has practically been formed or not.

3.2.6 Spectroscopic Studies

3.2.6.1 IR and Mass Spectra

In solution the rhenium complexes displays carbonyl stretching bands in the infrared (Table 1) indicative of a facial-stereochemistry for the $\text{ReX}(\text{CO})_3$ moiety. The IR spectrum of compound **8** exhibits two strong bands at 2021 and 1898 corresponding to the C-O stretch. Compound **10** gives four bands at 2039, 2020, 1933 and 1909. Among the first two bands 2039 is due to the cationic rhenium centre and 2020 for neutral rhenium centre. The cationic species show absorbances at higher

wave numbers due to decreased back-bonding into the π^* orbital of the carbonyl ligands. The IR bands of compound **10** supported the formation of a mono-acetonitrile compound, which is confirmed by X-ray crystallography discussed later.

Compound **9** seems to be an intermediate between **8** and **10** as it may be postulated that has a $\frac{1}{2}^+$ charge on each rhenium center and shows one strong broad band at 2023 and two split bands at 1914 and 1899. Compound **11** exhibits five bands at 2033, 2018, 1937, 1914 and 1901 which are red-shifted compared to those of compound **3** because of the strong σ -donor property of pyridine dominates over the π acceptor property of pyridine. Thus, replacing an acetonitrile with a pyridine donor enhances electron density on the metal centre and reduces the stretching frequency of the carbonyl groups. Compound **12** is almost identical with compound **9** and exhibits three bands at 2025, 1926 and 1907.

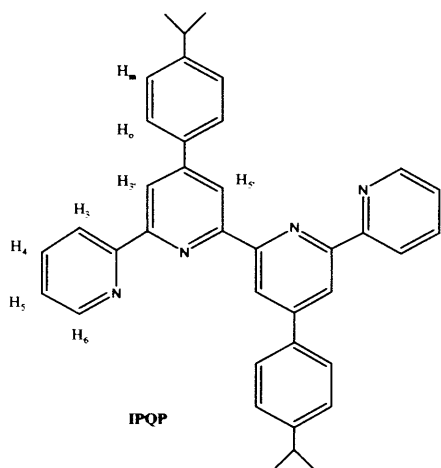
All complexes show masses for different isotopical arrangements of rhenium and chlorine in their mass spectrum. FAB mass spectrum of the complex **8** provides masses for the parent ion (23%) and an ion due to loss of chlorine (100%). Compound **9** shows good agreement with a mass of 1020.2 (70%) for $[\text{Re}_2(\text{Ph}_2\text{qpy})(\text{CO})_6(\text{OH})]^+$ by loosing a perrhenate ion. The electro spray mass spectrum of compound **10** exhibits masses due to the loss of a hexfluorophosphate ion (100%), and loss of hexfluorophosphate ion and acetonitrile molecule (100%). Electro spray mass spectrum of compound **11** shows masses at 1217.8(29%) for $[\text{Re}_2(\text{IPQP})(\text{CO})_6(\text{py-3-NH}_2)\text{Cl}]^+$ and 1161.9(100%) for $\{[\text{Re}_2(\text{IPQP})(\text{CO})_6(\text{py-3-NH}_2)\text{Cl}]^+ - 2\text{CO}\}$. Compound **12** gives a mass due to the loss of a hexfluorophosphate ion, $[\text{Re}_2(\text{IPQP})(\text{CO})_6(\mu\text{-Cl})]^+$, at 1122.7 m/z (100%).

Table 1: Infra-red and mass spectroscopic data for complexes **8-12**.

Complex	IR / ν_{max} ($\text{CH}_3\text{CN}/ \text{cm}^{-1}$)	MS (m/z)
$\text{Re}_2(\text{IPQP})(\text{CO})_6\text{Cl}_2$, 8	2020, 1897	1158/1123
$\text{Re}_2(\text{Ph}_2\text{qpy})(\text{CO})_6(\mu\text{-OH})\text{ReO}_4$, 9	2022, 1914, 1899	1020
$[\text{Re}_2(\text{IPQP})(\text{CO})_6(\text{CH}_3\text{CN})\text{Cl}]\text{PF}_6$, 10	2039, 2020, 1932, 1908	1164/1123
$[\text{Re}_2(\text{IPQP})(\text{CO})_6(\text{py-3-NH}_2)\text{Cl}]\text{PF}_6$, 11	2033, 2018, 1936, 1913, 1901	1218/1162
$[\text{Re}_2(\text{IPQP})(\text{CO})_6(\mu\text{-Cl})]\text{PF}_6$, 12	2024, 1925, 1906	1123

3.2.6.2 NMR Spectra

The ^1H NMR of the ligand (IPQP) shows sharp signals in the aromatic region which are similar to those found in qpy^5 , $4',4''\text{-Ph}_2\text{qpy}^6$, $4',4''\text{-bis}(4\text{-tert-butylphenyl})\text{-}2,2':6',2'':6'',2'''\text{-quaterpyridine}^{29}$ and in $4',4''\text{-diaryl-}2,2':6',2'':6'',2'''\text{-quaterpyridines}$ containing OMe, Me, CF_3 or Cl substituted phenyl group.¹⁹ A septet and a doublet for the isopropyl group also exist in the spectrum.



The assignments of the ^1H NMR shifts of rhenium complexes were made (Table 2) by comparison with corresponding shifts in $[\text{ReBr}(\text{CO})_3(\text{qpy})]$ and $[\{\text{ReBr}(\text{CO})_3\}_2\text{L}]$ ($\text{L} = 4',4''\text{-bis}(4\text{-tert-butylphenyl})\text{-}2,2':6',2'':6'',2'''\text{-quaterpyridine}$).²⁵ In compound **8** the symmetrical coordination of IPQP to two rhenium molecules means that the ^1H NMR exhibits eight ^1H chemical shifts arising from

equivalent pairs of aromatic hydrogens (Figure 3.1). The doublets centered at δ 9.09 and 8.37 ppm were due to the H_6 and H_3 protons, respectively. The triplets centered at δ 8.1 and 7.58 ppm were assigned to H_5 and H_4 protons, respectively. The H_7 and H_8 protons of the central two pyridine rings exhibit two singlets at δ 8.54 and 8.47 ppm. The two doublets twice the integral of other signals at 7.95 and 7.35 ppm were assigned to the protons H_9 and H_{10} of the para-substituted benzene rings.

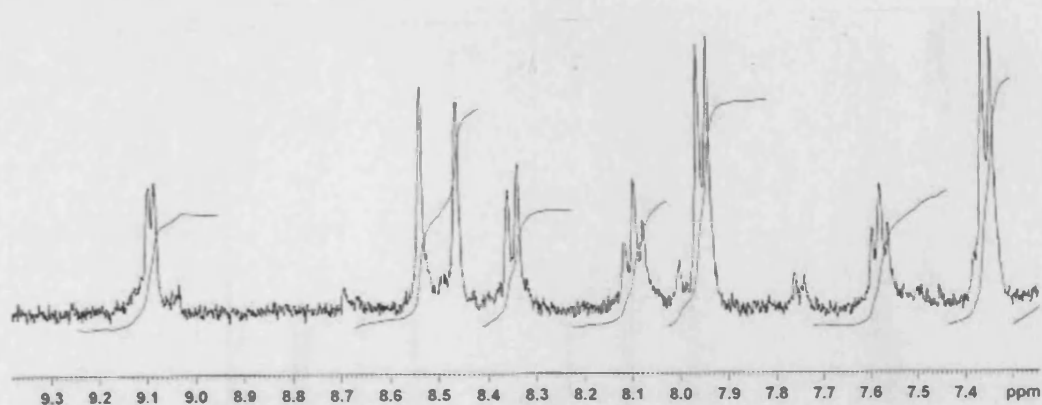
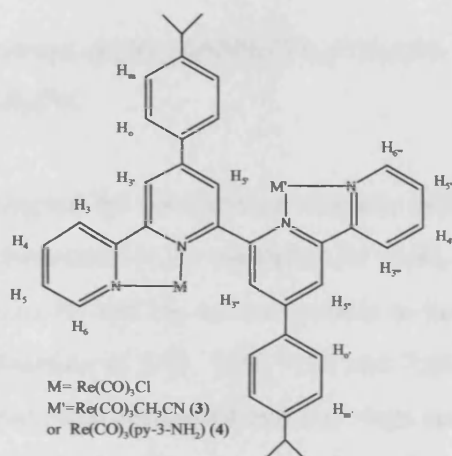


Figure 3.1 The 400 MHz ^1H NMR spectrum of $\text{Re}_2(\text{IPQP})(\text{CO})_6\text{Cl}_2(\mathbf{8})$ in CD_3CN .

Formation of the mono-acetonitrile compound, **10**, led to an increased complexity in its NMR spectrum (Figure 3.2). Several repetitions of the reaction generate reproducible NMR spectrum, though the spectrum is difficult to interpret. Now the two rhenium centres are inequivalent meaning that there is no longer a mirror plane of symmetry dissecting the $\text{C6}'\text{-C2}''$ bond and all 16 ring hydrogens become NMR distinguishable. A pseudo triplet at 9.03 ppm is attributed to the proton pairs H_6/H_6'' which are overlapping 1:1 doublets and a multiplet at 7.7 for H_5/H_5'' arose from two closely overlapping triplets. The doublets at 8.87, 8.83, 8.58 and 8.21 were due to the protons H_3 , H_5' , H_5 and H_3'' , respectively, with a small coupling constant, 1.9. These doublets were not observed in compound **8**. The doublets at 8.78 and 8.72 were due to the protons H_3 and H_3'' . The triplets at 8.32 and 8.24 were assigned to the protons H_4 and H_4'' . The doublets at 8.07, 7.91, 7.46 and 7.41 were assigned to the protons H_o , H_o' , H_m and H_m' of the para-substituted benzene rings. The larger difference in chemical shifts of proton pair H_o/H_o' ($\Delta\delta = 0.16$ ppm) compared to that of proton pair H_m/H_m' ($\Delta\delta = 0.05$ ppm) is due to the close proximity of protons H_o/H_o' to the rhenium centres compared to protons H_m/H_m' .



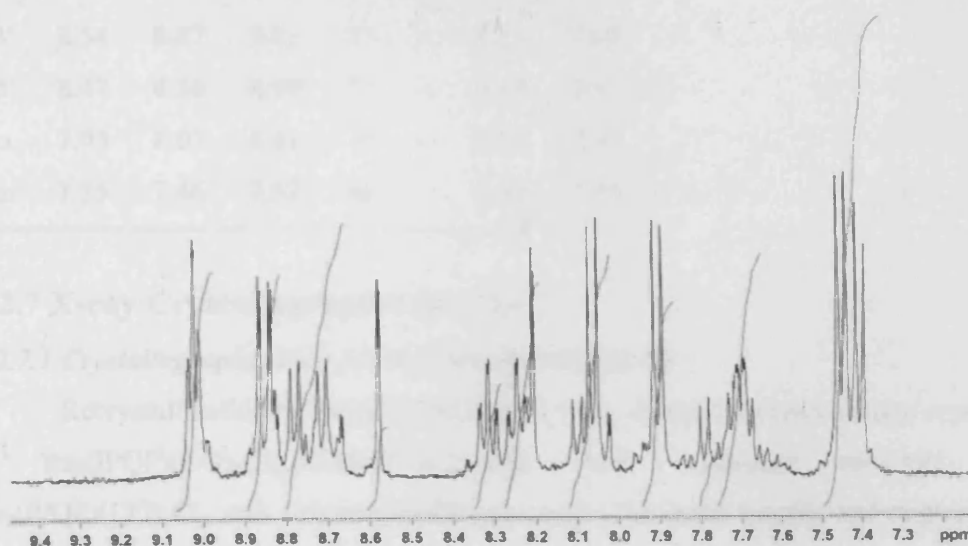


Figure 3.2 The 400 MHz ^1H NMR spectrum of $[\text{Re}_2(\text{IPQP})(\text{CO})_6(\text{CH}_3\text{CN})\text{Cl}]\text{PF}_6(\mathbf{10})$ in CD_3CN .

The spectrum of complex **11** can be assigned by comparison with the shift observed for **10**. In the ^1H NMR spectrum of compound **11**, the multiplet, for H_3/H_3' , at 7.97 and the triplets at 8.62 and 8.5 for protons H_2 and H_2' are comparable to the shift of those protons in compound **10**. The doublets at 8.41, 7.77, 7.57 and 7.48, assigned to the protons H_7 , H_7' , H_8 and H_8' of the para-substituted benzene rings are also of similar pattern to those of compound **10**. The incorporation of 3-aminopyridine rings in compound **11** gives the $\Delta\delta$ value for proton pair H_7/H_7' (0.64 ppm) which is larger than that of compound **10**.

The ^1H NMR spectra of complexes **9** and **12** were collected but it was not possible to assign any peaks due to the complicated nature of the spectra.

Table 2. ^1H NMR Shifts of IPQP protons in complexes **8**, **10** and **11**.

	^1H NMR shifts (δ) for different proton positions						
	8	10	11	8	10	11	
6	9.09	9.03	9.32	6'''	-	9.02	9.16
5	8.1	7.7	7.97	5'''	-	7.7	7.97
4	7.58	8.32	8.62	4'''	-	8.15	8.5

3	8.37	8.78	9.16	3'''	-	8.72	8.95
3'	8.54	8.87	9.25	3''	-	8.21	7.69
5'	8.47	8.58	8.94	5''	-	8.83	9.02
o	7.95	8.07	8.41	o'	-	7.91	7.77
m	7.35	7.46	7.57	m'	-	7.41	7.48

3.2.7 X-ray Crystallographic Studies

3.2.7.1 Crystallographic data for $\text{Re}_2(\text{IPQP})(\text{CO})_6\text{Cl}_2$ (8)

Recrystallization of $\text{Re}_2(\text{IPQP})(\text{CO})_6\text{Cl}_2$ from acetonitrile gave orange crystals of $\text{Re}_2(\text{IPQP})(\text{CO})_6\text{Cl}_2 \cdot 0.5\text{MeCN} \cdot 0.25\text{H}_2\text{O}$. The solid-state structure of $\text{Re}_2(\text{IPQP})(\text{CO})_6\text{Cl}_2$ was determined (Figure 3.3). The bond lengths and angles are given in Table 4.

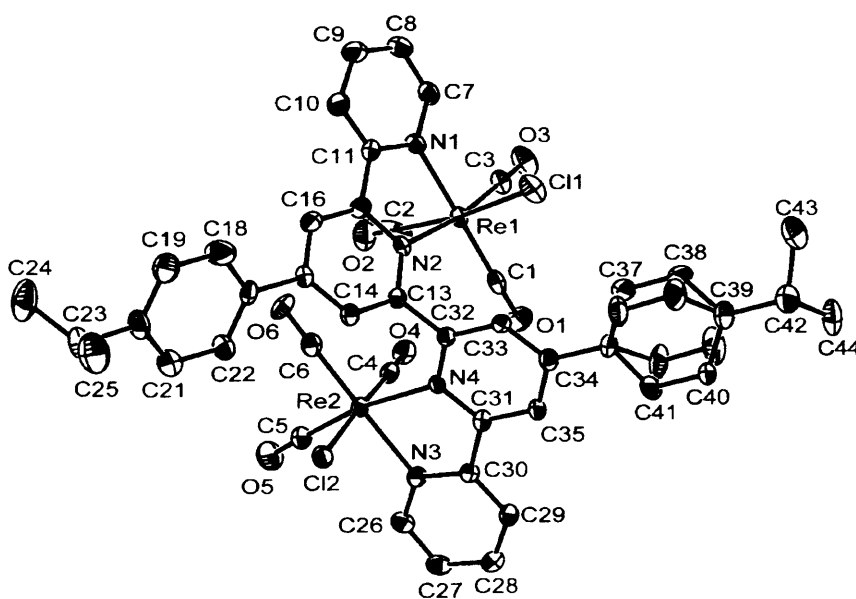


Figure 3.3 Ortep diagram of $\text{Re}_2(\text{IPQP})(\text{CO})_6\text{Cl}_2$ (8). Thermal ellipsoids are drawn at 50% probability.

The dirhenium $\text{Re}_2(\text{IPQP})(\text{CO})_6\text{Cl}_2$ consists of two independent rhenium centres. Each rhenium has an octahedral coordination sphere with a facial arrangement of the carbonyl groups, in addition there is one chloride donor and two pyridyl donors. The IPQP ligand is acting as two bidentate chelating ligands with a

cis, *trans*, *cis* conformation. In fact, this *trans* relationship favours the coordination of two rhenium moieties from opposite sides of the ligand. The principal twist of the interpyridyl bonds of the IPQP ligand in **8** occurs at C(13)-C(32) with a dihedral angle of $63.59(14)^\circ$ whereas in the complex $\text{Re}(\sigma^2\text{-terpy})(\text{CO})_3\text{Cl}$, containing an uncoordinated pyridine ring, the corresponding dihedral angle is $75.25(11)^\circ$. The N(2)-C(13)-C(32)-N(4) torsion angle is -123.0° whereas in the complex $\text{Re}(\sigma^2\text{-terpy})(\text{CO})_3\text{-Cl}$ the corresponding torsion angle is $-130.0(3)^\circ$.³³ The Re-C bond distances of the carbonyl groups are in the expected range and vary from 1.906(6) to 2.016(8) Å in the complex which is comparable to those found in $[\text{Re}_2(\text{bpy})_2(\text{CO})_6(\mu\text{-H})]\text{Cl}$ ³⁴ and $\text{Re}(\sigma^2\text{-terpy})(\text{CO})_3\text{Cl}$.³³ In addition, the Re-N bond distances vary from 2.165(5) to 2.225(5) Å which is also typical of $\text{Re}(\text{bpy})(\text{CO})_3\text{Cl}$ ³⁴ and $\text{Re}(\sigma^2\text{-terpy})(\text{CO})_3\text{Cl}$.³³ The Re atoms in the complex show a distorted octahedral geometry where the *cis* angles around the Re(1) atom are $75.08(17)$ - $102.4(2)^\circ$ and around the Re(2) atom are $74.0(4)$ - $102.5(5)^\circ$ showing a deviation away from the octahedral 90° . The *trans* angles around the Re(1) atom are $170.7(2)$ - $177.3(2)^\circ$ and around Re(2) atom are $170.2(2)$ - $177.76(17)^\circ$ reflecting the octahedral geometry. Again, these values are similar to those reported for related tricarbonylrhenium(I) complexes containing polypyridine ligands^{33, 34}. Therefore, there is not any significant steric strain observed for the dinuclear complex compared to the mononuclear complexes. The distance between two rhenium atoms is 5.244 Å, and there is no bonding interaction between the two metal centres. The structure is in agreement with solution state IR spectrum that reflects the facial arrangement of the carbonyl groups and ^1H NMR data which has 8 distinct proton signals as expected from the symmetry of the complex in the crystal structure.

3.2.7.2 Crystallographic data for $\text{Re}_2(\text{Ph}_2\text{qpy})(\text{CO})_6(\mu\text{-OH})\text{ReO}_4$ (9)

Recrystallisation of $[\text{Re}_2(\text{Ph}_2\text{qtpy})(\text{CO})_6(\mu\text{-OH})][\text{ReO}_4]$ from dichloromethane solution of the complex gave orange crystals of $[\text{Re}_2(\text{Ph}_2\text{qtpy})(\text{CO})_6(\mu\text{-OH})][\text{ReO}_4].0.5\text{CH}_2\text{Cl}_2$. The solid-state structure of $[\text{Re}_2(\text{Ph}_2\text{qtpy})(\text{CO})_6(\mu\text{-OH})][\text{ReO}_4]$ was elucidated (Figure 3.4). Corresponding relevant bond lengths and angles are shown in Table 4.

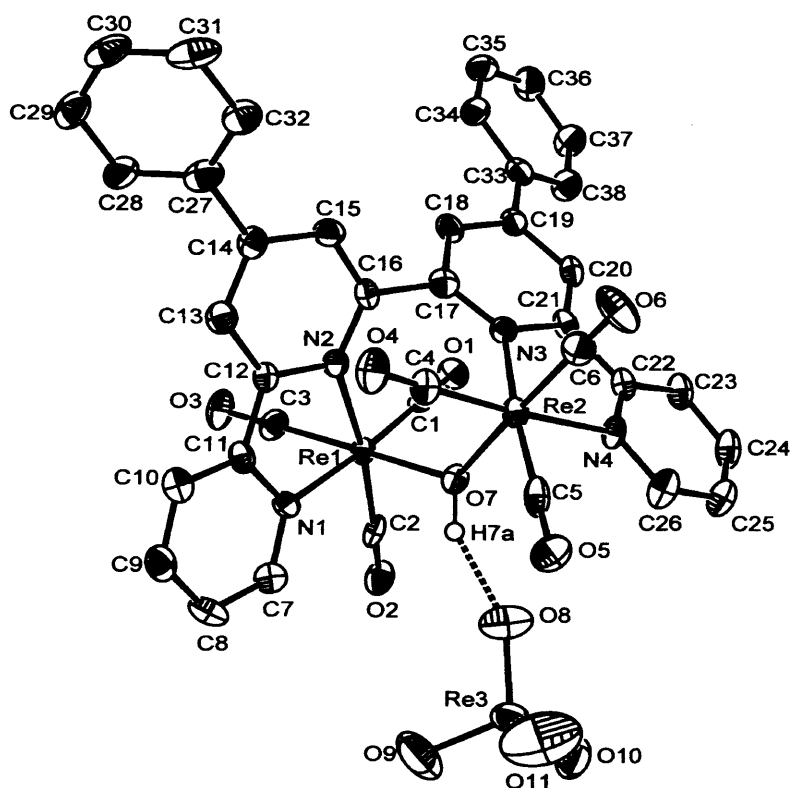


Figure 3.4 Ortep diagram of $\text{Re}_2(\text{Ph}_2\text{qpy})(\text{CO})_6(\mu\text{-OH})\text{ReO}_4(\mathbf{9})$. Thermal ellipsoids are drawn at 50% probability.

The cationic species contains two independent rhenium centres bonded to the quaterpyridine. Like compound **8** each rhenium possesses an octahedral geometry oriented by facially arranged carbonyl groups. The hydroxide group bridges the two metal centres and the $\text{Re}\dots\text{Re}$ distance is 3.863 Å which is shorter compared to the $\text{Re}\dots\text{Re}$ distance (5.244 Å) in complex **8**. Again, this distance does not correspond to a Re-Re bond. It is assumed that the hydroxide group pulls two positive rhenium centres closer in compound **9**. The quaterpyridine ligand is acting as two bipyridine moieties with a *cis, cis, cis* conformation. This *cis* relationship favours the coordination of two rhenium moieties from same sides of the ligand (Figure 3.5). The $\text{N}(3)\text{-C}(17)\text{-C}(16)\text{-N}(2)$ torsion angle is -52.1° whereas in complex $\text{Re}_2(\text{IPQP})(\text{CO})_6\text{-Cl}_2$ the corresponding torsion angle is -123.0° .

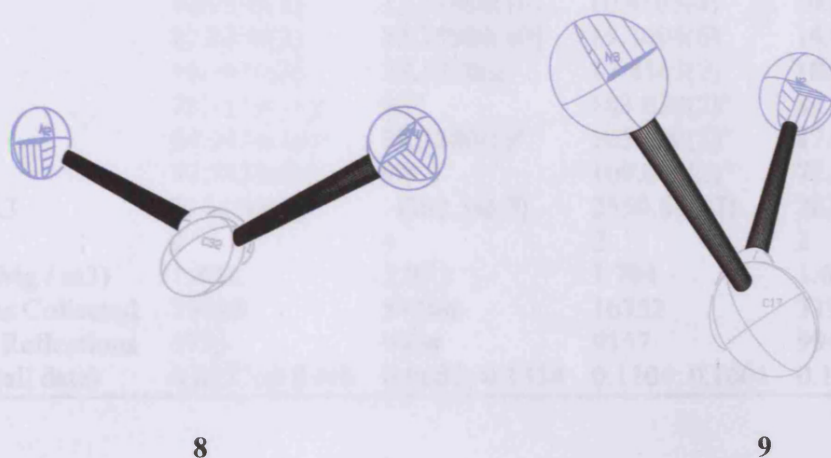


Figure 3.5 Comparison of torsion angles of complex 8 and 9.

The Re-C and Re-N bond distances are similar to those in compound 8 and lie within 1.900(10)-1.926(8) Å and 2.165(7)-2.212(7) Å respectively. The Re-O bond distances are 2.117(6) and 2.149(6) Å which are elongated than the corresponding bonds in $\text{Re}_2\text{O}_6(\mu_2\text{-OH})_2.3\text{C}_4\text{H}_8\text{O}_2$ [Re-O(bridge) 2.065],³⁵ $[\text{ReOCl}_2(\text{PPh}_3)\{\text{p-MeC}_6\text{H}_4\text{N}:\text{C}(\text{OEt})\text{S}\}]$ [1.671(4)],³⁶ $\text{Re}_2\text{O}_3\text{Cl}_4(\mu\text{-dippm})_2$ [bridging Re-O 1.921(8) and 1.904(8)]³⁷ but are comparable to the Re-OH₂ [2.142(7)] bond in $\text{Et}_4\text{N}[\text{ReO}(\text{H}_2\text{O})(\text{CN})_4].2\text{H}_2\text{O}$.³⁸ The Re atoms in the complex distorted from an ideal octahedral geometry. The *cis* angles around the Re(1) atom are 74.5(2)-102.7(3)° and around the Re(2) atom are 74.8(3)-102.4(3)° show much variations from the ideal value 90°. The *trans* angles around the Re(1) atom are 171.6(3)-176.0(3)° and around Re(2) atom are 170.3(3)-176.2(3)° slightly reduced from 180°. Again, no significant steric strain is observed in compound 9 though the two rhenium centres are incorporated from the same side of the ligand.

Table 3. Crystal and structure refinement data of complexes 8-11.

Compound	8	9	10	11
Empirical formula	$\text{C}_{45}\text{H}_{36}\text{Cl}_2\text{Re}_2$ N_4O_6	$\text{C}_{38}\text{H}_{23}\text{Re}_3\text{N}_4$ O_{11}	$\text{C}_{46}\text{H}_{37}\text{ClRe}_2\text{N}$ $5\text{O}_6\text{PF}_6$	$\text{C}_{49}\text{H}_{38}\text{ClRe}_2$ $\text{N}_6\text{O}_6\text{PF}_6$
Formula weight	1183.08	1311.66	1308.63	1359.67
Temperature K	150(2)	293(2)	293(2)	150(2)
Crystal system	Triclinic	Monoclinic	Triclinic	Triclinic

Space group	P -1	P 2 (1) / c	P -1	P -1
a Å	10.9559(2)	12.17800(10)	10.9105(4)	10.8560(3)
b Å	12.8359(2)	12.75800(10)	15.3094(6)	14.9350(4)
c Å	16.3916(3)	27.1270(3)	17.8143(7)	18.3430(7)
α	73.1119(11) $^\circ$	90 $^\circ$	103.038(2) $^\circ$	84.2630(10) $^\circ$
β	84.9434(10) $^\circ$	94.3380(5) $^\circ$	105.080(2) $^\circ$	87.0760(10) $^\circ$
γ	77.7225(6) $^\circ$	90 $^\circ$	109.089(2) $^\circ$	72.5540(10) $^\circ$
Volume Å ³	2154.42(7)	4202.56(7)	2550.68(17)	2822.32(15)
Z	2	4	2	2
Density (Mg / m ³)	1.824	2.073	1.704	1.600
Reflections Collected	37028	51106	16752	31946
Observed Reflections	9795	9454	9157	9945
R1, wR2 (all data)	0.0577; 0.0996	0.0682; 0.1334	0.1104; 0.1601	0.1197; 0.1907

Table 4: Bond lengths [Å] and angles [°] for **8- 11**

Compound	8	9	10	11
Re(1)-C(1)	1.937(7)	1.928(8)	1.915(13)	1.938(16)
Re(1)-C(2)	2.016(8)	1.907(10)	1.983(14)	1.961(18)
Re(1)-C(3)	1.916(6)	1.906(10)	1.943(15)	1.925(16)
Re(2)-C(4)	1.906(6)	1.915(9)	1.85(2)	1.953(18)
Re(2)-C(5)	1.932(6)	1.906(9)	1.948(15)	1.932(16)
Re(2)-C(6)	1.915(6)	1.921(9)	1.929(18)	1.94(2)
Re(1)-N(1)	2.165(5)	2.167(6)	2.209(8)	2.181(9)
Re(1)-N(2)	2.225(5)	2.212(7)	2.185(9)	2.210(9)
Re(2)-N(3)	2.178(5)	2.212(6)	2.179(10)	2.207(9)
Re(2)-N(4)	2.225(4)	2.182(6)	2.123(12)	2.159(12)
C(1)-Re(1)-C(2)	92.6(3)	86.6(3)	88.0(6)	86.1(6)
C(1)-Re(1)-C(3)	86.9(3)	85.6(4)	85.5(6)	88.6(6)
C(2)-Re(1)-C(3)	91.4(2)	88.2(4)	91.7(6)	88.3(5)
C(1)-Re(1)-N(1)	177.3(2)	176.3(3)	175.7(5)	177.1(5)
C(2)-Re(1)-N(1)	88.5(2)	96.3(3)	97.1(6)	96.8(5)
C(3)-Re(1)-N(1)	95.6(2)	92.1(3)	91.9(5)	92.3(5)
C(1)-Re(1)-N(2)	102.4(2)	102.4(3)	102.5(4)	170.7(5)
C(2)-Re(1)-N(2)	170.7(2)	170.4(3)	172.0(6)	102.8(4)
C(3)-Re(1)-N(2)	88.2(2)	95.7(3)	91.7(5)	94.3(5)
N(1)-Re(1)-N(2)	75.08(17)	74.8(2)	75.0(4)	74.3(4)
C(4)-Re(2)-C(5)	88.2(3)	85.5(3)	87.8(6)	92.0(6)
C(4)-Re(2)-C(6)	85.8(2)	88.5(3)	87.0(6)	90.9(6)
C(5)-Re(2)-C(6)	87.4(3)	88.8(4)	88.8(6)	86.4(6)
C(4)-Re(2)-N(3)	94.8(2)	102.9(3)	102.9(5)	102.5(5)
C(5)-Re(2)-N(3)	177.3(2)	171.4(3)	169.9(5)	171.1(5)
C(6)-Re(2)-N(3)	95.2(2)	89.7(3)	93.9(5)	88.0(5)
C(4)-Re(2)-N(4)	170.2(2)	175.9(3)	177.8(5)	176.0(5)
C(5)-Re(2)-N(4)	102.4(2)	97.3(3)	91.9(5)	97.5(6)
C(6)-Re(2)-N(4)	93.3(2)	88.6(3)	95.2(5)	88.4(5)
N(3)-Re(2)-N(4)	75.02(16)	74.2(2)	75.0(4)	73.6(4)

3.2.7.3 Crystallographic data for $[\text{Re}_2(\text{IPQP})(\text{CO})_6(\text{CH}_3\text{CN})\text{Cl}]\text{PF}_6$ (10)

Recrystallization by diffusing ether into an acetonitrile solution of $[\text{Re}_2(\text{IPQP})(\text{CO})_6(\text{CH}_3\text{CN})\text{Cl}]\text{PF}_6$ gave air sensitive and solvent dependent crystals which were not suitable for X-ray crystallographic studies. However, X-ray quality crystals obtained by layer diffusion of water into an acetonitrile solution of the compound and revealed the structure of $[\text{Re}_2(\text{IPQP})(\text{CO})_6(\text{CH}_3\text{CN})\text{Cl}]\text{PF}_6$. The crystal structure of compound **10** is shown in Figure 3.6. The relevant data are presented in table 3 and 4.

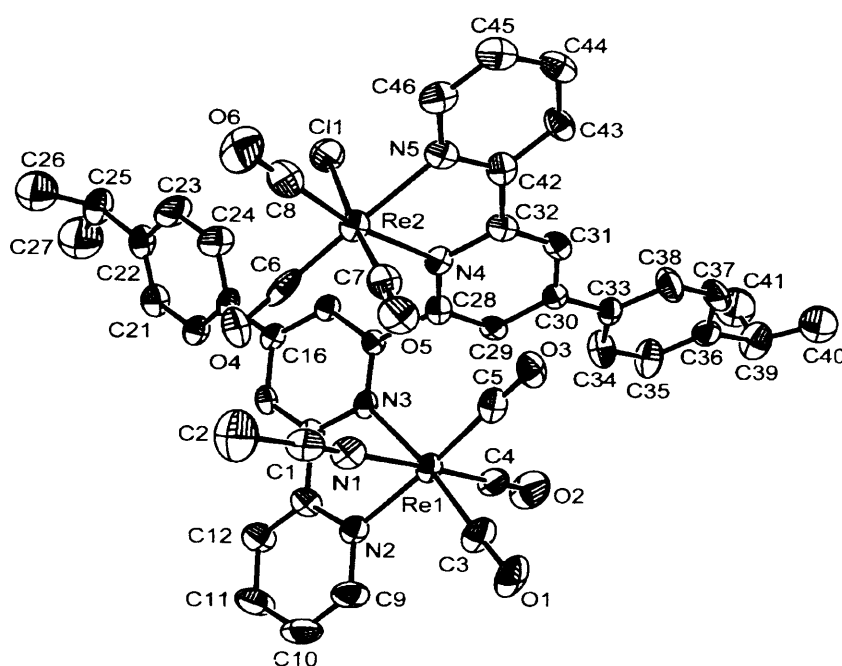


Figure 3.6 Ortep diagram of the cation present in $[\text{Re}_2(\text{IPQP})(\text{CO})_6(\text{CH}_3\text{CN})\text{Cl}]\text{PF}_6$ (**10**). Thermal ellipsoids are drawn at 50% probability.

The cationic species consists of two independent rhenium centres, one bearing a chloride donor and the other an acetonitrile donor. The structure of the complex shows two six coordinate $\text{Re}(\text{I})$ centres both with a pseudo-octahedral coordination geometry. The mode of coordination was once again facial. The ligand behaves as two bipy units with a *cis, trans, cis* conformation similar to that observed for **8** and the two rhenium moieties coordinate from opposite sides of the ligand. The $\text{N}(3)\text{-C}(18)\text{-C}(28)\text{-N}(4)$ torsion angle is -118.8° whereas the corresponding torsion angles for

compounds **8** and **9** are -123.0° and 52.1° , respectively. The Re-C bond distances [1.85(2) to 1.983(14) Å] and the Re-N bond distances of pyridine rings [2.137(10) - 2.185(9) Å] are also similar to those for compound **8** and **9**. The Re-N bond distances arising from the acetonitrile moiety is 2.123(12) Å may be compared to the corresponding bond lengths in complexes $[\text{NEt}_4][\text{Re}(\text{NO})\text{Br}_4(\text{MeCN})]$ (2.153(11) Å)³⁹, $[(\text{CO})_3\text{Re}(\text{NCCH}_3)_3]\text{BF}_4$ [2.132-2.125 Å]⁴⁰ and $[\text{Re}(\text{bpy})(\text{CO})_3(\text{CH}_3\text{CN})][\text{ClO}_4]$ [Re-N 2.140(3)].⁴¹ The *cis* angles around the Re(1) atom are $75.0(4)$ - $102.5(4)^\circ$ and around the Re(2) atom are $74.0(4)$ - $102.5(5)^\circ$ and the *trans* angles around the Re(1) atom are $172.0(5)$ - $175.7(5)^\circ$ and around Re(2) atom are $169.9(5)$ - $177.8(5)^\circ$. Again these values are similar to those of compound **8** and **9**. The structure is also supported by solution IR spectrum and ^1H NMR spectrum of the compound that gave evidence of a positive rhenium centre and a neutral rhenium centre in the complex.

3.2.7.4 Crystallographic data for $[\text{Re}_2(\text{IPQP})(\text{CO})_6(\text{py-3-NH}_2)\text{Cl}]\text{PF}_6$ (**11**)

Recrystallization of the compound from diethyl ether gave needle shaped air stable orange crystals having the structure $[\text{Re}_2(\text{IPQP})(\text{CO})_6(\text{py-3-NH}_2)\text{Cl}]\text{PF}_6$. The crystal structure of compound **11** is shown in Figure 3.7. The bond lengths and angles are presented in Table 4.

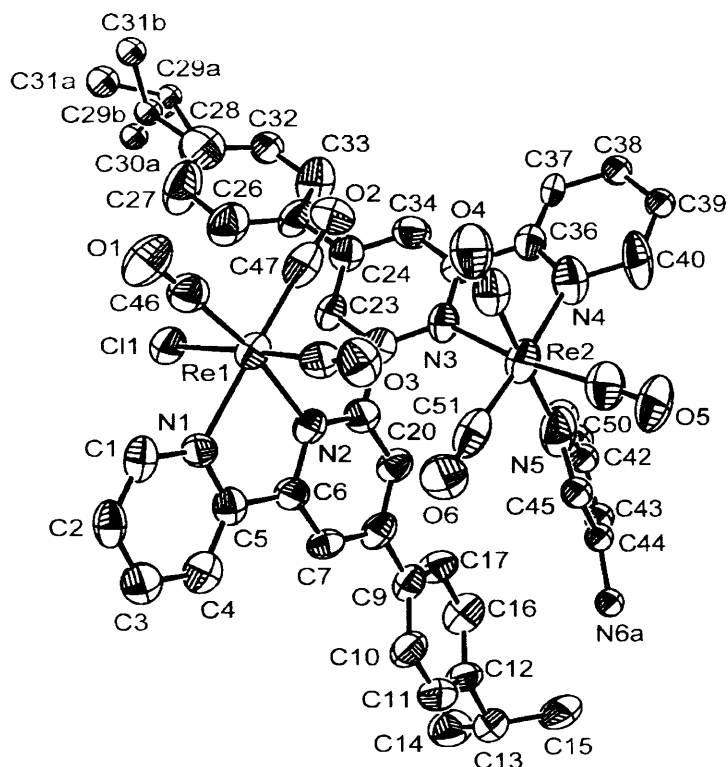


Figure 3.7 Ortep diagram of the cation present in $[\text{Re}_2(\text{IPQP})(\text{CO})_6(\text{py-3-NH}_2)\text{-Cl}]\text{PF}_6(11)$. Thermal ellipsoids are drawn at 50% probability.

The cationic species consists of two rhenium centres, one bearing a chloride donor and the other a 3-aminopyridine donor. Both of the rhenium centres are situated in a pseudo-octahedral coordination environment and the carbonyl groups are arranged in *facial* orientation. Like compound **8** and **10** the *cis*, *trans*, *cis* orientation of the pyridines in the quaterpyridine ligand provides enough space to coordinate the two rhenium moieties from opposite sides of the ligand. The $\text{N}(3)\text{-C}(21)\text{-C}(22)\text{-N}(3)$ torsion angle is -119.2° which is very similar to the corresponding torsion angle of compound **10** [$\text{N}(3)\text{-C}(18)\text{-C}(28)\text{-N}(4)$ -118.8°]. The Re-C bond distances [1.925(16) to 1.961(18) Å] and the C-O bond distances [1.127(16) to 1.159(16) Å] are almost the same as complex **10**. These values do not give any information for the lower stretching frequency of the carbonyl groups for complex **11** than compound **10**. The Re-N bond lengths [2.159(12)- 2.216(16) Å] are similar to those observed in related system, $[\text{Re}(\text{bpy})(\text{CO})_3(\text{py-3-NCS})\text{Cl}]\text{CF}_3\text{SO}_3$.⁴² The *cis* angles around Re(1) atom are $74.3(4)\text{-}102.8(4)^\circ$ and around Re(2) atom are $73.6(4)\text{-}102.5(5)^\circ$ and the *trans*

angles around Re(1) atom are $170.7(5)$ - $177.1(5)^\circ$ and around Re(2) atom are $171.1(5)$ - $177.4(5)^\circ$. Again these values are similar to those in compounds **8-11**.

In compound **8**, **10** and **11** the rotation about the C-C bond linking rings 2 and 3 is likely to be hindered by the interaction between two metal moieties i.e., the two metal chelated portions of the complex are locked with their planes being considerably angled to each other to minimize the interactions. Therefore, these compounds contain two chiral metal centres and an axially chiral centre through the C(2)-C(3) bond. There are eight possible permutations (RSS, SSR, RRS, SRS, SRR, RSR, SSS, RRR) for each of the complexes depending on the configuration at the metal centres and the axial centre. In fact, RSS and SSR are same compound and so are RRS and SRR. The pairs SSR, RRS are two enantiomers whereas the pairs SRS and RSR are two further enantiomers (and diastereomers of the previous enantiomers). The isomers SSS and RRR are again two further enantiomers. Thus, although there are three possible sets of diastereomers, ^1H NMR data implies that there is only one isomeric form observed for each of the complexes. This is also supported by the X-ray crystallographic studies of the compounds. Again, the ^1H NMR studies of the complexes also show only one set of signals, suggesting that there is only one diastereoisomer for each of the complexes.

3.2.8 Absorption spectra and luminescence properties

Absorption properties of complexes **8** and **10-12** are summarized in Table 5. All the complexes exhibit intense absorptions in the 252-314 nm intervals which are associated with LC and CT transitions centred on the corresponding quaterpyridyl unit. The absorptions in the region 342-372 nm can be assigned to metal(Re)-to-ligand(IPQP) charge transfer transitions.

Table 5. Absorption maxima of complexes **8** and **10-12**.

Complex	λ_{max} (nm) ($10^{-3}\epsilon$ ($\text{dm}^3 \text{mol}^{-1}\text{cm}^{-1}$))			
8			314 (44)	262(32)
10	372 (sh)	342 (sh)	312 (58)	
11	372 (sh)	342 (28)	312 (37)	252(35)
12		340 (sh)	312 (46)	

Regarding the luminescence properties of the $\text{Re}(\text{I})$ complexes, we noticed that complex **8** was the only one showing weak luminescence intensity in degassed acetonitrile solution. The other complexes show no luminescence. In fact, the $\text{Re}(\text{I})$ complexes of quaterpyridine ligand are generally not luminescent, in contrast to the strong luminescent intensity of the analogous mononuclear bipyridine complexes. The lack of luminescence of quaterpyridine complexes containing two mononuclear bipyridine units may arise due to the preference for rings 2 and 3 to adopt a *trans* orientation, thus lowering the energy of the π^* orbital or the presence of the substituted phenyl ring lowers the energy of the π^* orbital.

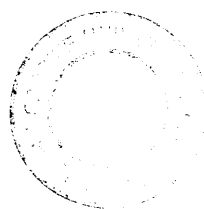
3.2.9 Concluding remarks

The complexes $[\text{Re}_2(\text{IPQP})(\text{CO})_6\text{Cl}_2]$ (**8**), $[\text{Re}_2(\text{IPQP})(\text{CO})_6(\text{CH}_3\text{CN})\text{Cl}]\text{PF}_6$ (**10**) and $[\text{Re}_2(\text{IPQP})(\text{CO})_6(\text{py}-3\text{-NH}_2)\text{Cl}]\text{PF}_6$ (**11**) were successfully prepared in a reasonable yield. These complexes have been characterized by ^1H NMR, IR and mass spectroscopy and X-ray crystallography. $\text{Re}_2(\text{Ph}_2\text{qpy})(\text{CO})_6(\mu\text{-OH})\text{ReO}_4$ (**9**) was obtained as a by product of the reaction of $\text{Re}_2(\text{CO})_{10}$ with 4',4''-diphenyl-2,2':6',2'':6'',2'''-quaterpyridine in presence of trimethylamine oxide. Complex **9** has been characterized by X-ray crystallography.

Several attempts have been made to obtain mono-rhenium complexes for making mono-dentate receptor site. This was not possible. All attempts at substituting the chloride ligand on the second rhenium centre have been unsuccessful. Even swapping the chloride for an iodide (which was successful in terpyridine analogues) resulted in the isolation of the starting material. The luminescence of these complexes is weak. No further investigation into the chemistry of these complexes was made.

3.3 Experimental

All preparations were carried out under an oxygen free inert atmosphere. Solvents were dried by standard procedures, distilled and used directly from the still. $\text{Re}(\text{CO})_5\text{Cl}$ and $\text{Re}(\text{CO})_{10}$ were purchased and were used without further purification. IR spectra were recorded in NaCl solution cells or in compressed KBr discs on a Perkin-Elmer 1600 or a Jasco 660 spectrophotometers. ^1H NMR was recorded on a Bruker DP-400 spectrometer. Electronic spectra were run in HPLC grade acetonitrile on a Perkin-Elmer 20 or a Jasco V-570 UV-Vis spectrophotometer. Fluorescence



spectra were recorded with a Perkin-Elmer LS 50B luminescence spectrometer. Spectra measured in a quartz SUPRASIL precision fluorescence cell. When necessary, samples were degassed by bubbling nitrogen through the solution. Perchlorate salts are potentially explosive. All compounds containing perchlorate should be handled with great care and in small amounts.

3.3.1 Preparation of 1, 6-bis(4-*iso*-propylphenyl)-1,5-diene-3,4-dione(Chalcone)

Piperidine (0.9 ml, 9 mmol) and glacial acetic acid (0.54 ml, 9 mmol) were added to a stirred solution of 4-*iso*-propylbenzaldehyde (28.8 g, 194 mmol) and diacetyl (3.96 g, 46 mmol) in methanol (30 ml). The mixture was heated under reflux for 2 h and then the methanol and unreacted diacetyl were removed in vacuo. The solution was placed in a freezer overnight and the orange crystals in a yield of 9% were isolated by filtration and washed with MeOH.

δ_{H} (400MHz, CDCl_3): 7.79(2H d, J 16.1, H_3), 7.56(4H, d, J 8.3, H_6), 7.38(2H, d, J 16.1, H_4), 7.26(4H, d, J 6.1, H_m), 2.89(2H, m, CH) and 1.21(12H, d, J 6.9, CH_3); IR (KBr): 2960m, 2922w, 1669s, 1598s, 1563m, 1509m, 1462m, 1418m, 1381w, 1361w, 1342w, 1322m, 1293m, 1203m, 1181m, 1116w, 1097w, 1057w, 1017m, 991s, 839m, 818s, 762m, 733w, 663m, 566m and 533w cm^{-1} ; Mass spectrum (CI): m/z 347($\text{C}_{12}\text{H}_{13}\text{O}$, 100%).

For the synthesis of the 4',4''-dipropylphenyl -2,2':6',2'':6'',2'''-quaterpyridine ligand benzaldehyde was used instead of 4-isopropylbenzaldehyde.

3.3.2 Preparation of 4',4''-bis(4-*iso*-propylphenyl) -2,2':6',2'':6'',2'''-quaterpyridine (IPQP)

1, 6-bis(4-*iso*-propylphenyl)-1,5-diene-3,4-dione (0.75 g, 2 mmol) was added to a solution of *N*-[1-oxo-2-(2-pyridyl)ethyl]pyridinium iodide (1.3 g, 4 mmol) and NH_4OAc (1.5 g, 20 mmol) in ethanol (50 ml) and the mixture was heated at reflux for 4 h. After cooling, the precipitate that had formed was collected by filtration to give the product as an off-white solid in a yield of 34%.

δ_{H} (400MHz, CDCl_3): 8.87(2H, s, $\text{H}_{3'+5'}$), 8.65-8.69(6H, m, $\text{H}_{5'+3'+\text{H}_{6+6''}+\text{H}_{3+3''}}$), 7.82(6H, d, J 8.1, $\text{H}_6+\text{H}_{4+4''}$), 7.36(4H, d, J 8.1, H_m), 7.30(2H, t, J 6.1, $\text{H}_{5+5'}$), 2.95(2H, m, CH) and 1.27(12H, d, J 6.9, CH_3); IR (KBr): 2960m, 2919w, 1595m, 1582s, 1550m, 1536m, 1502m, 1465m, 1383m, 1260w, 1096w,

1034w, 830m, 794m, 737w, 661w and 615w cm^{-1} ; Mass spectrum (EI): m/z 546($\text{C}_{38}\text{H}_{34}\text{N}_4$, 100%).

3.3.4 Preparation of $\text{Re}_2(\text{IPQP})(\text{CO})_6\text{Cl}_2$ (**8**)

Rhenium pentacarbonyl chloride (50 mg, 0.138 mmol) and 4',4''-bis(4-*iso*-propylphenyl)2,2':6',2'':6'',2'''-quaterpyridine (32 mg, 0.069mmol) were allowed to reflux in toluene (20 ml) under nitrogen atmosphere for 1 hour. The yellow precipitate was collected by filtration (81%).

Anal. Found: C 45.38, H 3.02, N 4.69%. Calc. for $\text{Re}_2(\text{IPQP})(\text{CO})_6\text{Cl}_2$: C 45.63, H 2.96, N 4.84%; δ_{H} (400MHz, CDCl_3): 9.09 (1H, d, J 4.6, H_6), 8.54 (1H, s, H_3), 8.47 (1H, s, H_5), 8.37 (1H, d, J 6.2, H_3), 8.1(1H, t, J 7.4, H_5), 7.95(2H, d, J 8.3, H_6), 7.58(1H, t, J 6.5, H_4), 7.35(2H, d, J 8.1, H_m), 2.9(1H, m, CH) and 1.21(6H, d, J 6.8, CH_3); IR (CH_3CN): 2021s and 1898s cm^{-1} ; Mass spectrum (positive FAB): m/z 1158[$\text{Re}_2(\text{IPQP})(\text{CO})_6\text{Cl}_2$, 23%] and 1123[$\{\text{Re}_2(\text{IPQP})(\text{CO})_6\text{Cl}\}^+$, 100%]; UV spectra: 262(32070) and 314(44290) nm.

Similar reaction was carried out by using 4',4''-diphenyl-2,2':6',2'':6'',2'''-quaterpyridine and IR spectrum of the product is analogous to compound **8**. Mass spectrum (positive FAB): m/z 1074[$\text{Re}_2(\text{Ph}_2\text{qpy})(\text{CO})_6\text{Cl}_2$, 18%]; IR (CH_3CN): 2022s and 1901s cm^{-1} . Due to the lower solubility of $[\text{Re}_2(\text{Ph}_2\text{qpy})(\text{CO})_6\text{Cl}_2]$ in most of the solvents the $^1\text{HNMR}$ spectrum of the compound was not obtained.

3.3.5 Preparation of $\text{Re}_2(\text{Ph}_2\text{qpy})(\text{CO})_6(\mu\text{-OH})\text{ReO}_4$ (**9**)

Dirhenium decacarbonyl (50 mg, 0.076 mmol), 4',4''-diphenyl-2,2':6',2'':6'',2'''-quaterpyridine (35 mg, 0.076 mmol) and trimethylamin-N-oxide (34 mg, 0.30 mmol) were stirred in dichloromethane for overnight under nitrogen atmosphere at room temperature. The solvent was then evaporated in a rotary evaporator and a mixture of orange (5%) and yellow (95)% powders was collected. Recrystallization of the powdered products in dichloromethane afforded a few orange crystals of the by-product, **9**, which were used for further analysis.

Anal. Found: C 35.79, H 1.81, N 4.36%. Calc. for $\text{Re}_2(\text{Ph}_2\text{qpy})(\text{CO})_6(\mu\text{-OH})\text{ReO}_4$: C 35.93, H 1.83, N 4.41%. IR (CH_2Cl_2): 2023s, 1914m and 1898m cm^{-1} . Mass spectrum (positive FAB): m/z 1020 [$\{\text{Re}_2(\text{diphenyl-qpy})(\text{CO})_6(\text{OH})\}^+$, 70%].

Due to small amount of the sample, the ^1H NMR spectrum of compound **9** was not obtained.

3.3.6 Preparation of $[\text{Re}_2(\text{IPQP})(\text{CO})_6(\text{CH}_3\text{CN})\text{Cl}]\text{PF}_6$ (**10**)

$\text{Re}_2(\text{IPQP})(\text{CO})_6\text{Cl}_2$ (50 mg, 0.043 mmol) and silver perchlorate (20 mg, 0.096 mmol) were refluxed in acetonitrile (25 ml) under a nitrogen atmosphere in the dark for overnight. After cooling the solution, concentrated aqueous solution of potassium hexafluorophosphate was added to the reaction mixture and acetonitrile was removed by slow evaporation under vacuum. The product was obtained as bright yellow crystals (43%).

Anal. Found: C 42.09, H 2.91, N 5.27%. Calc. for $[\text{Re}_2(\text{IPQP})(\text{CO})_6(\text{CH}_3\text{CN})\text{Cl}]\text{PF}_6$: C 42.22, H 2.85, N 5.35%; δ_{H} (400MHz, CD_3CN): 9.03 (1H, d, J 4.4, H_6), 9.02 (1H, d, J 4.4, H_6^m), 8.87 (1H, d, J 1.9, H_3), 8.83 (1H, d, J 1.9, H_5^m), 8.78 (1H, d, J 8.1, H_3), 8.72 (1H, d, J 8.3, H_3^m), 8.58 (1H, d, J 1.7, H_5), 8.32 (1H, td, J 8, 1.5, H_4), 8.24 (1H, td, J 8, 1.5, H_4^m), 8.21 (1H, d, J 1.9, H_3^m), 8.07 (2H, d, J 8.4, H_0), 7.91 (2H, d, J 8.3, H_0'), 7.7 (2H, m, $\text{H}_5, 5^m$), 7.46 (2H, d, J 8.2, H_m), 7.41 (2H, d, J 8.3, H_m); IR (CH_3CN): 2039s, 2020s, 1933m and 1909m cm^{-1} ; Mass spectrum (ES): m/z 1164 $[\{\text{Re}_2(\text{IPQP})(\text{CO})_6(\text{CH}_3\text{CN})\text{Cl}\}]^+$, 100% and 1123 $[\{\text{Re}_2(\text{IPQP})(\text{CO})_6\text{Cl}\}]^+$, 100%; UV spectra: 312(58400), 342(sh) and 372(sh) nm.

3.3.7 Preparation of $[\text{Re}_2(\text{IPQP})(\text{CO})_6(\text{py-3-NH}_2)\text{Cl}]\text{PF}_6$ (**11**)

$[\text{Re}_2(\text{IPQP})(\text{CO})_6(\text{CH}_3\text{CN})\text{Cl}]\text{PF}_6$ (40mg, 0.03 mmol) and 3-aminopyridine (55 mg, 0.6 mmol) were refluxed in THF (15 ml) under a nitrogen atmosphere for 2 hrs. After cooling, hexane was added slowly to precipitate the product as bright yellow crystals (75%).

Anal. Found: C 43.37, H 3.01, N 6.08%. Calc. for $[\text{Re}_2(\text{IPQP})(\text{CO})_6(\text{py-3-NH}_2)\text{Cl}]\text{PF}_6$: C 43.22, H 2.96, N 6.17%; δ_{H} (400MHz, CD_3CN): 9.32 (1H, d, J 5.4, H_6), 9.25 (1H, d, J 1.9, H_3), 9.16 (2H, d, J 7.4, H_6^m, H_3), 9.02 (1H, d, J 1.8, H_5^m), 8.95 (1H, d, J 5.5, H_3^m), 8.94 (1H, s, H_5), 8.62 (1H, t, J 8.7, H_4), 8.5 (1H, t, J 8.2, H_4^m), 8.41 (1H, d, J 8.3, H_0), 7.97 (2H, m, $\text{H}_5, 5^m$), 7.77 (2H, d, J 8.4, H_0), 7.69 (1H, d, J 2.3, H_3^m), 7.57 (2H, d, J 8.3, H_m), 7.51 (1H, d, J 5.1, py-NH₂), 7.48 (2H, d, J 8.4, H_m), 7.24 (1H, d, J 8.2, py-NH₂), 7.07 (1H, d, J 1.9, py-NH₂), 6.97 (1H, m, py-NH₂), 3.85 (2H, s, -NH₂); IR (CH_3CN): 2033s, 2018s, 1937w, 1914w and 1901w cm^{-1} ; Mass

spectrum (ES): m/z 1218 [$\{\text{Re}_2(\text{IPQP})(\text{CO})_6(\text{py-3-NH}_2)\text{Cl}\}^+$, 29%] and 1162 [$\{\text{Re}_2(\text{IPQP})(\text{CO})_6(\text{py-3-NH}_2)\text{Cl}\}^+ - 2\text{CO}$, 100%]; UV spectra: 252(35340), 312(37500), 342(28720) and 372(sh) nm.

3.3.8 Attempted preparation of $[\text{Re}_2(\text{IPQP})(\text{CO})_6(\mu\text{-Cl})]\text{PF}_6$ (12)

$[\text{Re}(\text{IPQP})(\text{CO})_6(\text{CH}_3\text{CN})\text{Cl}]\text{PF}_6$ (30mg, 0.023 mmol) was refluxed in toluene (15 ml) under a nitrogen atmosphere for overnight. The product was then obtained by evaporating the solvent.

Anal. Found: C 41.58, H 2.67, N 4.38%. Calc. for $[\text{Re}_2(\text{IPQP})(\text{CO})_6(\mu\text{-Cl})]\text{PF}_6$: C 41.69, H 2.70, N 4.42%; IR(KBr): 2025s, 1926m and 1907m; Mass spectrum (ES): m/z 1123 [$\{\text{Re}_2(\text{IPQP})(\text{CO})_6(\mu\text{-Cl})\}^+$, 100%].

3.3.9 Attempts to prepare $\text{Re}_2(\text{IPQP})(\text{CO})_6\text{I}_2$

$\text{Re}_2(\text{IPQP})(\text{CO})\text{Cl}_2$ (50 mg, 0.043 mmol) and Bu_4NI (32 mg, 0.086 mmol) were allowed to reflux in acetonitrile (20 ml) under nitrogen atmosphere for overnight. IR frequency and Mass spectrum observed are the same as the reactant.

References

1. E.C. Constable, *Adv. Inorg. Chem.*, 1989, **34**, 1.
2. E.C. Constable, *Adv. Inorg. Chem. Radiochem.*, 1986, **30**, 69.
3. J.-M. Lehn, J.-P. Sauvage, J. Simon, R. Ziessel, C. Piccinni-Leopardi, G. German, J.-P. Declercq and M. Van Meerssche, *Nouv. J. Chim.*, 1983, **7**, 413.
E.C. Constable, M.J. Hannon, A. Martin, P.R. Raithby and D.A. Tocher, *Polyhedron*, 1992, **11**, 2971.
4. F.H. Burstall, *J. Chem. Soc.*, 1928, 1662.
5. E. C. Constable, S.M. Elder, J. Healy and D.A. Tocher, *J. Chem. Soc., Dalton Trans.*, 1990, 1669.
6. E.C. Constable, M.J. Hannon and D.R. Smith, *Tetrahedron Lett.*, 1994, **35**, 6657.
7. N.A. Sorenson, E. Samuelsen and F.R. Oxaal, *Acta Chem. Scand.*, 1947, **1**, 458.
8. F. Kröhnke, *Synthesis*, 1976, 1.
9. E. C. Constable, S.M. Elder, J. Healy, M.D. Ward and D.A. Tocher, *J. Am. Chem. Soc.*, 1990, **112**, 4590.
10. C.-M. Che, Y.-P. Wang, K.-S. Yeung, K.-Y. Wong and S.-M. Peng, *J. Chem. Soc., Dalton Trans.*, 1992, 2675.
11. C.-W. Chan, C.-M. Che and S.-M. Peng, *Polyhedron*, 1993, **12**, 2169.
12. C.-W. Chan, C.-M. Che, M.-C. Cheng and Y.-P. Wang, *Inorg. Chem.*, 1992, **31**, 4874.
13. E.N. Maslen, C.L. Raston and A.H. White, *J. Chem. Soc., Dalton Trans.*, 1975, 323.
14. S.M. Yang, K.K. Cheung and C.-M. Che, *J. Chem. Soc., Dalton Trans.*, 1993, 3315.
15. E.C. Constable, S.M. Elder and D.A. Tocher, *Polyhedron*, 1992, **11**, 2599.
16. E.C. Constable, S.M. Elder and D.A. Tocher, *Polyhedron*, 1992, **11**, 1337.
17. C. M. Che, C.W. Chan, S.M. Yang, C.X. Guo, C.Y. Lee and S.M. Peng, *J. Chem. Soc., Dalton Trans.*, 1995, 2961.
18. E. C. Constable, S.M. Elder, M.J. Hannon, A. Martin, P.R. Raithby and D.A. Tocher, *J. Chem. Soc., Dalton Trans.*, 1996, 2423.
19. E.C. Constable, M.J. Hannon, P. Harverson, M. Neuburger, D.R. Smith, V.F. Wanner, L.A. Whall, M. Zehnder, *Polyhedron*, 2000, **19**, 23-34.

20. E.C. Constable, M.J. Hannon, A.M.W. Cargill Thompson, D.A. Tocher and J.V. Walker, *Supramol. Chem.*, 1993, **2**, 243.
21. R. Chotalia, E. C. Constable, M.J. Hannan and D.A. Tocher, *J. Chem. Soc., Dalton Trans.*, 1995, 3571.
22. E. C. Constable, S.M. Elder and D.A. Tocher, *Polyhedron*, 1992, **11**, 3571.
23. G. Baum, E.C. Constable, D. Fenske, C.E. Housecroft and T. Kulke, *Chem. Eur. J.*, 1999, **5**, 1862.
24. E.C. Constable, T. Kulke, G. Baum and D. Fenske, *Inorg. Chem. Commun.*, 1998, **7**, 80.
25. A. Gelling, K.G. Orrell, A.G. Osborne and V. Šik, *Polyhedron*, 1999, **18**, 1285.
26. P. de Wolf, S.L. Heath and J.A. Thomas, *Inorg. Chim. Acta*, 2003, **355**, 280.
27. P. de Wolf, S.L. Heath and J.A. Thomas, *Chem. Commun.*, 2002, 2540.
28. K.T. Potts, *Bull. Soc. Chim. Belg.*, 1990, **99**, 741.
29. K.T. Potts, K.M. Keshavarz, F.S. Tham, H.D. Abruna, C. Arana, *Inorg. Chem.*, 1993, **32**, 4436.
30. E.C. Constable, P. Harverson, D.R. Smith, L.A. Whall, *Tetrahedron*, 1994, **50**, 7799.
31. M. Wrighton, D.L. Morse, *J. Am. Chem. Soc.*, 1974, **96**, 998.
32. J.V. Casper and T.J. Meyer, *J. Phys. Chem.*, 1983, **87**, 952.
33. E.R. Civitello, P.S. Dragovich, T.B. Karpishin, S.G. Novick, G. Bierach, J.F. O'Connell and T.D. Westmoreland, *Inorg. Chem.*, 1993, **32**, 237
34. J. Guilhem, C. Pascard, J-M. Lehn and R. Ziessel, *J. Chem. Soc., Dalton Trans.*, 1989, 1449.
35. D. Fischer and B. Krebs, *Zeitschrift fuer Anorganische und Allgemeine Chemie* (1982), **491**, 73.
36. H.-F. Lang, P. E. Fanwick and R. A. Walton, *Inorg. Chim. Acta*, 2001, **322**, 17.
37. R. Rossi, A. Marchi, A. Duatti, L. Magno, U. Casellato and R. Graziani, *J. Chem. Soc., Dalton Trans.*, 1988, 1857.
38. W. Purcell, A. Roodt, S. S. Basson, J.G. Leipoldt, *Transition Met. Chem.*, 1990, **15**, 239.
39. G. Ciani, D. Giusto, M. Manassero and M. Sansoni, *J. Chem. Soc., Dalton Trans.*, 1975, 2156.
40. L. Y. Y. Chan, E. E. Isaacs and W. A. G. Graham, *Can. J. Chem.*, 1977, **55**, 111.
41. Y. -D. Chen, L. -Y. Zhang, Z. -N. Chen, *Acta Cryst.*, 2005, **E61**, m121.

42. K. K-W. Lo, D. C-M. Ng, W-K. Hui and K-K. Cheung, *J. Chem. Soc., Dalton Trans.*, 2001, 2834.

Chapter 4

**Functionalisation of the $[\text{Re}(\text{CO})_3\text{bpy}]^+$
moiety**

4.1 Introduction

The organometallic fragments $\text{Re}(\text{CO})_3(\text{bpy})^+$ have been widely used in coordination and organometallic chemistry. The spectroscopic, photochemical and photophysical properties of these complexes attract much attention ever since their interesting excited state properties, which are similar to those of the $\text{Ru}(\text{bpy})_3^{2+}$ analogues, were first recognized in the 1970s.¹ Later work by Meyer and co-workers helped elucidate the relationship in these systems between the nature of the chloride and/or polypyridyl ligand and the character of the photophysical properties.² By varying the coordinating polypyridyl ligand, the electronic properties of the system studied may be tuned. The electronic absorption spectrum of *fac*- $[\text{Re}(\text{CO})_3(\text{bpy})\text{Cl}]$ typically exhibits a number of high energy absorption bands. A high-energy feature at $\sim 295\text{nm}$ is associated with a bipyridyl based $\pi - \pi^*$ transition.¹ A lower energy band observed at $\sim 390\text{nm}$ is associated with a $\text{Re}-\pi^*$ (bpy) MLCT transition and Cl-bpy LLCT transition.³ This assignment was later confirmed with density functional theory (DFT) calculations.⁴

Such systems easily lend themselves to the design of luminescent sensors and materials for supramolecular devices.

4.1.1 Ruthenium based sensors

Recognition of common ions is of paramount importance due to the important roles of ions in industrial and biological processes. The coordination of anionic guest species by hydrogen bond donating receptors is amply demonstrated in nature itself. Thus, the transport of anions such as sulphate and phosphate across cell membranes is known to occur by formation of a host-guest species, in which a neutral receptor protein binds the anion via multiple hydrogen bonding interactions. In these cases, anion complexation is made selective by appropriately positioned hydrogen bond donors which make up the binding site, such that only specific anions can fit into the binding cavity.

Anions receptors based on ruthenium–bipyridyl complexes have been shown to be both electrochemical and optical sensors for anions (Figure 4.1).⁵ The receptor possesses a macrocyclic core containing hydrogen bond donating NH groups. The research group⁵ monitored the cathodic shifts of the first substituted bipyridyl redox wave by the adding various anionic guests. Interestingly the other bipyridyl moieties

are not significantly perturbed by the presence of anions, a finding that serves to confirm that the anion is bound within the macrocyclic core in solution. The bound anion is perturbing only the nearby substituted bipyridyl moiety and not the more distant unsubstituted ones.

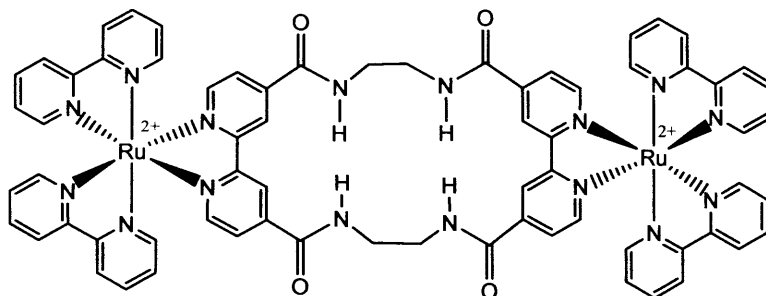


Figure 4.1 Ru based anion sensor

A combination of through bond and through space interactions together with a possible direct coordination pathway mediated via bpy $\text{C-H}\cdots\text{anion}$ hydrogen bonds are responsible for communicating the binding event to the bipyridyl moiety.

Ruthenium–bipyridyl based complexes have also been used for cation binding sensors.⁶ The complex $[\text{RuL}(\text{bipy})_2] [\text{PF}_6]_2$ (L = benzo-15-crown-5 ether) [Figure 4.2] has demonstrated spectrochemical recognition of Group IA and IIA metal cations (Na, Mg) in solution by the functionalised crown ethers.

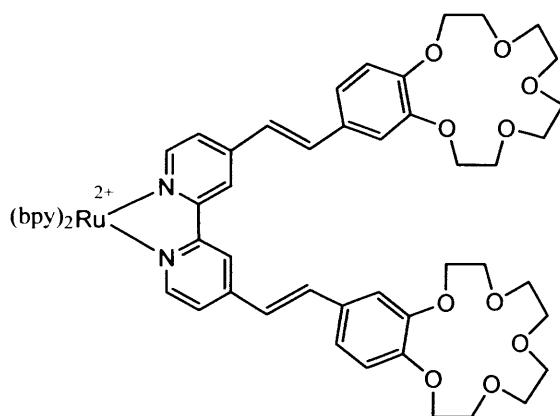


Figure 4.2 Ru based cation sensor

4.1.2 Rhenium based sensors

Interest in bipyridylrhenium(I)-based sensors has given rise to some very interesting and potentially useful molecular devices.⁷⁻⁸ In particular, systems designed to recognize anions have led to some sophisticated and complicated complexes. Elegant examples include the cationic molecular squares of Hupp and co-workers that selectively sense perchlorate,⁹ the rotaxane recently reported by the Beer group that shows a selectivity for hydrogensulfate,¹⁰ and the dimetallic diamide complex reported by Sun *et al.*¹¹

Hupp and coworkers studied the affinities of the rhenium–bipyridine rectangles (Figure 4.3).¹² The dimension of the cavity in the metallocyclic rectangle containing 4,4'-bpy is $5.89 \text{ \AA} \times 11.55 \text{ \AA}$. Proton NMR studies for the rectangle with bis-sodium salt of 2,6-naphthanedisulfonic acid gave association constants of $2.3 \times 10^3 \text{ M}^{-1}$, assuming the formation of a 1:1 host–guest complex. The authors concluded that the binding involves columbic interactions in addition to van der Waals interactions.

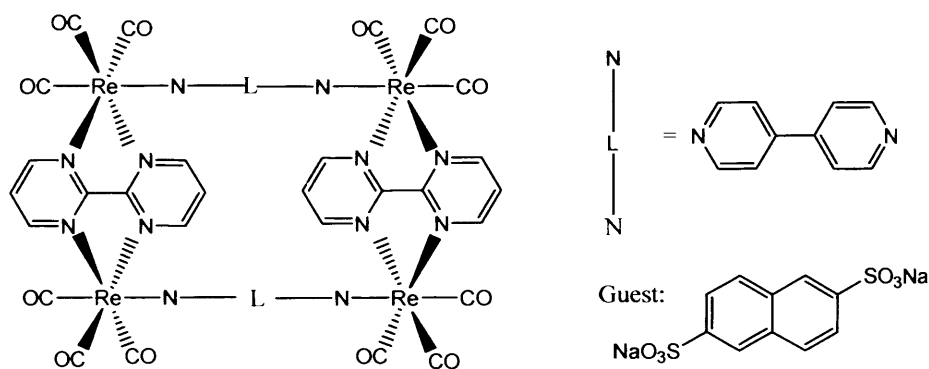


Figure 4.3 Re based sensor

Lo *et al.*¹³ has reported effective emission quenching of $[\text{Re}(\text{Me}_4\text{-phen})(\text{CO})\text{X}](\text{CF}_3\text{SO}_3)$ [$\text{Me}_4\text{-phen}$ = 3,4,7,8-tetramethyl-1,10-phenanthroline and X = Py-An, N-(1-anthraquinonyl)-N'-(4-pyridinylmethyl)thiourea and Py-Ph, N-(1-

phenyl)-N'-(4-pyridinylmethyl)thiourea] (Figure 4.4) upon binding the anions F^- , OAc^- and H_2PO_4^- .

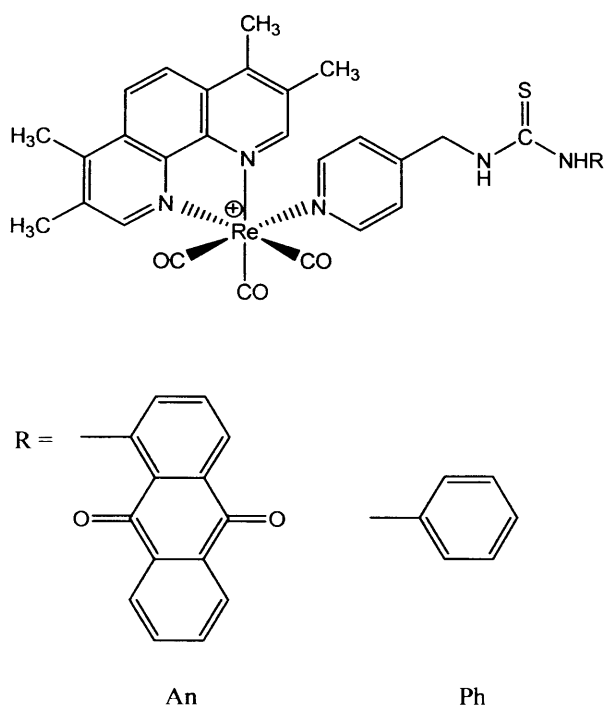


Figure 4.4: Anion binding rhenium complexes

Cation binding complexes of $\text{Re}(\text{CO})_3(\text{bpy})^+$ moiety have also been reported.¹⁴ The complex $[(\text{bpy})\text{Re}(\text{CO})_3\text{L}]^+$ (L = aza-15-crown-5 ether) [Figure 4.5] demonstrated significant blue shifts in the UV-Vis bands on protonation of the azacrown nitrogen atom or on complexation of alkali-metal (Li^+ , Na^+ and K^+) or alkaline-earth metal (Mg^{2+} , Ca^{2+} and Ba^{2+}) cations to the azacrown. Shifts in the azacrown ^1H NMR resonances reported on how the different metal cations interact with the macrocycle.¹⁴

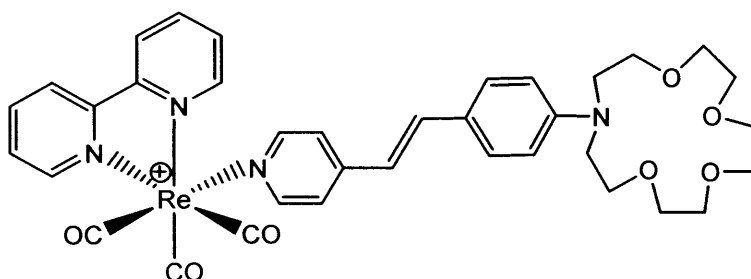


Figure 4.5 Re based cation sensor**4.1.3 Aim of the work**

This work mainly describes the synthesis and characterization of rhenium complexes of the $\text{Re}(\text{CO})_3(\text{bpy})^+$ moiety with their anion and cation binding capabilities, redox active properties and biological applications in mind.

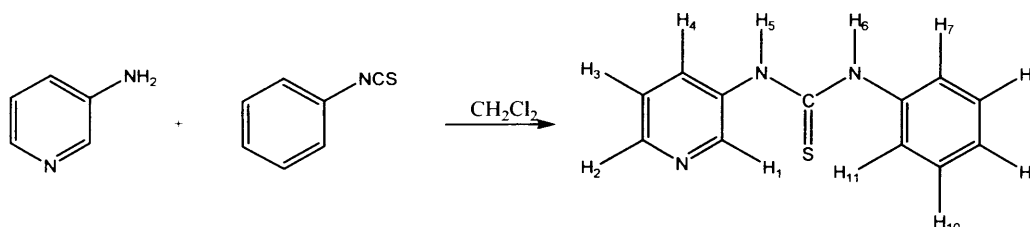
4.2 Results and Discussions**4.2.1 Anion binding switches:**

The development of anion sensors using various luminescent and redox-active systems has been investigated extensively.^{5, 7-12} While the amide group has been most commonly used to recognize anionic species,¹⁵ there is increasing interest in exploring other functional groups that show strong binding interaction with common anions. The thiourea moiety is one of the promising candidates. This unit has been attached to organic chromophores and fluorophores such as indoaniline,¹⁶ naphthalene¹⁷ and anthracene¹⁸ to produce effective anion sensors.

Here, we are interested in utilizing this thiourea unit to synthesis rhenium polypyridine complexes and to observe luminescence and anion binding properties of these complexes.

4.2.1.1 N-(3-pyridyl)-N'-phenylthiourea (L^1)

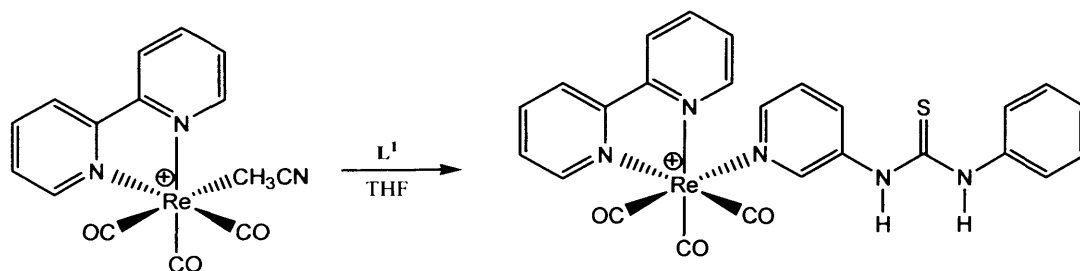
The ligand (L^1) was conveniently synthesized according to the literature method used by Avalos *et al.*¹⁹ Phenyl isothiocyanate and 3-aminopyridine was refluxed in a 1:1 molar ratio in dichloromethane to give the desired product in a quantitative yield (Scheme 4.1).

**Scheme 4.1: Synthesis of N-(3-pyridyl)-N'-phenylthiourea (L^1)**

The ligand was characterized by IR and ^1H NMR spectra. The IR spectrum shows characteristic $\text{C}=\text{S}$ peak at 1302 cm^{-1} . The ^1H NMR spectrum of the ligand shows two singlets at 10.2 and 9.87 ppm for H_5 and H_6 protons (N-H protons), respectively. The doublet at 8.31 ppm is due to the H_2 proton and the doublet of triplets at 7.94 ppm is due to the H_4 proton. The triplet at 7.15 ppm represents the H_3 proton. The H_1 proton should give a singlet, as there is no hydrogen to couple on neighbouring carbons, but it appears as a doublet at 8.6 ppm with a small coupling constant (2.5 Hz) which is due to coupling with H_2 proton. The phenyl group shows a doublet at 7.47 ppm for H_7 and H_{11} protons, and a multiplet at 7.37-7.33 ppm for H_8 , H_9 and H_{10} protons. The ligand L^1 can be utilized for anion recognition in biological processes. The recognition of an anion can take place through hydrogen bonding between the thiourea hydrogens and the anion. We expect that an anion sensory system could be achieved by the incorporation of an ion responsive chromophore into a lumophore. The anion uptake could change the absorption spectrum of the chromophore and hence potentially affect the luminescence properties of the lumophore.

4.2.1.2 $[\text{Re}(\text{CO})_3(\text{bpy})(\text{L}^1)]\text{PF}_6$ (13)

$[\text{Re}(\text{CO})_3(\text{bpy})(\text{py-3-NCS})]\text{PF}_6$ ²⁰ was prepared according to the literature procedure. Initial attempts to synthesize $[\text{Re}(\text{CO})_3(\text{bpy})(\text{L}^1)]\text{PF}_6$ involved the reaction of molar equivalent amounts of $[\text{Re}(\text{CO})_3(\text{bpy})(\text{py-3-NCS})]\text{PF}_6$ and aniline in acetonitrile. The resulting product was sticky and difficulties were encountered in obtaining and purifying the complex. However, the desired product was formed in a good yield (89%) by the substitution of acetonitrile from $[\text{Re}(\text{CO})_3(\text{bpy})(\text{CH}_3\text{CN})]\text{PF}_6$ by the ligand L^1 in refluxing THF (Scheme 4.2).



Scheme 4.2: Synthesis of $[\text{Re}(\text{CO})_3(\text{bpy})(\text{L}^1)]\text{PF}_6$ (13)

Complex **13** was characterized by IR, ^1H NMR and Mass spectrometry. The compound shows two strong IR absorption bands in the region associated with the carbonyl stretching frequencies and a medium band at 1295 cm^{-1} for the C=S group. The ^1H NMR spectrum of complex **13** was assigned by comparison to the shift observed for the ligand, L^1 , and $[\text{Re}(\text{CO})_3(\text{bipy})(\text{py-3-NCS})]\text{PF}_6$.²⁰ The spectrum exhibits two doublets and two triplets for the bipyridine protons and their shifts were consistent with those of $[\text{Re}(\text{CO})_3(\text{bipy})(\text{py-3-NCS})]\text{PF}_6$ ²⁰ and other $[\text{Re}(\text{CO})_3(\text{bpy})]^+$ containing compounds.²¹⁻²² The coordination of the ligand to the metal is apparent from the downfield shifts of the H_1 proton from 8.6 to 8.97 ppm and the upfield shift of the H_2 proton from 8.31 to 8.23 ppm. Significant upfield shifts were also observed for the N-H protons, H_5 and H_6 , from 10.02 to 9.65 and from 9.87 to 9.53, respectively. Mass spectroscopy (FAB) results support the formation of complex **13** and a molecular ion is evident at 652 m/z for $[\text{M-PF}_6]^+$. Attempts were made to grow X-ray quality crystals by diffusing ether into the acetonitrile solution, but these were unsuccessful.

Compound **13** offers visual luminescence under UV-lamp at room temperature in solid state. Upon excitation, a 10^{-4}M solution of **13** in acetonitrile excited at 340 nm gives an emission at 566 nm at room temperature. With reference to previous photophysical studies on rhenium (I) polypyridine systems,²¹⁻²² the emission of the complex is assigned to a MLCT $[\text{d}\pi(\text{Re}) \rightarrow \pi^*(\text{bpy})]$ excited state.

4.2.1.3 Test for anion binding

Lo's group¹³ found that the anion binding properties of anthraquinonyl free compound was reflected only by emission quenching while the anthraquinonyl compound showed significant quenching and red shifts in both absorption and emission spectra upon binding the anions.

Complex **13** and anthraquinonyl free compound have an almost similar structure. So, an initial attempt was taken to observe the anion-binding properties of the luminescent complex **13**. The experiment was done qualitatively by adding anions, such as phosphate (NH_4PO_3) and bromide (Bu_4NBr) to an acetonitrile solution of the compound to follow the changes in luminescence. Addition of phosphate did not have an effect on its luminescence property. This observation is not in line with the phosphate binding abilities of $[\text{Re}(\text{Me}_4\text{-phen})(\text{CO})\text{Py-Ph}]$ and is discouraging. The

reason for this may be due to the fact that the 3- position of the pyridyl thiourea group and the lack of methyl spacer higher the steric hindrance between complex **13** and the phosphate anion.

However, addition of bromide ion to a 10^{-4}M solution of complex **13** in degassed acetonitrile decreases relative luminescent intensity of the compound (20%) without shifting the emission maxima. Similar quenching was also observed for $[\text{Re}(\text{Me}_4\text{-phen})(\text{CO})\text{X}](\text{CF}_3\text{SO}_3)$ upon addition of I^- by Lo *et al.*¹³ But this quenching is not due to the binding of the ion, but the involvement of an excited-state association.²³

Due to small availability of complex **13** and lack of binding of phosphate ion we did not carry out further anion binding experiment for complex **13**.

4.2.1.4 $[\text{ReCl}(\text{CO})_3(\text{L}^1)_2]$ (**14**)

The concept of anion binding properties of compound **13** led us to prepare *bis*-[N-(3-pyridyl)-N'-phenylthiourea] rhenium complex. To investigate whether two thiourea groups in a complex could exhibit anion-binding properties in potentially a 'bidentate mode', compound **14** (Figure 4.5) was prepared.

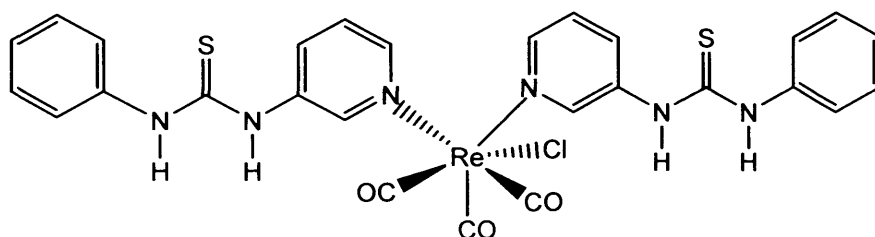
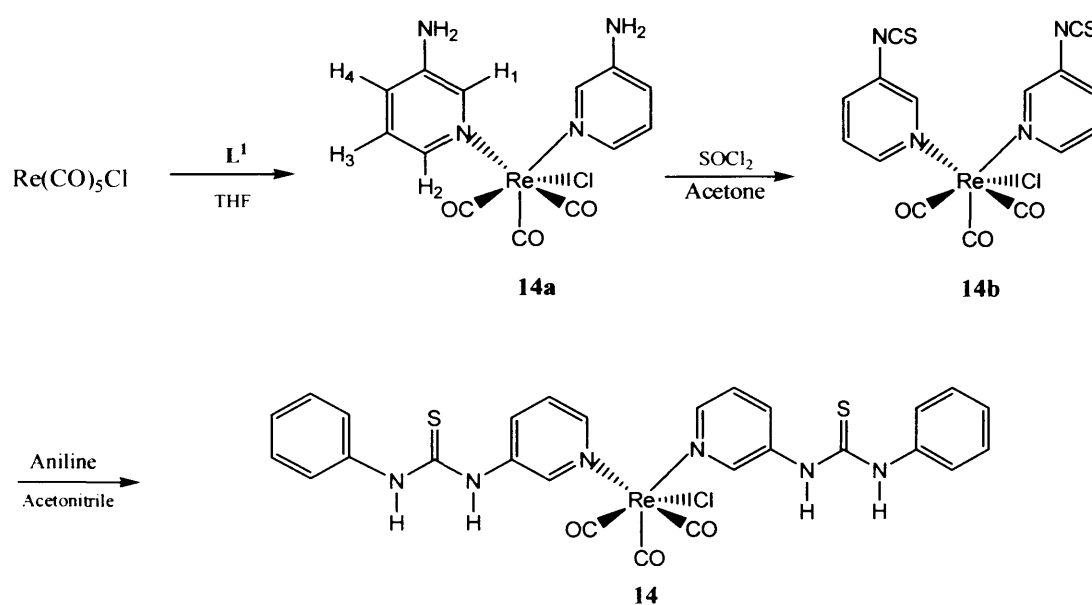


Figure 4.5: *Bis*-[N-(3-pyridyl)-N'-phenylthiourea] rhenium complex (**14**).

Attempts to synthesize compound **14** were made by following the general method for the preparation of the analogous compound, $[\text{Re}(\text{CO})_3(\text{py})_2\text{Cl}]$.²⁶ The reaction of $\text{Re}(\text{CO})_5\text{Cl}$ with two equivalents of L^1 in refluxing toluene were carried out until precipitation of the off-white product was observed. The product was insoluble in most of the solvents, such as, chloroform, methanol, acetonitrile, etc. The IR spectrum of the product showed facial arrangement of the carbonyl groups. The ^1H NMR spectrum of the product in DMSO was complicated and provided no conclusive evidence of complex formation. Electrospray mass spectrum suggested a compound

containing two rhenium atoms (^{186}Re) and two chlorine atoms (^{35}Cl) at 840 m/z but only one ligand molecule. However, this compound could be formed during the MS experiment when compound **14** was heated to get it into gas phase.

Afterwards, a three step route (Scheme 4.3) was followed to prepare compound **14**. The synthesis of intermediate **14a** required refluxing of $\text{Re}(\text{CO})_5\text{Cl}$ and 3-aminopyridine in a 1:2 molar ratio in toluene for 15 minutes. After cooling, the white precipitate was filtered and dried. The IR spectroscopy of the product showed $\text{C}\equiv\text{O}$ stretching frequencies at 2021, 1913 and 1886 cm^{-1} indicating the formation of a *fac*- tricarbonyl chlororhenium complex. The ^1H NMR spectrum of the complex exhibited a singlet at 8.18 ppm for H_1 , a doublet at 7.80 ppm for H_2 , a multiplet integrating to approximately two protons (H_3 and H_4) at 7.22-7.14 ppm and a singlet for two symmetrical N-H protons at 5.90 ppm. Significant downfield shifts were observed for H_1 and H_2 protons by 0.40 ppm in the complex compared to the free ligand. The formation of **14a** was also confirmed by the presence of the molecular ion at 512 mass unit (m/z) for $[\text{M}+\text{NH}_4]^+$.



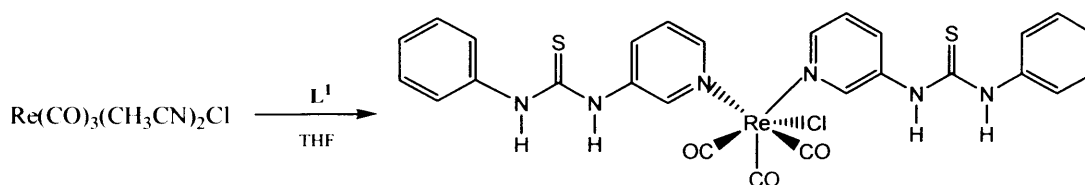
Scheme 4.3: Attempted synthesis of $[\text{Re}(\text{CO})_3(\text{bpy})(L^1)_2\text{Cl}]$ (**14**)

The preparation of **14b** followed a described literature method for the preparation of the isothiocyanate compounds.²² In this synthesis thiophosgene was added to **14a** in acetone in presence of calcium carbonate and the solution was

incubated in the dark overnight. The product was obtained by removing calcium carbonate by filtration and evaporating the solvent from the filtrate. The IR shows carbonyl peaks at 2021, 1906 and 1871 cm^{-1} and a distinctive peak at 2106 cm^{-1} for $\text{N}=\text{C}=\text{S}$ and the spectra is similar to that of $[\text{Re}(\text{bpy})(\text{CO})_3(\text{py-3-NCS})] \text{PF}_6$.²⁰ The ^1H NMR spectrum provided evidence of the complete disappearance of N-H protons. The ^1H NMR spectrum also showed the signals for H_1 and H_2 protons shifted downfield to 8.90 and 8.66 ppm for **14b** from the shifts, of those protons, 8.18 and 7.80 ppm for **14a**. The signals for protons H_3 and H_4 were also apparent separately with a triplet at 7.69 ppm and doublet at 8.27 ppm. The FAB mass spectroscopy also suggests the formation of **14b** with the presence of the molecular ion at 578 m/z .

Finally, the formation of **14** was performed by running the reaction of **14b** and aniline in acetonitrile in presence of triethylamine in the dark overnight. The product was obtained by complete evaporation of the solvent. The IR spectrum shows the complete disappearance of the $\text{N}=\text{C}=\text{S}$ peak and the presence of a peak at 1312 cm^{-1} for $\text{C}=\text{S}$ group indicating the formation of **14**. The ^1H NMR spectrum of **14** was complicated though two distinctive singlets appeared in the downfield shifts for N-H protons. Following the spectra one could expect that compound **14** might have been formed along with some impurity.

However, an easy and effective way to synthesize compound **14** is the substitution of acetonitrile from $[\text{Re}(\text{CO})_3(\text{CH}_3\text{CN})_2\text{Cl}]$ by L^1 and the reaction was carried out successfully in refluxing THF (Scheme 4.4). The product $[\text{Re}(\text{CO})_3(\text{L}^1)_2\text{Cl}]$, **14** was isolated by the addition of n-hexanes, which caused the precipitation of the white crystalline product in a yield of 65%.



Scheme 4.4: Synthesis of $[\text{Re}(\text{CO})_3(\text{bpy})(\text{L}^1)_2\text{Cl}]$ (**14**)

The product was characterized by IR, ^1H NMR and mass spectrum. The IR spectrum shows three strong peaks at 2022, 1919 and 1895 cm^{-1} for the facially arranged carbonyl groups and a peak at 1316 cm^{-1} for the $\text{C}=\text{S}$ group. The ^1H NMR

resonances of complex **14** are very similar to the corresponding signals of the ligand L^1 in DMSO-d_6 solution except H_1 proton shifted downfield from 8.6 to 9.04 ppm after complex formation.

Compound **14** does not exhibit luminescence in solid state or in solution. This observation is in agreement with other rhenium compounds containing non-chelated pyridines.²⁴

Attempts have been made to prepare an acetonitrile adduct of compound **14**, thus to facilitate the formation of $[\text{Re}(\text{CO})_3(\text{L}^1)_3]^+$ with the substitution of acetonitrile by L^1 . The reaction was carried out by using equimolar silver perchlorate and compound **14** in acetonitrile under nitrogen atmosphere in the dark overnight to replace the chloride ion with acetonitrile donor. The IR spectrum of the product remained the same as the chloride species which indicates the reaction did not occur. The insolubility of the compound in acetonitrile may prohibit the reaction from occurring.

Compound **14** did not show luminescence and the substitution of the chloride was not possible due to the insolubility of the compound in acetonitrile. As a consequence, the investigation of the anion-binding capabilities of this complex was stopped. Cation binding abilities of the $[\text{Re}(\text{CO})_3(\text{bpy})]^+$ moiety was then considered in the next section.

4.2.2 Cation binding switches:

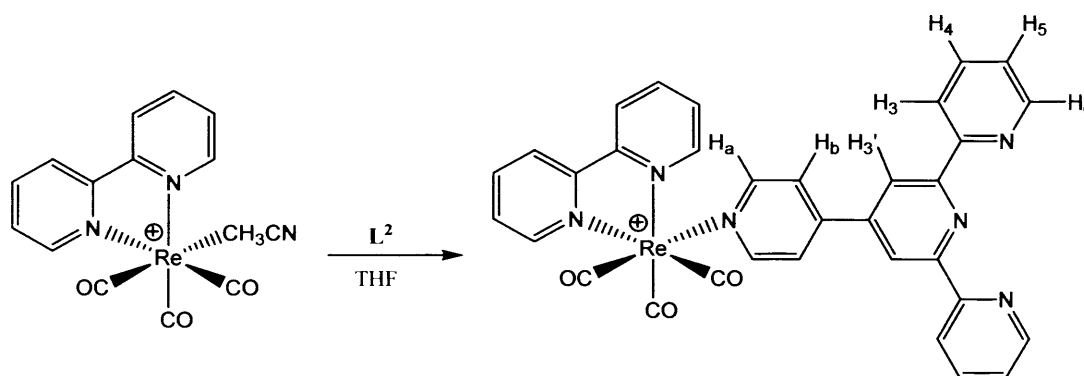
There is considerable interest in molecules which bind cations in solution, and which incorporate functional groups that signal cation binding *via* the change in a molecular property that is easily detected.²⁵ Such cation sensors have potential uses ranging from components in photonic communication devices to monitors of cation-dependent biological processes. Azacrown ethers are common motifs in cation sensors because the azacrown nitrogen atom has a lone pair that can form part of a delocalised electron system, and so can provide very effective electronic communication between the receptor and the rest of the molecule, including the signalling unit.

In particular, the signalling unit $[(\text{bpy})\text{Re}(\text{CO})_3]^+$ is being used increasingly in sensors because its metal-to-ligand charge-transfer (MLCT) excited state emits with a moderate quantum yield, and in photochemically active systems because it can undergo excited-state electron- and energy-transfer reactions.²⁶

The ligands we have investigated for use as potential cation binding switches are 4'-(4'''-pyridyl)-2,2':6',2''-terpyridine (L^2) and 4,4'-bipyridine (L^3) as they contain at least one pendent nitrogen. These ligands can be used to prepare luminescent rhenium complexes by using a pyridyl moiety at one end of the ligand to bind to the rhenium centre and the other end of the ligand have either a pyridyl or terpyridyl moiety which can coordinate with different metals and may change the luminescent behaviour of the rhenium lumophore, thus acting as a cation binding switch.

4.2.2.1 $[\text{Re}(\text{CO})_3(\text{bpy})(\text{L}^2)]\text{PF}_6$ (**15**)

The ligand, 4'-(4'''-pyridyl)-2,2':6',2''-terpyridine, L^2 was prepared following the literature procedure.²⁷ Compound **15** was obtained by the addition of the ligand L^2 to the precursor compound $[\text{Re}(\text{CO})_3(\text{bpy})(\text{CH}_3\text{CN})]\text{PF}_6$ in refluxing THF (Scheme 4.5). The product was isolated by the addition of hexane, which caused the precipitation of the yellow crystalline product in a yield of 60%.



*Scheme 4.5: Synthesis of $[\text{Re}(\text{CO})_3(\text{bpy})(\text{L}^2)]\text{PF}_6$ (**15**)*

The compound was characterized spectroscopically as well as crystallographically. The IR spectrum of compound **15** showed the presence of absorption bands characteristic of the carbonyl moiety. These absorptions have significantly shifted to lower energies relative to the $[\text{Re}(\text{bpy})(\text{CO})_3(\text{CH}_3\text{CN})]^+$ precursor complex which is typical for this type of complex.²⁰⁻²² The ^1H NMR spectrum of a CD_3CN solution of complex **15** is shown in Figure 4.6. The spectrum is sharp and well resolved. The spectrum was assigned by comparison with the ^1H NMR shifts observed for pyterpy²⁷ and $[\text{Re}(\text{CO})_3(\text{bipy})(4,4'\text{-bpy})]\text{PF}_6$.²¹⁻²²

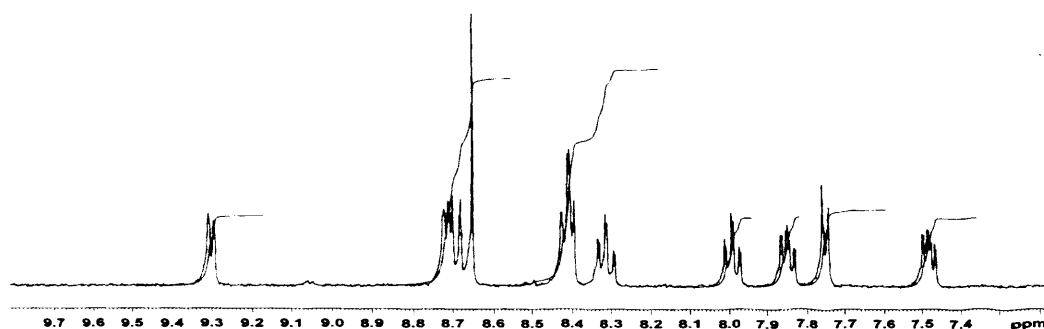


Figure 4.6 400 MHz ^1H NMR spectrum of $[\text{Re}(\text{CO})_3(\text{bpy})(\text{L}^2)]\text{PF}_6$ (**15**) in CD_3CN .

The spectrum exhibits two doublets and two triplets for the bpy protons and their shifts remain identical to those of the $[\text{Re}(\text{CO})_3(\text{bpy})]^+$ moiety.²⁰⁻²² The protons on the 4-pyridyl ring (H_a δ 8.69, H_b δ 7.75) were assigned with respect to the corresponding protons in $[\text{Re}(\text{CO})_3(\text{bipy})(4,4'\text{-bpy})]\text{PF}_6$ (H_a 8.81, H_b 7.95; with a general shift of ~ 0.2 ppm being observed due to the spectrum being recorded in DMSO). Since the pyterpy ligand has a significant localization of electron density on the pendant-ring nitrogen atom, we consider that the regioselective substitution is possible. Upon complex formation, the two doublets associated with the pyridyl protons of L^2 should be shifted significantly compared to the rest of the protons. However, in our experiment their shifts remained almost unchanged (0.08 ppm for H_a proton and 0.04 ppm for H_b proton) with those of the free ligand.²⁷ The two doublets for H_6 and H_3 protons of the terpyridine are overlapping and appear as a triplet, shifted to high field by approximately 0.3 ppm. The ES positive mass spectrum shows a peak at 737 m/z which corresponds to the calculated mass of $[\text{Re}(\text{CO})_3(\text{bpy})(\text{L}^2)]^+$.

X-ray quality light green crystals of compound **15** were obtained by diffusing diethyl ether into an acetonitrile solution of the compound. Crystallographic data for compound **15** is listed in Table 1, and the structure is shown in Figure 4.7. The details of crystallographic discussion will be presented in the section 4.2.2.3.

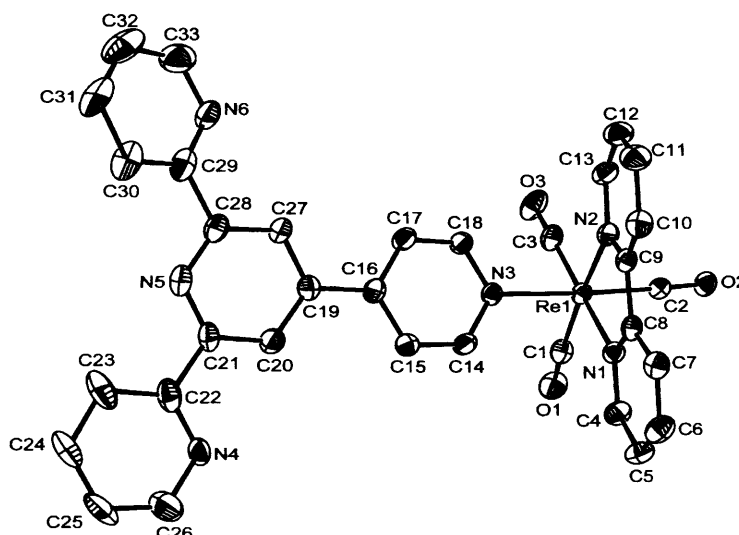


Figure 4.7 Ortep diagram of the cation present in $[\text{Re}(\text{CO})_3(\text{bpy})(\text{L}^2)]\text{PF}_6$ (**15**).

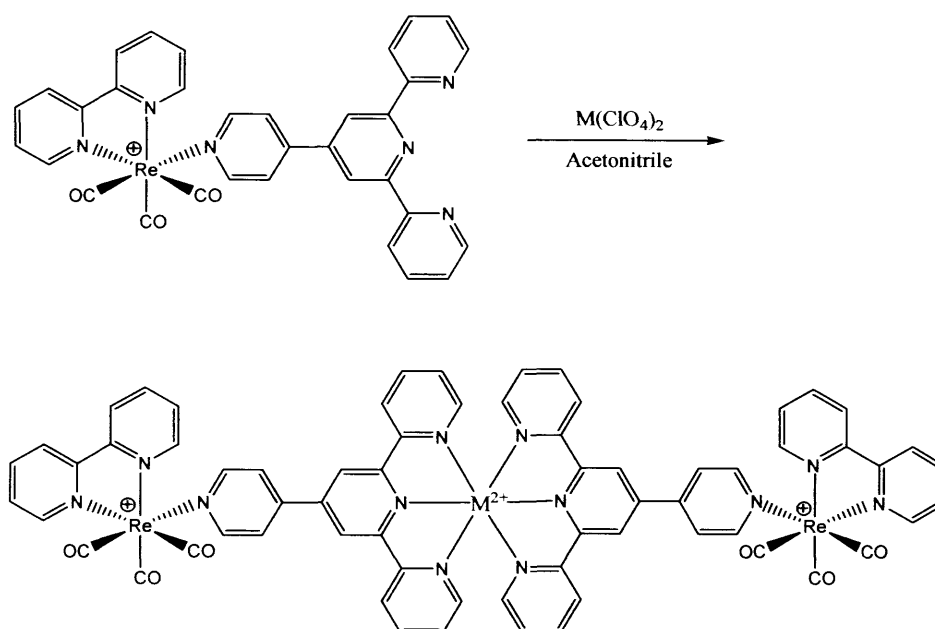
Thermal ellipsoids are drawn at 50% probability.

Cyclic voltammetric study of the compound in acetonitrile solution using *n*- Bu_4NBF_4 electrolyte in the solvent range +2.0 to -2.0 V demonstrated an irreversible oxidation at 1.3 V and a reversible reduction at -1.56 V vs SCE. Comparing with other $\text{Re}(\text{bpy})(\text{CO})_3$ containing compounds,²¹ the oxidation can be assigned to the rhenium based oxidation $[\text{Re}(\text{I})/\text{Re}(\text{II})]$ and the reduction may be assigned to the bipyridine based or py-terpy based reduction.

The compound is luminescent at room temperature. Upon excitation, at 390 nm, of a 10^{-4}M solution of compound **15** in acetonitrile, an emission peak at 565 nm was observed. The origin of the emission is a $^3\text{MLCT}$ [$d\pi(\text{Re}) \rightarrow \pi^*(\text{bpy})$] excited state. This compound has a coordinated pyridyl site and an uncoordinated terpy site. Because of these structural features, the complex can act as a ‘ligand-like’ coordinative unit through the terpy site and is expected to design polymetallic coordination compounds. Besides the structural feature, the luminescence property of the complex may also be tuned by the incorporation of the metal ions. Thus, it may be possible to construct optical sensors by using this precursor complex, **15**.

4.2.2.2 $[\text{Re}(\text{CO})_3(\text{bpy})(\text{L}^2)]_2\text{M}(\text{PF}_6)_2$ [$\text{M} = \text{Zn}(\mathbf{16})$ and $\text{Fe}(\mathbf{17})$]

Compound **16** and **17** were synthesized by the reaction of the corresponding perchlorate salt with compound **15** in a 1:2 molar ratio (Scheme 4.6). The reactions were carried out in acetonitrile at room temperature.



Scheme 4.6 Synthesis of $[\text{Re}(\text{CO})_3(\text{bpy})(\text{L}^2)]_2\text{M}(\text{PF}_6)_2$ [$\text{M} = \text{Zn}(\mathbf{16})$ and $\text{Fe}(\mathbf{17})$].

The zinc complex, **16**, was precipitated by adding diethyl ether to the acetonitrile solution of the complex. The formation of complex **16** was confirmed by the ¹H NMR spectrum (Figure 4.9) of the resulting precipitate that differs significantly from the starting material **15**. In order to assign the complete ¹H NMR spectrum of complex **16**, we also prepared $[\text{Zn}(\text{pyterpy})_2][\text{PF}_6]_2$ (**16a**). The reaction of zinc perchlorate with two equimolar pyterpy in acetonitrile resulted in the formation of $[\text{Zn}(\text{pyterpy})_2][\text{PF}_6]_2$. The ¹H NMR spectrum of a CD₃CN solution of this complex is shown in Figure 4.8 and shifts are listed in Table 1. The spectrum is relatively sharp and illustrates the high symmetry of the zinc(II) complex on the ¹H NMR time-scale.

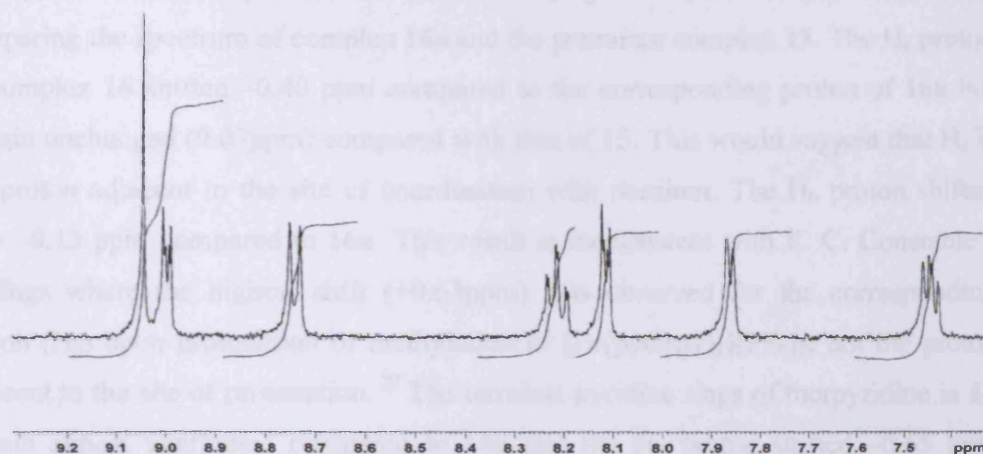


Figure 4.8 The 400 MHz ^1H NMR spectrum of $[\text{Zn}(\text{pyterpy})_2][\text{PF}_6]_2$ (**16a**) in CD_3CN .

The assignment of the resonances were made by comparison with the ^1H NMR spectrum of $[\text{Fe}(\text{pyterpy})_2][\text{PF}_6]_2$.²⁷ The main shifts were associated with H_6 (-0.86 ppm), H_4 (0.36 ppm), $\text{H}_{3'}$ (0.32 ppm), H_b (0.33 ppm) and H_a (0.25 ppm) protons in $[\text{Zn}(\text{pyterpy})_2][\text{PF}_6]_2$ comparing to the free ligand. Similar type of shifts were also observed for $[\text{Fe}(\text{pyterpy})_2][\text{PF}_6]_2$ [H_6 (-1.56 ppm), H_5 (0.28 ppm), $\text{H}_{3'}$ (0.47 ppm), H_b (0.44 ppm) and H_a (0.26 ppm)] compared to the free ligand.

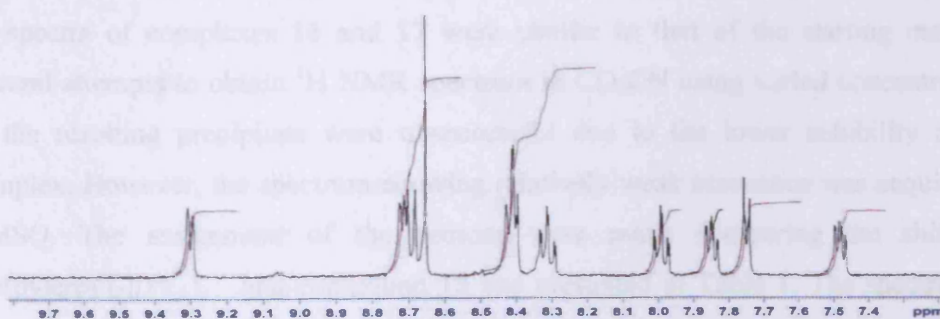


Figure 4.9 The 400 MHz ^1H NMR spectrum of $[\text{Re}(\text{CO})_3(\text{bpy})(\text{pyterpy})]_2\text{Zn}[\text{PF}_6]_2$ (**16**) in CD_3CN .

Finally, the ^1H NMR spectrum of complex **16** (Figure 4.9) was simply assigned by comparing the spectrum of complex **16a** and the precursor complex **15**. The H_a proton of complex **16** shifted -0.40 ppm compared to the corresponding proton of **16a** but remain unchanged (0.07 ppm) compared with that of **15**. This would suggest that H_a is the proton adjacent to the site of coordination with rhenium. The H_b proton shifted only -0.13 ppm compared to **16a**. This result is inconsistent with E. C. Constable's findings where the highest shift ($+0.63$ ppm) was observed for the corresponding proton (H_b) upon protonation or methylation of $[\text{Fe}(\text{pyterpy})_2][\text{PF}_6]_2$, not the proton adjacent to the site of protonation.²⁷ The terminal pyridine rings of terpyridine in **16** remain almost unaffected compared to **16a** and the H_6 proton shifted -0.65 ppm compared to **15** upon complexation with the Zn^{2+} ion. The ES mass spectrum of complex **16** exhibited peaks at $m/2$ 892 $[\text{M}-\text{PF}_6-\text{ClO}_4]$ and 737 $[\text{M}-2\text{PF}_6-2\text{ClO}_4-\text{Zn}]$.

Table 1: ^1H NMR shifts for pyterpy protons (δ).

	H_6	H_5	H_4	H_3	$\text{H}_{3'}$	H_b	H_a
$\text{L}^{2,27}$	8.73	7.37	7.89	8.68	8.76	7.79	8.77
$[\text{Re}(\text{CO})_3(\text{bpy})(\text{L}^2)]\text{PF}_6$	8.41	7.48	7.99	8.41	8.65	7.75	8.69
$[\text{Zn}(\text{L}^2)_2][\text{PF}_6]_2$	7.87	7.43	8.25	8.75	9.08	8.12	9.02
$[\text{Re}(\text{CO})_3(\text{bpy})(\text{L}^2)]_2\text{Zn}[\text{PF}_6]_2$	7.76	7.37	8.15	8.47	8.85	7.99	8.62
$[\text{Fe}(\text{L}^2)_2][\text{PF}_6]_2^{27}$	7.17	7.09	7.92	8.63	9.23	8.23	9.03
$^a[\text{Re}(\text{CO})_3(\text{bpy})(\text{L}^2)]_2\text{Fe}[\text{PF}_6]_2$	7.13	7.13	8.42	8.66	8.78	8.02	8.93

^a spectrum recorded in DMSO

The complexation of iron (II) in compound **17** was immediately apparent due to the observed colour change from yellow to violet and the precipitate formed. The IR spectra of complexes **16** and **17** were similar to that of the starting material. Several attempts to obtain ^1H NMR spectrum in CD_3CN using varied concentrations of the resulting precipitate were unsuccessful due to the lower solubility of the complex. However, the spectrum showing relatively weak resonance was acquired in DMSO. The assignment of the protons were made comparing the shifts in $[\text{Fe}(\text{pyterpy})_2][\text{PF}_6]_2$ and compound **15** and presented in Table 1. The spectrum of compound is in consistent with that of compound **16**.

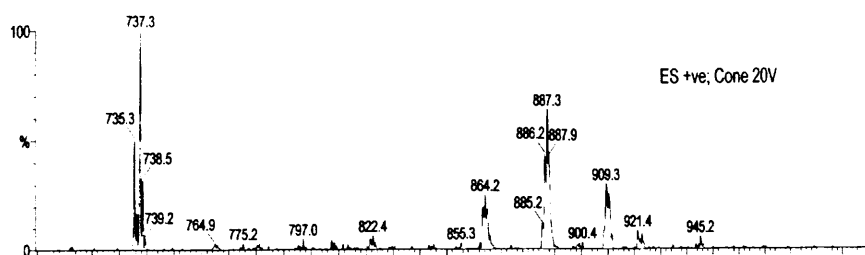


Figure 4.10 ES-MS spectrum of $[\text{Re}(\text{CO})_3(\text{bpy})(\text{L}^2)]_2\text{Fe}[\text{PF}_6]_2$ at $m/2$ (17).

From the mass spectroscopy, the presence of the trimetallic species has also been confirmed. The ES mass spectrum of complex 17 exhibited peaks at $m/2$ 887 $[\text{M}-\text{PF}_6-\text{ClO}_4]$, 864 $[\text{M}-2\text{PF}_6]$, 765 $[\text{M}-2\text{PF}_6-2\text{ClO}_4]$ and 737 $[\text{M}-2\text{PF}_6-2\text{ClO}_4-\text{Fe}]$ (Figure-4.10).

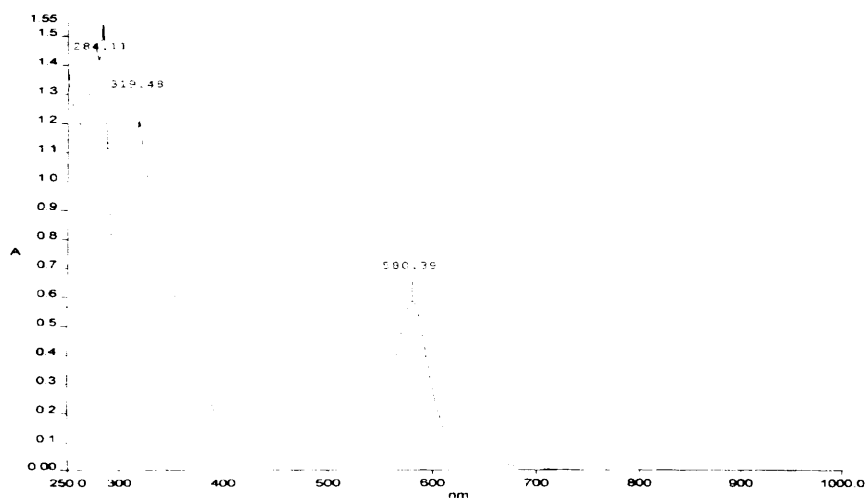


Figure 4.11 UV-vis absorption spectrum of $5 \times 10^{-4} \text{ M}$ CH_3CN solution of $[\text{Re}(\text{CO})_3(\text{bpy})(\text{pyterpy})]_2\text{Fe}[\text{PF}_6]_2$ (17) at 298 K

The UV spectrum of an acetonitrile solution of the trimetallic iron species exhibits band at 284 (sharp), 319 (sharp), 336 (shoulder), 364 (shoulder) and 580 (sharp) nm (Figure 4.11). The intense absorption at 580 (ϵ 28 500 $\text{dm}^3 \text{ mol}^{-1} \text{ cm}^{-1}$) nm can be assigned to metal(Fe)-to-ligand(pyterpy) charge transfer (MLCT) band and can

be compared to the MLCT band of $[\text{Fe}(\text{Hpyterpy})_2][\text{PF}_6]_4$ (594 nm) and $[\text{Fe}(\text{mepyperpy})_2][\text{PF}_6]_4$ (595 nm, ϵ 25 700 $\text{dm}^3 \text{mol}^{-1} \text{cm}^{-1}$).²⁷ The shift of MLCT band to lower energy compared to the MLCT band of $[\text{Fe}(\text{terpy})_2][\text{PF}_6]_4$ (552 nm, ϵ 11 900 $\text{dm}^3 \text{mol}^{-1} \text{cm}^{-1}$) and $[\text{Fe}(\text{pyterpy})_2][\text{PF}_6]_4$ (569 nm, ϵ 24 500 $\text{dm}^3 \text{mol}^{-1} \text{cm}^{-1}$)²⁷ is compatible with the lowering in energy of the π^* levels upon increasing the charge on the ligand. The other bands centred between 284 and 364 nm are assigned to pyterpy-based (π - π^* and n - π^*) bands and the Re-based MLCT band on consideration of the absorption spectra of pyterpy, $[\text{Re}(\text{CO})_3(\text{bpy})(4,4'\text{-bpy})]^+$ ²¹ and $\text{Re}(\text{CO})_3(\text{pyterpy})_2\text{Br}$.²⁸ No absorption band was observed for d-d transitions. This may be attributable to the weak nature of d-d transitions compared to other transitions.

The luminescence properties of complexes **16** and **17** were studied. A 10^{-4} M solution of compound **16** gave room temperature emission at 565 nm upon excitation at 390 nm, which is similar to the luminescence behavior of compound **15**. The result indicated that the Zn^{2+} ion has no influence on the luminescence of $[\text{Re}(\text{CO})_3(\text{bpy})(\text{pyterpy})]\text{PF}_6$. This observation is in line with the effect of Zn^{2+} ions on the fluorescence of ligand pyterpy.²⁹ No luminescence was detected upon excitation to the MLCT band for complex **17**. This is not surprising since Fe^{2+} terpyridine complexes bear low lying metal-centred states that provide non-radiative deactivation pathways for luminescence quenching.³⁰

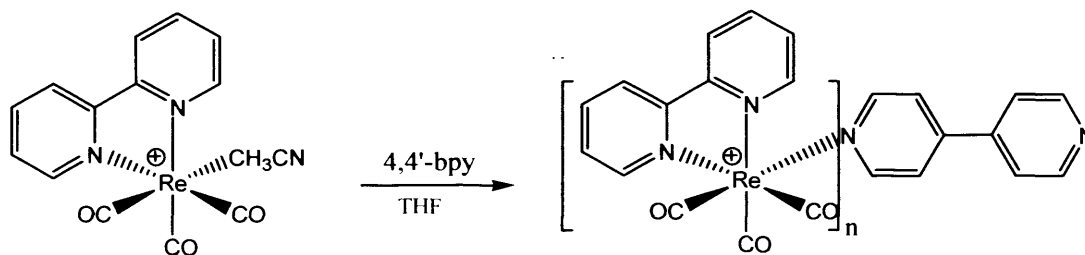
Since the luminescent behaviours of lanthanide ions, especially Eu^{3+} , have received great interest because of their unique luminescence emission,³¹ attempts have been made to synthesize a Eu^{3+} containing complex by the reaction of europium perchlorate and compound **15**. In the ^1H NMR spectrum of the perchlorate salt of the resulting compound a number of unexpected peaks were observed. Although the reaction was carried out in CH_3CN , we used an aqueous europium salt, and the complex may dissociate in presence of water, which is common for europium terpyridine complexes.³² In this case, mass spectral analysis of the compound might be helpful. However, electrospray mass spectrum only gave a molecular ion for a single unit of compound **15**. Attempts to grow crystals by diffusing diethyl ether into an acetonitrile solution of the compound afforded X-ray quality crystals of compound **15**.

We were interested in the luminescence spectrum of the complex to notice any traceable Eu^{3+} ion. Upon excitation a 10^{-4} M solution of the product at 390 nm gave

room temperature emission at 565 nm, which is Re-based emission. No sensitization of Eu^{3+} luminescence (600-615nm) was observed perhaps suggesting that Eu^{3+} did not coordinate with compound **15**. Thus, it has been confirmed that the complexation of **15** with Eu^{3+} ion was unsuccessful. The presence of the bulky substituents on pyterpy of the precursor complex may be responsible for the non formation of the expected product, probably as a result of pronounced steric constraints.

4.2.2.3 $[\text{Re}(\text{CO})_3(\text{bpy})]_n\text{L}^3(\text{PF}_6)_n$ [$n=1$ (**18**) and **2**(**19**), $\text{L}^3 = 4,4'$ -bpy]

Complexes **18** and **19** were prepared according to literature procedures (Scheme 4.7).²¹⁻²² The formation of compound **19** is quite straightforward and involved the reaction of 2:1 molar ratio of 4,4'-bpy with the precursor complex $[\text{Re}(\text{CO})_3(\text{bpy})(\text{CH}_3\text{CN})]\text{PF}_6$ in refluxing THF. The compound readily precipitates out from the solution with a reasonable yield (60%). The IR, ^1H NMR and mass spectra of the compound are in good agreement with the published work.¹⁸⁻¹⁹



Scheme 4.7 Synthesis of $[\text{Re}(\text{CO})_3(\text{bpy})]_n\text{L}^3(\text{PF}_6)_n$ [$n=1$ (**18**) and **2**(**19**), $\text{L}^3 = 4,4'$ -bpy]

Compound **18** was synthesized by the reaction of $[\text{Re}(\text{CO})_3(\text{bpy})(\text{CH}_3\text{CN})]\text{PF}_6$ with 10-fold excess of the ligand L^3 . During the course of the reaction a yellow precipitate of compound **19** was formed which was characterized by ^1H NMR. Compound **18** remained in the solution and hexane was added to precipitate the product. The ^1H NMR of the crude reaction mixture indicated the existence of the two products, **18** and **19**, in roughly a 4:1 ratio. The product was then dissolved in dichloromethane and ether was added to recrystallize the product. Complex **18** was obtained in a pure state, indicated by ^1H NMR, in low yield (35%). However, using

20-fold of L^3 , the reaction proceeded straightforward to give compound **18** in a higher yield of 55%.

The structures of both the complexes were determined by X-ray crystallography. The X-ray quality crystals of complex **18** were obtained by diffusing diethyl ether into dichloromethane solution of the compound whereas the crystals of compound **19** were obtained by layering an acetonitrile solution of the complex with water. The structures of complexes **18** and **19** are shown in Figs.4.12 and 4.13 respectively. However, the crystal structure of $[\text{Re}(\text{CO})_3(\text{bpy})(4,4'\text{-bpy})]^+$ with CF_3SO_3^- counterion has been published³³ concurrently as we obtained the structure of **18**. Details of the crystal parameters, data collection and refinement for the structures **18** and **19** along with the structure of **15** are collected in Table 2. Corresponding relevant bond angles are given in Table 3.

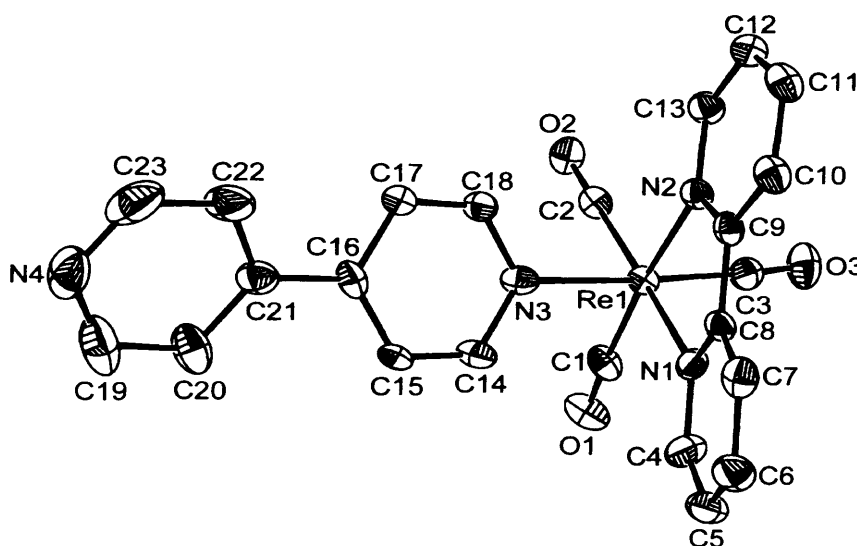


Figure 4.12 Ortep diagram of the cation present in $[\text{Re}(\text{CO})_3(\text{bpy})(\text{L}^3)]\text{PF}_6$ (**18**).

Thermal ellipsoids are drawn at 50% probability.

Table 2. Crystal data and structure refinement for **15**, **18** and **19**.

Compound	15	18	19
Empirical formula	C ₃₅ H ₂₅ Cl N ₇ O ₇ Re	C ₂₃ H ₁₆ F ₆ N ₄ O ₃ P Re	C ₄₀ H ₃₀ F ₁₂ N ₈ O ₆ P ₂ Re ₂
Formula weight	877.27	727.57	1381.06
Temperature	150(2) K	150(2) K	150(2) K
Wavelength	0.71073 Å	0.71073 Å	0.71073 Å

Crystal system	Triclinic	Orthorhombic	Monoclinic
Space group	P-1	P 212121	P2(1)/c
a Å	8.4510(2)	11.1580(2)	23.3031(2)
b Å	11.8890(3)	14.3180(3)	12.4413(2)
c Å	18.4520(4)	14.9470(4)	16.3796(2)
$\alpha/^\circ$	73.462(1)	90.00	90.11
$\beta/^\circ$	80.510(1)	90.00	108.9151(7)
$\gamma/^\circ$	74.044(1)	90.00	90.00
Volume Å ³	1701.21(7)	2387.94(9)	4492.35(10)
Z	2	4	4
Density (calculated) Mg/m ³	1.713	2.024	2.042
Absorption coefficient mm ⁻¹	3.710	5.238	5.562 mm ⁻¹
F(000)	864	1400	2648
Crystal size	0.25 x 0.13 x 0.10	0.55 x 0.40 x 0.35	0.28 x 0.24 x 0.20
θ -range for data collection (°)	3.10 - 27.52	3.07 - 30.03	2.98 - 27.49
Index ranges	-10 ≤ h ≤ 10 -15 ≤ k ≤ 15 -23 ≤ l ≤ 23	-10 ≤ h ≤ 15 -20 ≤ k ≤ 20 -20 ≤ l ≤ 21	-29 ≤ h ≤ 30 -16 ≤ k ≤ 16 -21 ≤ l ≤ 21
Reflections collected	18701	18488	54803
Independent reflections	7499 [R _{int} = 0.0476]	6905 [R _{int} = 0.0796]	10206 [R _{int} = 0.0943]
Completeness to θ = 30.03°	95.8 %	99.7 %	
Absorption correction	Semi-empirical from equivalents	Semi-empirical from equivalents	Semi-empirical from equivalents
Max. and min. transmission	0.7079 and 0.4573	0.2615 and 0.1608	
Refinement method	Full-matrix least- squares on F ²	Full-matrix least- squares on F ²	Full-matrix least- squares on F ²
Data / restraints / parameters	7499 / 0 / 446	6905 / 0 / 337	10206 / 0 / 642
Goodness-of-fit on F ²	1.098	1.038	1.024
Final R indices [I > 2σ (I)]	R ₁ = 0.0390 wR ₂ = 0.0999	R ₁ = 0.0463 wR ₂ = 0.1012	R ₁ = 0.0378 wR ₂ = 0.0831
R indices (all data)	R ₁ = 0.0447 wR ₂ = 0.1031	R ₁ = 0.0590 wR ₂ = 0.1081	R ₁ = 0.0561 wR ₂ = 0.0911

Table 3. Bond lengths [Å] and angles [°] for **15**, **18** and **19**.

Compound	15	18	19
Re(1)-C(1)	1.942(6)	1.929(7)	1.920(5)
Re(1)-C(2)	1.922(5)	1.924(8)	1.936(5)
Re(1)-C(3)	1.929(6)	1.927(8)	1.933(5)
Re(1)-N(1)	2.163(4)	2.181(6)	2.170(4)

Re(1)-N(2)	2.165(4)	2.165(6)	2.181(4)
Re(1)-N(3)	2.205(4)	2.217(6)	2.201(4)
C(2)-Re(1)-C(3)	90.1(2)	88.2(3)	90.1(2)
C(2)-Re(1)-C(1)	89.3(2)	87.8(3)	86.5(2)
C(3)-Re(1)-C(1)	88.7(2)	88.5(3)	91.1(2)
C(2)-Re(1)-N(2)	98.9(2)	99.4(3)	100.42(18)
C(3)-Re(1)-N(2)	92.49(17)	91.2(3)	94.93(18)
C(1)-Re(1)-N(2)	171.74(19)	172.8(3)	170.79(19)
C(2)-Re(1)-N(1)	173.22(18)	171.8(3)	174.39(18)
C(3)-Re(1)-N(1)	93.50(18)	97.7(3)	93.14(18)
C(1)-Re(1)-N(1)	96.5(2)	98.0(3)	98.0(2)
N(2)-Re(1)-N(1)	75.28(16)	74.9(2)	74.72(15)
C(2)-Re(1)-N(3)	91.19(18)	91.4(3)	90.47(18)
C(3)-Re(1)-N(3)	174.36(17)	175.8(3)	178.62(19)
C(1)-Re(1)-N(3)	96.79(19)	95.7(3)	90.21(18)
N(2)-Re(1)-N(3)	81.89(15)	84.7(2)	83.73(14)
N(1)-Re(1)-N(3)	84.65(15)	82.3(2)	86.23(14)
Re(1)-C(1)-O(1)	176.5(5)	176.7(8)	176.0(5)
Re(1)-C(2)-O(2)	178.1(4)	176.4(7)	178.2(5)
Re(1)-C(3)-O(3)	178.3(5)	176.5(7)	179.3(5)

The compounds have very similar geometries about the metal centre, with a *fac*-tricarbonyl disposition of ligands and a near octahedral geometry typical of Re(I)-diimine tricarbonyl complexes.^{20, 32} The compound **19** has a centre of symmetry through the C(4)-C(4') bond of 4,4'-bpy ligand. The octahedral geometry around the rhenium atom is observed from the *cis-trans* angles, the *trans* angles C(1)-Re(1)-N(2), C(2)-Re(1)-N(1) and C(3)-Re(1)-N(3) vary from 170.79(19)° to 178.62(19)° in the complexes. The *bpy cis* angles of N(1)-Re-N(2) [74.72(15) – 75.28(16)°] are far from 90°, due to the steric effects of the chelating bipyridyl ligand. The other *cis* angles vary from 81.89(15)° to 100.42(18)° in the complexes.

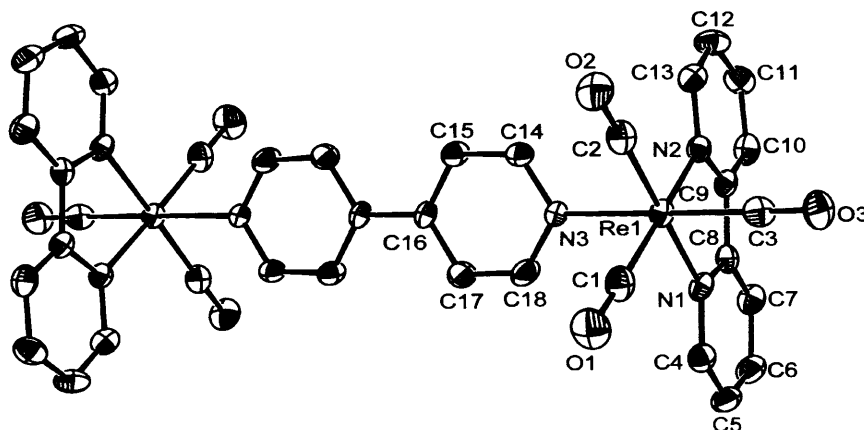


Figure 4.13 Ortep diagram of the cation present in $[\text{Re}(\text{CO})_3(\text{bpy})(\text{L}^3)]\text{PF}_6$ (**19**).

Thermal ellipsoids are drawn at 50% probability.

The axial ligands, 4,4'-bpy and pyterpy, lie normally to the equatorial plane of 2,2'-bpy and bisect the C(1)-Re(1)-N(1) and C(2)-Re(1)-N(2) bond angles. All the carbonyl groups make approximately linear angles with the nitrogen atoms of the 4,4'-bpy and 2,2'-bpy ligands in the complexes.

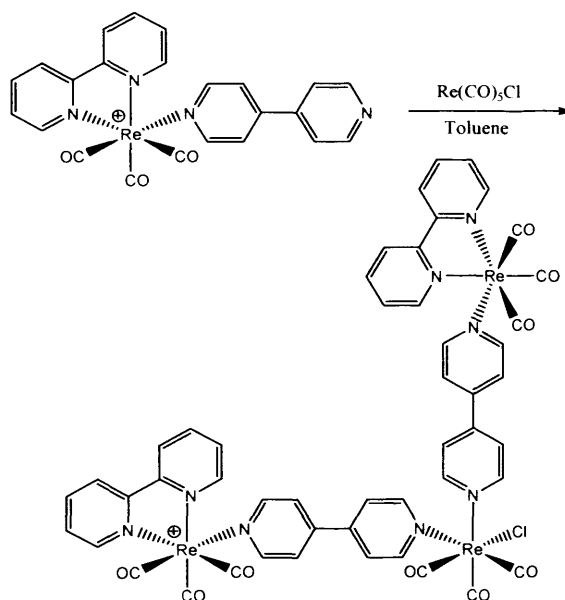
The bond distances for Re-N(2,2'-bpy) [2.163(4)- 2.181(6)Å] and Re-C [1.920(5)- 1.942(6)Å] in complexes **15**, **18** and **19** are similar to those of $[\text{Re}(\text{CO})_3(\text{bpy})(4,4'\text{-bpy})]\text{CF}_3\text{SO}_3$ and previously determined rhenium(I) tricarbonyl diimine structures.^{20, 34} The Re(1)-N(3) distances of the secondary donor (py-terpy or 4,4'-bpy) are slightly longer than that of the 2,2'-bipyridyl donors and they are 2.205(4), 2.217(6) and 2.201(4) in the complexes **15**, **18** and **19**, respectively. This is because the steric bulk of the secondary ligand prevents close approach to the rhenium centre. The Re-C-O angles for the carbonyl slightly deviates from linearity and are 178.3(5), 176.0(5)^o and 179.3(5)^o for complexes **15**, **18** and **19** respectively. steric bulk of the uncoordinated pyridyl, which is effectively a substituent on the central pyridyl, prevents close approach to the rhenium centre and the Re-N(2) distance is longer than the Re-N(1) distance.

Compounds **18** and **19** were emissive in room temperature and displayed luminescence in acetonitrile solution at 565-575 nm upon excitation at 360 nm. The emission spectra were broad and were consistent with ³MLCT origin. Again, compound **18** has a pendent nitrogen that can bind metals and act as a receptor for a cation. Thus, this compound could be utilized as a molecular switch as it may acquire

(1) an active subunit displaying fluorescence properties which can be switched on/off, (2) a control subunit, which is sensitive to the external stimulus (e.g, redox change) and affects the luminescence property of the active subunit.

Firstly, silver was used to serve this purpose as it can form a metal centered redox couple $[(\text{Ag}(\text{I})/\text{Ag}(\text{II}))]$. Attempts to synthesize silver complexes using the pendant nitrogen of compound **18** involved the reaction of silver perchlorate with complex **18** in a 1:2 molar ratio. The reaction was carried out by layer diffusion of an aqueous silver perchlorate solution to the acetonitrile solution of compound **18** in the dark for seven days. However, complexation of silver(II) was not successful as the ^1H NMR and mass spectroscopy analysis of the resulting precipitate is identical to that of the starting material.

Secondly, the synthesis of a tri-nuclear rhenium complex was attempted. The reaction was carried out by refluxing compound **18** and $\text{Re}(\text{CO})_5\text{Cl}$ in a 2:1 molar ratio in toluene (Scheme 4.8). In the IR spectrum two characteristic peaks were observed, one corresponds to the chloro species (2019 cm^{-1} , 80% T) and the other corresponds to the pyridinium species (2028 cm^{-1} , 75% T). However, the ^1H NMR spectrum of the complex produced broad, split and unresolved peaks. The MS spectral analysis of the complex did not give any relevant fragmentations to characterize the complex. Therefore, the formation of the tri-rhenium complex is uncertain.



Scheme 4.8 Attempted synthesis of $[\text{Re}(\text{bpy})(\text{CO})_3(4,4'\text{-bpy})]_2\text{Re}(\text{CO})_3\text{Cl}$.

4.2.3 Redox-active switches

The redox chemistry of Re complexes is extensive. These complexes show redox potentials for ligand reduction as well as metal oxidation. The latter is complicated by rapid decomposition of the resulting 17-electron Re(II) species. In contrast, in the ligand reduction region the electrochemical responses are typically chemically reversible. Low oxidation state Re complexes are often stabilized by π -acceptor ligands, in combination with neutral and anionic donor ligands. Choosing the right combination of the ligands is crucial: the ligands must complement rather than compete with each other, and the combination of the ligands should stabilize the complex better than each of the ligands does alone. Rhenium(I) polypyridyl tricarbonyl complexes, $[\text{Re}(\text{N-N})(\text{CO})_3\text{X}]^{n+}$, are ideal for redox chemistry studies. Again, these complexes are well known organometallic MLCT emitters with luminescent properties sensitive to changes in the electronic factors of the chromophoric polypyridyl ligands and the spectator ligand, X, (Figure 4.14) provides a convenient handle for the functionalization of complex. Variations of the non-carbonyl ligands can produce a considerable effect on the luminescence energies, lifetimes and quantum yields.

The recognition of the photoinduced redox activity of numerous Re(I) complexes has led to our interest to utilize the following spectator ligands.

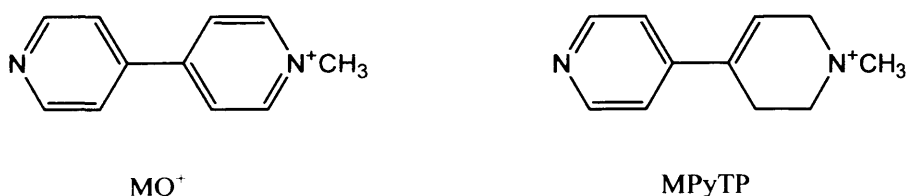


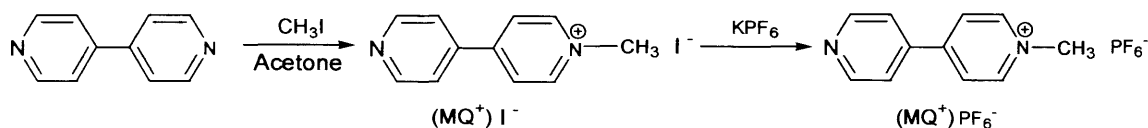
Figure 4.14 Redox active spectator ligands

We have prepared viologen (MQ^+) and reduced MPyTP then synthesized $[\text{Re}(\text{bpy})(\text{CO})_3\text{MQ}]^{2+}$ and $[\text{Re}(\text{bpy})(\text{CO})_3(\text{MPyTP})]^+$.

4.2.3.1 N-methyl-4,4'-bipyridinium(MQ^+) PF_6^-

The preparation of the ligand (MQ^+) PF_6^- has been reported in the literature.³⁵ The reaction of equimolar amounts of methyl iodide and 4,4'-bipyridine were carried

out in acetone at room temperature. But the resultant product was a mixture of N-methyl-4,4'-bipyridinium iodide and N,N'-dimethyl-4,4'-bipyridinium di-iodide which was confirmed by the presence of six different proton environments in its ^1H NMR spectrum. However, $(\text{MQ}^+)\text{I}^-$ was prepared successfully by the reaction of methyl iodide and a large excess (approximately 20 times) of 4,4'-bipyridine in acetone and it was then treated with potassium hexafluorophosphate to obtain its PF_6^- salt (Scheme 4.9). The purity of the ligand was determined by its ^1H NMR which exhibited four sharp aromatic signals, as expected.



Scheme 4.9 Synthesis of *N*-methyl-4,4'-bipyridinium(MQ^+) PF_6^-

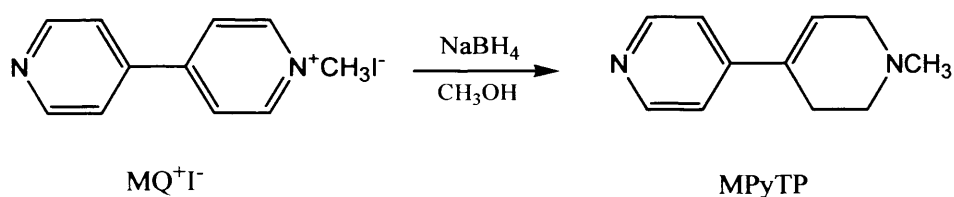
$(\text{MQ}^+)\text{PF}_6^-$ is a strong electron acceptor whose presence in the coordination sphere of a transition metal gives rise to very rich electrochemical, and photochemical behaviour. The pyridinium unit undergoes a reversible reduction to a radical species, which is a good candidate for a redox switch. When attached to a metal centre, MQ^+ can accept electrons from the metal and thus can change its optical properties. On the basis of earlier reports, it has been observed that MQ^+ acts as a luminescent quencher for many lumophores.³⁶⁻³⁷

4.2.3.2 1-methyl-4-pyridyltetrahydropyridine (MPyTP)

1-methyl-4-phenyl-1,2,3,6-tetrahydropyridine (MPTP) is a highly neurotoxic species that can easily be absorbed and transported to the brain.³⁸⁻³⁹ Here, monoamine oxidase A converts it to 1-methyl-4-phenyl pyridinium (MPP^+) which has been suggested to be responsible for destruction of the nigral-striatal pathway, leading to Parkinson's syndrome in man, monkeys, rat etc. In this work we were interested in preparing the ligand MPyTP, which is analogous to MPTP, and can cause a Parkinsonian condition. Synthesis of the corresponding Re complex would allow an investigation into the detection of Parkinsonian condition. Again, we were interested in oxidizing the resulting complex with monoamine oxidase A to observe the

accessibility for the synthesis of the MPP^+ analogue of rhenium complex in order to determine if it is a useful biological probe.

The ligand MPyTP was prepared in an analogous manner for the preparation of other tetrahydropyridine derivatives.⁴⁰ The synthesis involves the reduction of $(\text{MQ}^+)\text{I}^-$ with NaBH_4 in the presence of CH_3OH (Scheme 4.10). Purification was followed by extracting an aqueous solution of the ligand with diethyl ether and drying over MgSO_4 .

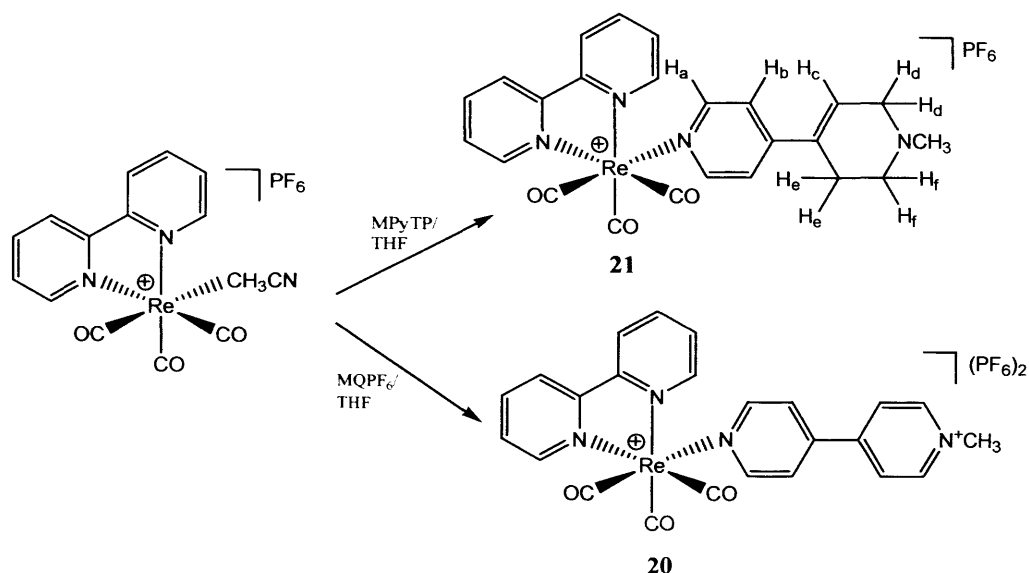


Scheme 4.10 Synthesis of 1-methyl-4-pyridyltetrahydropyridine (MPyTP)

The ^1H NMR spectrum of the ligand MPyTP showed the expected pattern⁴⁰ with six different signals for the ring hydrogens and a typical singlet for the methyl group.

4.2.3.3 $[\text{Re}(\text{CO})_3(\text{bpy})\text{L}^4][\text{PF}_6]$ [$\text{L}^4 = \text{MQ}^+\text{PF}_6^-$ (20) and MPyTP (21)]

Complex **20** was synthesized according to the published method³⁴ and a similar method was followed to prepare **21**, i.e., by the substitution reaction of the precursor complex $[\text{Re}(\text{CO})_3(\text{bpy})(\text{CH}_3\text{CN})]\text{PF}_6$ with MPyTP in THF under reflux conditions (Scheme 4.11).



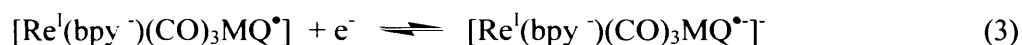
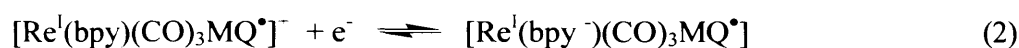
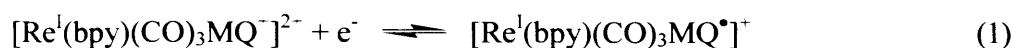
Scheme 4.11 Synthesis of $[\text{Re}(\text{CO})_3(\text{bpy})\text{L}^4][\text{PF}_6]$ [$\text{L}^4 = \text{MQ}^+\text{PF}_6^-$ (**20**) and MPyTP (**21**)]

Both the complexes were characterized by IR and ^1H NMR spectra. The spectra of complex **20** are similar to published work.³⁴ The ^1H NMR spectrum of complex **21** was also determined. The 2,2'-bipyridine protons appeared at 8.91, 8.29, 8.0 and 7.55 ppm and these shifts are similar to other complexes containing the $[\text{Re}(\text{CO})_3(\text{bpy})]^+$ moiety.²¹⁻²² Upon complexation, the signals of the ligand were shifted upfield with respect to the signals of the free ligand. The most significant shifts were observed for the protons H_a and H_b , though small shifts in other protons were also seen. The H_a proton next to the coordinated N-atom appeared at 7.78 ppm and shifted by 0.68 ppm and the H_b proton appeared at 6.96 ppm and shifted by 0.24 ppm. The $-\text{CH}_2$ protons, H_d and H_f , appeared as a singlet at 2.13 ppm integrating to approximately four protons. Several attempts to grow X-ray quality crystals of complex **21** were unsuccessful.

4.2.3.4 Cyclic Voltammetry

The electrochemical properties of compounds **20** and **21** have been determined (Figure 4.14, 4.15). The measurements were performed in acetonitrile, with 0.1 M $[\text{NBu}_4][\text{PF}_6]$, as supporting electrolyte and 1-2 mM concentration of the sample at room temperature. Ferrocene was added at the end of each experiment as an internal

reference, and all redox potentials are quoted vs. the ferrocene-ferrocenium couple. The measurements were carried out in the region from +2.00 to -2.00 V with a scan rate 200 mV s^{-1} . In agreement with the earlier report,⁴¹ it was observed that compound **20** undergoes four one electron reversible reductions. The first and third reduction waves were attributed to the sequential reductions of the MQ^+ ligand and the second and fourth reduction waves were attributed to the sequential reductions of coordinated bipyridine (step 1-4).



Thus the reductions at -1.103 and -1.730 V can be assigned as the MQ^+ based reductions (step 1 and 3) and the reduction at -1.58 V can be assigned as bipyridine based reduction (step 2). The other reduction (step 4) of the bipyridine ligand was in a more negative region than -2.0 V.

Compound **21** gave two irreversible oxidations at 0.669 and 1.384 V, one reversible reduction at -1.549 V and one irreversible reduction at -1.968 V (Figure 4.15). It is difficult to assign these redox potentials as the compound would possess redox potentials for oxidation of rhenium, oxidation of MPyTP, reduction of rhenium, bpy and MPyTP. However an attempt at assignment was made by comparing the position of the peaks with that of the MPTP ligand and $\text{Re}(\text{CO})_3(\text{bpy})^+$ containing complexes.

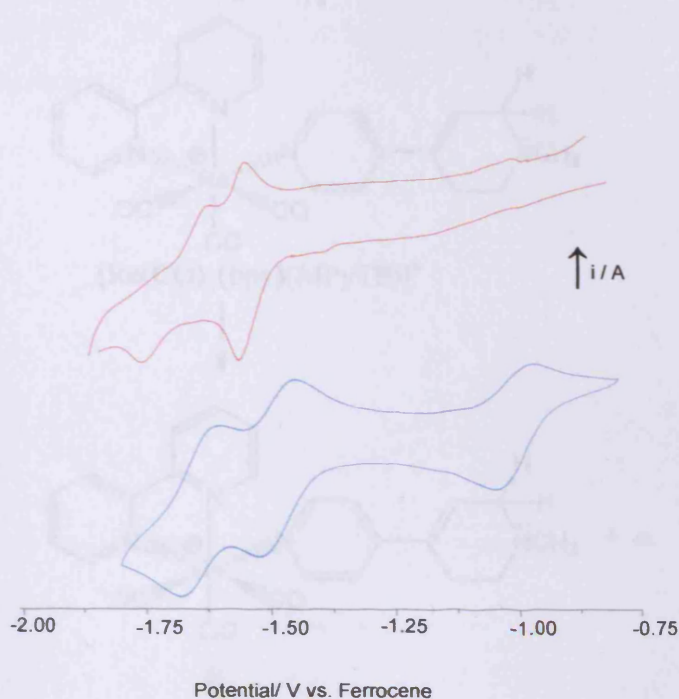
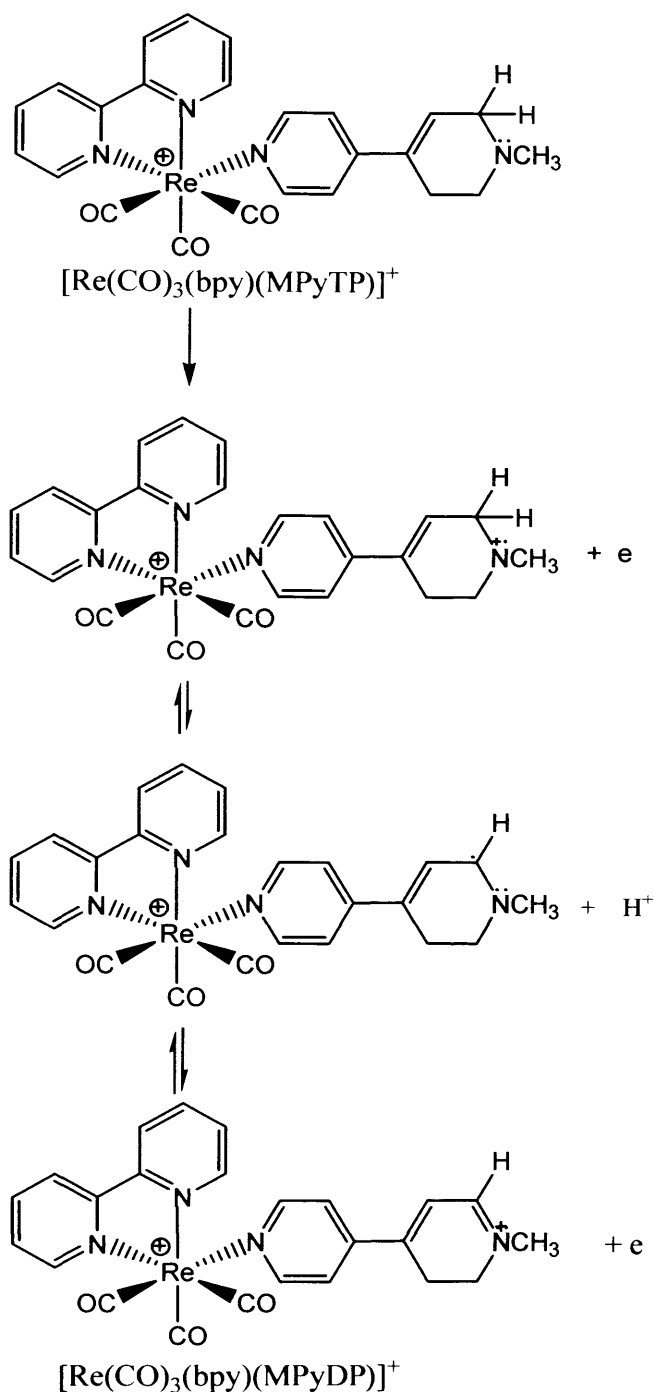


Figure 4.15 Cyclic voltammograms in the negative potential region of **20** (blue line) and **21** (red line) measured in acetonitrile solution containing $n\text{-Bu}_4\text{NBF}_4$ (0.1 M) as an electrolyte.

The analysis of the cyclic voltammetric result was performed by comparing the electrochemical behaviour of MPTP⁴² and other " $\text{Re}(\text{bpy})(\text{CO})_3$ " containing compounds.⁴¹ MPTP usually demonstrates 2-electron, 1-proton electrooxidation to MPDP^+ that can be reduced to the radical state followed by dimerization and other side reactions.⁴² Therefore, complex **21** would offer interesting electrochemical properties as deatomization of MPyTP might occur in the complex. Possible electrochemical reactions of MPyTP in compound **21** are shown in scheme 4.12.

Scheme 4.12 Possible electrochemical reactions of MPyTP in compound 21.

Thus it seems most likely that the oxidation at higher positive potential (Figure 4.16) can be assigned to the oxidation of MPyTP to MPyTP^+ . The irreversible reduction of the complex may arise from the reduction of deplete $(\text{Re}^{\text{II}}/\text{Re}^{\text{I}})$ or the



Scheme 4.12 Possible electrochemical reactions of MPyTP in compound 21.

Thus it seems more likely that the oxidation at higher positive potential (Figure 4.16) can be assigned to the oxidation of MPyTP to MPyDP^+ . The irreversible reduction of the complex may arise from the reduction of rhenium [Re^0/Re^1] or the

reduction of MPyDP^+ . The oxidation at lower positive potential can be assigned the oxidation of rhenium ($\text{Re}^{\text{I}}/\text{Re}^{\text{II}}$).

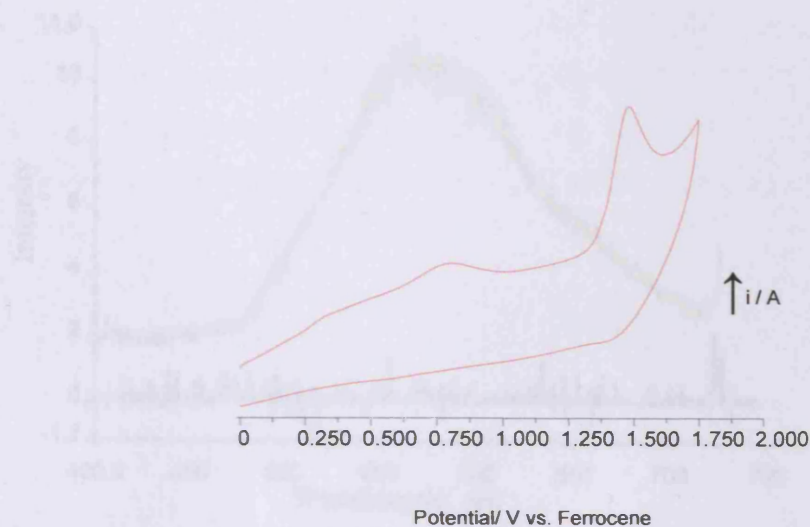


Figure 4.16 The anodic scan of **21** measured in acetonitrile solution containing $n\text{-Bu}_4\text{NBF}_4$ (0.1 M) as an electrolyte.

The only reversible reduction at -1.549 V can easily be confirmed as 2,2'-bipyridine based reduction. This result did not reveal all the corresponding redox reactions as some of the signals may be beyond the solvent limit.

4.2.3.5 Luminescence

The luminescent behavior of complexes **20** and **21** were determined. The measurements were carried out in degassed acetonitrile using 10^{-4} M solution of the corresponding complexes.

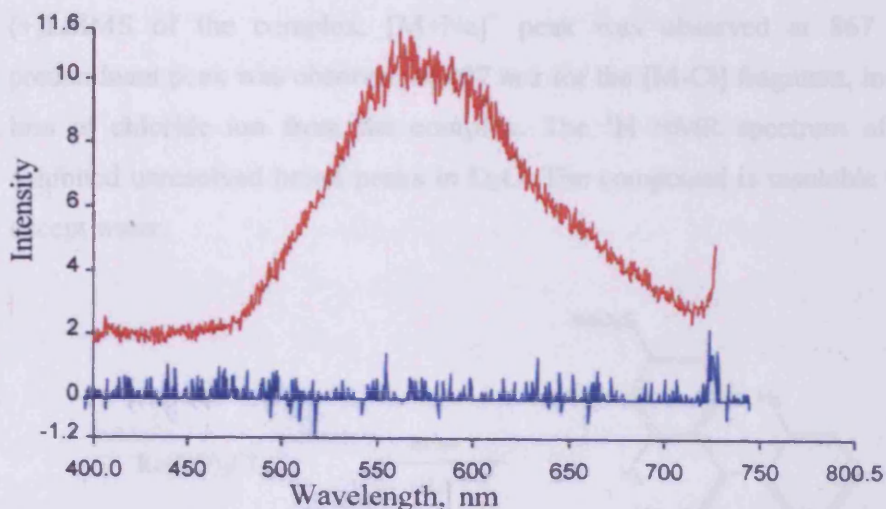


Figure 4.17 Luminescence spectra of compound **20** (blue line) and **21** (red line) in deoxygenated CH_3CN solution at 298K.

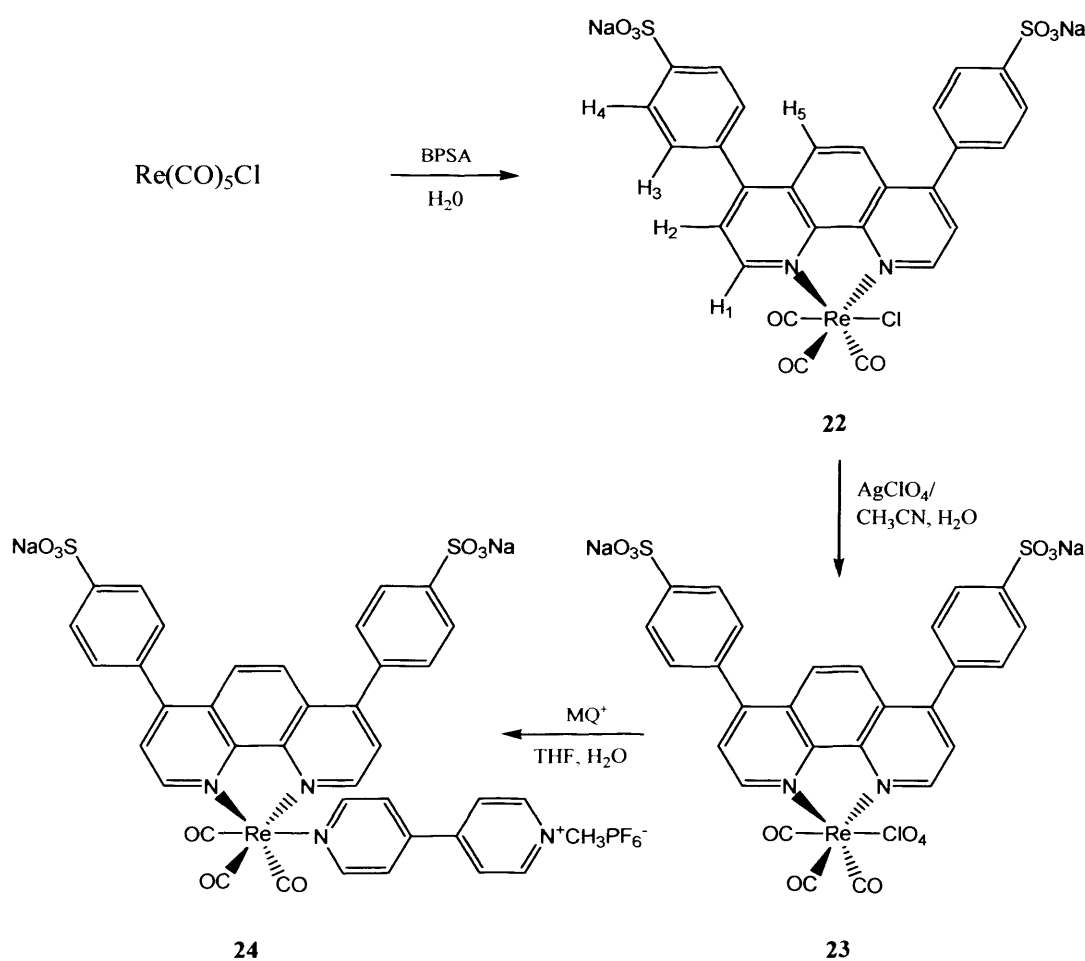
Upon excitation at 360 nm, significant quenching of luminescence was observed for **20** compared to **21** (Figure 4.17). These types of molecules may prove to be useful molecular probes for the biochemical research into the origin of Parkinsons-like conditions.

4.2.4 Water-soluble rhenium(I) complexes.

Complexes **20** and **21** are soluble in organic solvents. They cannot be used directly for the biochemical research as most of the biological reactions occur in aqueous medium. Thus, it is necessary to synthesis water soluble compounds to utilize them in biological system. We were interested in synthesizing water soluble analogues to **20** and **21** using the bathophenanthroline disulphonate ligand in order to assess their photophysical properties. We also aimed to react the MPyTP analogue with MAO-B to follow the changes in luminescence in aqueous solution.

These water soluble complexes were synthesized with slight modifications of the previous methods for the preparation of rhenium polypyridine complexes. Complex **22** was prepared by refluxing equimolar amounts of $\text{Re}(\text{CO})_5\text{Cl}$ and bathophenanthroline disulphonic acid disodium salt (BPSA) in water (Scheme 4.13). The product was precipitated from the solution on cooling and dried in a desiccator. The yield was 60%. The compound was then characterized spectroscopically. The

infrared stretching vibrations $\nu_{\text{C}=\text{O}}$ of the complex were found to be 2024 and 1896 cm^{-1} and these values are typical of $\text{Re}(\text{I})$ poly-pyridine chloride complexes. In the (+)LSIMS of the complex, $[\text{M}+\text{Na}]^+$ peak was observed at 867 m/z . Another predominant peak was observed at 807 m/z for the $[\text{M}-\text{Cl}]$ fragment, indicative of the loss of chloride ion from the complex. The ^1H NMR spectrum of the complex exhibited unresolved broad peaks in D_2O . The compound is insoluble in any solvent except water.



Scheme 4.13 Attempted synthesis of water soluble rhenium complexes (22-24)

Compound **23** was prepared by refluxing compound **22** and silver perchlorate in a mixture of water and acetonitrile for 24 hrs. The product was obtained by slow removal of the solvent under vacuum in a desiccator. The compound was then characterized by IR and mass spectrometry. The infrared vibration frequencies of the

Excitation of 10⁻⁴ M solutions of the complexes at 285 nm (absorption at 285 nm) of complex were observed at 2032, 1912, 1193 and 1097 cm^{-1} . The lower stretching vibrations $\nu_{\text{C}=\text{O}}$ of the complex compared to the analogous acetonitrile adduct of rhenium carbonyl compounds⁴³ and the presence of the strong peaks at 1193 and 1097 cm^{-1} for perchlorate ions predicted the molecular formula of the complex as $\text{Re}(\text{CO})_3(\text{bpsa})(\text{ClO}_4)$. This prediction is also supported by the mass spectrum of the complex. The complex showed molecular ions in its electrospray mass spectrum at 929 m/z [$\text{M}+\text{Na}^+$] and at 883 m/z with a loss of sodium ion from the molecule. The spectrum also demonstrated a strong molecular ion peak at 839 m/z [$\text{M}-\text{ClO}_4^- + \text{CH}_3\text{OH}$] and 816 m/z [$\text{M}-\text{ClO}_4^- + \text{CH}_3\text{OH}-\text{Na}^+$]. Unfortunately, the ^1H NMR spectrum of the complex was broad and was not clear enough to assign.

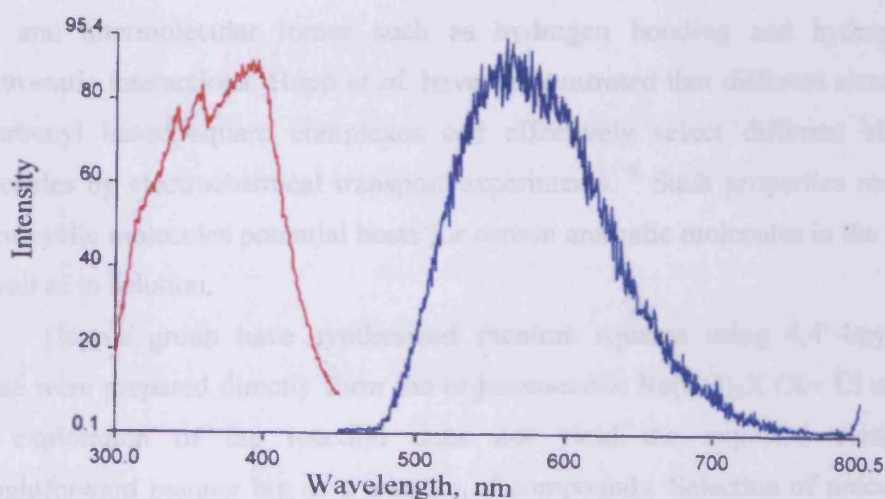


Figure 4.18 Luminescence spectra of compound **23** in deoxygenated CH_3CN solution at 298K

Compound **24** was obtained by the substitution reaction of **23** and $(\text{MQ})\text{PF}_6^-$ in THF and water under reflux condition. The IR of the product is almost identical to that of compound **23** and did not give any information about the formation of **24**. The ^1H NMR spectrum of the complex was not clear enough to assign any peak. No relevant fragments were observed in the mass spectrum of the product. Thus, the formation of the complex can not be established by spectroscopic methods. Several attempts to grow X-ray quality crystals were also unsuccessful.

Complexes, **22** and **23**, show strong emissive properties (Figure 4.18) Excitation of 10^{-4}M solutions of the complexes at 395 nm gives emission at 560 nm in aqueous solution. However, significant quenching of emission was observed in compound **24**. This observation is compatible with the luminescent behavior of other pyridinium containing species. Therefore, only the luminescence property of **24** provides evidence that suggests the complex might have been formed.

Since characterization of complex **24** was not possible, we could not investigate this complex any further.

4.2.5 Rhenium(I)-based supramolecules

Luminescent compounds with internal cavities have been shown to have potential applications as chemosensory devices in recent years. Many macrocyclic complexes have been studied for their molecular recognition capabilities toward small aromatic molecules, inorganic anions or porphyrin molecules, based on their cavity size and intermolecular forces such as hydrogen bonding and hydrophobic or electrostatic interactions. Hupp *et al.* have demonstrated that different sized rhenium tricarbonyl based square complexes can effectively select different sized guest molecules by electrochemical transport experiments.⁹ Such properties render these macrocyclic molecules potential hosts for certain aromatic molecules in the solid state as well as in solution.

Hupp's group have synthesized rhenium squares using 4,4'-bpy ligand.⁴⁴ These were prepared directly from the organometallic $\text{Re}(\text{CO})_5\text{X}$ ($\text{X} = \text{Cl}$ or Br). But the exploration of the reaction does not yield the expected compound in straightforward manner but as a mixture of compounds. Selection of precursors like $\text{Re}(\text{CO})_3(\text{CH}_3\text{CN})_2\text{Cl}$ and $[\text{Re}(\text{CO})_3(\text{CH}_3\text{CN})_3]^+$ might have a great influence in the preparation of rhenium-macromolecules. We were interested in synthesizing a rhenium cube using 4,4'-bpy. To achieve this goal, we first synthesised the precursor complex, $[\text{Re}(\text{CO})_3(\text{CH}_3\text{CN})_3][\text{PF}_6]$.

4.2.5.1 Synthesis of $[\text{Re}(\text{CO})_3(\text{CH}_3\text{CN})_3][\text{PF}_6]$ (**25**)

The preparation of $[\text{Re}(\text{CO})_3(\text{CH}_3\text{CN})_3]^+$ has been reported,⁴⁵ however, a more facile two step method has been reported here. The first step involves the replacement of the two carbonyl ligands from $\text{Re}(\text{CO})_5\text{Cl}$ by acetonitrile in toluene under reflux conditions and $\text{Re}(\text{CO})_3(\text{CH}_3\text{CN})_2\text{Cl}$ was precipitated as an analytically pure powder

in good yield (80%). The second step involves the replacement of chloride ion from $\text{Re}(\text{CO})_3(\text{CH}_3\text{CN})_2\text{Cl}$ by acetonitrile in refluxing acetonitrile solvent. On addition of KPF_6 salt to the solution, $\text{Re}(\text{CO})_3(\text{CH}_3\text{CN})_3\text{PF}_6$ (**25**) was obtained as transparent crystals in high yield (90%). The IR spectrum of the complex is similar to that of the reported $\text{Re}(\text{CO})_3(\text{CH}_3\text{CN})_3^+$ ⁴⁵ complexes.

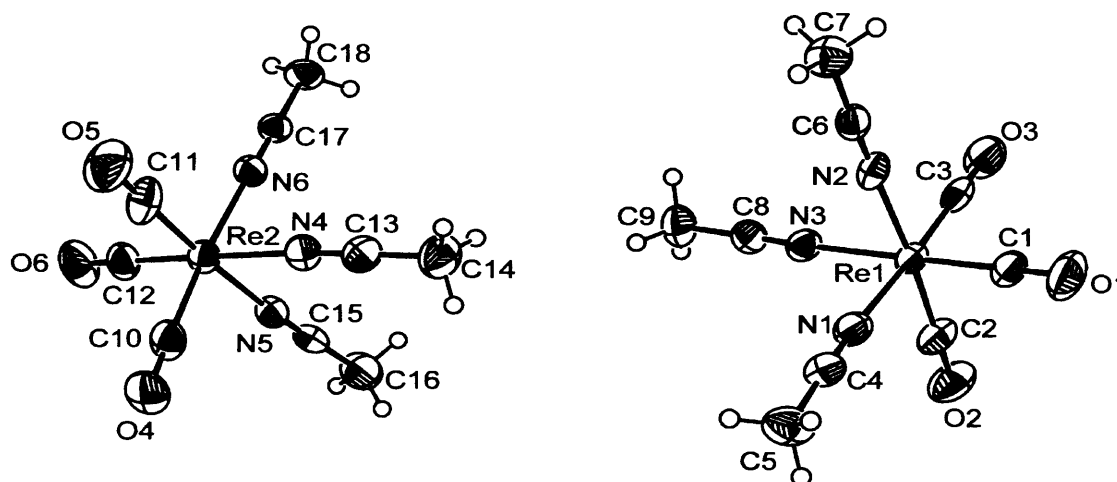


Figure 4.19 Ortep diagram of the cation present in $[\text{Re}(\text{CO})_3(\text{CH}_3\text{CN})_3]\text{PF}_6$ (**25**).

Thermal ellipsoids are drawn at 50% probability.

The crystal structure of $\text{Re}(\text{CO})_3(\text{CH}_3\text{CN})_3\text{PF}_6$ has been determined. The compound crystallizes in the monoclinic space group P21/a. The asymmetric unit of the structure contains two crystallographically independent complex units (molecule A and molecule B) (Figure 4.19). The two complex units are similar, with relatively minor differences in bond lengths and bond angles. $\text{Re}(\text{CO})_3(\text{CH}_3\text{CN})_3^+$ has been made before with different counter ions, such as, BF_4 ⁴⁵ and BrI_2 ⁴⁵. These molecules have also been structurally characterized by X-ray crystallography.

Table 4. Crystal data and structure refinement for **25**.

Empirical formula	C18 H18 F12 N6 O6 P2 Re2
Formula weight	1076.72
Temperature	150(2) K
Wavelength	0.71069 Å
Crystal system	Monoclinic
Space group	P 21/a
Unit cell dimensions	a = 13.257(5) Å α = 90.000(5)°.

	$b = 11.819(5) \text{ \AA}$	$\beta = 95.593(5)^\circ$
	$c = 21.514(5) \text{ \AA}$	$\gamma = 90.000(5)^\circ$
Volume	$3355(2) \text{ \AA}^3$	
Z	4	
Density (calculated)	2.132 Mg/m^3	
Absorption coefficient	7.412 mm^{-1}	
F(000)	2016	
Crystal size	$0.38 \times 0.38 \times 0.18 \text{ mm}^3$	
Theta range for data collection	3.09 to 30.03°	
Index ranges	$-18 \leq h \leq 18$, $-16 \leq k \leq 16$, $-28 \leq l \leq 30$	
Reflections collected	22856	
Independent reflections	9728 [R(int) = 0.0799]	
Completeness to theta = 30.03°	99.1 %	
Absorption correction	Semi-empirical from equivalents	
Max. and min. transmission	0.3488 and 0.1650	
Refinement method	Full-matrix least-squares on F ²	
Data / restraints / parameters	9728 / 0 / 411	
Goodness-of-fit on F ²	1.057	
Final R indices [I > 2sigma(I)]	R1 = 0.0574, wR2 = 0.1404	
R indices (all data)	R1 = 0.0824, wR2 = 0.1546	

Table 5. Bond lengths [\AA] and angles [$^\circ$] for **25**.

Re(1)-C(1)	1.930(8)	Re(1)-C(2)	1.933(9)
Re(1)-C(3)	1.908(9)	Re(1)-N(3)	2.135(6)
Re(1)-N(2)	2.135(6)	Re(1)-N(1)	2.144(8)
Re(2)-C(10)	1.921(9)	Re(2)-C(11)	1.933(9)
Re(2)-C(12)	1.933(9)	Re(2)-N(12)	2.128(7)
Re(2)-N(11)	2.139(7)	Re(2)-N(13)	2.143(6)
C(3)-Re(1)-C(1)	90.2(4)	C(3)-Re(1)-C(2)	90.3(4)
C(1)-Re(1)-C(2)	90.0(4)	C(3)-Re(1)-N(3)	92.3(3)
C(1)-Re(1)-N(3)	176.1(3)	C(2)-Re(1)-N(3)	93.0(3)
C(3)-Re(1)-N(2)	92.4(3)	C(1)-Re(1)-N(2)	93.4(3)
C(2)-Re(1)-N(2)	175.6(3)	N(3)-Re(1)-N(2)	83.5(2)
C(3)-Re(1)-N(1)	177.2(3)	C(1)-Re(1)-N(1)	91.9(3)
C(2)-Re(1)-N(1)	91.5(4)	N(3)-Re(1)-N(1)	85.5(2)
N(2)-Re(1)-N(1)	85.6(2)	C(10)-Re(2)-C(11)	90.7(4)
C(10)-Re(2)-C(12)	88.8(4)	C(11)-Re(2)-C(12)	89.4(4)
C(10)-Re(2)-N(12)	91.6(3)	C(11)-Re(2)-N(12)	176.6(3)
C(12)-Re(2)-N(12)	93.2(3)	C(10)-Re(2)-N(11)	93.5(3)
C(11)-Re(2)-N(11)	94.8(3)	C(12)-Re(2)-N(11)	175.2(3)
N(12)-Re(2)-N(11)	82.6(3)	C(10)-Re(2)-N(13)	175.4(3)
C(11)-Re(2)-N(13)	93.5(4)	C(12)-Re(2)-N(13)	93.2(3)
N(12)-Re(2)-N(13)	84.2(2)	N(11)-Re(2)-N(13)	84.2(2)

Details of the crystallographic data and selected bond lengths and angles of complex **25** are presented in Table 4 and 5. The geometry about the metal centre is only slightly distorted from octahedral. The greatest deviation from 90° were observed for angles $\text{N}(5)\text{-Re}(2)\text{-N}(4)$ [$82.6(3)^\circ$] and $\text{N}(3)\text{-Re}(1)\text{-N}(2)$ [$83.5(2)^\circ$]. The Re-C and Re-N bond distances of **25** are 1.921(9)-1.933(9)Å and 2.128(7)-2.143(6)Å in molecule A and 1.908(9)-1.933(9)Å and 2.135(6)-2.144(8)Å in molecule B, which are quite similar to those of the reported structures, $\text{Re}(\text{CO})_3(\text{CH}_3\text{CN})_3\text{BF}_4$ [Re-C 1.867(23)-1.931(24) and Re-N 2.125(18)-2.134(16)] and $\text{Re}(\text{CO})_3(\text{CH}_3\text{CN})_3\text{BrI}_2$ [Re-C 1.91(2)-1.94(2) and Re-N 2.12(1)-2.16(2)].

4.2.5.2 Attempted preparation of $[\text{Re}(\text{CO})_3]_8 [4,4'\text{-bpy}]_{12} [\text{PF}_6]_8$

As $\text{Re}(\text{CO})_3(\text{CH}_3\text{CN})_3^+$ is a cation with three available coordination sites, it might be possible to develop a supramolecular system (metal-mediated assembly of large architectures), involving the *in situ* preparation of stable Re compounds. The ligand which has been used to develop the supramolecule is 4,4'-bpy, because of its unique structural properties, containing two pendent nitrogen atoms that can coordinate more than one molecule with both ends of the ligand. Under suitable reaction environment these molecules can rearrange themselves to build a large molecular cube (Figure 4.20).

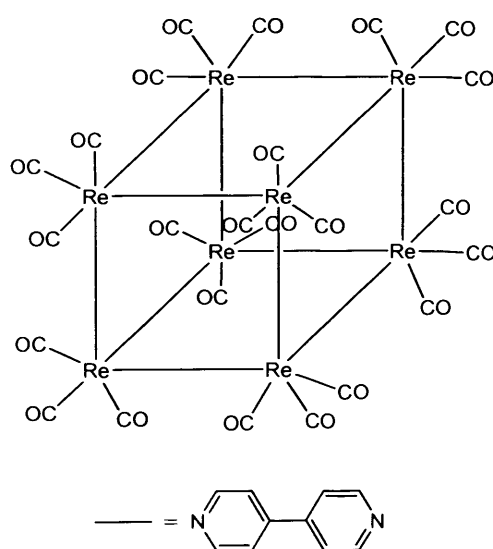
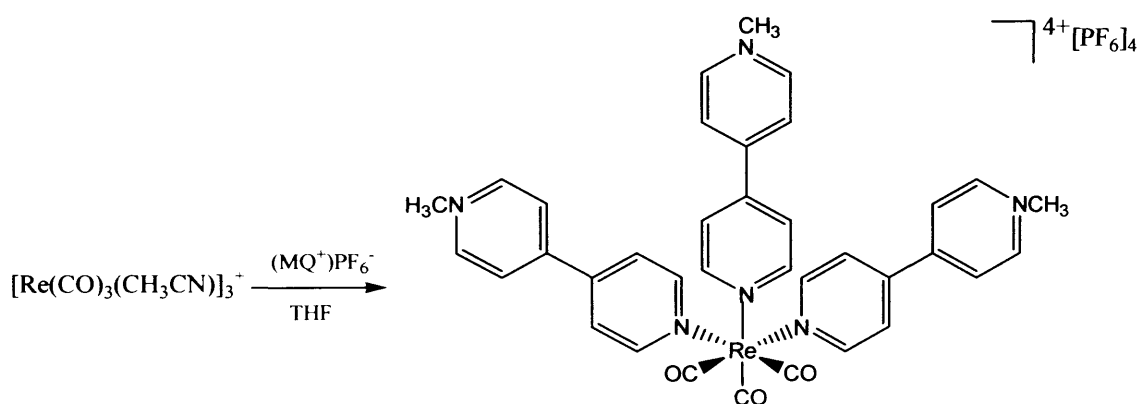


Figure 4.20 Structure of $[\text{Re}(\text{CO})_3]_8 [4,4'\text{-bpy}]_{12} [\text{PF}_6]_8$

To serve this purpose 4,4'-bpy was reacted with the precursor complex $[\text{Re}(\text{CO})_3(\text{CH}_3\text{CN})_3]\text{PF}_6$ in a ratio of 3:2 in acetonitrile (15 cm^3) at 60°C overnight. The formation of yellow precipitate indicated that the metal complex has been formed. The complex was then filtered and dried. The solid is sparingly soluble in acetonitrile, acetone and dichloromethane but fairly soluble in DMSO. ^1H NMR spectrum of the complex in DMSO does not indicate the formation a single compound but the presence of a mixture of compounds. The reaction was also carried out at room temperature. The reaction proceeded well but the ^1H NMR spectrum was not consistent with the expected product. The electrospray mass spectrum of the product did not provide any suitable ion to characterize the compound.

4.2.5.3 $[\text{Re}(\text{CO})_3(\text{MQ})_3][\text{PF}_6]_3$ (26)

$[\text{Re}(\text{CO})_3(\text{MQ})_3](\text{PF}_6)_3$ was prepared by the reaction of $\text{Re}(\text{CO})_3(\text{CH}_3\text{CN})_3$ and $(\text{MQ})\text{PF}_6^-$ in a 1:3 molar ratio in THF under reflux condition (Scheme 4.13). The complex was precipitated out from the solution.



Scheme 4.13 Synthesis of $[\text{Re}(\text{CO})_3(\text{MQ})_3](\text{PF}_6)_3$ (26)

The complex was characterized by IR and ^1H NMR spectrum. IR spectrum of the complex provides peaks at 2030 , 1924 and 1910 cm^{-1} corresponding the formation of *fac*- $[\text{Re}(\text{CO})_3(\text{MQ})_3](\text{PF}_6)_3$ complex. ^1H NMR spectrum exhibited eight doublets i.e., two sets of signals for the bipyridinium protons. This indicates that there is a lack of symmetry between the inner protons and outer protons of the corresponding rings.

All the protons shifted upfield compared to the ^1H NMR shift of the free ligand. Expected ions were not found in the mass spectral analysis. Attempts to grow X-ray quality crystals were unsuccessful in all occasions.

Compound **26** does not exhibit luminescence in solid state or in solution which is common for other rhenium compounds containing non-chelated pyridines.²⁴ Further investigation into the chemistry of this complex was stopped.

4.3 Experimental

All preparations were carried out under an oxygen free inert atmosphere. Solvents were dried by standard procedures, distilled and used directly from the still. $\text{Re}(\text{CO})_5\text{Cl}$ and $\text{Re}(\text{CO})_{10}$ were purchased and were used without further purification. IR spectra were recorded in NaCl solution cells or in compressed KBr discs on a Perkin-Elmer 1600 or a Jasco 660 spectrophotometer. ^1H NMR was recorded on Bruker DP-400 spectrometer. Electronic spectra were run in HPLC grade acetonitrile on a Perkin-Elmer 20 or a Jasco V-570 UV-Vis spectrophotometer. Cyclic voltammograms were recorded with an Autolab PGSTAT 12 Potentiometer with a Ag/AgNO_3 (0.1 M) reference electrode (BAS Non-aqueous Reference Electrode Kit). Electrochemical measurements were carried out in acetonitrile with 0.1 M $[\text{NBu}_4][\text{PF}_6]$ as supporting electrolyte. The supporting electrolyte was dried prior to use. Luminescence spectra were recorded with Perkin-Elmer LS 50B luminescence spectrometer. Spectra measured in a quartz SUPRASIL precision fluorescence cell. When necessary, samples were degassed by bubbling nitrogen through the solution.

Perchlorate salts are potentially explosive. All compounds containing perchlorate should be handled with great care and in small amounts. 1,4-Disubstituted tetrahydropyridines are potential nigrostriatal neurotoxins and should be handled using disposable gloves in a properly ventilated hood.

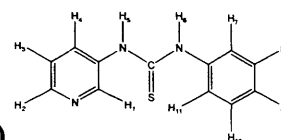
The precursor complexes $\text{Re}(\text{CO})_3(\text{bpy})\text{Cl}$,⁴³ $[\text{Re}(\text{CO})_3(\text{bpy})\text{CH}_3\text{CN}]\text{PF}_6$,⁴³ $[\text{Re}(\text{bpy})(\text{CO})_3(\text{py-3-NH}_2)]\text{PF}_6$ ⁴³ and $\text{Re}(\text{CO})_3(\text{CH}_3\text{CN})_2\text{Cl}$ ⁴⁶ were prepared according to the literature procedure.

4.3.1 Preparation of $[\text{Re}(\text{bpy})(\text{CO})_3(\text{py-3-NCS})]\text{PF}_6$:

Thiophosgene (44 mg, 0.36 mmol) was added to a mixture of $[\text{Re}(\text{bpy})(\text{CO})_3(\text{py-3-NH}_2)]\text{PF}_6$ (120 mg, 0.18 mmol) and calcium carbonate (73 mg,

0.72 mmol) in acetone (10 cm^3). The suspension was stirred in the dark for two hours at room temperature. The suspension was then filtered to remove calcium carbonate and the filtrate was evaporated to dryness.

Anal. Found: C 32.01, H 1.59, N 7.63%. Calc. for $[\text{Re}(\text{CO})_3(\text{bpy})(\text{py-3-NCS})]\text{PF}_6$: C 32.25, H 1.71, N 7.92%; δ_{H} (400MHz, acetone- d_6): 9.51 (2H d, J 4.9, $\text{H}_{6+6'}$), 8.79 (2H, d, J 8.2, $\text{H}_{3+3'}$), 8.66 (1H, d, J 1.9, H_2 , py-3-NCS), 8.55 (1H, d, J 5.5, H_6 , py-3-NCS), 8.49 (2H, m, $\text{H}_{4+4'}$), 8.07–8.00 (3H, m, $\text{H}_{5+5'}$, bpy + py-3-NCS), 7.58 (1H, dd, J 8.2, 5.5, py-3-NCS); IR (KBr), $\nu(\text{cm}^{-1})$ 2103.98 (N=C=S), 2029.30 and 1916.22. Mass spectrum (positive FAB): m/z 563 $[\text{M-PF}_6]$.



4.3.2 Preparation of N-(3-pyridyl)-N'-phenylthiourea (L^1)

3-aminopyridine (0.94g, 0.01 mol) was added dropwise to a stirred solution of phenylisothiocyanate (1.35g, 0.01 mol) in dichloromethane (50 cm^3). The solution was refluxed overnight and the resulting white solid was filtered, washed with cold dichloromethane and dried (60%).

IR(KBr), $\nu(\text{cm}^{-1})$ 3155 (NH), 1587 (NH), 2965 (NH), 1488 (CN) and 1302 (CS); δ_{H} (400MHz, DMSO): 10.02 (1H, s, H_5), 9.87 (1H, s, H_6), 8.6 (1H, d, J 2.5, H_1), 8.31 (1H, d, J 4.6, H_2), 7.94 (1H, d, J 8.2, H_4), 7.47 (2H, d, J 7.9, $\text{H}_{7,11}$), 7.37-7.33 (3H, m, $\text{H}_{8,9,10}$) and 7.15 (1H, t, J 7.3, H_3). Mass spectrum (EI): m/z 229 (100).

4.3.3 Preparation of $[\text{Re}(\text{CO})_3(\text{bpy})(\text{L}^1)]\text{PF}_6$ (13)

$[\text{Re}(\text{bpy})(\text{CO})_3(\text{CH}_3\text{CN})]\text{PF}_6$ (54 mg, 0.088 mmol) and N-(3-pyridyl)-N'-phenylthiourea (25 mg, 0.1 mmol) were allowed to reflux in THF (20 cm^3) under nitrogen atmosphere for two hours. After cooling the mixture was filtered and the filtrate was evaporated to dryness to give an orange solid. Recrystallization from dichloromethane/diethyl ether afforded the pure product in 50% yield.

Anal. Found: C 37.24, H 2.25, N 8.68%. Calc. for $[\text{Re}(\text{CO})_3(\text{bpy})(\text{N-(3-pyridyl)-N'-phenylthiourea})]\text{PF}_6$: C 37.50, H 2.39, N 8.75%. IR(CH_3CN), $\nu(\text{cm}^{-1})$ 2031, 1920 and 1295 (CS); δ_{H} (400MHz, DMSO): 9.65 (1H, s, H_5), 9.53 (1H, s, H_6), 9.32 (2H, d, J 5.4, bpy), 8.97 (1H, s, H_1), 8.61 (2H, d, J 8.3, bpy), 8.32 (2H, td, J 7.9, 1.5, bpy), 8.23 (1H, d, J 5.2, H_2), 7.87- 7.84 (2H, m, bpy), 7.41 (1H, t, J 7.9, H_4),

7.33-7.21 (5H, m, H_{7-11}) and 7.11 (1H, t, J 4.1, H_3). Mass spectrum (positive FAB): m/z 656 (100) $[\text{M}-\text{PF}_6]$.

4.3.4 Attempted preparation of $[\text{Re}(\text{CO})_3(\text{L}^1)_2\text{Cl}](14)$

Rhenium pentacarbonyl chloride (50 mg, 0.138 mmol) and *N*-(3-pyridyl)-*N'*-phenylthiourea (63 mg, 0.274 mmol) were allowed to reflux in toluene (30 cm^3) under a nitrogen atmosphere for 1 hour. After the CO evolution had ceased, the precipitated complex, formed upon cooling to room temperature, was filtered out, washed with diethyl ether and dried under vacuum (45%).

IR(CH_3CN), $\nu(\text{cm}^{-1})$ 2023, 1917 and 1865; Mass spectrum (ES): m/z 833 (98) $[\text{M}-\text{L}^1+\text{Re}(\text{CO})_3\text{Cl}]$. Several attempts to obtain a clean ^1H NMR spectrum were unsuccessful.

4.3.5 Preparation of $[\text{Re}(\text{CO})_3(\text{py-3-NH}_2)_2\text{Cl}](14\text{a})$

$\text{Re}(\text{CO})_3\text{Cl}$ (50 mg, 0.138 mmol) and 3-aminopyridine (26 mg, 0.276 mmol) were allowed to reflux in toluene under nitrogen atmosphere for 15 minutes. After cooling, the white precipitate was filtered and dried to yield the product (82%).

Anal. Found: C 31.44, H 2.31, N 11.15%. Calc. for $[\text{Re}(\text{CO})_3(\text{py-3-NH}_2)_2\text{Cl}]$: C 31.61, H 2.45, N 11.34%; IR(CH_3CN), $\nu(\text{cm}^{-1})$ 2021, 1913, 1886; δ_{H} (400MHz, DMSO): 8.18 (1H, s), 7.80 (1H, d, J 5.2), 7.19 (2H, m) and 5.90 (2H, s, NH_2); Mass spectrum (ES): m/z 494(35).

4.3.6 Preparation of $[\text{Re}(\text{CO})_3(\text{py-3-NCS})_2\text{Cl}](14\text{b})$

Thiophosgene (37 mg, 0.32 mmol) was added to a mixture of $[\text{Re}(\text{CO})_3(\text{py-3-NH}_2)_2\text{Cl}]$ (40 mg, 0.08 mmol) and calcium carbonate (60 mg, 0.6 mmol) in acetone (10 cm^3). The suspension was stirred in the dark for two hours at room temperature. The suspension was then filtered to remove calcium carbonate and the filtrate was evaporated to dryness.

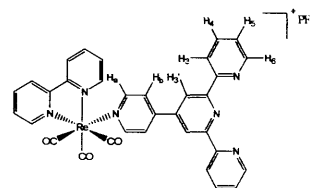
Anal. Found: C 31.23, H 1.32, N 9.51%. Calc. for $[\text{Re}(\text{CO})_3(\text{py-3-NCS})_2\text{Cl}]$: C 31.17, H 1.39, N 9.69%; IR (KBr), $\nu(\text{cm}^{-1})$ 2106 ($\text{N}=\text{C}=\text{S}$), 2021, 1906 and 1871; δ_{H} (400MHz, DMSO): 8.90 (1H, s), 8.66 (1H, d, J 5.4), 8.27 (1H, d, J 8.2) and 7.69 (1H, t, J 6.9); Mass spectrum (positive FAB): m/z 578(25).

4.3.7 Preparation of $[\text{Re}(\text{CO})_3(\text{L}^1)_2\text{Cl}](14)$

1. $\text{Re}(\text{py-3-NCS})_2(\text{CO})_3\text{Cl}$ (40 mg, 0.068 mmol) and aniline (13 mg, 0.103 mmol) were allowed to reflux in dichloromethane (20 cm^3) under nitrogen atmosphere in dark overnight. The product was obtained by evaporating of the solvent (55%).

2. $\text{Re}(\text{CO})_3(\text{CH}_3\text{CN})_2\text{Cl}$ (20 mg, 0.051 mmol) and N-(3-pyridyl)-N'-phenylthiourea (23 mg, 0.103 mmol) were allowed to reflux in THF (20 cm^3) under nitrogen atmosphere for 2 hrs. After the solution had cooled, hexane was added to precipitate the product. The white precipitate was then filtered and dried (65%).

Anal. Found: C 42.24, H 2.92, N 10.89%. Calc. for $\text{Re}(\text{CO})_3(\text{N}-(3\text{-pyridyl})\text{-N}'\text{-phenylthiourea})_2\text{Cl}$: C 42.43, H 2.90, N 11.00%; IR (KBr), $\nu(\text{cm}^{-1})$ 2022, 1919, 1895 and 1312 (CS); δ_{H} (400MHz, DMSO): 10.27 (1H, s, H₅), 10.14 (1H, s, H₆), 9.04 (1H, d, J 2.3, H₁), 8.31 (1H, d, J 4.6, H₂), 7.94 (1H, d, J 8.2, H₄), 7.47 (2H, d, J 7.9, H_{7,11}), 7.37-7.33 (3H, m, H_{8,9,10}) and 7.15 (1H, t, J 7.3, H₃); Mass spectrum (ES): m/z 729(10) [M-Cl].



4.3.8 Preparation of $[\text{Re}(\text{CO})_3(\text{bpy})(\text{py-terpy})][\text{PF}_6] (15)$

$[\text{Re}(\text{bpy})(\text{CO})_3(\text{CH}_3\text{CN})]\text{PF}_6$ (80 mg, 0.124 mmol) and 4'-(4'''-pyridyl)-2,2':6',2''-terpyridine (38 mg, 0.124 mmol) were allowed to reflux in THF (40 cm^3) under nitrogen atmosphere for two hours. After the solution had cooled, hexane was added, resulting in the precipitation of the product, which was then filtered and dried (67%).

Anal. Found: C 44.57, H 2.32, N 9.45%. Calc. for $[\text{Re}(\text{CO})_3(\text{bpy})(\text{py-terpy})]\text{PF}_6$: C 44.95, H 2.51, N 9.53%; IR(CH_3CN), $\nu(\text{cm}^{-1})$ 2033, 1930; δ_{H} (400MHz, Acetonitrile- d_6): 9.3 (1H, d, J 5.5, H₆, 6', bpy), 8.72 (1H, d, J 5.3, H₃, 3', bpy), 8.69 (1H, d, J 8, H_a), 8.65 (1H, s, H_{3'}), 8.41 (2H, t, J 6.3, H₃ and H₆), 8.31 (1H, td, J 7.9, 1.4, H₄, 4', bpy), 7.99 (1H, td, J 7.7, 1.7, H₄), 7.85 (1H, td, J 7.2, 1.3, H₅, 5', bpy), 7.75 (1H, dd, J 5.2, 1.6, H₆) and 7.48 (1H, td, J 6.6, 1.1, H₅); Mass spectrum (ES): m/z 737(100) (M- PF_6).

4.3.9 Preparation of $[\text{Zn}(\text{py-terpy})_2][\text{PF}_6]_2$ (16a)

$\text{Zn}(\text{ClO}_4)_2$ (15 mg, 0.04 mmol) and py-terpy (25 mg, 0.08 mmol) were allowed to stir in acetonitrile (20 cm^3) at room temperature under nitrogen for overnight. The solution was then reduced to half of the volume and diethyl ether was added to precipitate the product.

δ_{H} (400MHz, Acetonitrile- d_6): 9.08 (1H, s, H_3), 9.02 (H, d, J 6.7 H_a), 8.75 (1H, d, J 7.2, H_3), 8.25 (1H, t, J 7.4, 1.2, H_4), 8.12 (1H, d, J 6.7, H_b), 7.87 (1H, d, J 6.5, H_6), 7.43 (1H, t, J 5.8, 1.1, H_5); Mass spectrum (ES): m/z 686(70) [M-2 PF_6].

4.3.10 Preparation of $[\text{Re}(\text{CO})_3(\text{bpy})(\text{py-terpy})]_2\text{Zn}[\text{PF}_6]_2[\text{ClO}_4]_2$ (16)

$[\text{Re}(\text{CO})_3(\text{bpy})(\text{py-terpy})]\text{PF}_6$ (30 mg, 0.032 mmol) and $\text{Zn}(\text{ClO}_4)_2$ (6 mg, 0.016 mmol) were allowed to stir in acetonitrile (20 cm^3) at room temperature under nitrogen for overnight. The solution was then reduced to half of the volume and diethyl ether was added to precipitate the product.

Anal. Found: C 38.84, H 2.01, N 8.35%. Calc. for $[\text{Re}(\text{CO})_3(\text{bpy})(\text{py-terpy})]_2\text{Zn}(\text{PF}_6)_2(\text{ClO}_4)_2$: C 39.09, H 2.19, N 8.29%; IR(CH_3CN), $\nu(\text{cm}^{-1})$ 2036, 1932; δ_{H} (400MHz, Acetonitrile- d_6): 9.37 (1H, d, J 5.2, H_6 , δ , bpy), 8.85 (1H, s, H_3), 8.62 (2H, m, H_3 , β , bpy, H_a), 8.47 (1H, d, J 8.2, H_3), 8.34 (1H, td, J 9.1, 1.5, H_4 , α , bpy), 8.15 (1H, td, J 7.8, 1.5, H_4), 7.99 (1H, d, J 6.8, H_b), 7.88 (1H, td, J 5.7, 1.2, H_5 , β , bpy), 7.76 (1H, d, J 4.8 H_6) and 7.37 (1H, td, J 5.1, 2, H_5); Mass spectrum (ES): m/z 892(45) (M- PF_6 - ClO_4), 737(85) (M-2 PF_6 -2 ClO_4 -Zn).

4.3.11 Preparation of $[\text{Re}(\text{CO})_3(\text{bpy})(\text{py-terpy})]_2\text{Fe}[\text{PF}_6]_2[\text{ClO}_4]_2$ (17)

$\text{Fe}(\text{ClO}_4)_2$ (4 mg, 0.016 mmol) was added to an acetonitrile (20 cm^3) solution of $[\text{Re}(\text{CO})_3(\text{bpy})(\text{py-terpy})]\text{PF}_6$ (30 mg, 0.032 mmol) at room temperature and the yellow solution immediately turned into purple colour indicating the formation of the complex. The precipitate was then filtered and dried (45%).

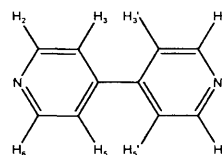
Anal. Found: C 39.45, H 2.05, N 8.21%. Calc. for $[\text{Re}(\text{CO})_3(\text{bpy})(\text{py-terpy})]_2\text{Fe}(\text{PF}_6)_2(\text{ClO}_4)_2$: C 39.28, H 2.20, N 8.33%; IR(CH_3CN), $\nu(\text{cm}^{-1})$ 2035, 1931; δ_{H} (400MHz, DMSO): 9.53 (1H, d, H_6 , δ , bpy), 8.93 (1H, d, H_a), 8.86 (1H, d, H_3 , β , bpy), 8.78 (1H, s, H_3), 8.66 (1H, d, H_3), 8.48 (1H, t, H_4 , α , bpy), 8.42 (1H, t, H_4), 8.02

(2H, m, H_5 , s' , bpy, H_b) and 7.13 (2H, m, H_4 and H_5); Mass spectrum (ES): m/z 887(60) (M- PF_6 - ClO_4), 864(25) (M- 2PF_6), 765(5) (M- 2PF_6 - 2ClO_4), 737(98) (M- 2PF_6 - 2ClO_4 -Fe).

4.3.12 Attempted preparation of $[\text{Re}(\text{CO})_3(\text{bpy})(\text{py-terpy})]_3\text{Eu}[\text{PF}_6]_3$

$[\text{Re}(\text{CO})_3(\text{bpy})(\text{py-terpy})]\text{PF}_6$ (31 mg, 0.035 mmol) and $\text{Eu}(\text{ClO}_4)_3$ (7 mg, 0.012 mmol) were allowed to stir in acetonitrile (20 cm^3) at room temperature under nitrogen for overnight. The solution was then reduced to half of the volume and diethyl ether was added to precipitate the product.

IR(CH_3CN), $\nu(\text{cm}^{-1})$ 2035, 1932; Mass spectrum (ES): m/z 737 $[\text{Re}(\text{CO})_3(\text{bpy})(\text{py-terpy})]^+$; ^1H NMR spectrum produces unpredictable broad peaks. Mass spectrum shows relevance peak for the starting material at m/z 737(M- PF_6).



4.3.13 Preparation of $[\text{Re}(\text{CO})_3(\text{bpy})(4,4'\text{-bpy})][\text{PF}_6]$ (18)

Synthesized according to the literature.²⁰ $[\text{Re}(\text{CO})_3(\text{bpy})\text{CH}_3\text{CN}]\text{PF}_6$ (100 mg, 0.195 mmol) was added to a stirred solution of 20 fold excess 4,4'-bpy (710 mg, 3.905 mmol) in THF (30 cm^3) under nitrogen atmosphere. The solution was refluxed for 2 h. The resulting yellow solution was allowed to cool and evaporated to dryness, and the residue was then dissolved in CH_2Cl_2 , to which hexane was added to precipitate the product. The bright yellow solid obtained was washed with diethyl ether to remove excess free ligand and recrystallized by diffusion of diethyl ether into dichloromethane solution of the product (55%).

Anal. Found: C 37.78, H 2.15, N 7.81%. Calc. for $[\text{Re}(\text{CO})_3(\text{bpy})(4,4'\text{-bpy})]\text{PF}_6$: C 37.97, H 2.22, N 7.70%; δ_{H} (400MHz, DMSO): 9.48 (2H, d, J 5.4, $\text{H}_{6,6'}$, bpy), 8.84 (2H, d, J 8.3, $\text{H}_{3,3'}$, bpy), 8.81 (2H, d, J 6.5, $\text{H}_{2,6}$, 4,4'-bpy), 8.63 (2H, d, J 6.3, $\text{H}_{2',6'}$, 4,4'-bpy), 8.50 (2H, td, J 8, 2, $\text{H}_{4,4'}$, bpy), 8.02 (2H, t, J 5.3, $\text{H}_{5,5'}$, bpy), 7.95 (2H, dd, J 6.5, 1.5, $\text{H}_{3,5}$, 4,4'-bpy) and 7.86 (2H, dd, J 6.1, 1.8, $\text{H}_{3',5'}$, 4,4'-bpy); IR(KBr), $\nu(\text{cm}^{-1})$ 2035, 1931; Mass spectrum (positive FAB): m/z 583(100)[M- PF_6].

4.3.14 Preparation of $[\text{Re}(\text{CO})_3(\text{bpy})]_2(4,4'\text{-bpy})[\text{PF}_6]_2$ (19)

$[\text{Re}(\text{CO})_3(\text{bpy})\text{CH}_3\text{CN}]\text{PF}_6$ (30 mg, 0.058 mmol) and $[\text{Re}(\text{CO})_3(\text{bpy})(4,4'\text{-bpy})]\text{PF}_6$ (36 mg, 0.058 mmol) were allowed to reflux in THF (20 cm^3) under nitrogen

atmosphere for 2 h. After cooling, the yellow precipitate formed during the course of the reaction was filtered and dried. After cooling to room temperature, a saturated solution of KPF_6 was added. The mixture was concentrated in a rotary evaporator to one-third of the original volume to precipitate the yellow product. The solid was washed with ether and dried (60%).

Anal. Found: C 33.31, H 1.84, N 6.31%. Calc. for $[\text{Re}(\text{CO})_3(\text{bpy})]_2(4,4'\text{-bpy})(\text{PF}_6)_2$: C 33.29, H 1.86, N 6.47%. IR (CH_3CN), $\nu(\text{cm}^{-1})$ 2032, 1923. δ_{H} (400MHz, Acetone): 9.39 (2H, d, J 5, $\text{H}_{6,6'}$), 8.74(2H, d, J 8.2, $\text{H}_{3,3'}$), 8.57 (2H, d, J 6.6, $\text{H}_{2,6,4,4'\text{-bpy}}$), 8.44 (2H, td, J 8, 1.3, $\text{H}_{4,4'}$), 7.96 (2H, t, J 6.5, $\text{H}_{5,5'}$) and 7.78 (2H, d, J 6.9 $\text{H}_{3,5,4,4'\text{-bpy}}$). Mass spectrum (ES): m/z 1153 (98)[M-PF_6] and 1008 (17)[M-2PF_6].

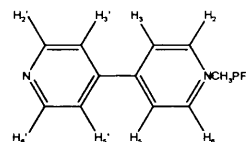
4.3.15 Attempted preparation of $[\text{Re}(\text{CO})_3(\text{bpy})(4,4'\text{-bpy})]_2 \text{Ag}(\text{PF}_6)_2$

$[\text{Re}(\text{CO})_3(\text{bpy})(4,4'\text{-bpy})]\text{PF}_6$ (30 mg, 0.041 mmol) was dissolved in acetonitrile (2 cm^3) and AgNO_3 was dissolved in distill water (2 cm^3). Acetonitrile solution was added to the aqueous solution slowly by layer diffusion and left in dark for seven days.

No evidence of complex formation was observed by ^1H NMR and Mass spectrum.

4.3.16 Attempted preparation of $[\text{Re}(\text{CO})_3(\text{bpy})(4,4'\text{-bpy})]_2 [\text{Re}(\text{CO})_3\text{Cl}][\text{PF}_6]_2$

$\text{Re}(\text{CO})_3\text{Cl}$ (29 mg, 0.039 mmol) and $[\text{Re}(\text{CO})_3(\text{bpy})(4,4'\text{-bpy})]\text{PF}_6$ (7.2 mg, 0.0195 mmol) were allowed to reflux in toluene under nitrogen atmosphere for 1 hr. After cooling the precipitate was filtered and dried. ^1H NMR showed broad splitted peaks. Mass spectrum didn't provide expected ions.



4.3.17 Preparation of N-methyl-4,4'-bipyridinium(MQ^+) PF_6^-

4,4'-bpy (1.35 g, 8.68 mmol) and MeI (0.68g, 4.85 mmol) were stirred in acetone (100 cm^3) at room temperature for overnight. The yellow precipitate was collected by filtration, washed with acetone and dried. Recrystallization in ethanol and water afforded a golden product, which was then collected by suction filtration and dried. The yellow filtrate was then reduced to dryness using a rotary evaporator

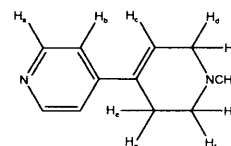
and the redissolved in water. Conc. aqueous KPF_6 was added to the solution to yield off white precipitate of the hexafluorophosphate salt. The precipitate was collected by suction filtration and dried (55%).

δ_{H} (400MHz, DMSO): 9.2 (2H, d, J 6.7, $\text{H}_{2,6}$), 8.94 (2H, d, J 6.1, $\text{H}_{2',6'}$), 8.68 (2H, d, J 6.7, $\text{H}_{3,5}$), 8.1 (2H, dd, J 4.6, 1.5, $\text{H}_{3',5'}$), 4.44 (3H, s, CH_3). Mass spectrum (EI): m/z 171 (70)[M-PF_6].

4.3.18 Preparation of $[\text{Re}(\text{CO})_3(\text{bpy})(\text{MQ})][\text{PF}_6]_2$ (20)

$[\text{Re}(\text{CO})_3(\text{bpy})\text{CH}_3\text{CN}]\text{PF}_6$ (100 mg, 0.16 mmol) and $(\text{MQ})^+\text{PF}_6^-$ (50 mg, 0.16 mmol) were allowed to reflux in THF (20 cm^3) under nitrogen atmosphere for 2 h. After the solution had cooled, hexane was added to precipitate the product. The precipitate was filtered and purified by repeated recrystallization from methanol (85%).

Anal. Found: C 32.23, H 2.01, N 6.47%. Calc. for $[\text{Re}(\text{CO})_3(\text{bpy})(\text{MQ})](\text{PF}_6)_2$: C 32.48, H 2.16, N 6.31%; IR(KBr), $\nu(\text{cm}^{-1})$ 2036, 1933. δ_{H} (400MHz, DMSO): 9.43 (2H, d, J 4.7, $\text{H}_{6,6'}$, bpy), 9.13 (2H, d, J 6.8, $\text{H}_{2,6}$, MQ), 8.77 (2H, d, J 8.2, $\text{H}_{3,3'}$, bpy), 8.71 (2H, d, J 6.7, $\text{H}_{2',6'}$, MQ), 8.52 (2H, d, J 6.7, $\text{H}_{3,5}$, MQ), 8.45 (2H, td, J 8, 1.3, $\text{H}_{4,4'}$, bpy), 8.00 (2H, d, J 6.8, $\text{H}_{3',5'}$, MQ), 7.97 (2H, t, J 6.2, $\text{H}_{5,5'}$, bpy) and 4.36 (3H, s, NCH_3); Mass spectrum (positive FAB): m/z 598 (100)[M-2PF_6].



4.3.19 Preparation of 1-methyl-4-pyridyltetrahydropyridine (MPyTP)

Sodium borohydride (120 mg, 0.43 mmol) was added to a stirred solution of MQ^+I^- (80 mg, 0.265 mmol) in methanol (20 cm^3) at 0°C . The mixture was then stirred for 1 h at room temperature and the solvent was removed in vacuum. The residue was dissolved in water (20 cm^3) and was extracted 4 times with diethyl ether. The combined organic layers were dried over MgSO_4 , filtered to remove the solid and the filtrate was dried under vacuum to obtain the desired product.

δ_{H} (400MHz, CDCl_3): 8.46 (2H, d, J 4.7, H_a), 7.2 (2H, dd, J 4.8, 1.4, H_b), 6.24 (1H, m, H_c), 3.08 (2H, dd, J 6, 2.9, H_e), 2.61 (2H, t, J 5.7, $\text{H}_{d/f}$), 2.5 (2H, m, $\text{H}_{d/f}$) and 2.34 (3H, s, $-\text{CH}_3$); Mass spectrum (EI): m/z 174 (75)[M-PF_6].

4.3.20 Preparation of $[\text{Re}(\text{CO})_3(\text{bpy})(\text{MPyTP})][\text{PF}_6]$ (21)

$[\text{Re}(\text{CO})_3(\text{bpy})\text{CH}_3\text{CN}]\text{PF}_6$ (49 mg, 0.08 mmol) and freshly prepared MPyTP (23 mg, .08 mmol) were allowed to reflux in THF (20 cm^3) under nitrogen atmosphere for 2 h. After the solution had cooled, hexane was added to precipitate the product (95%).

Anal. Found: C 38.42, H 2.78, N 7.35%. Calc. for $[\text{Re}(\text{CO})_3(\text{bpy})(\text{MPyTP})](\text{PF}_6)_2$: C 38.66, H 2.97, N 7.51%; IR(KBr), $\nu(\text{cm}^{-1})$ 2035, 1932; δ_{H} (400MHz, DMSO): 8.91 (2H, d, J 5.1, bpy), 8.29 (2H, d, J 8.1, bpy), 8.0 (2H, td, J 7.9, 1.2, bpy), 7.78 (2H, d, J 6.5, H_a), 7.55 (2H, t, J 6.4, bpy), 7.24 (4H, s, CDCl_3) and 6.96 (2H, d, 6.6, H_b), 6.11(1H, s, H_c), 3.04 (2H, s, H_e), 2.27 (3H, s, $-\text{CH}_3$) and 2.13 (4H, s, H_d , t); Mass spectrum (positive FAB): m/z 601(85) [M- PF_6].

4.3.21 Preparation of $[\text{Re}(\text{CO})_3(\text{bps})\text{Cl}]$ (22)

Rhenium pentacarbonyl chloride (100 mg, 0.276 mmol) and 4,7- diphenyl-1,10-phenanthrolinedisulfonic acid disodium salt (148 mg, 0.276 mmol) were allowed to reflux in water (30 cm^3) for 1 hour. The solution turned into orange colour over this time. The solution was then cooled to room temperature. The orange precipitate formed upon cooling was filtered and dried in a desiccator (75%).

IR (KBr), $\nu(\text{cm}^{-1})$ 2024 and 1895; Mass spectrum (FAB): m/z 865(42) [M+Na] and 807(100) [M-Cl]. ^1H NMR of the compound in D_2O gives broad splitted peaks.

4.3.22 Preparation of $[\text{Re}(\text{CO})_3(\text{bpsa})(\text{ClO}_4)]$ (23)

$\text{Re}(\text{bpsa})(\text{CO})_3\text{Cl}$ (50 mg, 0.058 mmol) and silver perchlorate (13 mg, 0.06 mmol) were allowed to reflux in acetonitrile (30 cm^3) and water, enough to dissolve the reactants, under a nitrogen atmosphere in the dark for overnight. After cooling, the solution was filtered to remove silver chloride. The solvent was removed from the solution under vacuum line in a desiccator to obtain the crystalline product (57%).

IR(KBr), $\nu(\text{cm}^{-1})$ 2032, 1912, 1193 and 1097(ClO_4). Mass spectrum (ES): m/z 929(10) [M+Na], 883(5) [M-Na], 839(75) [M + MeOH - ClO_4], 816(30)[M+ MeOH - ClO_4 -Na].

4.3.23 Attempted preparation of $[\text{Re}(\text{CO})_3(\text{bpsa})(\text{MQ})][\text{PF}_6][\text{ClO}_4]$ (24)

$[\text{Re}(\text{CO})_3(\text{bpsa})(\text{CH}_3\text{CN})]\text{ClO}_4$ (20 mg, 0.0215 mmol) and $(\text{MQ})^+\text{PF}_6^-$ (7 mg, 0.0215 mmol) were allowed to reflux in THF (20 cm^3) and water under nitrogen atmosphere for 2 h. After cooling, the solution was filtered. The solvent was removed from the solution under vacuum line in a desiccator to obtain the product (50%).

IR(KBr), $\nu(\text{cm}^{-1})$ 2030, 1911.

4.3.24 Preparation of $[\text{Re}(\text{CO})_3(\text{CH}_3\text{CN})_3]\text{PF}_6$ (25)

$\text{Re}(\text{CO})_3(\text{CH}_3\text{CN})_2\text{Cl}$ (70mg, 0.18 mmol) and AgClO_4 (41mg, 0.198 mmol) were allowed to reflux in acetonitrile (25 cm^3) under a nitrogen atmosphere in the dark for overnight. After cooling the solution, concentrated aqueous solution of potassium hexafluorophosphate was added to the reaction mixture and acetonitrile was removed by slow evaporation under vacuum. The product was obtained as colorless crystals. The yield was 95%.

IR(KBr), $\nu(\text{cm}^{-1})$ 2293w (CN), 2253w (CN), 2052s and 950s; δ_{H} (400MHz, CDCl_3): 2.45 (9H, s, CH_3CN).

4.3.25 Attempted preparation of $[\text{Re}(\text{CO})_3]_{12}(\text{4,4'-bpy})_8[\text{PF}_6]_{12}$

$[\text{Re}(\text{CO})_3(\text{CH}_3\text{CN})_3]\text{PF}_6$ (12 mg, 0.022 mmol) and 4,4'-bpy (6.5 mg, 0.041 mmol) were allowed to react in acetonitrile (15 cm^3) at 20⁰ C for overnight. During the course of the reaction yellow precipitate was formed which was then filtered and dried. The solid is sparingly soluble in acetonitrile, acetone and dichloromethane but fairly soluble in DMSO.

¹H NMR and Mass spectrum provide no evidence of complex formation.

4.3.26 Preparation of $[\text{Re}(\text{CO})_3(\text{MQ})_3](\text{PF}_6)_3$ (26)

$[\text{Re}(\text{CO})_3(\text{CH}_3\text{CN})_3]\text{PF}_6$ (30 mg, 0.055 mmol) and MQ^+ (52 mg, 0.164 mmol) were allowed to reflux THF (20 cm^3) under nitrogen atmosphere for 2 h. During the course of the reaction yellow precipitate was formed which was collected by filtration. Hexane was added to the filtrate to precipitate the rest of the product. The solid was then washed with ether and dried (70%).

IR (CH_3CN), $\nu(\text{cm}^{-1})$ 2030, 1924 and 1910. δ_{H} (400MHz, CD_3CN): 8.76 (1H, dd, J 4.7, 1.3), 8.74 (1H, dd, J 5.2, 1.5), 8.67 (1H, d, J 6.8), 8.63 (H, d, J 6.7), 8.22 (2H, d, J 6.5), 7.85 (1H, dd, J 5.1, 1.5) and 7.74 (1H, dd, 4.5, 1.5).

References

- 1 M. Wrighton and D. L. Morse, *J. Am. Chem. Soc.*, 1974, **96**, 998; J.C. Luong, L. Nadjio and M.S. Wrighton, *J. Am. Chem. Soc.*, 1978, **100**, 5790;
- 2 J.V. Casper and T.J. Meyer, *J. Phys. Chem.*, 1983, **87**, 952; L.A. Worl, R. Duesing, P. Chen, L. Della Ciana and T.J. Meyer, *J. Chem. Soc., Dalton Trans.*, 1991, 849.
- 3 B.D. Rossenaar, D.J. Stufkens and A. Vl̇cek, *Inorg. Chem.*, 1996, **35**, 2902.
- 4 A. Vl̇cek and S. Żalijs, *Coord. Chem. Rev.*, 2007, **251**, 258.
- 5 P.D. Beer, F. Szemes, V. Balzani, C.M. Sala, M.G.B. Drew, S.W. Dent and M. Maestri, *J. Am. Chem. Soc.*, 1997, 119, 11864.
- 6 P. D. Beer, O. Kosian, R. J. Mortimer and C. Ridgway, *J. Chem. Soc., Dalton Trans.*, 1993, 2629.
- 7 P. D. Beer and E. J Hayes, *Coord. Chem. Rev.*, 2003, **240**, 167.
- 8 M. H. Keefe, K. D. Benkstein and J. T. Hupp, *Coord. Chem. Rev.*, 2000, **205**, 201.
- 9 R. V. Slone, D. I. Yoon, R. M. Calhoun and J. T. Hupp, *J. Am. Chem. Soc.*, 1995, **117**, 11813.
- 10 D. Curiel and P. D. Beer, *Chem. Commun.*, 2005, 1909.
- 11 S. S. Sun and A. J. Lees, *Chem. Commun.*, 2000, 1687.
- 12 K.D. Benkstein, J.T. Hupp and C.L. Stern, *J. Am. Chem. Soc.*, 1998, **120**, 12982.
- 13 K. K. -W. Lo, J. S.-Y. Lau, V. W.-Y. Fong and N. Zhu, *Organometallics*, 2004, **23**, 1098.
- 14 J. D. Lewis and J. D. Moore, *Dalton Trans.*, 2004, 1376.
- 15 K.-S. Jeong, Y.L. Cho, S.-Y. Chang, T.-Y. Park and J.U. Song, *J. Org. Chem.*, 1999, **64**, 9459.
- 16 D. H. Lee, H. Y. Lee and J. I. Hong, *Tetrahedron Lett.*, 2002, **43**, 7273.
- 17 Y. Kubo, M. Tsukahara, S. Ishihara, and S. J. Tokita, *Chem. Soc., Chem. Commun.*, 2000, 653.
- 18 T. Gunnlaugsson, A. P. Davis, and M. J. Glynn, *Chem. Soc., Chem. Commun.*, 2001, 2556.
- 19 M. Avos, R. Babino, A. Cabanillas, P. Cintas, F. J. Highes, J. L. Jiménez, and J. C. Palacios, *J. Org. Chem.*, 1996, **61**, 3738.

- 20 K. K. -W. Lo, D. C.-M. Ng, V. W.-K. Hui and K. K. Cheung, *J. Chem. Soc., Dalton Trans.*, 2001, 2634.
- 21 W. -M. Xue, F. E. Kühn and E. Herdtweck, *Polyhedron*, 2001, **20**, 791.
- 22 G. Tapolsky, R. Duesing and T. J. Meyer, *Inorg. Chem.*, 1990, **29**, 2285.
- 23 S. S. Sun, A. J. Lees and P. Y. Zavalij, *Inorg. Chem.*, 2003, **42**, 3445.
- 24 P. J. Giordano and M. S. Wrighton, *J. Am. Chem. Soc.*, 1979, **101**, 2888.
- 25 L. Fabbrizzi and A. Poggi, *Chem. Soc. Rev.*, 1995, 197.
- 26 J. D. Lewis, R. N. Perutz and J. N. Moore, *J. Phys. Chem. A*, 2002, **106**, 12202.
- 27 E. C. Constable and A. M. W. C. Thompson, *J. Chem. Soc., Dalton Trans.*, 1992, 2947.
- 28 S. S. Sun and A. J. Lees, *Coord. Chem. Rev.*, 2002, **230**, 171.
- 29 C.-F. Zhanga, H.-X. Huangb, B. Liub, M. Chena and D.-J. Qiana, *J. Lumin.*, 2008, **128**, 469.
- 30 E. Amouyal, M. Mouallem-Bahout and G. Calzaferri, *J. Phys. Chem.*, 1991, **95**, 7641.
- 31 R. Reisfeld, T. Saraidarov, E. Ziganski, M. Gaft, S. Lis and M. Pietraszkiewicz, *J. Lumin.*, 2003, **243**, 102.
- 32 C. Mallet, R. P. Thummel, C. Hery, *Inorganica Chimica Acta*, 1993, **210**, 223.
- 33 M. Casanova, E. Zangrando, F. Munini, E. Iengo and E. Alessio, *Dalton Trans.*, 2006, 5033.
- 34 P. Chen, M. Curry and T. J. Meyer, *Inorg. Chem.*, 1989, **28**, 2271.
- 35 B.J. Coe, M.C. Chamberlain, J.P. Essex-Lopresti, S. Gaines, J.C. Jeffery, S. Houbrechts and A. Persoons. *Inorg. Chem.*, 1997. **36**, 3284; M. Seiler and H. Durr. *Synthesis*, 1994, 83.
- 36 J. R Schoonover, P. Chen, W. D. Bates, R. B Dyer and T. J. Meyer, *Inorg. Chem.*, 1994, **33**, 793.
- 37 P. Chen, E. Danielson and T. J. Meyer, *J. Phys. Chem.*, 1988, **92**, 3708.
- 38 N.N. Mateeva, L.L. Winfield and K.K. Redda, *Current Medicinal Chemistry*, 2005, **12**, 551.
- 39 M. Yamada, M. Onodera, Y. Mizuno and H. Mochizuki, *Neuroscience*, 2004, **124**, 173.
- 40 C. Franot, S. Mabic and N. Castagnoli, *J. Bioorganic & Medicinal Chemistry*, 1997, **5**, 1519.

- 41 S. Berger, A. Klein, and W. Kaim, *Inorg. Chem.*, 1998, **37**, 5664.
- 42 C. A. Linkous, K. M. Schaich, A. Foman and D. C. Borg, *Bioelectrochemistry and Bioenergetics*, 1988, **19**, 477.
- 43 T. D. Westmoreland, H. Le Bozec, R. W. Murray, and T. J. Meyer, *J. Am. Chem. Soc.*, 1983, **105**, 5952.
- 44 R.V. Slone, J. T. Hupp, C. L. Stern, and T. E. Albrecht-Schmitt, *Inorg. Chem.*, 1996, **35**, 4096.
- 45 N.G. Connelly and L. F. Dahl, *Chem. Commun.*, 1970, 600; M. G. B. Drew, D. G. Tisley and R. A. Walton, *Chem. Commun.*, 1970, 800; Y. Y. Lilian, E. E. Chan and W. A. G. Graham, *Can. J. Chem.*, 1977, **55**, 111; P. K. Baker, M.G. B. Drew and M. M. Meehan, *Inorg. Chem. Commun.*, 2000, **3**, 393.
- 46 M. F. Farona and K. F. Kraus, *Inorg. Chem.*, 1970, **9**, 1700.

